

**COMMUNITIES IN TRANSITION:
A MULTI-PHASE STUDY OF THE
TSUGA HETEROPHYLLA / *ABIES AMABILIS* ECOTONE
IN THE OREGON CASCADES**

by

Todd Lookingbill

University Program in Ecology
Nicholas School of the Environment and Earth Science
Duke University

Date: _____

Approved:

Dean Urban, Supervisor

Lawrence Band

Norman Christensen

James Clark

Dissertation submitted in partial fulfillment of
the requirements for the degree of
Doctor of Philosophy
in the University Program in Ecology
in the Graduate School
of Duke University

2003

ABSTRACT

**COMMUNITIES IN TRANSITION:
A MULTI-PHASE STUDY OF THE
TSUGA HETEROPHYLLA / *ABIES AMABILIS* ECOTONE
IN THE OREGON CASCADES**

by

Todd Lookingbill

University Program in Ecology
Nicholas School of the Environment and Earth Science
Duke University

Date: _____

Approved:

Dean Urban, Supervisor

Lawrence Band

Norman Christensen

James Clark

An abstract of a dissertation submitted in partial
fulfillment of the requirements for the degree of
Doctor of Philosophy
in the University Program in Ecology
in the Graduate School
of Duke University

2003

ABSTRACT

Gradient analysis as a study of community pattern has a long and distinguished history in montane systems. The elevation complex stands out from these studies as the most consistent environmental correlate with changes in forest community composition. As a result, major vegetation zones typically are described along elevation gradients. Trees are not affected by elevation, however, but rather by variables such as temperature and precipitation that covary with elevation. Because these variables are difficult to measure at large spatial scales, I propose an iterative approach of leveraging traditional gradient analysis studies to (1) develop new hypotheses regarding the dynamics of forest communities, (2) identify major data needs and shortcomings, and (3) target locations on the landscape that are best suited to test new hypotheses and fill data gaps.

I developed a working model of community pattern from a landscape sample of old-growth forest stands in the Lookout Creek Watershed of the H.J. Andrews Experimental Forest, Oregon. Analytic techniques in classification, ordination, and spatial regression were used in synthesis to identify major forest communities and the terrain and soil factors influencing their distribution. Elevation and spatial location were highlighted as the strongest explanatory variables. These results, though typical of a gradient analysis study, allow for considerable variability in the interpretation of the underlying mechanisms. To make educated predictions of how these forests may respond to environmental change, such as that predicted under greenhouse warming scenarios, requires a more detailed description of the interactions between forest communities and their environment.

To refine the working model, I developed a series of novel sampling and analytic approaches to study fine-grain environmental patterns over large geographic areas. These methods include:

- new approaches to empirically interpolate relative differences in temperature, radiation and soil moisture across landscapes; and
- a replicated study of plant demographics (growth, mortality and regeneration) at the dominant community ecotone.

These studies were intended to replace elevation and basal area from the working model with more plant-relevant explanatory variables and the demographic components that they affect. The landscape-scale models illustrate that using elevation to approximate environmental variability ignores the multi-scale structure of the physical template. Similarly, the focused study of the *Tsuga heterophylla*-*Abies amabilis* ecotone illustrates that a coarse-scale analysis of community distributions might not accurately reflect the dynamics within active areas of community transition. I conclude with a summary of the findings and approach, an example of how the results could be relevant to management under potential climate change scenarios, and a discussion of how the methods can be transferred to other montane systems.

ACKNOWLEDGMENTS

First and foremost, I thank my advisor and mentor, Dean Urban, whose guidance has been dead-on at every step of this journey. I also thank my committee, Larry Band, Norm Christensen and Jim Clark, for helping me to see the forest when I would wander off into the trees.

This dissertation is presented as a collection of related papers. In addition to the invaluable contributions by my advisor and committee members throughout the work, I recognize Ken Pierce (Chapter 3.1), Christina Tague, Georgianne Moore and Steven Petersen (Chapter 3.4) as co-authors on papers related to individual chapters.

The Duke Landscape Ecology Lab improved this work considerably with their ideas, comments and encouragement. This amazing group included Ken Pierce, Monique Rocca, Emily Minor, Rob MacDonald, Eric Trembl, Yolanda Wiersma, Pat Halpin, Peter Harrell, Andy Bunn and Katie Bickel. Thanks for contributing your time, expertise and friendship.

None of this work would have been possible without the assistance of the incredible research and support teams at the H.J. Andrews Experimental Forest. Special acknowledgments to Bonnie West, Chris Bigelow, John Moreau, Art McKee, Julia Jones, Fred Swanson, Mark Harmon and Steve Garman. I was helped with the dirty work (literally) by a tireless field crew: Scott Powell, Mike Dietz, Rachel Tallmadge, Andrew Black, Hilary Lookingbill, Neal Goldenberg and Brian Williams.

Finally, I especially thank my parents for years of support that extend far beyond the duration of this dissertation and my wife Nicole, whose love, encouragement and understanding were paramount to the completion of this project. I look forward to returning these gifts with interest over the years ahead.

TABLE OF CONTENTS

CHAPTER 1 Introduction	1
Gradient Analysis.....	1
Ecotones: Communities in Transition.....	3
Study Goals and Objectives	5
SECTION 2: A PRELIMINARY MODEL	9
CHAPTER 2 A 3D Exploration of Landscape Pattern in the Oregon Cascades: Three Techniques Based on Ecological Dissimilarity.....	9
Abstract.....	10
Introduction.....	11
Methods.....	13
Site description.....	13
Data	14
Analysis.....	19
Bray-Curtis dissimilarity index.....	20
Biotic patterns/species associations	21
Environmental patterns	23
Species-environment interactions	24
Results	29
Species associations	29
Environmental patterns	32
Species-environment Interactions.....	34
Discussion.....	42
Species patterns.....	42
Traditional gradient analysis approach	43
Extending community ecology to landscapes.....	45
Conclusion	46

SECTION 3: THE PHYSICAL SETTING	48
CHAPTER 3.1 A Simple Method for Estimating Potential Relative Radiation (PRR) for Landscape-Scale Vegetation Analysis.....	48
Abstract.....	49
Introduction.....	50
The geometry of radiation.....	51
Radiation proxies	53
Radiation models	56
Methods.....	59
Study site.....	59
Potential relative radiation (PRR).....	60
Other radiation proxies	62
Results	64
Discussion.....	69
CHAPTER 3.2 Spatial Estimation of Air Temperature Differences for Landscape-scale Studies in Montane Environments	73
Abstract.....	74
Introduction.....	75
Methods.....	78
Study area.....	78
Data	80
Analysis.....	84
Results	85
Model fits.....	85
Model validations.....	89
Discussion.....	89
CHAPTER 3.3 An Empirical Approach Towards Improved Spatial Estimates of Soil Moisture for Vegetation Analysis	95
Abstract.....	96
Introduction.....	97

Methods.....	101
Study area.....	101
Exploratory studies	103
Empirical model.....	107
Spatial scale of variability.....	110
Results.....	112
Comparison among permanent TDR sites.....	112
Comparison within permanent TDR sites.....	115
Gravimetric sampling.....	116
Empirical model.....	116
Variograms.....	119
Discussion.....	124
CHAPTER 3.4 Estimating Spatial Patterns of Summer Soil Moisture: Model Comparison	131
Abstract.....	132
Introduction.....	133
Site description.....	136
Model Descriptions	137
Soil moisture indices.....	137
Statistical model.....	140
Process models.....	142
TOPOG	144
RHESSys.....	147
Validation Data	150
Model Comparisons.....	153
Three watersheds, single day	153
Landscape, multiple days.....	155
Discussion.....	157

SECTION 4: A FOCUSED INVESTIGATION.....	167
CHAPTER 4 Factors Controlling Community Transition at the <i>Tsuga heterophylla</i>/<i>Abies amabilis</i> Ecotone.....	167
Abstract.....	168
Ecotone hypotheses.....	171
Study area.....	176
<i>Tsuga heterophylla</i> [Raf.] Sarg. (western hemlock).....	177
<i>Abies amabilis</i> [Dougl.] Forbes (Pacific silver fir).....	177
<i>Abies procera</i> Rehd. (noble fir).....	178
Methods.....	180
Plot selection.....	181
Field methods.....	182
GIS methods - development of spatial data layers.....	185
Statistical methods.....	190
Results.....	193
Plot descriptions.....	193
Biotic patterns.....	193
Environmental patterns.....	197
Environmental controls on demography.....	205
Landscape-level associations.....	205
Ecotone level associations.....	209
Discussion.....	215
T. heterophylla.....	215
A. amabilis.....	218
A. procera.....	220
Conclusions.....	222
CHAPTER 5 Summary and Conclusions.....	223
Summary.....	223
Beyond Elevation.....	225
Demographics are Important, too.....	226
Implications for Global Climate Change.....	228
Applicability of Approach to Other Montane Systems.....	230
REFERENCES.....	232

LIST OF TABLES

Table 2.1. Seven dominant species observed on 164 plots	15
Table 2.2. Summary of environmental variables collected on the 164 plots	18
Table 2.3. Group membership assignment for four-cluster solutions	31
Table 2.4. Species loadings on MDS axes and direct elevation axis	33
Table 2.5. Correlation matrix for environmental variables	33
Table 2.6. Correlations between species abundance and environmental variables	35
Table 2.7. Mantel coefficients for aggregated analysis	38
Table 3.1.1. Correlations between proxies and modeled radiation for 175 plots	68
Table 3.1.2. Correlations between proxies and modeled radiation for 1000 points	68
Table 3.2.1. Mean, minimum, maximum temperature models	88
Table 3.3.1. Environmental statistics for permanent meteorological stations	105
Table 3.3.2. Potential predictor variables for empirical moisture models	108
Table 3.3.3. Summer 1999 permanent meteorological station data	113
Table 3.3.4. Regression statistics for empirical moisture models	118
Table 3.4.1. Tests of model predictions for three small-watershed samples	154
Table 3.4.2. Tests of model predictions after removing 2 transects with large error	154
Table 3.4.3. Tests of model predictions for landscape-wide samples	154
Table 4.1. Summary of geospatial data layers built for ecotone analysis	187
Table 4.2. Summary descriptions of five ecotone plots	194
Table 4.3. Summary of ecotone canopy openings and aspect values	198
Table 4.4. Summary of ecotone soil moisture measurements	198

Table 4.5. Summary of ecotone temperature data	204
Table 4.6. CART analysis results for ecotone data	212

LIST OF FIGURES

Figure 1.1. Schematic overview of research approach	8
Figure 2.1. Dominance-diversity curve for 20 species sampled on 164 plots	15
Figure 2.2. Locations of 164 sample plots	16
Figure 2.3. Stratified cluster sampling design	18
Figure 2.4. Maximum indicator values recorded for 7 dominant species	30
Figure 2.5. Group membership of species in clusters	30
Figure 2.6. Species clusters projected into NMS space	31
Figure 2.7. Direct ordination of dominant species on elevation	37
Figure 2.8. Mantel path diagram for aggregated variables	38
Figure 2.9. Mantel path diagram for individual variables	40
Figure 2.10. Classification tree of 164 landscape plots	41
Figure 3.1.1. Schematics of solar geometry	52
Figure 3.1.2. Illustration of radiation indices at Moro Rock	65
Figure 3.1.3. Comparison of radiation proxies to modeled radiation	67
Figure 3.2.1. HJA locator map	79
Figure 3.2.2. Location of micro-loggers	82
Figure 3.2.3. Comparison of micro-logger and CR10X datalogger data	83
Figure 3.2.4. Maps of spatial residuals for the mean July temperature models	87
Figure 3.2.5. Temperature model validations	90
Figure 3.3.1. State of Oregon with HJA identified	102
Figure 3.3.2. Map of soil moisture sample locations	104

Figure 3.3.3. Surface soil gravimetric samples vs. volumetric samples	108
Figure 3.3.4. Summer 1999 soil moisture levels for permanent TDR sites	114
Figure 3.3.5. Gravimetric moisture as a function of elevation	117
Figure 3.3.6. Analysis of residuals from regression model	118
Figure 3.3.7. Variograms of soil moisture and factors important to water budget	120
Figure 3.3.8. Variogram of fine-scale trend in soil moisture	123
Figure 3.3.9. Spatial mapping of statistical surface soil moisture model	128
Figure 3.3.10. Variogram of fitted values from regression analysis	130
Figure 3.4.1. Spatial mapping of TCI and IMI	138
Figure 3.4.2. Spatial mapping of Topog and RHESSys	143
Figure 3.4.3. Locations of 2002 soil moisture validation samples	152
Figure 3.4.4. Moisture measurements from permanent sampling stations	156
Figure 4.1. Tree size class distributions for four major species	179
Figure 4.2. Schematic of ecotone plot sampling design	183
Figure 4.3. Comparison of kriging vs. IDW as DEM interpolation techniques	187
Figure 4.4. Ecotone plot locations	194
Figure 4.5. Seedling size class distributions	196
Figure 4.6. Kriged soil moisture coverage for Ecotone Plot 2	200
Figure 4.7. Snowdepth transect on Ecotone Plot 2	201
Figure 4.8. SNOBO melt data for a location on Ecotone Plot 2	201
Figure 4.9. Landscape trends in basal area, seedling density, and mortality	206
Figure 4.10. Landscape trends in relative growth rates	208
Figure 4.11. Landscape trends in <i>T. heterophylla</i> seedling distribution	210

Figure 4.12. Ecotone trends in relative growth rates	210
Figure 4.13. Logistic regression results for ecotone data	214
Figure 4.14. Seedling distributions of all species with respect to aspect	221
Figure 5.1. Areas of HJA potentially sensitive to climate change	229

CHAPTER 1 Introduction

Gradient Analysis

Community ecology conducted over landscape scales has been largely an inferential science dependent on correlations between vegetation and easily derived environmental “proxy” variables (Hobbs 1997, Wiens 1999). In montane systems, these studies largely have taken the form of gradient analyses (Merriam 1899, Whittaker 1956, Zobel et al. 1976, Gauch et al. 1981). The elevation complex stands out from this work as the most consistent environmental correlate with pattern. As a result, major vegetation zones typically are described along elevation gradients (Vankat & Major 1978, Ohmann & Spies 1998, Franklin & Halpern 2000).

A major shortcoming of these studies is that elevation is not directly relevant to plants. Although elevation may be strongly correlated with landscape pattern, elevation differences are not responsible for landscape pattern. Trees do not respond to elevation, but rather to variables such as temperature and precipitation that covary with elevation. Gradient studies with largely topographic explanatory variables can be thought of as a guide for more sophisticated analyses that attempt a more mechanistic description of ecological patterns (Austin 1987, Levin 1992). Stephenson (1990, 1998) presents a detailed discussion of how biologically meaningful variables are better predictors of plant distributions than commonly used environmental surrogates.

Correlative relationships with biologically irrelevant proxy variables may work well for describing pattern under reference conditions, but if conditions were to change,

these relationships might no longer be valid. For example, in response to rising atmospheric CO₂ levels, temperature is projected to increase by 1.4-5.8 °C over the next 100 years (IPCC 2001). Potential changes in precipitation due to global climate change are less certain, and features that affect water storage and drainage, such as soil depth and local topography, are unlikely to change. Predicting vegetation responses to climate change scenarios requires an understanding of how each of these specific factors is related to plant distributions (Halpin 1997, Urban et al. 2000). Using elevation as a proxy variable to study plant-environment relationships is complicated by the fact that elevation is highly related to many of these factors. For example, temperature is correlated with elevation, but so are soil properties. Loose soil particles creep downslope over time and collect on gentler slopes and lower elevations, while rock outcrops and volcanic ejecta are more common at higher elevations. Amount and persistence of snowpack, climate, and disturbance also are correlated with elevation (Franklin & Dyrness 1988, Clark 1990).

Despite the importance of isolating more biologically meaningful determinants of landscape pattern, few ecological studies attempt to quantify and relate the variability in these factors to plant community pattern at the landscape scale. This is largely due to the difficulty of studying ecosystems at this scale. Intensive, fine-grain studies are able to capture the complex patterns in environmental variability explicitly (*e.g.*, Yeakley et al. 1998), and much of this fine-scaled detail averages away at regional to global scales (*e.g.*, Neilson 1991). But at landscape scales, detailed environmental variability cannot be ignored, nor can its influence be captured empirically using conventional sampling

techniques (Chen et al. 1999). Despite the lack of information, management decisions typically must be made at the landscape scale (Christensen et al. 1996, 2000).

Ecotones: Communities in Transition

I offer an examination of plant-relevant explanatory variables to attempt to understand the spatial transition in community dominance from the *Tsuga heterophylla* (western hemlock) to *Abies amabilis* (Pacific silver fir) vegetation zones in the Oregon Western Cascades. An improved understanding of this ecotone is needed to assess the potential impacts of changes in climate or management that may alter the correlation structure among environmental variables in these prized forests. This type of assessment is not possible without extending our knowledge base beyond the simple correlation of plant communities with the elevation gradient complex.

Ecologists historically have focused on homogeneous environments to understand ecological processes (Whittaker 1956, Peet 1981, Acker et al. 1998). Ecotones need further study. These are areas of maximum habitat variability and often maximum diversity (Neilson 1991). Because many species are at the competitive limits of their ecological tolerances at ecotones, these regions may be especially sensitive to environmental change (Fortin et al. 2000). Neilson (1991) suggests that ecotones could be used as early warning systems of regional change, particularly for global climate change.

The *T. heterophylla*-*A. amabilis* ecotone has been well documented in the Pacific Northwest (Fonda & Bliss 1969, Zobel et al. 1976, Franklin & Dyrness 1988), but efforts to identify the ultimate causes of the transition have been minimal. Those studies that

have focused on describing mechanisms for this transition are somewhat contradictory (e.g., Krajina 1969, Thornburgh 1969).

Thornburgh (1969) suggested that the influence of snowpack on *T. heterophylla* seedlings might be critical to this transition. According to his line of reasoning, *T. heterophylla* seedlings do not establish until up to a month after the first snowmelt, while *A. amabilis* can germinate almost immediately. The *T. heterophylla* seedlings therefore have limited growth over their first growing season. This low growth combined with the drooping nature of *T. heterophylla* seedlings make them highly susceptible to damage by snowpack and accompanying debris over their first winter. Although the logic of this snowpack theory is compelling and has been invoked in simulation modeling (Urban et al. 1993) and general descriptions of the system (Franklin & Dyrness 1988), empirical support for the theory is limited. Krajina (1969) suggested an alternative hypothesis. He argued that low drought limited the distribution of *A. amabilis* and described the transition from *T. heterophylla* to *A. amabilis* along an increasing precipitation gradient.

The long history of gradient analysis provides an additional potential explanation. Implicit in these studies is the assumption that community transitions are caused by trade-offs in tolerances and growth rates. Species develop tolerances to low levels of environmental resources at the cost of reduced growth rates even when resources are not limiting. Following the general model described by Smith and Huston (1989), *T. heterophylla* would not be competitive at higher elevations because of limited cold tolerance (Packee 1990). *A. amabilis*, conversely, would not be competitive at lower elevations because of slower growth rates.

The competing postulates have different implications under greenhouse warming scenarios. For example, an ecotone formed primarily by differences in growth rates associated with temperature may respond linearly to changes in temperature, while an ecotone maintained primarily by winter snowpack may exhibit less predictable shifts in response to increasing temperature. In this analysis, I consider directly the effect of temperature, snowpack, radiation and moisture on seedling establishment and relative growth rates of trees.

Study Goals and Objectives

The primary goals of this study are twofold: (1) to better understand the mechanisms behind the spatial transition from *T. heterophylla* to *A. amabilis* communities, and (2) to develop general approaches to capture multi-scale environmental variability in montane ecosystems. These goals are tightly entwined in this dissertation and it is only through the latter that I am able to accomplish the former.

The dissertation is organized chronologically, in a sense, and represents a systematic approach to extending popular methods of community ecology to large spatial extents. The approach follows closely Levin's (1992) description of how to analyze ecological pattern with attention to scale: (1) describe pattern, (2) look for correlations with pattern to suggest potential mechanisms, and (3) improve understanding of pattern through careful examination of relationship with new 'mechanistic' variables. Though a true mechanistic understanding of ecological pattern may not be possible without experimentation (Platt 1964), I argue that well-designed observational studies can go a

long way towards disentangling the complex environmental gradients that are often invoked to explain ecological patterns.

I begin by developing a working model that delineates the major vegetation zones of the H.J. Andrews Experimental Forest, a Long Term Ecological Research site in the Oregon Western Cascades (Chapter 2). The model uses an efficient sampling design and a traditional community ecology approach to classify communities and ordinate them along common environmental surrogates. I complement the community analysis with partial regression techniques from landscape ecology in an attempt to quantify the relative importance of potential explanatory variables in a spatial context. Predictably, elevation and spatial location are identified as the strongest predictors of community composition. The results would constitute an end-product for many community studies, but I use them as a point of departure to suggest further studies. Specifically, I dissect the complex elevation gradient into its relevant environmental components and use the model to identify locations on the landscape for a focused study of the relationships between fine-scale environmental variability and demographic processes (Figure 1.1).

In the next part of the dissertation, I describe new empirical approaches to quantify the landscape-level distribution of environmental variables that likely are important controls of vegetation pattern, but were left out of the working model because of lack of data. These variables include radiation (Chapter 3.1), temperature (Chapter 3.2) and soil moisture (Chapter 3.3). I also include in this section a comparison of my empirical moisture model to models of greater and lesser complexity (Chapter 3.4). I emphasize the scaling of fine-grain environmental detail to large spatial extents in this

section, because without this information it would not be possible to extend relationships revealed in the subsequent section to the landscape level.

In the final part, I use the working model from Chapter 2 to identify sites of active community transition for a focused investigation of the effects of temperature, moisture, radiation and snowpack on establishment, growth and mortality at the *T. heterophylla*-*A. amabilis* ecotone (Chapter 4). Here, I show how forest demographics interact with the physical template in creating spatial pattern.

The study concludes (Chapter 5) with a summary of the findings and approach and a discussion of how the methods can be transferred easily to other montane systems. I revisit the working model armed with new information regarding the landscape-level distribution of physiologically important physical variables. I also address how demographic processes provide more valuable descriptions of forest community transitions than simple trends in the relative abundance of tree species. The specific results are applicable to the dynamics of transition at the most common forest-forest ecotone in the Oregon Western Cascades. The general approach, however, is more generic and this study may be viewed as a case study in ecology by iteration, whereby field samples are used to build models, which guide future sampling to answer new hypotheses and build better models.

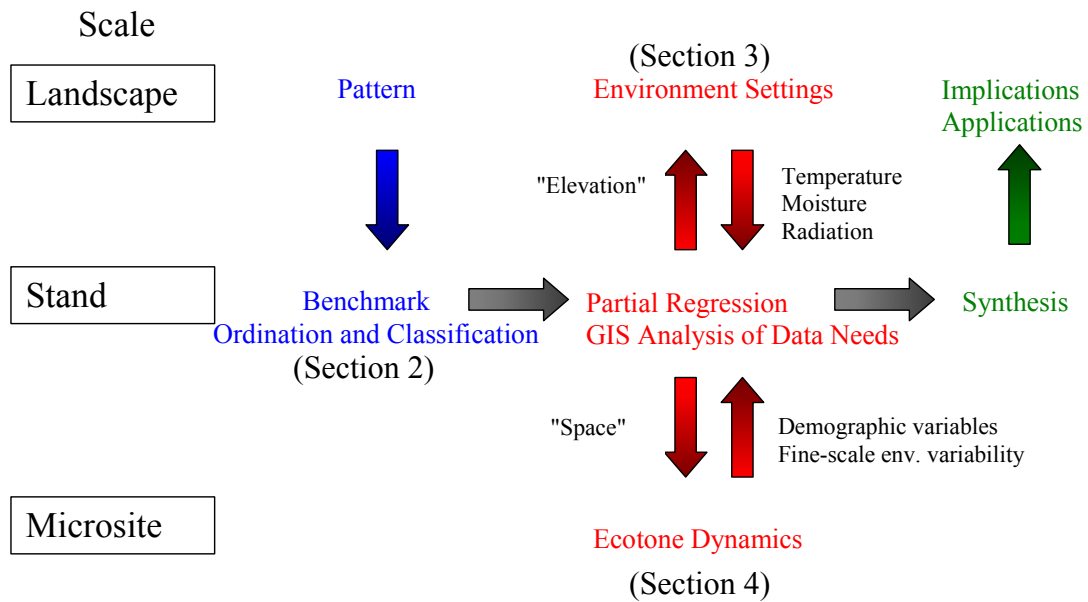


Figure 1.1. Schematic overview of research approach. The study follows an iterative process, alternating between field sampling and modeling, to explain community pattern at the landscape scale. First, I describe the current state of the system using measures of forest composition and common environmental proxy variables such as elevation, slope, aspect and soil attributes (Chapter 2). In the next phase, I replace the proxies with variables relevant to plant performance and examine how demographics such as growth, mortality and reproduction influence pattern. Hierarchical patch dynamics dictates that pattern at a given, focal level can be derived from constraints at higher levels and mechanisms at lower hierarchical levels (Urban et al. 1987, Wu & Luocks 1995). Here, I scale environmental variables down (Chapter 3) and scale biotic processes up (Chapter 4) to a common level of study.

SECTION 2: A PRELIMINARY MODEL

CHAPTER 2 A 3D Exploration of Landscape Pattern in the Oregon Cascades: Three Techniques Based on Ecological Dissimilarity

Abstract

Management of species and ecological communities requires a landscape perspective. Yet, information at these scales is sparse. Methods in community ecology have been applied to landscape extents with limited success. The most direct route to landscape ecology from community ecology (*i.e.*, do the same sorts of studies but over larger areas) does not admit that there are aspects of landscapes that call for different tactics in data collection, analysis, and modeling. Analytic techniques in classification, ordination, and spatial regression can be used in synthesis to identify broad scale patterns in forest communities. Tree abundance levels and common environmental variables on 164 plots were sampled in the western Oregon Cascades using a multi-scale stratified cluster sampling design. Spatial location significantly influenced observed species composition. Conventional community ecology methods ignore important spatial dependencies and, as a result, may overemphasize the importance of autocorrelated environmental variables. Elevation was highly correlated with the transition in basal area from *Tsuga heterophylla* to *Abies amabilis* community types, even after accounting for significant autocorrelation within the data. Results from studies that explicitly track spatial location can be mapped back into geographic space and used to identify new field locations for follow-up studies to test model uncertainties.

Keywords: classification analysis, ordination, Mantel test, Bray-Curtis, Classification and Regression Tree

Introduction

Analyses of community data rely heavily on techniques in classification and ordination to identify relationships between species composition and the environment. Patterns in species composition are typically described in terms of species groups. Classification analysis is a useful tool in uncovering these associations. A variety of classification techniques have been developed to relate compositional trends in vegetation to environmental variables, each with its own strengths and weaknesses (Sneath & Sokal 1973, Gauch & Whittaker 1981). Ordination techniques are well suited for examining continuous patterns on the landscape. The study of species responses to continuous environmental gradients also has a long history in community ecology (Shreve 1922, Whittaker 1956, Stephenson 1990). Temperature and moisture consistently emerge from these studies as proposed determinants of pattern. Because measuring gradients in these variables directly is often logistically impossible, factors such as elevation, slope, aspect and soil variables are frequently used as proximate measures.

Used together, ordination and classification can provide a broad interpretation of ecological pattern (Jongman et al. 1995, Legendre & Legendre 1998). This combination of complementary tools can describe discrete groupings of species along continuous environmental gradients. They do not account, however, for collinearities or spatial autocorrelation in the environmental data complex. Although tools exist that explicitly attend to the spatial structure of ecological data, community ecologists have not as a group embraced their use. By ignoring important spatial relationships, studies can overemphasize the importance of autocorrelated environmental variables (*e.g.*, elevation).

Ecologists can better interpret their results in a landscape context by thinking more explicitly about the spatial elements to their data. These analyses also can lead to new hypotheses about spatial processes not considered in more traditional studies of community pattern.

I present a synthetic approach to identifying potential natural communities in species distributions and associating these communities with environmental patterns in a spatial context. Specific objectives of the study include an investigation of the following questions.

- 1) Are species grouped into discrete clusters?
- 2) If so, what species indicate groups?
- 3) How do these groups map onto a continuous gradient?
- 4) How do patterns in the environment relate to patterns in species distributions?
- 5) How do spatial relationships confound plant-environment associations?
- 6) Are there significant spatial residuals in species composition that are not accounted for by commonly measured environmental variables?

Zobel et al. (1976) argued that topography is more important than soil differences in controlling vegetation in these forests. On a regional basis, Ohmann and Spies (1998) suggested that elevation and associated macroclimate are the major correlates with community composition throughout Oregon. My study reexamines these relationships in a spatially explicit context. I conclude with a discussion of the ecological significance of observed trends and a perspective on how to view the current results. The statistical

model created can be readily mapped back into geographic space and used to identify new field locations for follow-up studies to test model uncertainties. In a sense, gradient studies of this sort can be viewed as providing a framework within which to pursue a more refined understanding of species-environment relationships. What historically have been viewed as final, static models that describe ecological patterns can be recharacterized as preliminary, dynamic models that dictate where to proceed next.

Methods

Site description

The H.J. Andrews Experimental Forest (HJA) is located on the west slope of the Cascade Mountains. It is comprised of the Lookout Creek watershed, 80 km east of Eugene, Oregon. The Long Term Ecological Research (LTER) site covers 6400 ha and ranges in elevation from 410 m to 1630 m (McKee 1998). The watershed lies within the Blue River Adaptive Management Area, one of 10 such areas devoted to the development and evaluation of progressive management strategies for northwestern forests (Cissel et al. 1999). At the time of its establishment in 1948, the HJA was an intact forest with about 65 percent of the land in old-growth (*i.e.*, 400-500 years old). Since that time, old-growth forest has been reduced to 40 percent of the total area due to logging activities.

Climate is characteristic of the Pacific Northwest, with dry summers and wet winters. Annual precipitation ranges from 2200 mm at the base of the watershed to 3400 mm at upper elevations, with less than 300 mm normally falling during the summer growing season (Grier & Logan 1977). Soils are mostly deep, well-drained Inceptisols.

In the Western Cascades, soils are derived primarily from colluvial and residual parent materials. Andesitic, basaltic, and pyroclastic rock types are most common, but are mixed with some volcanic ejecta (Franklin 1965). Lower-elevation soils of the HJA are older than upper-elevation soils, dating back to the Oligocene-lower Miocene. Upper-elevation soils are composed of younger andesite lava flows and High Cascade rocks. Textures range from gravelly, silty clay loam to very gravelly, clay loam (Grier & Logan 1977). Rooting occurs almost entirely in the upper 200 cm of soil.

Pseudotsuga menziesii (Douglas-fir), *Tsuga heterophylla* (western hemlock), and *Thuja plicata* (western red cedar) are the dominant species at lower elevations, while *Abies amabilis* (Pacific silver fir), *Abies procera* (noble fir), and *Tsuga mertensiana* (mountain hemlock) dominate upper elevations (Franklin & Dyrness 1988). The seven species with the greatest basal area in the study plots were analyzed in this study (Figure 2.1). These species are tallied in Table 2.1. None of the other species recorded contributed as much as one percent to the total basal area observed in the sampling.

Data

The data for this study were collected over three years of sampling (1997-1999) in old-growth stands within the HJA. We collected georeferenced data on vegetation and site characteristics at 164 plots (Figure 2.2). Data were gathered using a stratified-cluster sampling design, whereby 20x20-m (0.04 ha) plots were clustered along transects across the landscape. Clusters consisted of three or four plots located at random distances (<100 m) and random azimuths from a cluster center-point on the transect (Figure 2.3). Cluster center-points were separated by 200 m to 400 m. Transects were separated by

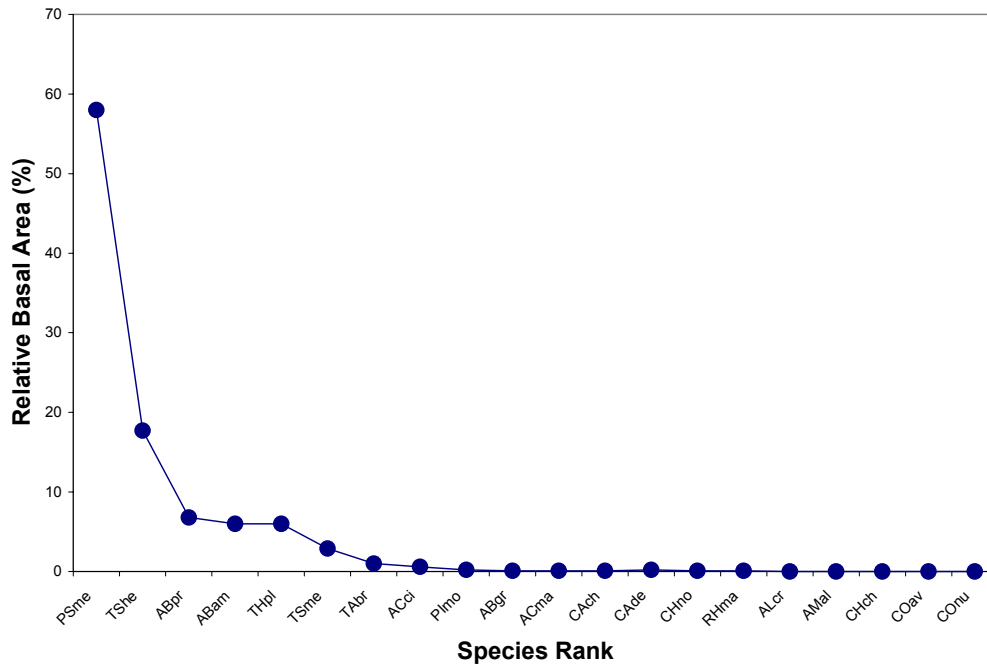


Figure 2.1. Dominance-diversity curve for 20 species sampled on 164 plots in the HJA. Species are ordered on the x-axis according to the percentage of total basal area contributed by that species. Species codes are provided in Table 2.1 for the seven species that contributed at least 1 percent to the total observed basal area on the plots.

Table 2.1. Seven dominant species observed on 164 plots in HJA, along with the frequency, mean density and mean, maximum and standard deviation basal area of each observed in the study.

Code	Scientific Name	Common Name	Frequency (%)	Density (#/ha)	BA (m ² /ha)		
					Mean	Max.	St. Dev.
ABAM	<i>Abies amabilis</i>	Pacific silver fir	42.7	173.6	5.2	57.9	10.7
ABPR	<i>Abies procera</i>	Noble fir	24.4	47.6	6.0	96.4	16.0
PSME	<i>Pseudotsuga menziesii</i>	Douglas fir	78.0	110.1	50.5	168.2	42.6
TABR	<i>Taxus brevifolia</i>	Pacific yew	40.9	58.4	0.9	13.3	2.2
THPL	<i>Thuja plicata</i>	Western redcedar	38.4	52.7	5.2	83.1	12.2
TSHE	<i>Tsuga heterophylla</i>	Western hemlock	82.9	231.4	15.5	71.0	16.6
TSME	<i>Tsuga mertensiana</i>	Mountain hemlock	13.4	42.2	2.6	107.8	12.1

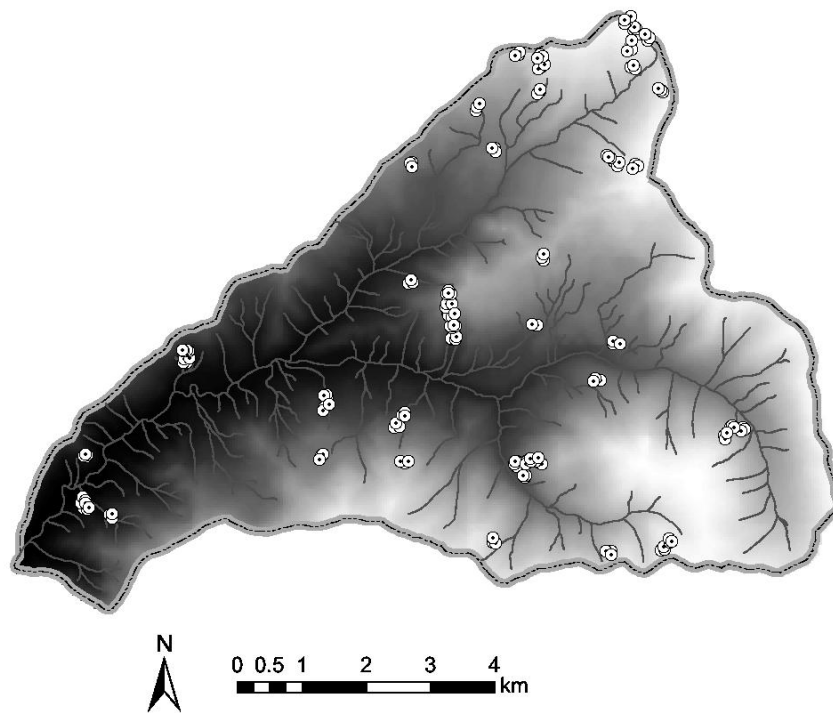


Figure 2.2. Locations of 164 sample plots in the HJA. Sampling of vegetation was conducted in old-growth stands, stratified across elevation, slope/aspect, and vegetation type. Shading indicates decreasing elevation with increasing shading. Elevation ranges from 410 m to 1630 m.

100s to 1000s of meters. The stratified cluster design integrates information across multiple scales, collecting the same data at the stand (plots), facet (clusters of plots), and landscape scales (transects). Stratified clusters have been shown to be more efficient at capturing fine-scaled pattern over large extents than either random or stratified random sampling (Urban et al. 2002). The diameter and species of all trees on the plots were recorded. Diameters were converted to basal area, which was summed for each of the species on each plot.

Topographic variables collected on the plots included slope, aspect, and slope in each of the four cardinal directions (Table 2.2). Aspect was transformed to a more direct measure of relative heat load on a scale of -1.0 (northeast-facing slopes with low afternoon radiation) to 1.0 (southwest-facing slopes with high afternoon radiation): $T_{\text{aspect}} = -\cos(45 - \text{Aspect})$ (after Beers et al. 1966). Percent slope measurements in each of the four cardinal directions were averaged to generate a Terrain Shape Index (TSI; McNab 1989), which ranged from -12.75 to 14 with positive numbers indicating coves and negative numbers indicating domes. Elevation was derived from GPS measurements and ranged from 485 m to 1567 m.

Information on the soils also was collected at the sites (Table 2.2). Three 10-m transects were marked on 1-m intervals in each of the plots. Soil depth was recorded with a tile probe at each 1-m interval to a maximum depth of 100 cm. A $\frac{3}{4}$ -inch soil probe was used to collect soil samples at a random location along each of the three transects. These samples were then air-dried and sieved for laboratory analysis of

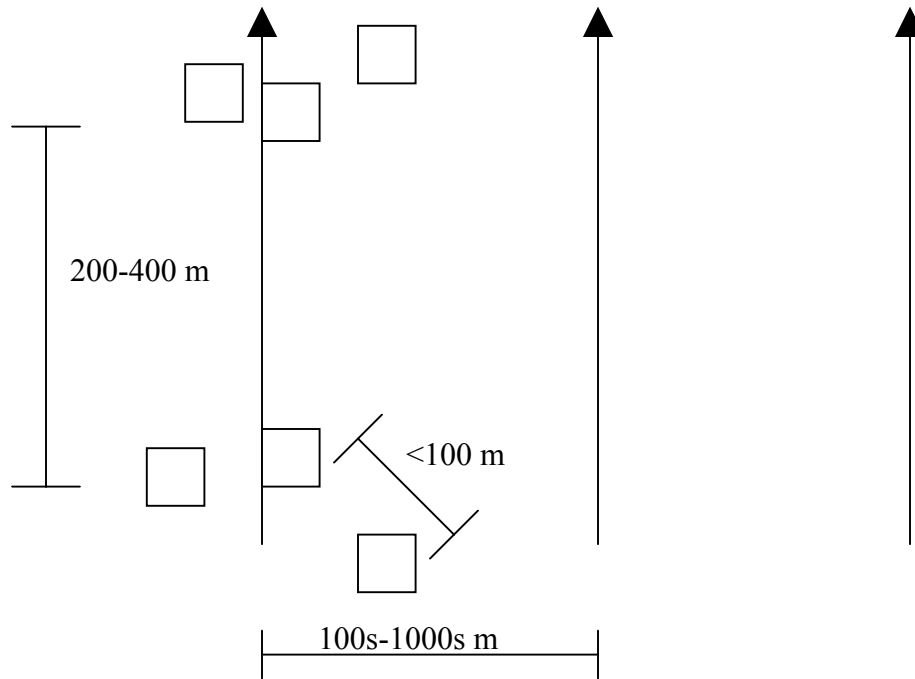


Figure 2.3. Stratified cluster sample design. Plots are clustered along transects across the landscape to capture variability at multiple scales.

Table 2.2. Summary of environmental variables collected on the 164 sample plots.

Name	Mean	Stand. Dev.	Minimum	Maximum
Elevation (m)	1018	284	485	1567
Slope (°)	26	10	0	50
TAspect	0.0	0.6	-1.0	1.0
TSI	-0.7	3.0	-12.8	14.0
Soil Depth (cm)	47.9	18.3	10.2	92.7
pH	4.59	0.25	3.79	5.18
Acidity (cmol(+)/kg)	1.73	1.45	0.2	8.24
Ca (cmol(+)/kg)	6.9	6.5	0.5	35.3
K (cmol(+)/kg)	0.54	0.35	0.14	2.37
Mg (cmol(+)/kg)	1.56	1.88	0.13	8.54
P (ug/g)	22.0	24.8	0.6	120.7
Clay (%)	5.1	3.1	0	18.9
Sand (%)	56.3	8.9	26.8	76.7
Silt (%)	38.6	7.3	21.2	55.8

exchangeable nutrient cations (Ca, Mg, P, and K), total exchangeable acidity, C, N, pH and texture (percent silt, sand, and clay).

Analysis

I used a combination of classification, ordination, and regression analyses to describe trends in community composition and environmental condition within these data (details follow in the sections below). All three of these analyses were based on the same Bray-Curtis dissimilarity index. A clustering analysis was conducted on the species abundance data to partition the data into discrete groups. Species that differentiate clusters were identified using Indicator Species Analysis (ISA). These clusters were mapped into ordination space using nonmetric multidimensional scaling (NMS). The environmental data matrix was examined by direct correlation analysis and principal components analysis (PCA). The relationship between species and the environment was examined through direct ordination with environmental overlays, Mantel regression, and classification and regression tree (CART) analysis. The multivariate statistical software package PC-ORD version 4.09 (McCune & Mefford 1999) was used to conduct all clustering and ordination analyses. S-PLUS 2000 (1999) was used for the CART analysis and Mantel tests with the RPART (Therneau and Atkinson 1997) and Mantel (Urban et al. 2002) S-PLUS libraries.

Bray-Curtis dissimilarity index

“Ecological distance” is expressed as the dissimilarity (1 - similarity) between sample units. A large number of indices have been developed to quantify dissimilarity (see Legendre & Legendre 1998 for a comprehensive discussion of potential dissimilarity indices). When species abundance data are being considered, these indices must account for the common finding of shared absence, which ecologically is not equivalent to a finding of shared presence. In this analysis, I make use of the Bray-Curtis index (Bray & Curtis 1957) as a measure of dissimilarity for all analyses of species abundance patterns. The Bray-Curtis distance matrix is a Sorensen index computed on quantitative data such as species abundance as:

$$d_{ij} = \frac{\sum_{k=1}^s |y_{ik} - y_{jk}|}{\sum_{k=1}^s (y_{ik} + y_{jk})} \quad (\text{eqn. 2.1})$$

where d_{ij} is the ecological distance between samples i and j , y_{ik} is the abundance of species k on sample i , y_{jk} is the abundance of species k on sample j , and there are s species included in the analysis.

The Bray-Curtis index is commonly preferred over other indices such as Jaccard's for species abundance data because it retains its sensitivity in more heterogeneous data sets and gives less weight to outliers (McCune & Grace 2002). Measured as percent dissimilarity, the index provides ecological distance between samples as elements of a data matrix. The resulting matrix can be used as input in a variety of multivariate statistical analyses that can be applied to interpret forest community patterns. These

include the common community ecology tools of classification and ordination (Whittaker 1967, Fasham 1977, Gauch et al. 1981). The matrix also can be used in a Mantel regression framework to quantify the ability of different environmental variables to explain patterns in species dissimilarity (Leduc et al. 1992). Within this framework it is possible to compare the matrix of ecological distance to a matrix of simple Euclidean distance that measures the absolute distance in space between sample pairs. The resulting analysis allows spatial dependencies in the data to be considered explicitly, a practice too often ignored in community analyses but central to the field of landscape ecology.

The dissimilarity index is an integral component of the analytic method described below. The clustering analysis uses the Bray-Curtis index to identify compositional groups in a data set. NMS uses the dissimilarity matrix to map samples into ordination space, preserving the ecological distance among samples. The Mantel analysis uses the matrix to quantify the relative importance of environmental variables to species composition in a spatial context.

Biotic patterns/species associations

Clustering analyses are used to identify natural breaks or groups in a data set (Sneath & Sokal 1973). Clustering analyses are highly dependent upon the choice of distance measure used to assess group similarity and the linkage criteria used to determine the distance between groups for joining purposes (Legendre & Legendre 1998). Multiple joining criteria were considered for this analysis. Ultimately, unweighted pair-group method, arithmetic (UPGMA) was chosen (Sneath & Sokal 1973). UPGMA averages all distances equally for all possible groups. This approach resulted in the

lowest amount of chaining (5.6 percent). Chaining, the sequential addition of small groups to a few large groups, can cause difficulties in defining subgroups (McCune & Grace 2002).

Since groups are defined at multiple levels in hierarchical clustering algorithms, choosing the level of clustering is an important decision. Indicator Species Analysis (ISA) was used as a test of the appropriate level of clustering (Dufrene & Legendre 1997). Indicator values combine information on species relative abundance and relative frequency in different groups. Relative abundance is calculated as the average abundance of a species in a given group of plots divided by the average abundance of that species in all plots. Relative frequency is calculated as the percentage of plots in a given group where a species is present. Indicator values range from 0 to a maximum of 100 for a perfect indicator. In addition to identifying key species for groups, ISA can be used to decide the appropriate number of groups for species data. Indicator values will be low for poorly defined clusters and typically peak at an intermediate level of clustering (Dufrene & Legendre 1997).

Ordination is the ordering of objects (*e.g.*, species or plots) along axes to emphasize underlying trends in the data (McCune & Grace 2002). The objective is to orient the objects in such a way that proximity in ordination space resembles proximity in ecological space. Ordination techniques can be direct or indirect. In direct ordination, objects are organized with respect to some ancillary variable, such as elevation. Indirect ordination does not require ancillary data to orient objects in ordination space; objects are oriented based solely on internal associations within the species data matrix.

I rely on nonmetric multidimensional scaling (NMS; Kruskal 1964) as an indirect ordination technique to describe relationships among species. NMS uses a dissimilarity measure of ecological distance, here the Bray-Curtis index, to map objects into ordination space, preserving the ecological distance among objects. Because objects are oriented along all axes simultaneously, the solution is dependent upon the number of axes used. The number of axes to include in an analysis can be selected by plotting the stress (a “badness of fit” metric associated with reducing the dimensionality of the dissimilarity matrix) for model runs of decreasing dimensionality. The final solution should include the minimum number of axes that do not result in large jumps in model stress.

NMS is preferred over other conventional ordination methods because it has no underlying assumption regarding the distribution of input variables. Other techniques commonly must assume that input variables are unimodally distributed with similar maxima, an assumption frequently violated by environmental data (Legendre & Legendre 1998). NMS also is particularly good at finding groups or disjunctions in species data when they exist.

Environmental patterns

A simple correlation matrix can be used to describe the relationship among environmental factors. This measure of association focuses on the pairwise relationships among variables. Although the assumption of linear relationships required of this analysis is frequently violated by environmental data (Legendre & Legendre 1998), relationships found through alternative techniques can be easily supported or discredited by examining this correlation matrix.

Principle components analysis (PCA; Goodall 1954) is perhaps the most popular technique used to analyze multivariate patterns among environmental variables. PCA reduces the dimensionality of multivariate data by focusing on the correlations among variables. The data are rotated in principal component space to align the first axis with the longest possible vector of the data cloud. The second axis is the longest vector orthogonal to the first principal component; the third axis is the longest vector orthogonal to the first two and so on. Because there is so much correlation in environmental data, this rotation can result in a huge compression of information on relatively few principal components. I conducted a PCA on a correlation matrix of the environmental data to determine major trends in the environmental data.

Species-environment interactions

Direct ordination with suspected environmental determinants of pattern remains one of the most effective analytic techniques for deciphering relationships between species and the environment. Since elevation is frequently referenced as a major correlate with pattern (Franklin & Dyrness 1988, Ohmann & Spies 1998), I present species abundances as a direct ordination of elevation. Using the sample elevation scores as weights, I calculate the average position of each of the species along the elevation axis. This weighted average score provides a straightforward and powerful summary of species response to elevation, reducing the entire distribution of a species across a gradient to a single value (Jongman et al. 1995).

The correlation of variables is classically tested using parametric tests, such as Pearson's product-moment correlation. These tests require all the usual assumptions of

parametric tests, including the independence of data observations. Specifically, this assumption of independence is frequently violated by autocorrelated environmental variables related to climate, topography and soils (Legendre & Fortin 1989, Fortin & Gurevitch 1993). To isolate specific explanatory variables in a spatial context, Legendre & Fortin (1989) proposed the use of simple and partial Mantel tests. The Mantel test (Mantel 1967) is a nonparametric linear regression technique applied to distance (or dissimilarity) matrices representing geostatistical data. The test overcomes the lack of independence problem by computing significance through permutation of the data. To permute the data, matrices are generated that can be rearranged for successive iterations of the calculation of the statistic. Partial Mantel tests assess the explanatory power of variables after controlling for other factors.

The simple Mantel test is based on a comparison of two distance matrices describing the same set of sampling stations (Legendre & Fortin 1989). It can be used to assess the explanatory power of predictor variables singly. Spatial location is naturally represented by a distance matrix. For ecological data, indices of dissimilarity such as the Bray-Curtis index can be used for analysis at the community level (Leduc et al. 1992). At the single species level, similarity in abundance can be used to compute ecological distance.

Partial Mantel tests can be used to compute the correlation of two distance matrices while controlling for the effect of other predictor variables (Smouse et al. 1986). The simple Mantel test estimates how much of the dissimilarity in one variable (*e.g.*, species composition) can be explained by dissimilarity in a second variable (*e.g.*, spatial

location or environmental variability). The residuals of such a regression can be analyzed further following a multiple regression model, to get partial correlations. This approach is particularly useful to account for the spatial structuring of environmental data. Partial correlation analysis can help to isolate the pure partial effect of specific environmental variables that may be collinear and autocorrelated (Leduc et al. 1992). The partial Mantel test also can be used to determine how much of the dissimilarity in species data is determined purely by spatial context.

I conducted Mantel tests at two levels of abstraction: (1) a community level analysis comparing the influence of spatial relationships to that of environmental variability, and (2) an analysis of the influence of specific environmental variables on overall community composition and on specific species. The first series of tests addresses the questions: *Are samples that are environmentally similar also similar with regards to species composition?* and *Are samples that are close in space similar in species composition?* The second set of tests address the questions: *Which environmental variables are most associated with overall changes in community composition?* and *Which environmental variables are most associated with the distributions of individual species of interest?*

The species, environmental, and geographic distance data were synthesized into three matrices for Mantel analysis. All environmental variables (Table 2.2) were standardized using z-scores and combined into a single environmental matrix. Relative basal areas of the main tree species (Table 2.1) were standardized using a Wisconsin double relativization (McCune & Grace 2002) and combined into a single species matrix.

With these two synthetic matrices and a matrix of geographic distance for the 164 plots, I conducted the community-level analyses. I expected both space and environmental variability to influence species composition. To estimate the pure influence of the environment on species composition, I conducted a partial Mantel test on the species and environmental data, controlling for space. I also ran Mantel tests on overall community composition and on individual species with the environmental variables separately to determine the relative contribution of each to overall community pattern. By controlling for environmental variability and conducting a partial Mantel test on species and geographic space, I tested for residuals in the data that could be explained purely by spatial context. Biological processes (*e.g.*, seed dispersal), disturbance, or unquantified environmental variability could cause such unexplained pure spatial correlations.

The information from the Mantel tests was used to construct path diagrams. Legendre & Trousselier (1988) show how significant results from partial matrix association tests can be interpreted as indicating “causal” relationships. Mantel statistics were used to highlight significant causal relationships between species distributions, explanatory environmental variables, and space.

To determine how key environmental variables influence the species clusters, I also created a classification tree of the species groups using the environmental data as predictor variables. Classification and regression tree (CART) analysis is a divisive analysis that attempts to partition a data set by recursively dividing it into subsets based on the strongest predictor variable (Breimann et al. 1984). The technique offers several advantages over the regression approach. It allows the distribution of multiple categories

of data to be considered simultaneously. The interpretation of the tree is rather intuitive and can be easily converted to a geographic information system context for visualization of the results (Moore et al. 1991). The data structure allows for the incorporation of substitution and compensatory relationships. The hierarchical structure of the model allows the data to be partitioned at multiple levels of complexity. Because each branch of the tree is defined independent of other branches and the decision rules rely on no assumptions regarding the underlying model structure, CART allows a data set to be classified with great accuracy.

Unfortunately, the high degree of accuracy in CART analysis can result in an over-fitting of the models to most ecological data sets (Legendre & Legendre 1998). The resulting tree will explain the input data extremely well, but can be too specific to those data to be generalized to broader patterns. To account for this tendency to over-fit, I used cross-validations of one-tenth of the entire data set to prune the tree. The effect of this cross-validation was to penalize trees that over-fit the data. Classification accuracy was determined from an average of the 10 cross-validated trees. The final tree was trimmed to eliminate branches that caused an increase in the average misclassification rate. I also conducted a validation of the final tree with 11 independent samples that were collected in 2002. These samples were targeted to be in areas of the watershed deemed most difficult to classify by the models.

Results

Species associations

ISA found a weak natural break in the groupings derived from the cluster analysis (Figure 2.4). The maximum indicator values (IVs) averaged across all seven species peaked at 68 percent for the four-cluster solution. Further partitioning of the data resulted in a lower mean IV. *A. amabilis*, *P. menziesii*, and *T. heterophylla* were the primary indicators for the two-cluster solution. *T. heterophylla* and *P. menziesii* were associated with one cluster, while *A. amabilis* was associated with the second (Figure 2.5). The four-cluster solution partitioned the *A. amabilis* cluster into additional groups. By eight clusters, all species were associated with separate groups. Species associations for the four-cluster solution (*i.e.*, the solution with the highest average IVs) are provided in Table 2.3.

The species clusters can be interpreted in the context of ordination space (Figure 2.6). Because NMS proceeds from the same Bray-Curtis distance matrix as the clustering analysis, it provides a compatible analysis in an interpretable space. The step-down NMS procedure recommended a three-axis solution as optimal (stress = 12.3). The final solution of the three-axis analysis suggested that one of the axes was considerably stronger than the other two. The cumulative coefficient of determination (R^2) for the correlation between ordination distance and distance in the original n-dimensional space was 0.9 for the three axes combined. The r^2 for axis one was 0.52 while axis three, the next strongest axis, had an r^2 value of 0.24.

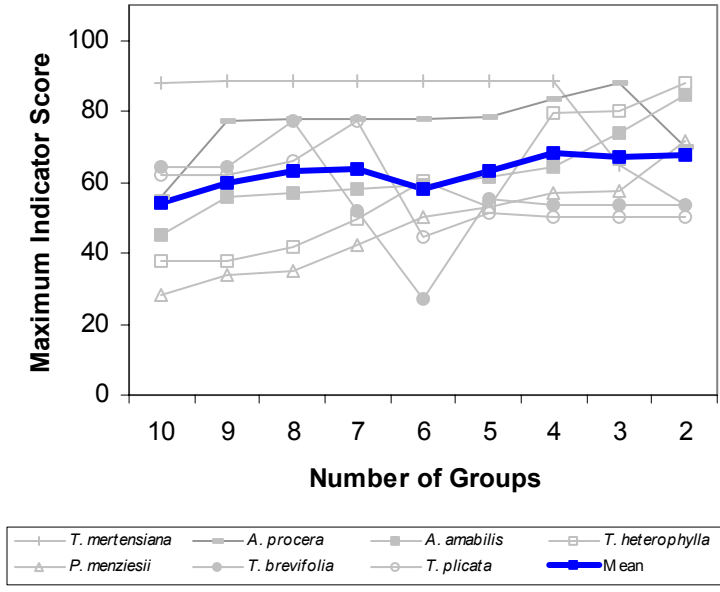


Figure 2.4. Maximum indicator values recorded for each of the 7 dominant species by successive ISAs. Grouping the data into four clusters resulted in the highest indicator values. Groups were determined by a clustering analysis on species abundance data.

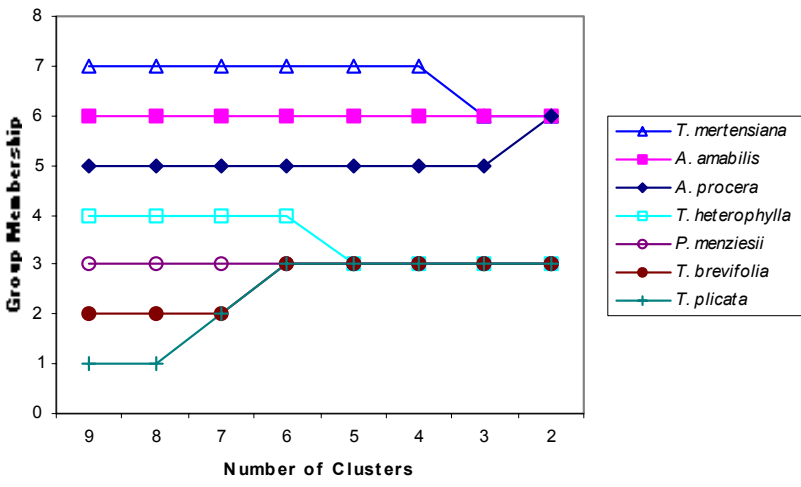


Figure 2.5. Group membership of species in clusters. Species were assigned to the group for which they had the largest indicator value. The four-cluster solution was used throughout most of this study.

Table 2.3. Group membership assignment for four-cluster solution based on species abundance data. Species were assigned to the group for which they had the largest indicator value.

Group	Cluster on Species Abundance	Indicator Value
1	<i>T. heterophylla</i>	80
	<i>P. menziesii</i>	57
	<i>T. brevifolia</i>	54
	<i>T. plicata</i>	50
2	<i>A. amabilis</i>	64
3	<i>A. procera</i>	84
4	<i>T. mertensiana</i>	89
Mean		68

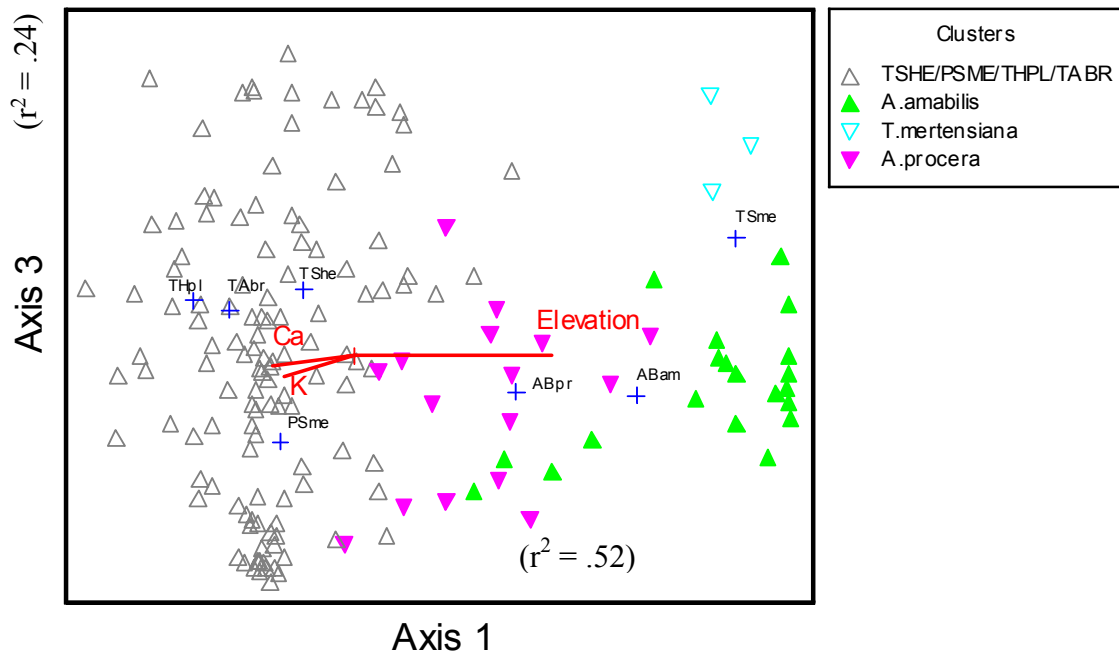


Figure 2.6. Clustered sample plots projected into NMS space. Two-dimensional projection of three-dimensional space showing only the two strongest axes. Different symbols represent four clusters based on species abundance data. The length of the vectors for the environmental variables represents the strength of correlation with the ordination axes. See Table 2.1 for species codes.

The species loadings along axis one ranged from a maximum of 0.6 for *T. plicata* to a minimum of -1.5 for *T. mertensiana* (Table 2.4). *A. amabilis* had the strongest correlation with axis one ($r = 0.79$), followed by *P. menziesii* ($r = -0.50$).

Environmental patterns

The cations were all strongly correlated with each other and with pH (Table 2.5). Total P was the least strongly correlated with the other cation variables. Total acidity was negatively correlated with pH as expected, but also positively correlated with soil depth. C and N were strongly correlated with each other, positively correlated with silt, and negatively correlated with the cation concentrations. Elevation was significantly correlated with slope and all the soil variables. Elevation was not significantly correlated with transformed aspect or TSI.

The PCA corroborated that the environmental variables were correlated among themselves. The correlation of variables allowed for substantial reduction in the dimensionality of the data. Thirty-five percent of the total variance of the environmental data matrix could be explained by the first principal component alone. An additional 19 percent was explained by the second axis. Hence, over 50 percent of the information content of the environmental matrix could be represented in two-dimensional space by PCA. The first axis was strongly correlated with elevation ($r = 0.69$) and negatively correlated with several of the cations (*i.e.*, Ca, Mg and K all with r values < -0.88). The second axis was most strongly correlated with acidity ($r = 0.83$) and soil depth ($r = 0.76$). Weaker negative correlations were found between axis two and pH, slope, and P ($r = -0.49$, -0.38 , and -0.36 , respectively).

Table 2.4. Species loadings on NMS axes and direct elevation axis. The order on axis 1 from highest to lowest corresponds closely to a gradient from low to high elevation, as shown by a comparison to the weighted average species scores on elevation.

	Axis 1	Axis 2	Axis 3	WA
<i>T. plicata</i>	0.63	-0.10	0.28	853
<i>T. brevifolia</i>	0.49	-0.30	0.24	848
<i>P. menziesii</i>	0.29	-0.22	-0.28	925
<i>T. heterophylla</i>	0.20	-0.32	0.33	923
<i>A. procera</i>	-0.64	0.94	-0.08	1383
<i>A. amabilis</i>	-1.11	0.20	-0.09	1330
<i>T. mertensiana</i>	-1.51	0.54	0.53	1484

Table 2.5. Correlation matrix for environmental variables. Bold Pearson product moment correlation coefficients are significant at $P < 0.0001$ level. Correlations not significant at the $P = 0.05$ level are not shown.

	Elev	Slope	TAsp	TSI	Depth	pH	Acid	Ca	K	Mg	P	C	N	Clay	Sand	Silt	
Elevation	1.00																
Slope	-0.14	1.00															
TAspect			1.00														
TSI				1.00													
Xdepth	-0.23	-0.23		0.20	1.00												
pH	-0.22	0.25	0.26			1.00											
Acidity	-0.21					0.40	-0.50	1.00									
Ca	-0.52	0.34	0.16				0.54	1.00									
K	-0.59	0.27			0.18	0.40		0.80	1.00								
Mg	-0.55	0.28			0.31	0.41	0.23	0.90	0.76	1.00							
P	-0.35	0.20			-0.31	0.25	-0.16	0.50	0.45	0.30	1.00						
C	0.66	0.33			-0.32	-0.31		-0.22	-0.28	-0.37		1.00					
N	0.66	0.28			-0.24	-0.24		-0.19	-0.24	-0.31		0.95	1.00				
Clay	-0.53	-0.32	-0.21		0.34		0.50	0.25	0.24	0.27		-0.36	-0.32	1.00			
Sand		0.22	0.34		-0.32	0.22	-0.45					0.38	-0.22	-0.30	-0.65	1.00	
Silt	0.26		-0.33		0.24	-0.21	0.33					-0.42	0.42	0.50	0.37	-0.95	1.00

Species-environment Interactions

Of the topographic variables measured, elevation showed the clearest associations with the species data via simple correlation analyses (Table 2.6). Elevation was highly correlated with five of the seven species abundances (absolute r -values > 0.30). As expected, species described by Zobel et al. (1976) as high elevation species were positively correlated with elevation; low elevation species were negatively correlated with elevation. Weaker correlations between *T. plicata*, *T. brevifolia*, and elevation were due to nonlinearities in these relationships. Few significant correlations were observed between the other topographic variables and species abundances. *T. plicata* was negatively correlated with slope; *T. brevifolia* was negatively correlated with TSI; *A. procera* was positively correlated with transformed aspect.

Of the soil variables, carbon and nitrogen trends were the most consistent. The high elevation species were positively correlated with carbon and nitrogen levels, negatively correlated with cation concentrations, and positively correlated with silt. The low elevation species were negatively correlated with carbon, nitrogen and silt levels. *P. menziesii* abundance was positively associated with cation concentrations, while the rest of the low elevation species were not significantly correlated with the cations.

Overlaying the environmental vectors on the NMS ordination corroborated that elevation and the concentration of cations were highly related to patterns of species composition (Figure 2.6). Elevation was the environmental variable most associated with the first axis ($r = 0.75$), followed by Ca, K, Mg and P ($r < -0.4$ for all the cations).

Table 2.6. Correlations between species abundance levels (m²/ha) and environmental variables. Values are Pearson product moment correlation coefficients (*r*). Correlations that are not significant (*P* > 0.05) are not shown. Values are bolded for *P* < 0.0001. See Table 2.1 for species codes.

	THPL	TABR	PSME	TSHE	ABPR	ABAM	TSME
Elevation	-0.30	-0.25	-0.39	-0.31	0.48	0.54	0.35
Slope	-0.16						
TAspect					0.20		
TSI		-0.27					
xDepth				0.19			
pH			0.26	-0.23		-0.24	
Acidity	0.16			0.23			
Ca			0.33		-0.24	-0.38	-0.17
K			0.41		-0.22	-0.35	-0.17
Mg			0.23		-0.22	-0.32	
C	-0.22	-0.26	-0.25	-0.22	0.34	0.36	
N	-0.23	-0.26	-0.26	-0.25	0.38	0.35	
P			0.38		-0.24	-0.29	-0.16
Clay	0.19					-0.23	
Sand		0.22	0.19		-0.20	-0.17	
Silt		-0.27	-0.26	-0.22	0.30	0.31	

Environmental correlations with the second strongest axis were much weaker (no correlation coefficients had absolute r -values > 0.3).

Direct ordination with elevation indicated a transition in the composition of dominant tree species at elevations from 1150 m to 1350 m (Figure 2.7). No *T. plicata* were observed above 1100 m in elevation. The relative basal area of *P. menziesii* and *T. heterophylla* also declined sharply around this altitude. *A. amabilis* increased in dominance in this transition zone. *A. procera* were not observed below 1100 m and *T. mertensiana* were not observed below 1350 m. Table 2.4 presents the weighted average species scores on elevation.

At the community level, the three simple Mantel tests (above the diagonal in Table 2.7) on community composition, geographic space, and the grouped environmental data all provided significant results at the $P = 0.05$ level (in every case, significance tests were based on 1000 permutations). Both space and environmental variability were significantly correlated with species composition, and environmental variability and species composition were both significantly autocorrelated according to these tests. The partial Mantel tests (below the diagonal in Table 2.7) provided significant pure partial associations between species composition and environmental variability, but not between species composition and space. This finding suggests spatial location is not a significant influence on community composition after accounting for the spatial component of environmental variability. Figure 2.8 provides a path diagram of the relationship between these three variables derived from the simple and partial Mantel statistics. Environmental variability is significantly associated with community composition by both the simple

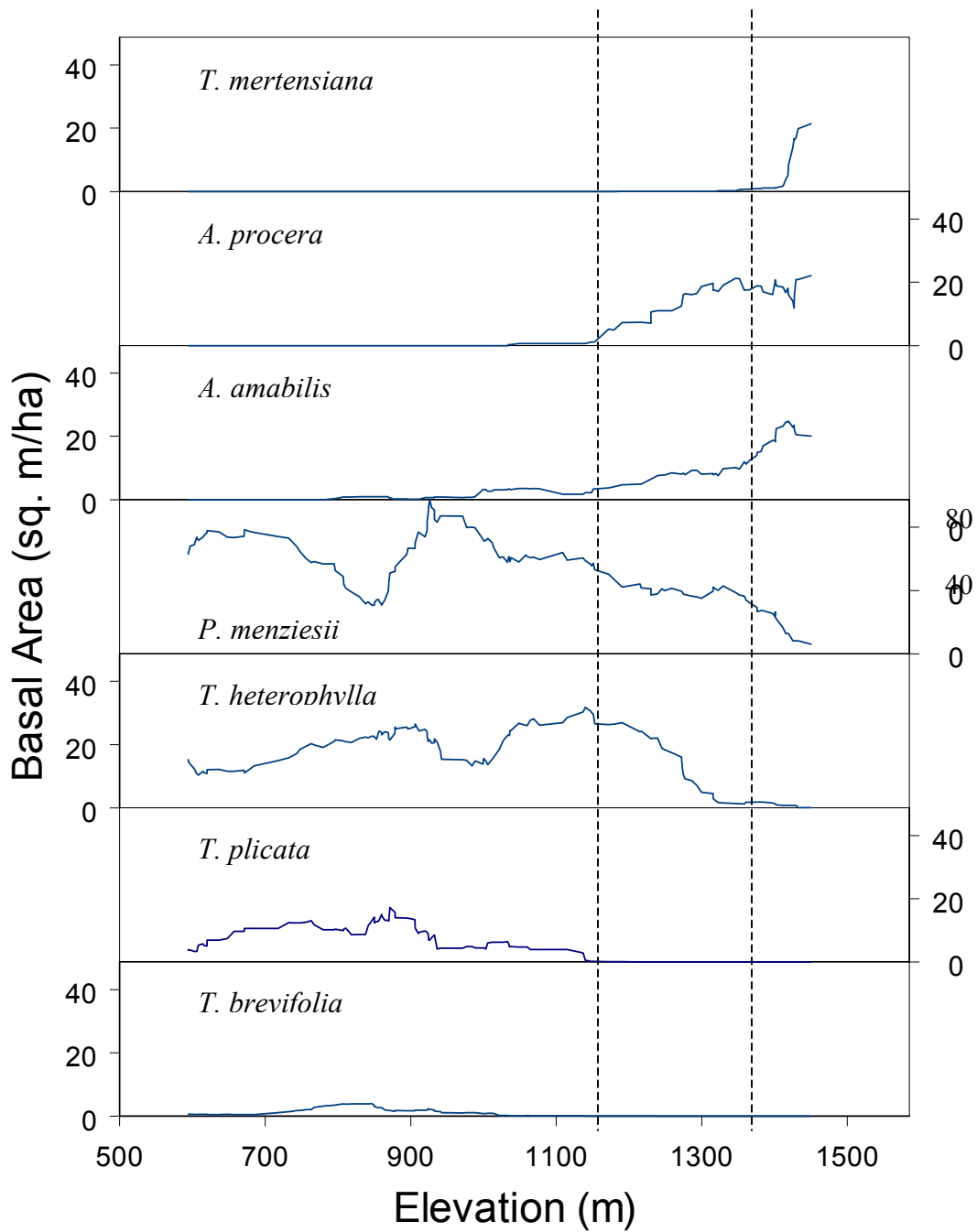


Figure 2.7. Direct ordination of basal area of dominant species on elevation. Lines represent twenty-point moving averages. Vertical dotted lines represent the proposed transition zone.

Table 2.7. Mantel coefficients for aggregated analysis. Values in table are Mantel correlation statistics (r) and P -values from a one-tailed test of significance. Results of simple Mantel tests are reported above the diagonal. Results of partial Mantel tests are below the diagonal.

	Community Composition	Environment	Space
Community Composition	----	0.38 $P = 0.001$	0.18 $P = 0.001$
Environment	0.35 $P = 0.001$	----	0.14 $P = 0.001$
Geographic Space	n.s.	----	----

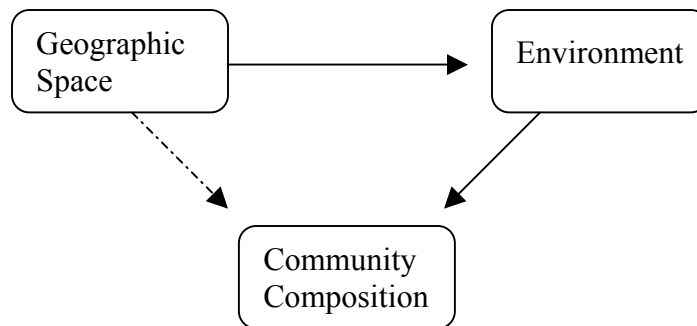


Figure 2.8. Mantel path diagram for aggregated variables. Solid lines represent causal factors (significant partial Mantel value; $P = 0.05$). Dotted line represents spurious relationship (significant simple Mantel value but nonsignificant partial Mantel value; $P = 0.05$).

and partial Mantel tests. This relationship is considered causal. Space is significantly associated with community composition by the simple Mantel test but not the partial test. This relationship is considered spurious, with space related to community composition only through environmental variability.

When considering the environmental variables individually, the Mantel tests confirmed that community composition was significantly correlated with elevation (Figure 2.9). The high elevation species (*A. amabilis*, *A. procera*, and *T. merteniiana*) showed the strongest correlation. *P. menziesii* and *T. plicata* were significantly correlated with elevation only after removing the effects of pure spatial influences. None of the other environmental variables analyzed had significant correlations with the species data.

Community composition, the distribution of the high elevations species, and the distribution of *T. heterophylla* all were found to be autocorrelated by the simple Mantel tests. Only *A. amabilis* was significantly correlated with space, however, after accounting for variation in elevation via partial Mantel tests. Elevation and aspect also were strongly autocorrelated. The other variables did not have strong spatial structure. The results are summarized in a schematic path diagram in which projected causal relationships between variables are shown by solid arrows (Figure 2.9).

The CART analysis indicated that elevation, transformed aspect, and K concentration were the environmental variables that most strongly sort the four species clusters (Figure 2.10). Elevation was the strongest predictor variable, separating the *T. heterophylla*/*P. menziesii* community from the high elevation species at the first branch

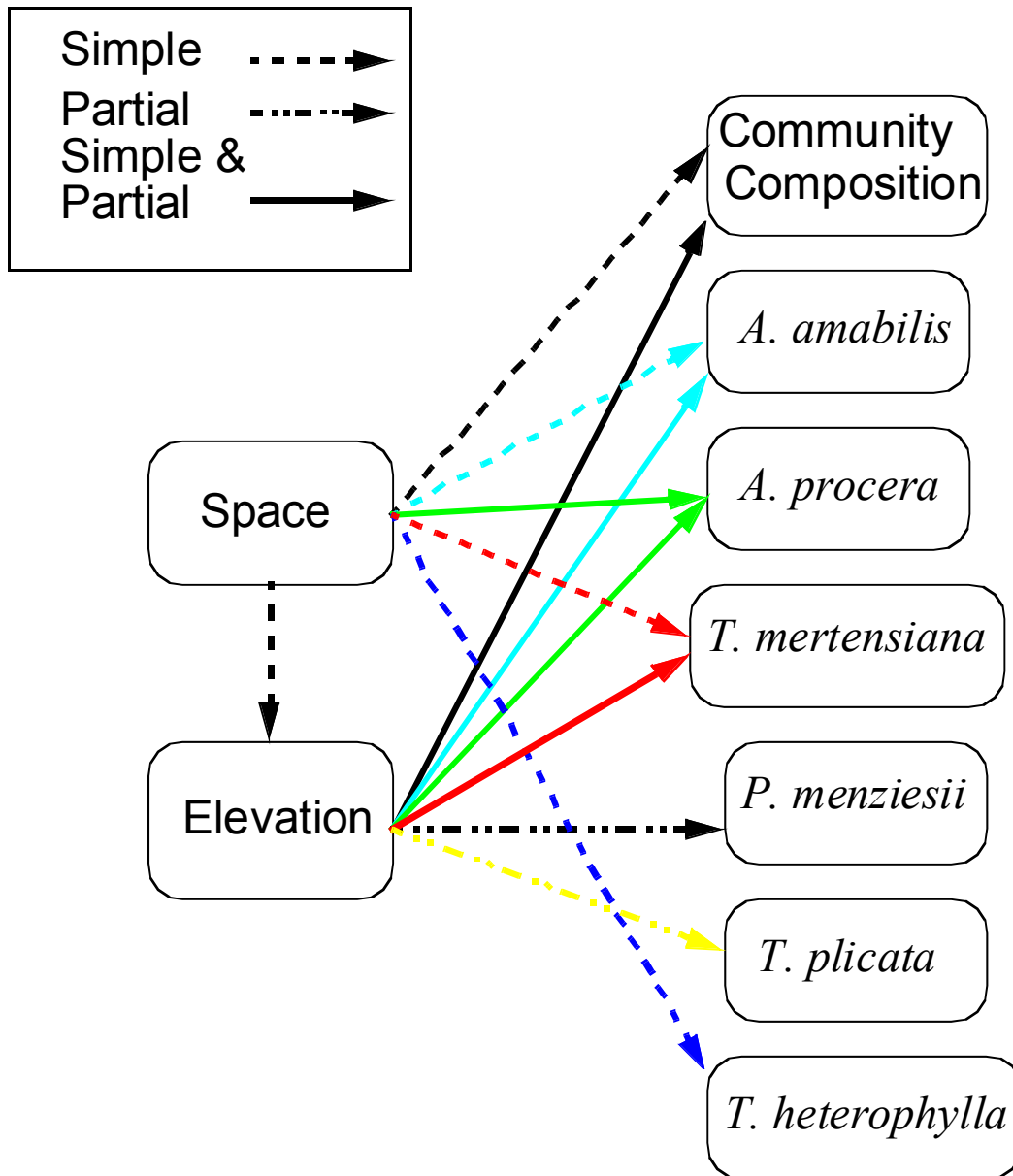


Figure 2.9. Mantel path diagram for individual variables. Arrows indicate significant correlations at the $P = 0.05$ level. *T. brevifolia* was not significantly autocorrelated or correlated with elevation and is not shown. None of the other environmental variables analyzed had significant correlations with the species data.

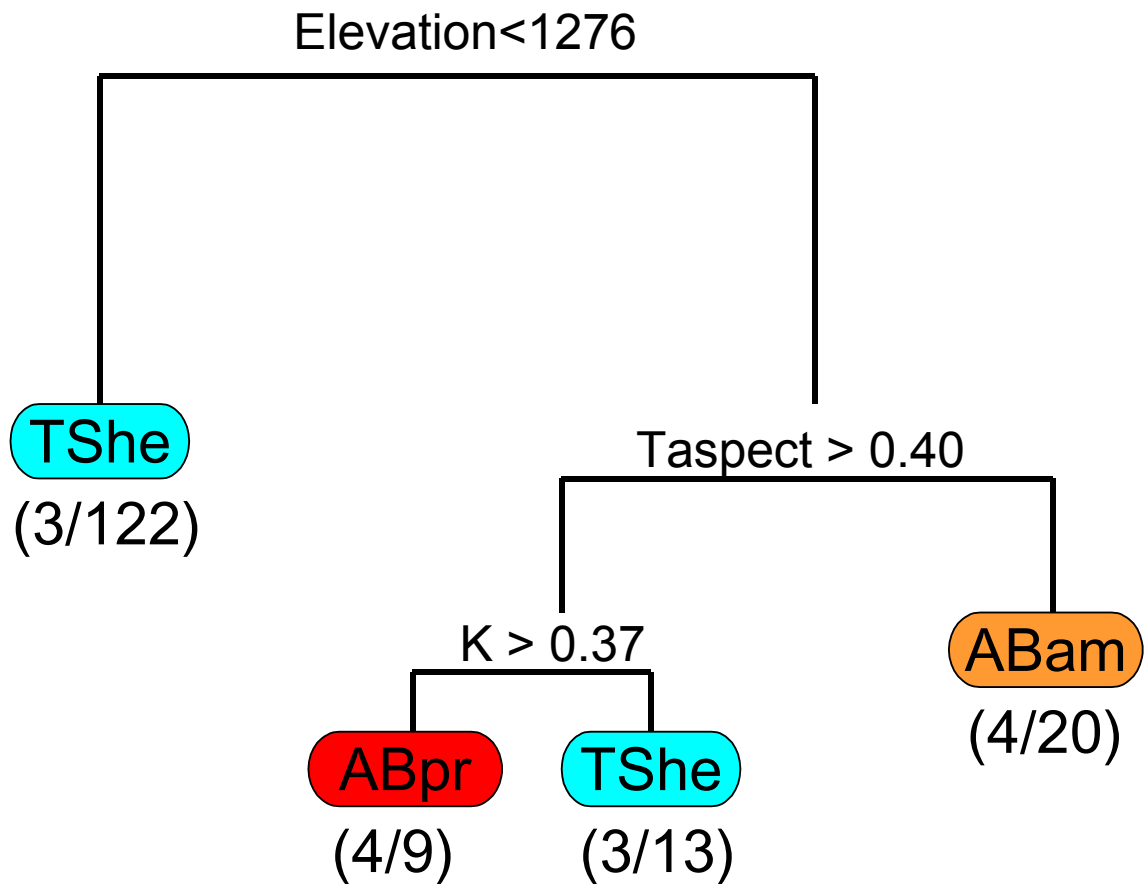


Figure 2.10. Classification tree from CART analysis. Groups were determined by a clustering analysis on species abundance data and are designated on the tree by the species with the highest indicator value in the group. Species codes are provided in Table 2.1. Parentheses at terminal nodes provide the misclassification errors as number misclassified / total N in node.

of the tree. Misclassification rates provide a measure of the ability of the model to discriminate among groups. Total misclassification in the tree was 8.5 percent. The highest misclassification rate was between the *T. heterophylla* and *A. procera* communities at high elevations.

Four of the 11 validation plots were misclassified by this classification scheme: two plots dominated by *T. mertensiana*, one *A. procera* plot that was misclassified as *T. heterophylla*, and one *T. heterophylla* plot that was misclassified as *A. procera*. When I reran the analysis including these 11 plots with the original 164, a *T. mertensiana* end-node was identified at elevations greater than 1450 m. The most effective variable at discriminating between *A. procera* and *T. heterophylla* in this revised analysis also switched from K concentration to pH.

Discussion

Species patterns

Species do appear to sort into discrete communities within the watershed. The four major communities can be described as follows.

- *T. mertensiana* group: indicated by *T. mertensiana* with *A. amabilis* also present but in lower abundance. No other dominants common.
- *A. amabilis* group: dominated by *A. amabilis* with *T. mertensiana* and *A. procera* often represented.

- *A. procera* group: indicated by *A. procera* with some *A. amabilis* and *P. menziesii*. Small abundances of *T. heterophylla* also commonly observed.
- *T. heterophylla*/*P. menziesii* group: characterized by *T. heterophylla* and *P. menziesii*. *T. plicata* and *T. brevifolia* present about 50 percent of the time. The latter two species are never found in the other three communities.

The level at which the different species separate into distinct clusters gives some indication of their similarity (Figure 2.5). According to the species clustering analysis, *T. plicata* and *T. brevifolia* have the most similar affinities. Both are more similar to *P. menziesii* in distribution than to *T. heterophylla*. All of these species have stronger community ties than do the three other dominant species in the HJA. The environmental data can be examined further to gain an understanding about which factors might be associated with the differences in composition.

Traditional gradient analysis approach

Both topographic and soil features can affect species distributions (Cole 1990, Davis & Goetz 1990). I have collected information on both types of environmental variables in hopes of attaining a more complete understanding of the observed species patterns in the HJA watershed.

The NMS analysis indicates that elevation may be the primary correlate with the two species communities. The first axis alone explains over 50 percent of the variance in the data and elevation is the environmental variable most associated with this axis. The species loadings along this first axis are in nearly the same order as the weighted average

species scores from the direct ordination with elevation. These findings are consistent with the simple correlation coefficients between the species and environmental variables and they conform to the general community trends described for the Pacific Northwest (Franklin & Dyrness 1988, Ohmann & Spies 1998).

Other environmental variables might contribute to the observed species distributions. Both the NMS environmental overlays and the PCA analysis suggest that cation concentration in the soil might be negatively associated with the primary axis. This is supported by the inverse correlation between elevation and the cations observed in the simple correlation tests. The higher order axes in the ordinations provide additional insight into what might be important in partitioning species within elevation zones. The PCA suggests that pH, acidity, and soil depth might be important environmental variables that are orthogonal to elevation.

The CART analysis provides testable hypotheses regarding what might be differentiating these species. It provides corroborating evidence that the main communities are separated along the elevation gradient, with the transition occurring around 1275 m. Although soil chemistry differences (K or pH) might explain some of the observed partitioning at high elevations, topographic effects appear to be the primary determinant of the observed pattern. Additional sampling at contrasting topographic locations within the elevation of the transition zone could further refine the model.

Extending community ecology to landscapes

Techniques derived from landscape ecology complement these traditional analyses of forest communities. Specifically, spatial sampling and analysis methods can support community analyses to provide the following:

- Increased understanding of the importance of scale,
- Synoptic coverages of large extents,
- Greater resolution of physical variables, and
- Explicit studies of spatial processes.

Here, I provide two examples of how spatial relationships (“space”) can be considered in landscape studies of community pattern. First, sampling designs should carefully consider the multi-scale variability inherent in ecological data. Both community composition and environmental variables can vary at scales of 10s to 1000s of meters (Urban et al. 2000). It is important for field samples to capture these variances in order to relate biotic and abiotic patterns. Stratified clusters are one example of the family of sampling schemes that are specifically designed to measure multi-scale trends over large spatial extents (see Nusser 1998 and Urban 2002 for additional examples).

Second, analytic methods can be employed that account for spatial relationships in the ecological data. I present an example of how “space” can have a significant impact on the interpretation of species-environment relationships by including spatial separation distance explicitly as a variable in Mantel analyses. The effect of including space was to reduce the significance of the relationship with elevation for some species (all species

combined, *A. amabilis* and *A. procera*) and strengthen the observed relationship for other species (*P. menziesii* and *T. plicata*). Differences in space also were correlated with the overall species patterns and with several of the individual species (*A. amabilis*, *A. procera* and *T. mertensiana*) via the simple Mantel tests. Fortin and Jacquez (2000) list four potential sources of spatial autocorrelation. The first two, spurious and interpolation autocorrelation, are considered artifacts of sampling and analytic methods. True (arising from causal interactions among close samples) and induced autocorrelation (arising from a causal relationship with another spatially autocorrelated variable) stem from ecological processes of direct scientific interest. These cannot be removed by improved sampling and analytic methods, and suggest potential effects of unmeasured environmental variability and/or the presence of spatial biological or physical processes. The fact that several of the species had significant simple Mantel coefficients but not significant partial Mantel coefficients suggests that some of the observed autocorrelation might be spurious, but enough significant spatial relationships remain to warrant further study of the causes of these relationships.

Conclusion

This study contributes to the large body of gradient analysis studies by explicitly considering spatial location and scale in both the sampling and analysis phases. Although the analyses suggest relationships between species and the environment, no general theory has been developed to explain the relationships via causative mechanism. The results, therefore, should be viewed as an initial phase in the investigation of forest community pattern in the HJA. They are unsatisfying in at least two important ways:

- Elevation, the strongest environmental correlate even after accounting for spatial autocorrelation, is not directly relevant to plants, and
- The significance of spatial location in the analyses indicates biologic processes or environmental factors not represented in the basal area data.

The remainder of this dissertation addresses these issues by attempting to incorporate more plant-relevant explanatory variables and focusing on biologic processes such as growth and regeneration rather than sheer abundance. In essence, I replace elevation and basal area with more meaningful environmental and biotic data.

None of the techniques offered here offer an unambiguous description of the pure effects of environmental factors on species' distributions. In fact, no single technique currently available to ecologists can offer this output (Griffith 1992). In combination, however, this blend of multi-scaled field samples and statistical tools provides a clearer picture of community patterns in the HJA. Of equal importance, the results highlight specific locations on the landscape for future sampling and ecological hypotheses that should be addressed next to bring this picture into sharper focus.

SECTION 3: THE PHYSICAL SETTING

CHAPTER 3.1 A Simple Method for Estimating Potential Relative Radiation (PRR) for Landscape-Scale Vegetation Analysis

Abstract

Radiation is one of the primary influences on vegetation composition and productivity. Topographic orientation is often used as a proxy for relative radiation load due to its effects on evaporative demand and local temperature. Common methods for incorporating this information (*i.e.*, site measures of slope and aspect) fail to include daily or annual changes in solar orientation and shading effects from local topography. As a result, these static measures do not incorporate the level of spatial and temporal heterogeneity required to examine vegetation patterns at the landscape level. We developed a widely applicable method for estimating potential relative radiation (PRR) using digital elevation data and a common geographic information system (Arc/Info). We found significant differences among four increasingly comprehensive radiation proxies. Our GIS-based proxy compared well with estimates from a more data-intensive and computationally rigorous radiation model. We note that several recent studies have not found strong correlations between vegetation pattern and landscape-scale differences in radiation. We suggest that these findings may be due to the use of proxies that were not accurately capturing variability in radiation, and we recommend PRR for use in future vegetation analyses.

Keywords: aspect, DEM, GIS, proxy variables, relative radiation, slope, topography, vegetation analysis

Introduction

Plants respond to solar radiation through multiple pathways (Geiger 1965). Photosynthetically active radiation (PAR) provides the driving energy for photosynthesis (Raven et al. 1992). Radiation influences ambient temperature and, consequently, the rates of photosynthesis and respiration (Kozlowski et al. 1991). Radiation affects the water supply (*e.g.*, ground surface evaporation; Brady & Weil 1999) as well as the water demand (potential evapotranspiration) components of the water balance (Stephenson 1998), and has been shown to have a significant effect on the distribution of surface water through simulation modeling (Vertessy et al. 1990, Band 1991) and empirical sampling (Yeakley et al. 1998, Chapter 3.3). These multiple influences can result in complex responses to radiation loads. For example, high radiation leads to the ability to convert large amounts of carbon to sugar while simultaneously decreasing soil moisture levels. The strong association between radiation and plant processes has been reported to shape the landscape-scale distribution of plants in numerous studies (Davis & Goetz 1990, Urban et al. 2000), but others, somewhat surprisingly, have not been able to document a strong correlation between radiation estimates and plant pattern (Brown 1994, Parker 1995, Park 2001).

Direct measurements of radiation are uncommon and these are especially rare in topographically rugged terrain (most meteorological stations are on level ground at low elevations). Acquiring fine-scale information about climatic factors over large extents is logistically problematic. This has led to many attempts to find alternatives to actual measurements of solar radiation. There are two common approaches to account for

radiation effects over landscape scales. The simpler approach relies on static topographic proxies based on slope and aspect, either from field measurements or from digital terrain data (*e.g.*, Beers et al. 1966). A more complicated approach involves numerical integration of radiation values through simulation modeling using terrain and climate data (Running et al. 1987, Daly et al. 1994, Thornton et al. 1997).

Here we offer a third alternative: a physical proxy that captures some of the solar geometry of more complicated radiation models yet can be quickly implemented for any landscape with digital terrain data. This level of detail should correspond with the data needs of a growing number of ecologists who are interested in landscape-scale vegetation analysis.

The geometry of radiation

The amount of radiation impinging on a surface is the sum of three components: direct, diffuse and reflected radiation. Direct-sky radiation is the fraction of extra-atmospheric solar radiation that reaches the earth's surface without being scattered by molecules in the atmosphere (Figure 3.1.1a). Diffuse-beam radiation is the component resulting from atmospheric scattering. Reflected radiation bounces off other surfaces before impinging on a target (Campbell & Norman 1999).

Under clear sky conditions, direct radiation is largely a function of the geometry between the earth surface and the sun. Topography acts as a filter on radiation loads in two important ways: (1) through shading effects and (2) through attenuation of the solar flux by altering the apparent solar inclination angle. The position of the sun in relation to

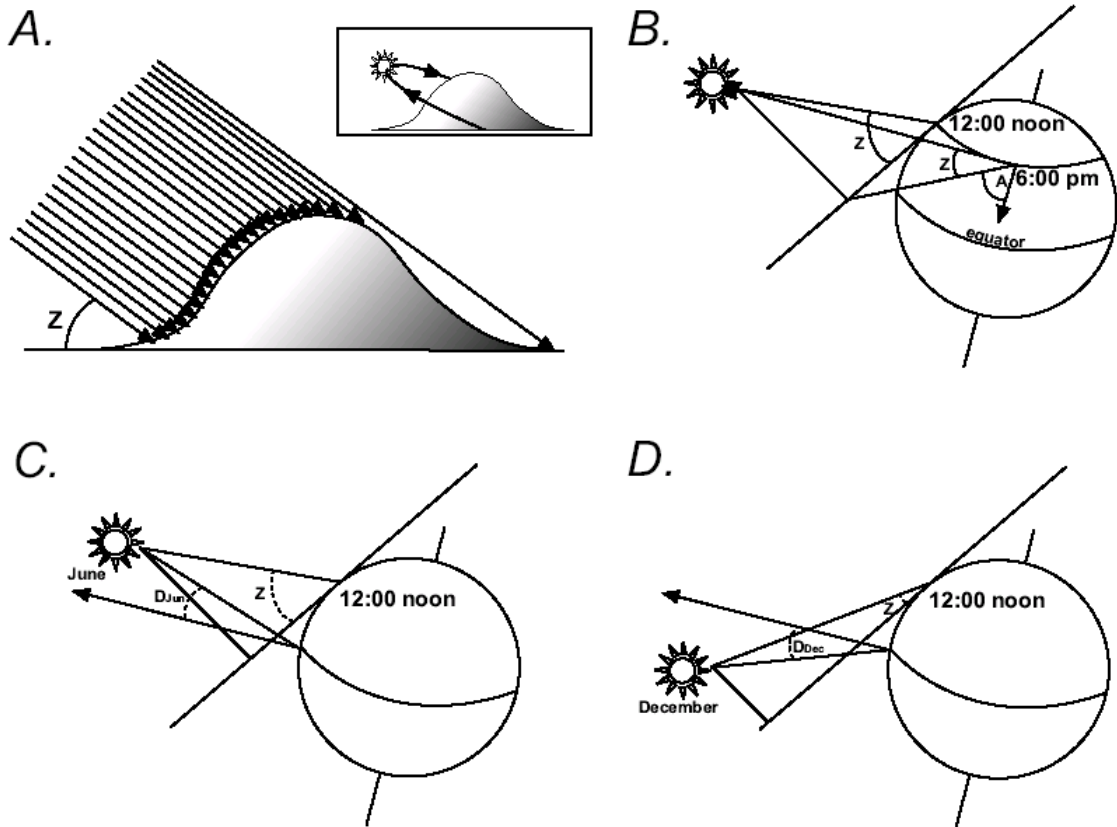


Figure 3.1.1. (A) Solar azimuth and inclination create a topographic shading effect. (B) This shading is continuously shifting as the earth rotates causing changes in solar inclination and azimuth. The change in the orientation of the earth's tilt in relation to the sun creates the basis for our seasons. The lower two panels depict the apparent solar zenith for the same location during the summer (C) and winter (D) solstices. (after Bonan 2002)

the earth is well understood. The orientation between a slope and the sun's position therefore can be calculated with a high degree of precision given position and time.

This relationship is not static. The relative position of the sun changes through the course of the day and year. The rotation of the earth causes the daily solar orientation to change, affecting irradiance and shading (Figure 3.1.1a-b). The tilt and orbit of the earth causes an annual change in the topographic orientation of a site in relation to the sun, affecting the solar zenith (Z), the highest daily inclination angle, and solar period (Figure 3.1.1c-d). The complexity of topography and the changing orientation of the sun create a dynamic but important problem for estimating radiation loads across landscapes. Too often this complexity is ignored in simple radiation proxies.

Diffuse and reflected radiation are more difficult to quantify, and are not addressed in this study. In general, these components tend to minimize spatial differences in radiation. Under clear sky conditions, the largest share of radiation is direct-beam. This condition provides the maximum contrast in radiation load between sites with different topographic orientations. As the partitioning of radiation shifts from direct to diffuse with increasing cloud cover, sites are affected similarly and the relative differences between sites are reduced. Calculating a measure of potential direct radiation thus provides an upper bound on differences in solar insolation.

Radiation proxies

Slope and aspect have been used as radiation proxies in hundreds of studies because, until recently, they have been the easiest way to estimate relative radiation without extensive direct sampling or complex computer programming.

Early gradient analysis studies categorized topographic aspects as factors along a moisture continuum (*e.g.*, Whittaker 1956). Frank & Lee (1966) standardized these discrete relationships between relative radiation and slope and aspect in tables that accounted for latitudinal differences. These tables were based on a 16-quadrant measure of aspect and are still in use today (Parker 1995, McCay et al. 1997, Donnegan & Rebertus 1999). As categorical factors, however, slope and aspect have a limited ability to capture the full range of topographic variability. With too few factor levels, there is a loss in precision; and with too many levels, between-level contrasts become diluted. The 16-quadrant model has been used in several studies in similar southeastern forests with varying results (Day & Monk 1974, Clinton et al. 1994, McCay et al. 1997, Bolstad et al. 1998).

Representing aspect as a continuous rather than discrete variable is complicated by the discontinuity at due north where the measure repeats itself going from 360 to 0. Transformations can be used to remove the discontinuity by reorienting the variable along a specified axis. These require a specific orientation of interest to be defined, such as a north-south axis. One common approach is to use “absolute aspect” computed as $ABS(180 - \text{aspect})$, which solves the circularity problem while aligning the index on a N-S axis. Beers et al. (1966) transformed aspect along an axis running from NE to SW to reflect the combined influence of bright illumination with warm afternoon temperatures maximally affecting SW-facing slopes. Beers transformation indexes radiation explicitly as a proxy for heat load or evaporative demand. Depending on the landscape, choosing an *a priori* transformation axis might bias results.

The relationship between aspect and radiation is modified by local slope. The proper way to incorporate slope is to use the solar angle, which is the difference between the normal vector from the slope surface and the vector pointing towards the sun, a value that changes throughout the day and year (Dozier & Frew 1990). Sine or cosine transformations of the local slope angle often are used as a surrogate measure.

McCune and Dylan (2002) recently described an approach for incorporating topographic effects on radiation (N-S axis) and heat load (NE-SW axis) through fitted linear regression equations. Using stepwise linear regression with slope, latitude, and folded (*i.e.*, transformed) aspect as explanatory variables, they were able to explain potential direct incident radiation differences as tabulated in common lookup tables (Buffo et al. 1972) with R^2 values > 0.95 . Though convenient in their simplicity, these equations might not be adequate for many applications in complex terrain for at least two reasons: (1) they do not account for variation through time and (2) they do not account for shading by adjacent topography.

Radiation levels vary through time in several ways that are not captured by simple topographic proxies. For instance, east-facing slopes experience higher radiation loads in morning hours, while west-facing slopes experience higher radiation in later afternoon hours. This effect also changes with the time of year. Solar period shortens in accordance with decreasing solar inclination. Therefore, incorporation of daily and annual solar path is essential when comparing solar exposure between two sites.

Even with proper consideration, slope and aspect alone might not be able to resolve radiation differences between sites. The proxies by necessity imply that observed

slopes are in a landscape devoid of other features (*i.e.*, isolated mountains or hills). But obstructions to direct-beam radiation can result from not only “self-shading” by the slope itself, but also from shading by nearby ridges. Two sites with identical topographic orientation (slope, aspect and elevation) can have widely differing solar exposure based on their topographic context. For example, sites could differ by being at the bottom of a drainage or the top of a nearby ridge but be characterized similarly by simple measures of slope and aspect. Radiation proxies, as well as many radiation models, do not incorporate shading effects from adjacent land features.

Radiation models

The relative permanence of topography and the deterministic position of the sun make assessing direct relative solar exposure a simple matter of calculation, depending only on latitude, time, slope orientation, and topographic context. This geometry serves to attenuate direct-beam radiation by decreasing the solar angle from perpendicular to the surface to some smaller angle and thereby increasing the cross-sectional area illuminated by a quantum of radiant energy. To estimate radiation quantitatively involves the addition of the diffuse and reflected components. Thus, direct-beam, diffuse-beam and reflected radiation can be estimated as:

$$R_b = R_{ea} * t^m \quad \text{(eqn. 3.1.1)}$$

$$R_d = 0.3 (1 - t^m) R_{ea} \cos(Z) \quad \text{(eqn. 3.1.2)}$$

$$R_r = r (R_b + R_d). \quad \text{(eqn. 3.1.3)}$$

Direct-beam radiation (R_b) is extra-atmospheric radiation (R_{ea}) attenuated by atmospheric transmittance (t) and modified by the optical air mass number (m). Transmittance is largely a function of climate and necessitates estimating daily relative humidity and cloudiness. The optical air mass number is a function of atmospheric pressure and latitude. Latitude is important because it is used to calculate the path length through the atmosphere. The longer the path length the more molecules a beam may encounter in order to become scattered.

Diffuse-beam radiation (R_d) is the fraction of radiation scattered by air molecules and aerosols and then attenuated by the solar zenith angle (Z):

$$\cos(Z) = \sin(L) * \sin(D) + \cos(L) * \cos(D) * \cos(15 (T-T_0)) \quad (\text{eqn. 3.1.4})$$

where L is latitude, T is the time of day, and T_0 is the longitude corrected base time or zero. Solar declination (D), the angle between the Sun and a position directly above the earth's surface, accounts for the tilt of the earth. It depends only on time (Julian day J) and can be estimated for each day of the year as:

$$\sin(D) = 0.3978 \sin[279.0 + 0.9856 J + 1.9165 \sin(356.6+0.9856 J)] \quad (\text{eqn. 3.1.5})$$

Reflected radiation (R_r) is the sum of the direct and diffuse components multiplied by the average local surface reflectivity (r) [see Campbell & Norman 1998 or Bonan 2002 for a more detailed accounting of these components].

The radiation calculations as described above are for a flat surface perpendicular to the direct-beam radiation. Radiation is modified by local topography using tilt factors and view angles. First, the R_b is multiplied by the cosine of the solar azimuth (A), the

angle between the normal vector to the surface and the vector directed towards the sun's current position.

$$\cos(A) = -[(\sin(D) - \cos(Z) * \sin(L)) / [\cos(L) * \sin(Z)]] \quad (\text{eqn. 3.1.6})$$

The R_d is then modified by taking into account the proportion of the sky visible from the point of estimation (*i.e.*, the angular percentage of the hemispherical view). This is a small fraction in a deep chasm and close to one on a large flat plain.

Atmospheric scientists have used these calculations to develop sophisticated models for predicting solar radiation in complex terrain (Bonan 1989, Dozier & Frew 1990, Nikolov & Zeller 1992, Dubayah & Rich 1995, Greenland 1996, Wilson & Gallant 2000). Running these models requires considerable site data or the acquisition of special programs. For instance, SRAD requires up to 16 parameters to calculate a radiation map (Wilson & Gallant 2000). Our method uses the common geographic information system Arc/Info (ESRI 1994) to produce a spatially explicit representation of variation in radiation and is widely applicable with minimal investment in time or resources.

In summary, most existing proxies are insufficient for use in landscape-scale ecological studies because they do not account for changes in solar orientation and/or do not account for topographic shading. More sophisticated radiation models do have the capability to account for these factors, but at a cost of decreasing simplicity for the user. Our goal in calculating a new radiation proxy was to develop a dimensionless index to support community vegetation analysis. Decades of gradient studies have found primary "elevation" gradients with small-scale topography and soils playing a secondary role in structuring plant communities (Whittaker 1960, Dyrness et al. 1974, Kessell 1979). We

were interested in the way local topography influences relative radiation load and thus evaporative demand. Previous studies suggest that this might be an important mechanism controlling vegetation distributions (Callaway et al. 1987, Franklin et al. 2000, Mackey et al. 2000). For these applied uses, we felt a new method of estimating relative radiation was needed that incorporated the important components of more complicated models but the ease of calculation of simple proxies. We present here what we believe to be such an approach.

Methods

Study site

We demonstrate our approach for one of our study sites of complex topography. The H.J. Andrews Experimental Forest (HJA) is located on the west slope of the Cascade Mountains. It is comprised of the Lookout Creek watershed, 80 km east of Eugene, Oregon. The Long Term Ecological Research (LTER) site covers 6400 ha and ranges in elevation from 410 m to 1630 m (McKee 1998). Climate is characteristic of the Pacific Northwest, with dry summers and wet winters. Annual precipitation ranges from 2200 mm at the base station to 3400 mm at upper elevations, with less than 300 mm normally falling during the summer growing season (Grier & Logan 1977). Major vegetation types range from *Pseudotsuga menziesii* (Douglas-fir), *Tsuga heterophylla* (western hemlock), and *Thuja plicata* (western red cedar) at lower elevations to *Abies amabilis* (Pacific silver fir), *Abies procera* (noble fir) and *Tsuga mertensiana* (mountain hemlock) at upper elevations (Franklin & Dyrness 1988). The LTER's research emphasis includes the

effects of climate on vegetation pattern and we have been actively involved in this research.

Potential relative radiation (PRR)

To account for temporal variability in radiation, we developed potential relative radiation (PRR) as an integrative index, which sums hourly estimates of radiation over the day and then sums daily grids over the summer growing season. Each point estimate accounts for topographic shading by surrounding landscape features. The method can be summarized as follows.

1. Calculate solar declination and solar azimuth for daylight hours for the day of the month representing the average solar period for each month of the growing season (equations 3.1.5 and 3.1.6; these data are also available on many websites).
2. Obtain a digital elevation model (DEM) of the study site (USGS).
3. Calculate hourly hillshaded radiation grids using DEM, solar azimuth and solar declination (Arc/Info HILLSHADE function with MODEL SHADOWS option).
4. Sum hourly grids to get daily totals, which represent monthly averages.
5. Sum monthly averages to get seasonal maps of PRR.

The approach is outlined in greater detail below.

There are many sources for finding solar azimuth and declination for a specific location and time of day. Since solar path changes in a continuous manner throughout the year we decided to use a single day from each month to represent that period (Klein 1977, Bonan 1988). We chose the day of the month that was closest to the average solar period for that month. This was not always the 15th of the month, but depended on the

trajectory of the solar period for the month (*e.g.*, we choose June 11 to represent the average solar period for June). Solar position can be calculated using equations 3.1.5 and 3.1.6. These values also can be obtained by supplying the locations, dates and times desired to several commonly available sources of solar calculation such as Image Processing Workbench (Frew 1990) and several web sites. These sources all provide the same data with slight formatting differences.

We obtained a digital elevation model (DEM) for our study site from the USGS, being careful to incorporate enough surrounding area to properly capture topographic shading. We imported the DEM into Arc/Info and used our solar position information with the HILLSHADE function,

$$HS = 255 [\cos(90-D) \sin(s) \cos(\alpha-A) + \sin(90-D) \cos(s)] \quad (\text{eqn 3.1.7})$$

where D is the solar declination, s is the local slope, A is the solar azimuth and α is the azimuth of the slope facet (ESRI 1994).¹ This function calculates relative reflectance based on surface orientation, solar position, and self-shading by calculating the angle between the vector normal to the plane of ground and solar position (ESRI 1994). We used the MODEL SHADOWS option to set areas shaded by surrounding topographic features to zero illumination. We performed this operation for each hour of daylight on the representative day of each month from March to September. To calculate monthly radiation maps we summed over the hourly grids. To calculate relative seasonal radiation maps we summed the monthly grids. The index, therefore, can be summarized as:

$$PRR = \Sigma \Sigma (\text{monthly, hourly (HS)}). \quad (\text{eqn. 3.1.8})$$

¹ HILLSHADE uses the solar inclination angle, which is the complement of declination (90-D).

Other radiation proxies

To compare the variation captured by our method to other common indices we calculated three other radiation proxies. Two were derived both from field measurements and from DEM-based calculations. The first proxy was a simple measure of transformed aspect (Urban et al. 2000) similar to Beers et al.'s (1966) measure but varying from -1 for NE facing slopes to 1 for southwest facing slopes:

$$TA = -1 * \cos(\alpha - 45) \quad (\text{eqn. 3.1.9})$$

The second proxy incorporated slope information by multiplying TA by the sine of the slope angle:

$$TASL = -1 * \cos(\alpha - 45) * \sin(s) \quad (\text{eqn. 3.1.10})$$

We analyzed both DEM and field-based indices for these proxies to determine how well the digital data corresponded to on-the-ground measurements. We had topographic information from 175 (20x20 m) plots, which we used for the field calculations. We compared estimates from the DEM-based proxies for these same 175 plots.

The third radiation proxy we considered was a single HILLSHADE map. This proxy accounted for the effect of topographic shading without considering solar track. HILLSHADE requires the user to supply an azimuth and solar inclination angle (eqn. 3.1.7). We used a solar azimuth of 225 degrees and solar inclination of 45 degrees to mirror our TA calculation.

Because we are interested in radiation as a relative variable in community ecology studies, not as an absolute variable in an atmospheric model, we did not correct insolation for atmospheric transmittance. We also ignore the effect of cloudiness. For landscape-scale vegetation analyses dealing with small-to-medium sized watersheds in mountainous regions, relative radiation estimates should be sufficient. We attempted to ascertain the effect of the simplifying assumptions in our method by comparing the results to those from a more complex radiation model. We used a model of radiation recently completed for the HJA that synthesizes meteorological data from the LTER using PRISM (Parameter-elevation Regressions on Independent Slopes Model: Daly et al. 1994). These mean monthly estimates of radiation account for topography, cloudiness and their effects on direct and diffuse radiation (Smith 2002). We summed monthly values over the growing season (June through September) and compared the values to those calculated from the different proxies.

In total, we compared our PRR proxy (eqn. 3.1.8) to a more explicit radiation model and three less rigorous radiation proxies: transformed aspect (eqn. 3.1.9, field and DEM-based), transformed aspect modified by slope (eqn. 3.1.10, field and DEM-based), and Arc/Info HILLSHADE (eqn. 3.1.7, $A = 225$, $S = 45$). It was our intent that PRR achieve a much higher level of realism than the simple proxies with considerably less computational effort than the more complicated model.

Results

We have chosen a severe topographic feature from another one of our study sites in order to illustrate the differences among the different proxies. Figure 3.1.2 depicts the area around Moro Rock, a large granite dome in southern Sequoia National Park. The digital elevation map (Figure 3.1.2b) is provided for reference to the four proxies (Figure 3.1.2c-f).

This feature demonstrates many of the advantages to be gained by a more comprehensive index. The transformed aspect image (Figure 3.1.2c) illustrates the difficulty in not including a measure of local slope in formulating a proxy. The dark streak across the center of the figure is the northeast face of Moro Rock. The equally dark region in the upper right is a low-relief valley that also has a slight northeast aspect. When slope is accounted for (Figure 3.1.2d), the dark streak in the upper right becomes a lighter shade of gray, giving a much better representation of the contrast in topographic orientation.

The region depicted in Figure 3.1.2 lies in a region of the Park where the only major shading feature is Moro Rock. When topographic shading is considered (Figure 3.1.2e), the area of low light on the northeast side of Moro Rock is widened. No other shading effects are observed. The biggest change in the picture occurs when daily solar track is included (Figure 3.1.2f). The darkness in the upper right corner disappears and the darkness in the lower center becomes considerably lighter. This change occurs because in the morning hours the sun is shining directly on some of these eastern-facing features for several hours. Morning sun is not captured by the other simple aspect

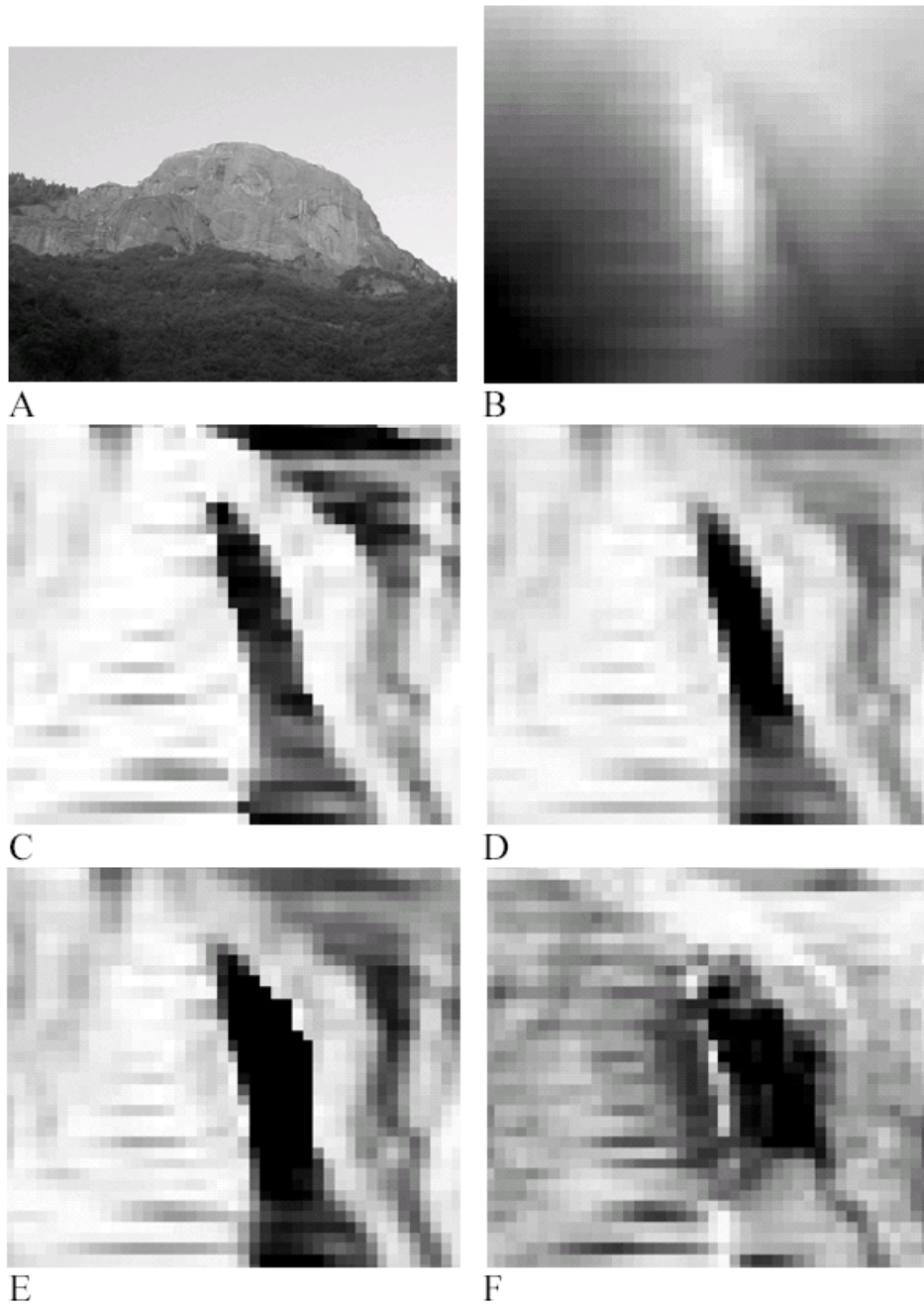


Figure 3.1.2. (A) Moro Rock is a large narrow granitic outcrop about 1.2 km long. The photo is from the west. The following maps are oriented towards the north. (B) DEM of the Moro Rock area is used to illustrate the differences between the radiation proxies draped over a severe terrain feature (high elevations are lighter). (C) Transformed aspect map (high radiation areas are lighter). (D) Transformed aspect modified by slope. (E) HILLSHADE with $A = 225$, $S = 45$. (F) Potential relative radiation (PRR).

proxies, which are transformed along a NE-SW axis. By integrating across the entire day, the PRR index also highlights features that get continuous full sun with distinctive radiation signatures. For example, the white diagonal in the center of the picture is the ridgeline of Moro Rock. Also, the flat area in the upper middle of the image is readily identifiable in Figure 3.1.2f.

To illustrate the amount of variation captured by the different DEM-based indices we compare them to the radiation figures generated by the Smith (2002) model for the 175 plots scattered across the HJA watershed (Figure 3.1.3; Table 3.1.1). Many of the sites with the most negative transformed aspect have relatively high radiation according to the Smith model (Figure 3.1.3a). Adding the slope modification actually decreases the explanatory power of the model (Figure 3.1.3b). Arc/Info's HILLSHADE function mirrors the assumptions from transformed aspect, adding the effects of shading by adjacent topography (Figure 3.1.3c). The HILLSHADE proxy simulates solar conditions at one point in time. The PRR proxy captures any potential shading that occurs throughout the course of the day and year (Figure 3d). The index is highly correlated with radiation values obtained from the Smith model (Table 3.1.1).

Correlations between the DEM-derived indices and the Smith model also were compared for 1000 points randomly sampled across the landscape (Table 3.1.2). PRR again is highly correlated with the modeled radiation. Transformed aspect does as good a job as HILLSHADE in predicting this larger dataset of radiation values.

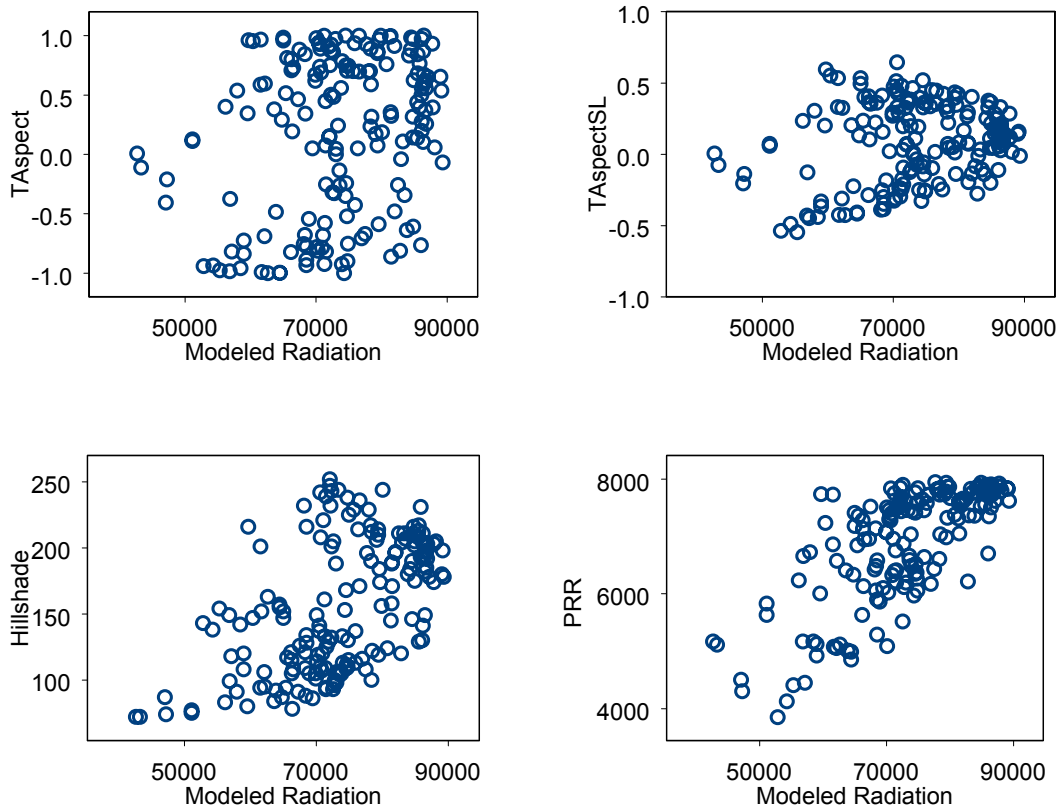


Figure 3.1.3. Comparison of the different radiation proxies to the modeled radiation from the Smith model. (A) DEM-derived transformed aspect graphed against modeled radiation. (B) The effect of slope on relative radiation is added. (C) HILLSHADE adds topographic hillshading from a single point in time. (D) Potential relative radiation (PRR) accounts for topographic shading and integrates over different solar positions.

Table 3.1.1. Correlations between field- and DEM-derived proxies with the modeled radiation for 175 sample plots.

	Radiation Model (r^2)	<i>P</i> -value
Transformed field aspect	0.06	0.001
Transformed field aspect * sine slope	0.05	0.003
Transformed DEM aspect	0.09	<0.0001
Transformed DEM aspect* sine DEM slope	0.05	0.0002
Hillshade	0.31	<0.0001
PRR	0.54	<0.0001

Table 3.1.2. Correlations between DEM-derived proxies with the modeled radiation for 1000 random samples.

	Radiation Model (r^2)	<i>P</i> -value
Transformed DEM aspect	0.20	<0.0001
Transformed DEM aspect* sine DEM slope	0.14	<0.0001
Hillshade	0.20	<0.0001
PRR	0.59	<0.0001

Field-derived measurements of transformed aspect and sloped-modified transformed aspect correspond poorly with the modeled radiation and the other radiation proxies. They explain less than seven percent of the variation in the Smith-modeled radiation values (Table 3.1.1). Correspondence between the field-based proxies and PRR are equally poor. These low correlations underscore that field measures of many environmental variables, including slope and aspect, are taken at a very different scale than measures derived from a 30-m DEM and the two approaches can differ substantially in their final estimates.

Discussion

The two major methods for incorporating solar radiation information into vegetation analyses are radiation proxies and radiation models. Slope and aspect proxies require specific transformations and neglect temporal variation and local topographic shading. Computationally intensive techniques are easily capable of modeling radiation explicitly in complex terrain, but require extensive input data and also frequently neglect local topographic shading. Our calculation of potential relative radiation (PRR) accounts for both temporal variation and topographic shading by adjacent landforms and requires only digital elevation data and access to Arc/Info or similar GIS software. The method can be implemented for most study areas with only an afternoon's time investment on a reasonably fast computer. We feel the index provides a good compromise between the simplicity of common radiation proxies and the complexity of more sophisticated models. It captures the dynamics important to radiation in mountainous terrain, but remains accessible to a wide user group.

Studies that explicitly model radiation in topographically heterogeneous areas regularly find radiation effects to be important correlates with vegetation pattern (Davis & Goetz 1990, Franklin 1998). Studies based on crude proxies such as aspect tend to be more variable in their conclusions (Parker 1995, Guisan et al. 1998, Donegan & Rebertus 1999, Park 2001). Proxy variables continue to be used in vegetation analysis, however, because they are much easier to derive. Slope and aspect can be obtained from digital terrain data, which is readily available for most study sites. We show that these proxies can correspond poorly with modeled radiation for sample sizes realistic of a rigorous field effort. Given enough samples, transformed aspect predicts radiation as well as HILLSHADE (Table 3.1.2). With smaller sample sizes, the differences might be considerable, particularly if many of the samples are in topographic shade as was the case for the 175 sample plots considered in this study (Table 3.1.1).

The HILLSHADE and PRR indices, which also can be calculated easily from digital terrain data, provide a much better match to the modeled data for the field samples. Much of this increased correlation can be explained by the improved ability of these indices to account for topographic shading. Shadows from adjacent ridges produce areas that are considerably darker during certain hours of the day, and aspatial models that do not incorporate local topography can greatly overestimate radiation at these sites. Incorporation of these effects is only feasible using a GIS-based method. Because many more complicated radiation models are essentially aspatial with regards to topographic context, we expect PRR to provide a more accurate description of relative radiation differences than many of these models for topographically complex study areas.

It is important to reiterate that our method provides relative estimates only. We modeled the most predictable source of heterogeneity, direct-beam radiation with clear-sky conditions and no diffuse-beam radiation. While this is not completely realistic, it approximates the most common growing season condition in the mountainous western US systems in which we work. We present our proxy as an upper bound of potential radiation differences. Radiation from diffused sources tends to attenuate the overall variability caused by topography, as overcast skies cast a reasonably uniform light across the entire landscape (Dubayah & Rich 1995).

By focusing on relative radiation as derived from a measure of direct radiation only, we are able to greatly simplify our calculations and data needs. A major difficulty in predicting actual radiation is in accurately partitioning radiation between its direct and diffuse components. Radiation is affected from minute to minute by clouds and from day to day by weather patterns. Our approach completely ignores climatic fluctuations; therefore, we do not require the additional data needed to incorporate these fluctuations into a model. Because we consider only direct-beam radiation neither cloudiness nor the presence of aerosols as scattering agents are considered. We also ignore reflected radiation and the detailed algorithms that would be required to estimate this component in complex terrain.

Finally, because our method is so reliant on DEM data, any inherent errors in the DEMs will cascade throughout the results. We did not employ DEM correction algorithms as they sometimes introduce as many errors as they remove (Dubayah 1994, Dubayah & Rich 1995) and we wanted to keep our method as simple as possible. We

advise that all DEMs be examined for apparent systematic errors and stress the importance of obtaining the best terrain data possible.

Radiation is a fundamental influence on many ecological patterns. Current approaches to estimate radiation might be sufficient for some sites (*e.g.*, areas of little topographic relief where topographic shading is not important), but they produce flawed estimates that might downplay the importance of radiation in many other environmental settings (Brown 1994). We developed our approach for use in forest community studies to respond to the following common data needs. (1) Our study areas encompass large landscapes in mountainous terrain, in which empirical measures of radiation are not available. (2) In the complex terrain in which we work, we felt differences associated with topographic shading were important to include in our estimates of radiation. We also felt that it was important to represent the dynamic nature of radiation loads, which change over the course of the day and year. (3) Because our requirements for vegetation analysis are less stringent than for atmospheric scientists, we did not desire to spend the effort to account for the comprehensive suite of factors used in solar radiation models such as attenuation by atmospheric transmittance or cloudiness. This is partially due to the scale of our study, and partially due to the fact that our analyses of vegetation distributions require only relative radiation values. We felt it was important that the estimates be readily calculable and the approach be accessible to a wide audience. The resulting PRR index should provide a powerful tool for estimating fine-scale variability in radiation across large spatial extents.

CHAPTER 3.2 Spatial Estimation of Air Temperature Differences for Landscape-scale Studies in Montane Environments

Abstract

Capturing fine-grain environmental patterns at landscape scales cannot be accomplished easily using conventional sampling techniques. Yet increasingly, the landscape is the scale at which ecosystems are managed. Temperature variability is an important control of many ecological processes. Elevation is often used as a proxy for temperature in montane ecosystems, partly because few direct measurements are available. We propose a low-cost and logistically practical approach to collecting spatially explicit temperature data using a network of portable temperature micro-loggers. These data can be used to generate simple, site-specific models for estimating temperature differences across complex terrain. We demonstrate the approach in a predominantly old-growth watershed in the Oregon Western Cascades. Environmental lapse rates are generated for July mean, maximum and minimum temperatures. Temperature estimates are improved substantially over these lapse rate estimates by including measures of relative radiation and relative slope position as additional explanatory variables in the model. The development of temperature estimates that explicitly account for topography has important implications for ecological analysis, which frequently relies upon the simplifying assumptions associated with lapse rates in describing the environmental template.

Keywords: H.J. Andrews Experimental Forest, lapse rate, old-growth forest, temperature modeling, terrain analysis

Introduction

Efforts to describe vegetation patterns in montane systems historically have relied on elevation as an ecological “proxy” variable to represent complex environmental gradients (Whittaker 1978). While elevation is reasonably correlated with distributions of species, this indirect correlation is unsatisfying. It has been understood for some time that variability in temperature and soil moisture is a major determinant of plant distributions (Whittaker 1967, Stephenson 1990). Elevation is merely a convenient way of representing these environmental factors (Barry 1992). Since the relationships among ecological variables likely will change with any changes in climate, it is important to develop more descriptive models of key ecological constraints such as temperature in order to model future ecological processes.

Attaining data to develop these models is hampered by at least two logistical issues. First, better models are needed at the landscape scale, because this is the level at which management decisions typically are made (Christensen et al. 1996, 2000). Describing complex environmental patterns at this scale can be extremely data intensive. Fine-grain studies are able to capture environmental variability explicitly (*e.g.*, Yeakley et al. 1998, Chen et al. 1999), and much of this fine-scaled detail averages out at regional to global scales (*e.g.*, general circulation models, Henderson-Sellers & McGuffie 1987, VEMAP 1995). At landscape scales, however, detailed environmental patterns cannot be ignored. Novel sampling techniques often are required to capture fine-scaled detail over large spatial extents (Urban et al. 2002).

Second, obtaining sufficient data to calibrate and validate temperature models is frequently difficult in montane environments where weather-monitoring stations are sparse (Running et al. 1987, Yeakley et al. 1998). Weather stations tend to be at low elevations in watersheds and therefore tend to overestimate temperature across steep terrain (Phillips et al. 1992, Daly et al. 1994). Working in the southern Appalachian Mountains, Bolstad et al. (1998) suggested that spatially extrapolated estimates of temperature from a few low-elevation weather stations are consistently biased due to the inability to account for local topographic effects. Extending the network of monitoring stations to account for these phenomena has been logistically and economically prohibitive (Chen et al. 1999).

Local topography can modify substantially the relationship between elevation and temperature. Primary topoclimatic effects result from differences in hillslope angle and aspect (Barry 1992). These effects are governed largely by the relationship of slope orientation to solar radiation. In the northern hemisphere, north-facing slopes experience less radiation than south-facing slopes. McCutchan and Fox (1986) showed that aspect differences can be even more important than elevation in controlling temperature. Bolstad et al. (1998) suggested that temperature maxima, in particular, are sensitive to topographic exposure.

Secondary topoclimatic effects can result from the influence of terrain on mountain winds and the generation of airflow effects such as cold air drainage (Barry 1992). As a result, mountain valleys, midslopes, and ridges can be characterized by very different temperature regimes. Evaporative cooling can further accentuate these

differences for riparian areas along valley bottoms. While temperature maxima might be particularly sensitive to radiation differences, temperature minima might be more strongly influenced by relative slope position and mountain air currents (Bolstad et al. 1998).

In this analysis, we consider a nested series of temperature regression models. We begin with a simple elevation model, in which we collect data to develop a site-specific lapse rate – a quantitative description of the decrease in temperature with increase in elevation. This first model serves as an improvement over the generic environmental lapse rate of 6 °C per km elevation gain (Barry 1992). We then consider more complicated models that include measures of relative radiation and relative slope position as additional potential explanatory variables. We test the importance of each factor in explaining temperature means, minima, and maxima.

Ecological predictions that rely upon the loose correlation between vegetation and temperature as proxied by elevation may be adequate for national and regional analyses, but they will not suffice at the landscape scale. The ultimate objective of our research is to isolate the fraction of the ubiquitous elevation gradient (Whittaker 1967, Kessell 1979, Stephenson 1998) that can be attributed to temperature. To do this effectively we must develop an efficient means of including fine-scale topographic effects in our temperature models. This paper addresses the following specific objectives:

- 1) To develop a site-specific lapse rate model of a mountainous study area.
- 2) To test this model against increasingly complex models that include fine-scale topographic factors as potential explanatory variables.

- 3) To test hypotheses that radiation differences strongly influence temperature maxima and relative slope position influences temperature minima.
- 4) To develop a simple approach to data collection and statistical analysis that could be applied in mountainous study areas to create site-specific temperature models with minimal investment in time and money.

Methods

Study area

Located predominantly in old-growth forest of the Oregon Western Cascades (Figure 3.2.1), the H.J. Andrews Experimental Forest (HJA) is a Long Term Ecological Research (LTER) site covering 6400 ha and ranging in elevation from 410 m to 1630 m (McKee 1998). The HJA was established in 1948 within a forested watershed with about 65 percent of the land in old-growth (*i.e.*, 400-500 years old). A preliminary vegetation survey of the site suggests that elevation is the primary correlate with community pattern. *Pseudotsuga menziesii* (Douglas-fir), *Tsuga heterophylla* (western hemlock), and *Thuja plicata* (western redcedar) are the dominant species at lower elevations in the forest, while *Abies amabilis* (Pacific silver fir), *A. procera* (noble fir), and *Tsuga mertensiana* (mountain hemlock) dominate upper elevations. Vegetation sampling in the HJA suggests a transition in forest community composition at elevations around 1200 m, consistent with trends found elsewhere in the Oregon Western Cascades (Dyrness et al. 1976, Franklin & Dyrness 1988).

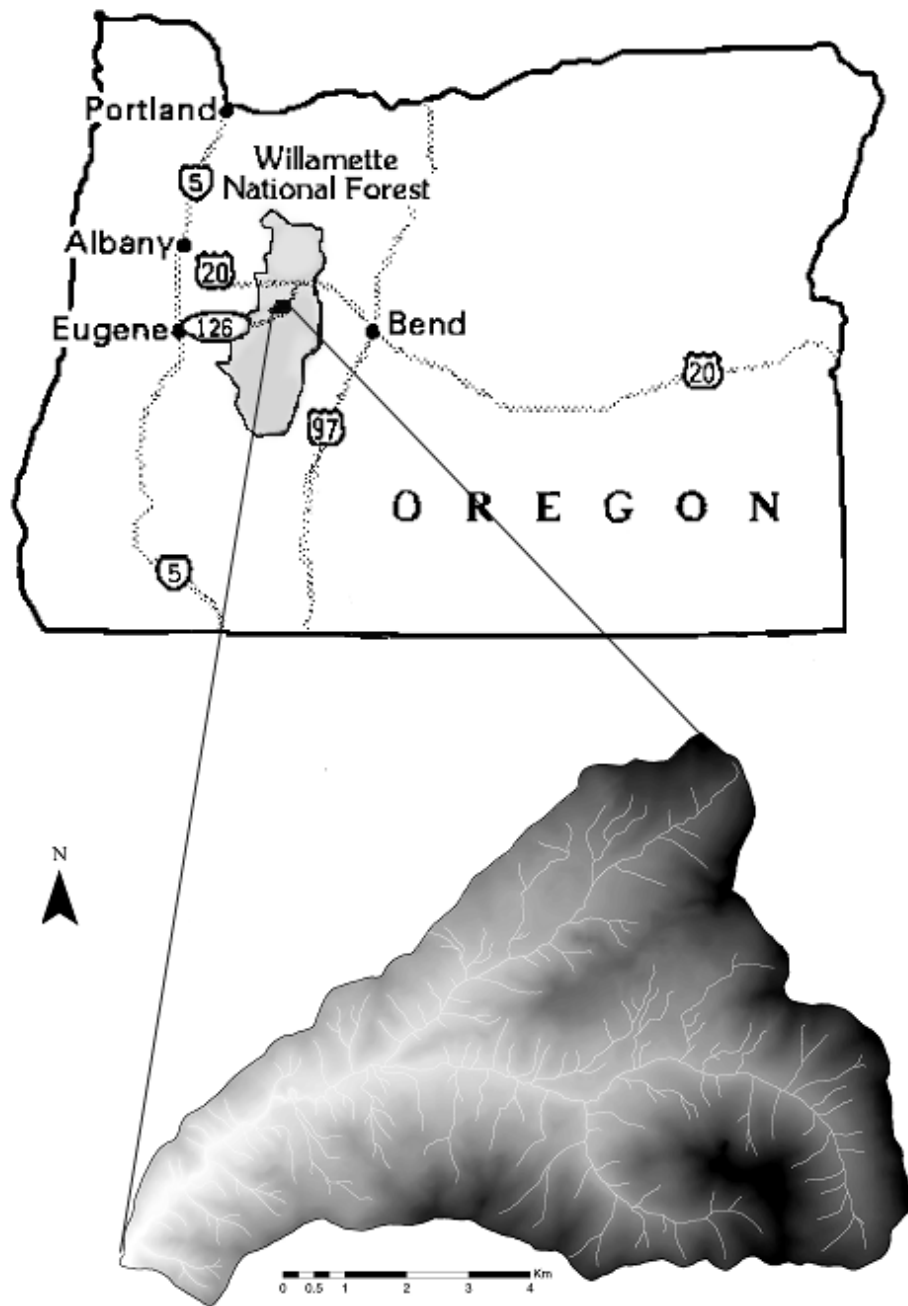


Figure 3.2.1. Locator map for the H.J. Andrews Experimental Forest LTER. The study site is located on the west side of the Cascade Mountains approximately 80 km east of Eugene, Oregon.

As an LTER site, the HJA maintains an extensive database of meteorological data (Bierlmaier & McKee 1989). Climate is characteristic of the Pacific Northwest, with dry summers and wet, mild winters. Only about one-tenth of the annual precipitation falls from June to September in the Western Cascades (Daly et al. 1994). At larger scale, Greenland (1994) has placed the climate of the HJA into a regional context based on monthly temperature and precipitation data. Sea and Whitlock (1995) have reconstructed the vegetational and climatic history of the region and suggested that vegetation changes have been influenced heavily by changes in temperature over the past 14,000 years.

Data

Temperature measurements were recorded hourly using a sampling network of portable temperature micro-loggers (HOBO: Onset Computer Corporation). The micro-loggers were hung from trees at a height of 1.3 m above ground level. Sensors were kept on the northwest side of trees to minimize exposure to direct radiation. All measurements were taken in undisturbed, old-growth forest in an effort to control biotic variability, while varying only topographic factors. Stand variation in stem density and total basal area was minimized. Relative temperature differences, therefore, should be applicable across the old-growth components of the landscape. While absolute temperatures may not reflect accurately temperatures experienced in tree canopies or by regeneration on the forest floor, relative differences should be scalable to the different vertical strata of old-growth forests.

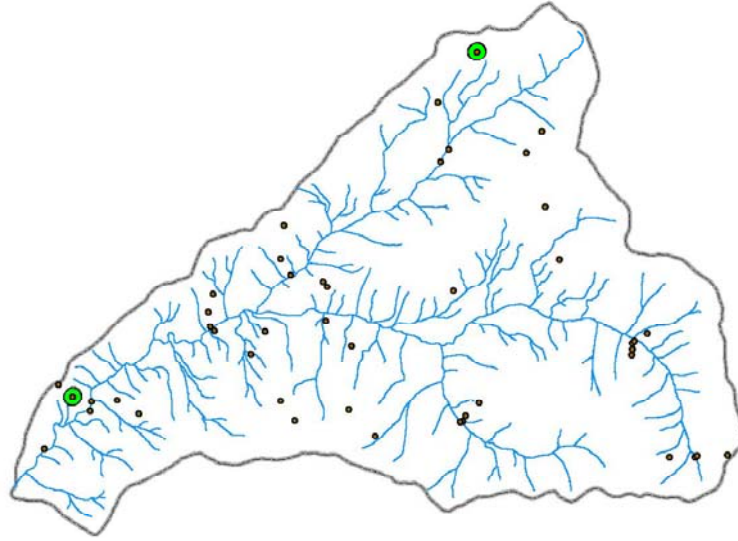
Data were gathered for the month of July over two successive years in 1999-2000. In examining the existing meteorological network at the HJA, Rosentrator (1994)

identified the late spring/early summer as the time of greatest temperature spatial and temporal variability. Greene and Klopsch (1985) also choose July as a key month for developing their lapse rate models for Mount Rainier National Park in the Washington Cascade Range.

Two year-long datalogger stations (CR10X: Campbell Scientific Incorporated) were linked to the temporary networks by placing micro-loggers at each of the permanent datalogger stations in both 1999 and 2000 (Figure 3.2.2). The dataloggers recorded measurements from temperature probes (CS107: Campbell Scientific Incorporated), which also were located at 1.3 m above ground but protected in louvered radiation shields open to the environment. These continuous records provide the potential of extending the July micro-logger trends over a longer time frame. Measurements taken by the two sampling devices were highly correlated at both the high elevation (1292 m) and low elevation (642 m) locations (Figure 3.2.3). The micro-logger data were, on average, 0.2 °C higher for the low elevation site and 0.3 °C higher for the high elevation site.

Models were developed using data from 45 micro-loggers deployed over the summer of 2000. A stratified sampling design was used, whereby sample locations were stratified across elevation, aspect and relative slope position for each of seven major watersheds of the HJA determined by geographic information systems analysis (Figure 3.2.2A). These factors represent the predominant altitudinal and topoclimatic controls on temperature (Barry 1992). Aspect is associated with differences in relative radiation load, while relative slope position is associated with airflow effects such as cold air drainage. Additional data were available from 33 micro-loggers deployed across the watershed

A) 2000



B) 1999

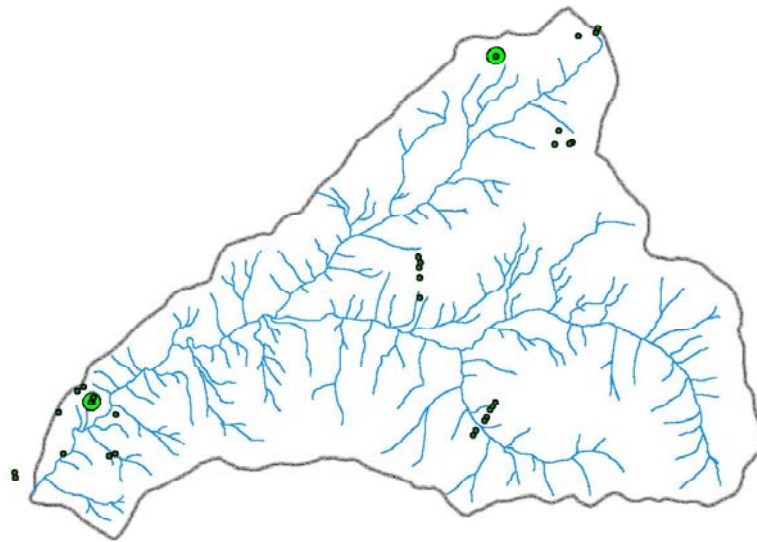


Figure 3.2.2. A) Locations of 45 micro-loggers for July 2000. B) Locations of 33 micro-logger locations for 1999. Larger circles represent locations of permanent CR10X stations.

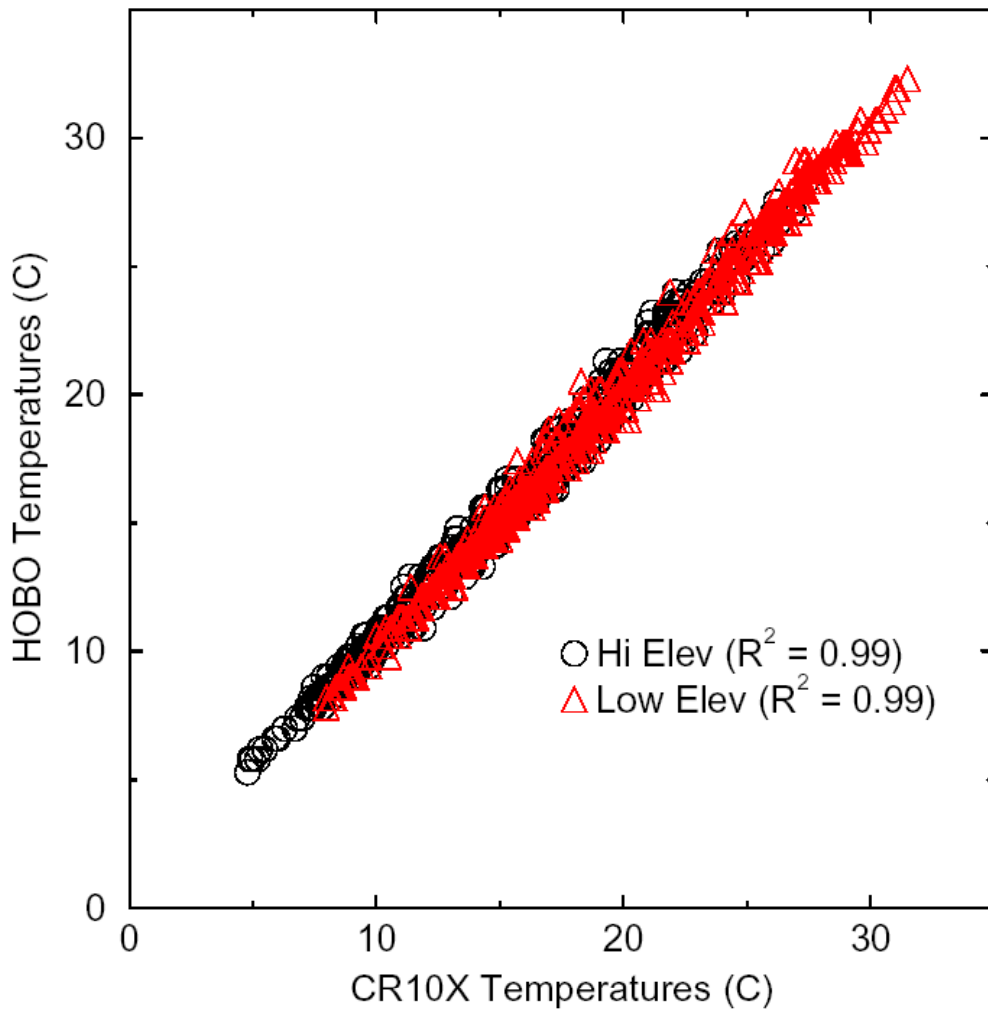


Figure 3.2.3. Comparison of 1999 temperature data collected from micro-loggers with data collected from two CR10X dataloggers. The high elevation site was located at 1292 m. The low elevation site was located at 642 m (n = 744 hourly measurements at each site).

over the summer of 1999 (Figure 3.2.2B). These data were used for validation purposes. The locations of the micro-loggers in 1999 overlapped with the 2000 locations only at the permanent CR10X datalogger stations and at the HJA's primary meteorological station at the base of the watershed.

Analysis

The monthly average, daily minimum, and daily maximum temperatures were calculated for each location from the hourly measurements. The 2000 data were used to compare a series of increasingly more complex regression models attempting to describe temperature differences across the watershed. The models were nested so they could be compared by simple likelihood ratio tests (Sokal & Rohlf 1995). Variables were added to the models in order of increasing explanatory power until additional variables no longer significantly improved the model.

Each of the variables chosen as a candidate for the models was selected because of its potential influence on temperature. Additionally, all of the variables could be derived easily from commonly available geographic information systems data (*e.g.*, digital elevation model (DEM), streams coverage). Besides elevation, we considered relative slope position, distance from stream (log transformed because the strength of the relationship decreases with distance), and a wide range of radiation proxies ranging from simple transformed aspect (Beers et al. 1966) to a potential relative radiation (PRR) measure developed from DEM data. Chapter 3.1 describes the radiation proxies in detail. The PRR index, developed specifically for use in community level vegetation analysis, is a measure of how topography translates to spatial differences in relative radiation. It both

accounts for hillshading and shadowing effects and integrates over time to account for the fact that solar position changes over the course of the day and year.

Once models were calibrated, they were confronted with the 1999 data as a validation exercise. Models therefore were evaluated in terms of their ability to describe the 2000 data from which they were generated and their ability to predict temperature differences in the 1999 data attained from different sampling locations and a different year. Using data from separate years for calibration and validation purposes was a practical decision. By redeploying the same micro-loggers for a second time in order to gather sufficient data for model testing, we were able to reduce greatly the cost of the analysis.

Results

Model fits

Mean July temperatures ranged from 12.9 to 17.6 °C at the 45 sites sampled in 2000. In order of increasing complexity, the three best models for predicting mean July temperature are as follows:

$$\hat{y} = \beta_0 + \beta_1 \textit{Elevation} + \varepsilon \quad (\text{eqn. 3.2.1})$$

$$\hat{y} = \beta_0 + \beta_1 \textit{Elevation} + \beta_2 \log(d_{\textit{strm}}) + \varepsilon \quad (\text{eqn. 3.2.2})$$

$$\hat{y} = \beta_0 + \beta_1 \textit{Elevation} + \beta_2 \log(d_{\textit{strm}}) + \beta_3 \textit{Radiation} + \varepsilon \quad (\text{eqn. 3.2.3})$$

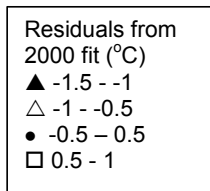
where \hat{y} is the estimated mean temperature, β 's are constants, $d_{\textit{strm}}$ is the distance from the nearest stream in meters, *Radiation* is our DEM derived estimate of potential relative

radiation (PRR index), and ε is an error term. Other variables considered do not improve the model fit.

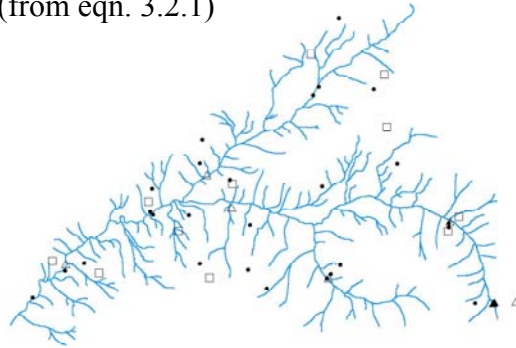
Elevation, which ranges from 433-1359 m, is the explanatory variable best able to explain the differences in mean temperature among the sites. This case mimics a traditional lapse rate model where elevation can be viewed as the primary forcing variable in the system. Local effects, as captured by the distance from stream and radiation terms, are also important. Model 2 is a significant improvement over Model 1 (F-statistic = 39.79, $P < 0.001$). Model 3 is able to describe the spatial variability in temperature slightly better than Model 2 (F-statistic = 3.80, $P = 0.058$).

The spatial residuals from each of the three models are shown in Figure 3.2.4. Model 1, the elevation model, does a reasonable job of fitting the data, but with 19 of the 45 points over- or underestimated by greater than 0.5 °C. Adding distance to stream to the model reduces this number to 10. In particular, the model fit is improved for many of the sites in the higher-elevation, eastern portion of the study area. Adding radiation to the model further reduces to six the number of points over- or underestimated by greater than 0.5 °C. This factor seems to be more important to the lower-elevation, western portion of the watershed with more deeply incised stream channels.

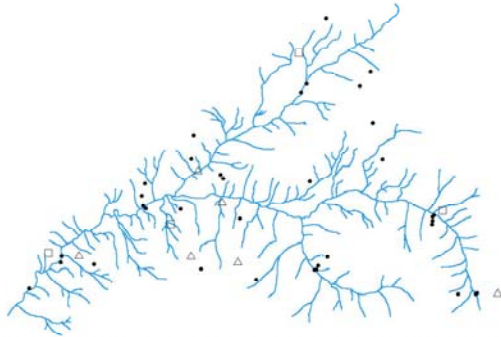
For daily maximum temperature, the simple lapse rate model is significantly improved upon by including radiation as an additional explanatory variable (Table 3.2.1). Relative slope position as measured by distance from stream has little effect.



(from eqn. 3.2.1)



(from eqn. 3.2.2)



(from eqn. 3.2.3)

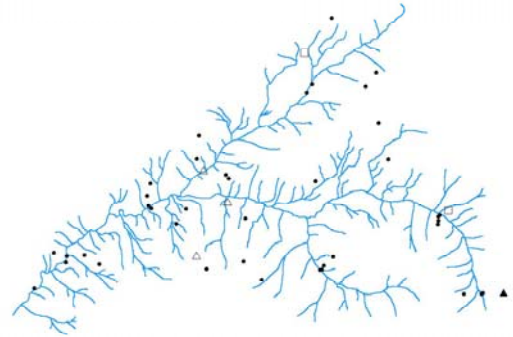


Figure 3.2.4. Maps of spatial residuals for the mean July temperature models. Squares represent locations that were warmer than predicted by the models by at least 0.5°C . Triangles represent locations that were cooler than predicted by the models by at least 0.5°C .

Table 3.2.1. Monthly average, daily maximum and daily minimum temperatures were modeled for July 2000. Variables were added to the models in order of increasing explanatory power until additional variables no longer significantly improved the model fit.

Mean Temperature			
	R ²	F-statistic	p-value
Model 1 = MeanTemp~Elevation	0.82	189.56	<0.001
Model 2 = MeanTemp~Elevation+Log(d_{strm})	0.90	36.79	<0.001
Model 3 = MeanTemp~Elevation+Log(d_{strm})+Radiation	0.91	3.80	0.058
Daily Maximum Temperature			
	R ²	F-statistic	p-value
Model 1 = MaxTemp~Elevation	0.41	30.30	<0.001
Model 2 = MaxTemp~Elevation+Radiation	0.48	5.74	0.020
Model 3 = MaxTemp~Elevation+Radiation+Log(d_{strm})	0.49	0.13	0.725
Daily Minimum Temperature			
	R ²	F-statistic	p-value
Model 1 = MinTemp~Elevation	0.58	59.98	<0.001
Model 2 = MinTemp~Elevation+Log(d_{strm})	0.67	11.77	0.001
Model 3 = MinTemp~Elevation+Log(d_{strm})+Radiation	0.67	0.002	0.965

In contrast, distance from stream is more important than any of the radiation proxies in explaining variability in daily minimum temperature (Table 3.2.1). The combination of distance from stream and elevation provides the most parsimonious model. Radiation differences have little effect on minimum temperatures.

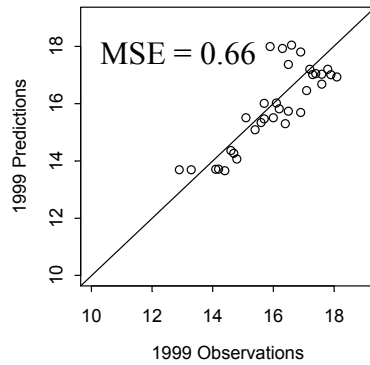
Model validations

The model validations confirm that mean temperature can be better described using a combination of elevation and fine-scale environmental variables than it can by using elevation alone. An analysis of the bias and spread of the predictions can be made by graphing the predicted against the observed values (Figure 3.2.5). The one-to-one line on this graph represents a perfect fit of the data to the model. Points above this line were warmer than predicted by the model; points below this line were cooler than predicted by the model. The scatter of points around the one-to-one line represents the spread of the error. Although there is not a systematic bias in any of the models, the spread is reduced in the more detailed models (Mean Square Error of the predictions (MSE) = 0.66 for elevation alone vs. MSE = 0.44 and 0.45 for the other two models).

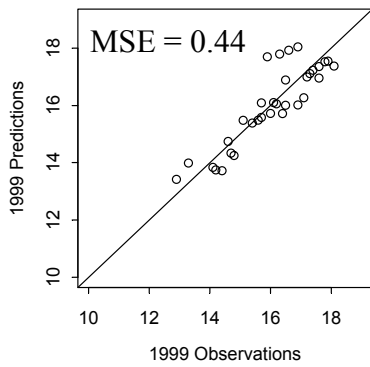
Discussion

It has been argued that temperature is the single most important component of mountain climate (*e.g.*, Barry 1992). Detailed temperature data certainly are required to understand plant community dynamics. Among the long list of ecological processes influenced by temperature are photosynthesis, evapotranspiration, respiration, carbon fixation and decomposition (Running et al. 1987, Bolstad et al. 1998). Potential

Elevation Model



Elevation, Distance Stream Model



Elevation, Distance Stream, Radiation Model

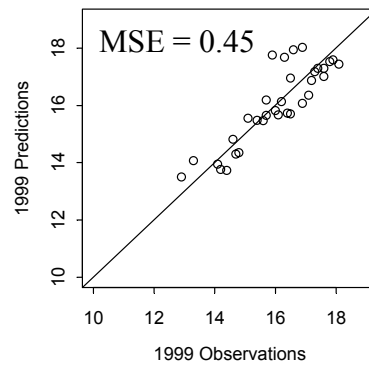


Figure 3.2.5. Comparison of the ability of the models calibrated with 2000 data to explain relative differences in 1999 temperatures. Predictions that match observations exactly would be on the one-to-one line.

applications of improved temperature estimates covering a variety of spatial scales include studies of global climate change, global vegetation dynamics, regional hydrologic balances, and local photosynthesis and transpiration capabilities (Running et al. 1987, Miller & Urban 1999). But it is at the landscape scale that our current climate models are particularly insufficient (Chen et al. 1999). With the growing popularity of geographic information systems, the demand for regularly distributed meteorological information is likely only to increase (Daly et al. 1994).

Unfortunately, the data typically do not exist to develop detailed temperature models in montane study areas. For most systems, available data are limited to a small number of base station measurements. Further, these base stations are typically situated at locations that are not representative of the landscape as a whole (Phillips et al. 1992). The use of inexpensive, portable micro-loggers allowed us to collect data and model temperature over a large spatial coverage given practical economic, time and human resource constraints.

Although more expensive recording devices are available, we found the relatively low-end micro-loggers to be sufficient for our purposes. Agreement between micro-logger and permanent datalogger measurements were good, although the micro-loggers showed a slight tendency to heat up more slowly in the morning and retain heat longer into the afternoon and evening. This observed lag was likely due to differences in the weatherproofing of the sensors rather than any differences between the recording equipment. The plastic weatherproofing containers holding the micro-loggers may have created a slight greenhouse effect around the sensors. For a small increase in cost,

weatherproof micro-loggers could be purchased, thus removing the need for the plastic containers. Protective containers also could be designed that are partially open to the atmosphere and would experience less of a greenhouse effect. Since we observed primarily a slight lag in the timing of temperature changes and little difference between the mean, daily maximum or daily minimum measurements, we do not feel that the use of the weatherproof containers substantially influenced our results.

Use of the micro-loggers allowed us to generate site-specific lapse rates for July temperature means, maxima, and minima across the HJA. The mean temperature lapse rate ($4.5\text{ }^{\circ}\text{C}/\text{km}$) and maximum temperature lapse rate ($7.0\text{ }^{\circ}\text{C}/\text{km}$) are similar to the generic environmental lapse rate of $6\text{ }^{\circ}\text{C}/\text{km}$. Given that our study area covers little more than a km of elevation change, the equations differ in their predictions by no more than $1\text{--}2\text{ }^{\circ}\text{C}$. The influence of elevation on temperature minima, however, is less severe ($3.8\text{ }^{\circ}\text{C}/\text{km}$). The finding of a lower lapse rate for temperature minima than for other measures of temperature is in agreement with others who have examined these relationships at a much larger spatial scale for the northwestern US (Thornton et al. 1997).

The results of our analysis suggest that temperature estimates that consider additional fine-scale topographic variability describe temperature more accurately for our study area than do estimates derived from simple lapse rate models. The lapse rate approach completely ignores local effects associated with differences in aspect and relative slope position. As shown here, these factors can have measurable effects on temperature. Our results are consistent with others who found daily minima to be

influenced heavily by relative slope position and daily maxima to be more affected by topographic exposure (Bolstad et al. 1998). Both types of effects influence mean temperatures.

It is important to emphasize that the results presented in this analysis are applicable to only a very narrow range of conditions. As with any statistical model, these models should not be extrapolated beyond the range of conditions specified by the input data. These include the topographic and climatic conditions of the study area, the timing of the sampling in mid-summer, and the stand structure of old-growth forest. Further, the absolute temperatures derived from measurements taken at 1.3 m above ground may not be the values most directly relevant to tree growth or reproductive success, but the relative temperature differences between different locations within the landscape should be robust across different vertical strata. For many ecological applications, it is these relative differences that are of primary interest. For example, we developed these models to help explain transitions in community composition for old-growth forests of the HJA. These transitions are more strongly correlated with our model predictions of relative July temperature differences than any single temperature “proxy” variable (*e.g.*, elevation, slope, aspect; Chapter 4).

Though the results themselves may have limits on their applicability, the approach is widely applicable. The sensors are relatively inexpensive and minimal labor is involved in deploying and downloading data. With some attention paid to sample design *a priori*, statistical analysis and model generation should follow easily. We have applied

the techniques described in this paper to other study sites with success (*e.g.*, Kaweah Basin of Sequoia National Park).

Since temperature is such an important component of mountain climate, we suggest that developing a simple geographic model of temperature differences should be an important first-step in many landscape-scale ecological studies. Our approach offers an economic means of quickly assessing spatial temperature trends for topographically complex environments.

CHAPTER 3.3 An Empirical Approach Towards Improved Spatial Estimates of Soil Moisture for Vegetation Analysis

Abstract

Landscape-level spatial estimates of soil water content are critical to understanding ecological processes and predicting watershed response to environmental change. Moisture patterns are shaped by the balance between water supply and demand. Because these influences are highly variable at the landscape scale, most meteorological datasets are not detailed enough to capture the variability in the water balance. We propose a tactical approach to gather high-resolution field data for use in soil moisture models. Specifically, we (1) describe general soil moisture trends for a watershed in the Oregon Western Cascades, (2) use this description to identify environmental variables to stratify across in collecting data for a statistical explanatory model of summer soil moisture spatial pattern, and (3) examine the spatial scale of variability in soil moisture measurements and compare this scale with the characteristic scales at which potential moisture influences vary. Although none of the individual explanatory variables mimic exactly the complex scaling pattern of the moisture measurements, by combining factors in the regression model we are able to reproduce observed moisture patterns. The model incorporates both macroscale (climate) and mesoscale (topographic drainage and radiation) influences on the water balance. We use the regression model to extrapolate estimates of relative soil moisture across the watershed for the beginning of the dry growing season.

Keywords: gravimetric and volumetric soil moisture content, H.J. Andrews Experimental Forest, landscape-scale, regression, semivariance analysis, spatial variability

Introduction

Improved spatial estimates of soil water content as a basic environmental resource are urgently needed to predict vegetation responses to potential climate change (Pastor & Post 1988, Stephenson 1990). Soil moisture levels influence such fundamental ecological processes as photosynthesis, respiration, and nutrient uptake (Band et al. 1993). Moisture acts as a primary constraint on forest productivity (Vertessy et al. 1996), affects species composition (Stephenson 1998), and plays a major role in determining forest flammability and fire regime (Clark 1990; Miller & Urban 1999, 2000). It influences erosion (Moore et al. 1988), pedogenesis (Jenny 1980), geomorphology (Beven & Kirkby 1993), and controls infiltration-runoff partitioning in response to precipitation events (Grayson et al. 1997). For these reasons, spatial explorations of soil water are critical to understanding and predicting ecological processes at the watershed level.

Soil moisture is highly variable in time and space. A major challenge for hydrology and ecology is the estimation of the temporal and spatial distribution of moisture at the catchment scale (Crave & Gascuel-Oudoux 1997). *In time*, seasonal climatic patterns influence rates of precipitation, evaporation and soil water uptake by vegetation (D'Odorico et al. 2000, Mackay & Band 1997). Grayson et al. (1997) describe two distinct states in soil moisture patterns for seasonal watersheds in Australia: one for the wet season when nonlocal controls (terrain) dominate and the other for the dry season when local controls (soils, vegetation, radiation) are more important. Yeakley et al. (1998) also describe two distinct states in soil moisture, though they credit a different

seasonal mix of local and nonlocal controls. They collected soil moisture content measurements along a hillslope gradient at the Coweeta Hydrologic Laboratory in the southern Appalachian Mountains of western North Carolina. In this watershed, drainage (terrain) was particularly important in controlling moisture levels in upper soils, and in deeper soils during periods of drought. Storage properties (soils) seemed to control moisture content in lower horizons during watershed recharge. An important conclusion of the Yeakley work that we test in our analysis is that shallow and deep soils can have very different hydrologic controls.

For a given point in time, the *spatial* distribution of soil water is determined by the balance between water supply and demand (Stephenson 1990, 1998). Demand is influenced by relative radiation load (related to slope and aspect) and temperature (related to elevation). In the northern hemisphere, south-facing slopes receive more insolation than north-facing slope. This relationship is modified by latitude, which determines the solar angle; local slope, which affects the incident angle; and landscape context, which can create topographic shading (Chapter 3.1, Dubayah & Rich 1995). Cloud cover also can reduce solar radiation (Nikolav & Zeller 1992). Temperature differences are traditionally estimated using lapse rates, simple regression equations that describe how air cools as it moves uphill (Barry 1992). The relationship between temperature and elevation is similarly confounded by primary (*e.g.*, hillslope angle and aspect) and secondary (*e.g.*, cold air drainage and evaporative cooling) topoclimatic effects (Chapter 3.2, Lookingbill & Urban 2003).

Supply is determined by water inputs and storage. Inputs are influenced by precipitation (elevation) and drainage (relative slope position). Storage is influenced by soil water holding capacity (soil depth and texture). As air rises in altitude, density and temperature decrease, resulting in a decreased capacity for water storage and increases in precipitation (Barry 1992). At higher elevations, this precipitation falls in the form of snow during the winter months, and snowmelt can act as an additional input when temperatures rise in the summer (Running et al. 1987). Drainage moves water from upslope to downslope positions. In terms of inputs, therefore, precipitation generally increases with elevation while hillslope drainage results in soil water decreasing with local elevation. In terms of storage, volumetric water-holding capacity varies with soil texture and depth (Brady & Weil 1999). In general, soils with high clay content have higher moisture content than sandy soils in similar environments. For a given soil type, the greater the soil depth, the greater the potential for storing water. Several studies have found that soil storage properties can be at least as important as topographic variables in dictating soil water distributions (Helvey et al. 1972, Boyer et al. 1990).

These underlying influences to the soil water balance vary at different characteristic spatial scales. For example, temperature and precipitation influence soil moisture at regional scales, while topographic drainage and soil water storage are important at more local scales (Neilson 1991). Generally, the environmental factors that govern soil moisture act at three different spatial scales (Urban et al. 2000): climate (macroscale), topography (mesoscale), and soil depth and texture (microscale). As for the common physical surrogates for the water balance, elevation typically varies along large-

scale hillslope gradients in mountain watersheds. Drainage indices, such as the topographic convergence index (TCI; Beven & Kirkby 1979) and the terrain relative moisture index (TRMI; Parker 1982), are designed to capture local topography. In this analysis, we investigate patterns of soil moisture at multiple scales in a montane ecosystem and try to discern how these patterns can be reproduced by a composite of physical factors.

Several shortcomings hamper the use of existing climate datasets in modeling ecological response to such things as global climate change scenarios (Cramer et al. 1999). Available data are usually sparsely (and often irregularly) sampled, necessitating some form of interpolation to smooth across gaps. Common smoothing techniques are not appropriate when it is important to represent the variability between point measurements. Although techniques do exist for modeling unmeasured variance (*e.g.*, Richardson's (1981) weather generator algorithm), the data required to parameterize these models are often difficult to collect (Cramer et al. 1999). It is important to capture variability at the landscape scale and finer, because these are the scales at which the supply and demand components, and consequently the entire water balance, vary. These are also the scales that are most relevant to ecosystem management (Christensen et al. 1996).

In this study, we examine the summer soil moisture regime of the H.J. Andrews Forest, an experimental watershed in the Oregon Western Cascades. The goal is not to exhaustively characterize the complex temporal dynamics of this highly seasonal system, but instead to develop an estimate of spatial differences in soil moisture during the peak

of the summer growing season. The need for such information grew out of our landscape-scale vegetation studies of these forests. We begin with a cursory examination of the general spatial and temporal trends in soil moisture during the period of summer draw down. We next develop a statistical model for combining potential explanatory variables. We then examine the spatial scale of variability in soil moisture measurements and compare this scale with the characteristic scales at which potential moisture influences vary in the study area. Finally, we map the spatially implicit model back onto the landscape to give a spatial representation of soil moisture that can be tested with future samples.

Methods

Study area

The H.J. Andrews Experimental Forest (HJA) is located on the west slope of the Cascade Mountains (Figure 3.3.1). It is comprised of the Lookout Creek watershed, 80 km east of Eugene, Oregon. The Long Term Ecological Research (LTER) site covers 6400 ha and ranges in elevation from 410 m to 1630 m (McKee 1998). At the time of its establishment in 1948, the HJA was an intact forest with about 65 percent of the land in old-growth (*i.e.*, 400-500 years old). Since that time, old-growth forest has been reduced to roughly 40 percent of the total area due to logging activities.

As an LTER site, the HJA maintains an extensive database of meteorological data. Climate is characteristic of the Pacific Northwest, with dry summers and wet winters. Annual precipitation ranges from 2200 mm at the watershed base to 3400 mm at

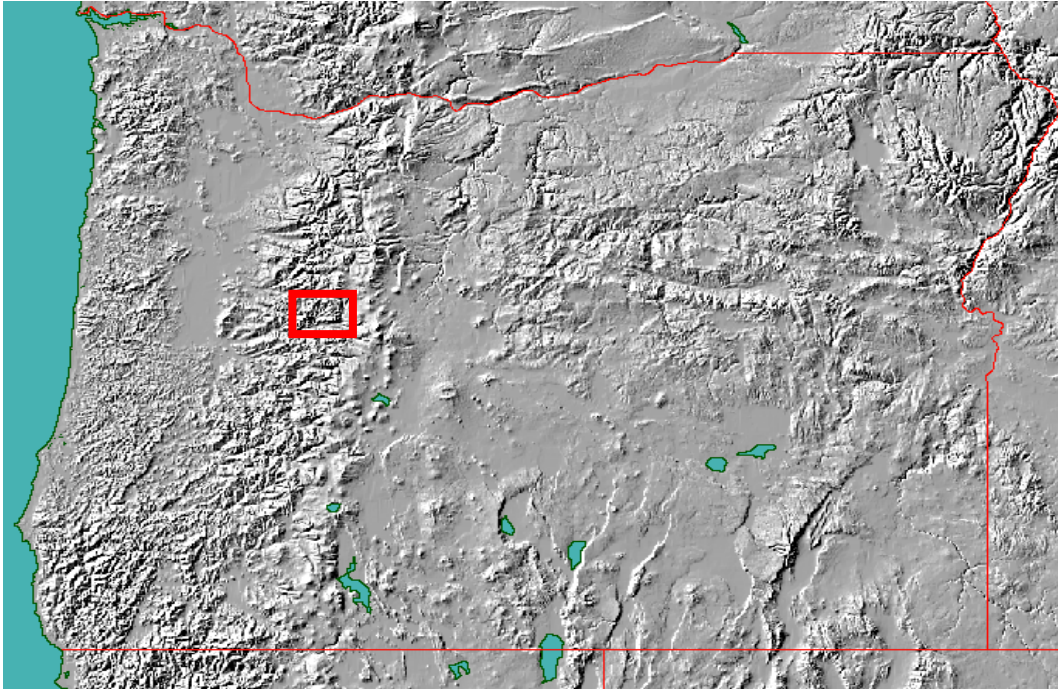


Figure 3.3.1. Locator map for the H.J. Andrews Experimental Forest LTER. The study site is located on the west side of the Cascade Mountains approximately 80 km east of Eugene, Oregon.

upper elevations, with less than 300 mm normally falling during the growing season (Grier & Logan 1977). Soils are mostly deep, well-drained Inceptisols. Rooting occurs almost entirely in the upper 200 cm of soil. Textures range from gravelly, silty clay loam to very gravelly, clay loam. Lower-elevation soils are older than upper-elevation soils, dating back to the Oligocene-lower Miocene. Upper-elevation soils are comprised of younger andesite lava flows and High Cascade rocks.

Topographic position is an important control on vegetation in this region (Zobel et al. 1976). *Pseudotsuga menziesii* (Douglas fir), *Tsuga heterophylla* (western hemlock), and *Thuja plicata* (western redcedar) are the dominant species at lower elevations. *Abies amabilis* (Pacific silver fir), *Abies procera* (noble fir), and *Tsuga mertensiana* (mountain hemlock) dominate upper elevations (Franklin & Dyrness 1988). Ohmann and Spies (1998) suggest that elevation and associated macroclimate are the major correlates with regional patterns of forest community composition throughout Oregon.

Exploratory studies

In an initial effort to better understand the general dynamics of the watershed, we installed a network of three permanent datalogger stations in 1999. The three stations were located at low, mid and high elevation sites within the HJA (Figure 3.3.2; Table 3.3.1). Two sampling stations were located in the *T. heterophylla* zone at low elevation. The third was located in the *A. amabilis* zone. All sites were installed on southwest-facing slopes.

Time domain reflectometry (TDR) units were run from each datalogger to three locations along a hillslope gradient (Table 3.3.1). At each location, we took

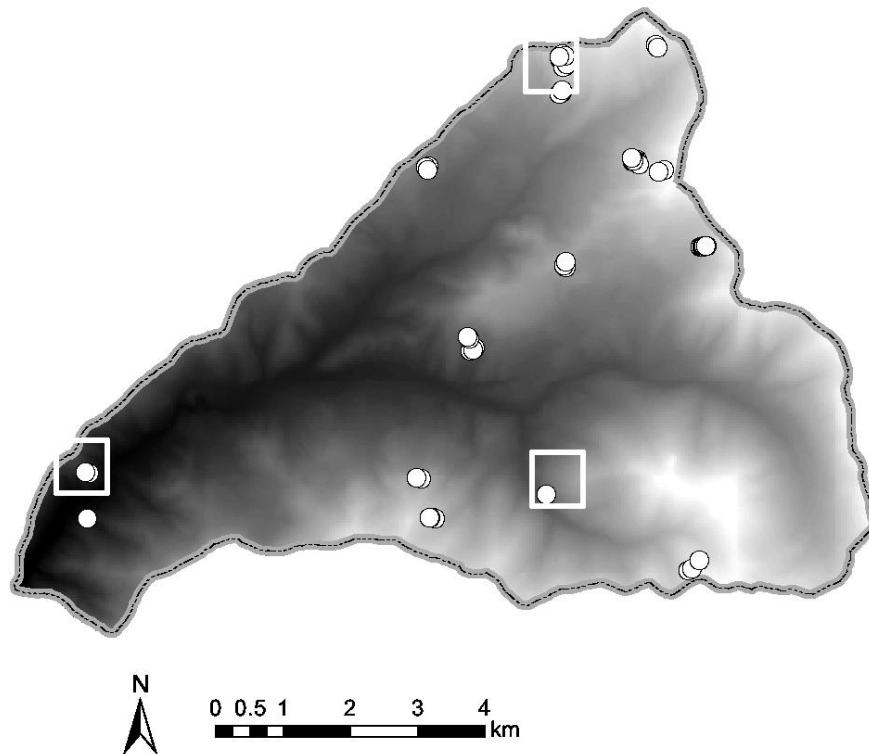


Figure 3.3.2. Map of soil moisture sample locations. Boxes identify small watersheds containing permanent dataloggers and from which samples for regression analysis were collected. Points represent 60 20x20-m plots used for semivariance analysis. Underlying image is a digital elevation model in which higher elevation areas are lighter in color.

Table 3.3.1. Environmental statistics for permanent meteorological stations established in 1999. A surface soil (0-20 cm) and a deep soil (80-100 cm) sensor were located at each location.

	Site Average	Upper Slope TDR Location	Mid Slope TDR Location	Down Slope TDR Location
Elevation (m)				
MetHigh	1288	1299	1287	1278
MetMid	887	899	887	876
MetLow	642	652	643	632
Aspect (°)				
MetHigh	227	220	234	228
MetMid	236	231	241	235
MetLow	225	220	240	214
Slope (°)				
MetHigh	28	26	28	29
MetMid	34	36	29	36
MetLow	29	22	30	35

continuous measurements at two depths (0-20 cm and 80-100 cm). TDR determines soil moisture content by measuring the travel velocity of electromagnetic waves as they pass through the soil (Herkelrath et al. 1991). The velocity of the waves is strongly correlated with the soil water content. The probes were oriented along hillslope gradients of approximately 20 m in relief. Over the summer 1999, data were collected every 60 seconds from these units and hourly statistics (average, maximum and minimum) were stored in dataloggers (CR10X, Campbell Scientific Incorporated).

From this exploratory study, we hoped to capture the temporal pattern of soil moisture drawdown during the dry summer growing season. This information would be used to guide the timing of future synoptic sampling. We also hoped to identify primary physical constraints on the watershed moisture regime. Additional sampling would stratify across these variables. The data from these stations were meant to represent the amount of baseline data typically available for montane study sites. In fact, these three stations probably overestimate the amount of available data for most watersheds.

To help identify potentially important variables to stratify across in later sampling, we collected two small synoptic samples of gravimetric moisture during summer 1999. These samples covered a much larger spatial area than the three TDR stations. Soil samples were collected from 30 (1x1 m) plots spread across the entire HJA, once on July 22 and once on August 12, six days after the largest rainstorm of the summer season. Samples from the top 0-20 cm of soil were weighed wet, oven dried, then weighed again to provide gravimetric moisture estimates.

Empirical model

On July 4 2001, we collected one-time synoptic moisture measurements to build a simple regression model that would capture important components of the water balance in a statistical relationship. Measurements were taken using handheld reflectometers (Hydrosense, Campbell Scientific Incorporated). These portable sensors allowed us to collect measurements of soil moisture rapidly over a large area. They offer two major advantages over the gravimetric method of sampling. First, measurements are provided instantaneously in the field. Samples need not be brought back to the lab for weighing, drying and reweighing. Consequently it is easier to collect larger sample sizes. Second, soil moisture is provided on a volumetric rather than mass basis. Although relative differences should be similar for similar soil types using the two different measures (Figure 3.3.3), variation in soil bulk density will affect greatly gravimetric results.

The sample design met two objectives: (1) it stratified across variables deemed as potentially important to the water balance in the exploratory analyses and (2) it covered a range of spatial scales. At each of the permanent datalogger stations we extended the spatial network of data points up and down the hillslopes and to different slope-aspect combinations within the local watersheds. Samples were taken along short transects (no more than 110 m) with a separation distance of 5-10 m between samples. Each sample represented the average of three measurements taken within 1 m². Measurements integrated over the top 0-20 cm of soil. A total of 79 samples were taken: 19 at low elevation, 31 at mid elevation and 29 at high elevation. An additional nine samples were added to the analysis from the permanent datalogger stations at the center of each of the

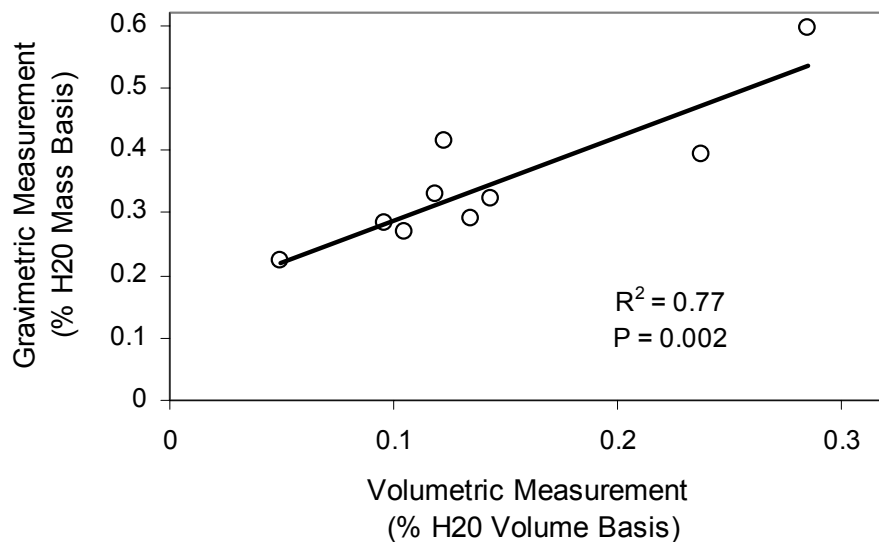


Figure 3.3.3. Comparison of surface soil gravimetric samples to volumetric samples taken from the same locations, three each at the low, mid, and high elevation small watersheds.

Table 3.3.2. Potential predictor variables for empirical moisture models.

Variable	Definition	Comment
Temperature and Precipitation Proxy		
Elev	elevation (m)	relationship commonly represented via lapse rates (Running et al. 1987, Daly et al. 1994)
Drainage Proxies		
Slope	hillslope angle (°)	steep slopes drain quicker than shallow slopes
Dstrm	distance to stream (m)	water drains towards stream channels
RSP	relative slope position	high values: ridges; low values: valleys
TCI	topographic convergence index ($\ln(a/\tan\beta)$)	high values: convergent; low values: well drained (Beven & Kirkby 1979; Moore et al. 1991)
Evaporative Demand Proxies		
TAsp	transformed aspect ($-1 * \cos(\alpha - 45)$)	varies from -1 for NE facing slopes to 1 for SW facing slopes (Beers et al. 1966, Urban et al. 2000)
TASL	slope-corrected transformed aspect ($-1 * \cos(\alpha - 45) * \sin(s)$)	values increased for steep SW facing slopes and decreased for steep NE facing slopes
HS	hillshade ($255 [\cos(S) \sin(s) \cos(\alpha - A) + \sin(S) \cos(s)]$)	corrects for local topographic features; solar azimuth set to 225 degrees and solar inclination set to 45 degrees (ESRI 1994)
PRR	potential relative radiation $\Sigma\Sigma$ (monthly, hourly HS)	integrates solar azimuth and inclination over the course of the day and entire summer (Chapter 3.1)

three sampling areas. For a small subset of the locations we dug pits 80 cm deep in order to sample moisture at 80-100 cm in depth. The time required to create suitable pits in rocky soil constrained our sampling considerably and the interpretation of the deep soil model should be tempered by this limited sample size. From these data, we developed a set of regressions to describe deep (n=16) and shallow (n = 88) soil water trends.

Forward stepwise regression analysis (Sokal & Rohlf 1995) was used to select the most important variables to explain the observed trends in moisture. Each of the variables chosen as a candidate for the models was selected because of its potential influence on soil moisture (Table 3.3.2). Additionally, we considered only variables that could be derived easily from commonly available geographic information systems (GIS) data. These restrictions allowed us to map the results back into geographic space.

Unfortunately, it precluded the use of field measurements such as canopy cover and soil properties in the model. Soil spatial information is generally the least known of the land surface attributes (Band & Moore 1995), and reliable, landscape-scale soils estimates were not available for our study area at the fine-scale resolution needed to capture the variability in this attribute. Variables considered for the model include elevation, slope, distance from stream, relative slope position, and a topographic convergence index calculated according to the formula:

$$TCI = \ln(a/\tan\beta) \quad (eqn. 3.3.1)$$

where a is the upslope contributing area and β is the local slope angle (Beven & Kirkby 1979).

We also examined a wide variety of radiation proxies ranging from simple transformed aspect (Beers et al. 1966) to a potential relative radiation (PRR) measure developed from a digital elevation model (DEM). Chapter 3.1 describes the radiation proxies in detail. The PRR index, developed specifically for use in community level vegetation analysis, is a measure of how topography translates to spatial differences in relative radiation.

$$\text{PRR} = \Sigma \Sigma (\text{monthly, hourly hillshade (HS)}) \quad (\text{eqn. 3.3.2})$$

$$\text{HS} = 255 [\cos(S) \sin(s) \cos(\alpha - A) + \sin(S) \cos(s)] \quad (\text{eqn. 3.3.3})$$

where S is the solar inclination, s is the local slope, A is the solar azimuth and α is the azimuth of the slope facet. PRR both accounts for hillshading effects and integrates over time to account for the fact that solar position changes over the course of the day and year. For this analysis, we integrated PRR over the entire summer growing season.

Spatial scale of variability

In July 2002, we collected 540 field measurements of volumetric soil moisture to test whether our moisture model was able to reproduce the spatial scaling of the water balance (Figure 3.3.2). The synoptic measurements were spread across the landscape in 60 20x20 m plots, covering a range of separation distances from 10's to 1,000's of m. Three 2x2 m quadrats were located randomly within each 20x20 m plot and three randomly located measurements were taken within each quadrat. The variance of the nine plot measurements increased slightly with the mean soil moisture content for the 60

plots ($r^2 = 0.15$, $P = 0.002$). We assessed the characteristic scaling of this dataset through semivariance analysis (Legendre and Fortin 1989) with 250 m lag distance intervals (resulting in 70 to over 200 plot pairs per distance interval) and 5 km set as the largest lag distance (*i.e.*, one-half the smallest dimension of the study area).

Semivariograms are a central tool in geostatistics and are an effective means of describing soil moisture spatial scaling (Western et al. 1998). The features of note in a variogram are the sill (value at which semivariance asymptotes), range (the lag distance at which the sill is reached), and nugget (the Y-intercept, reflecting variation finer-scaled than the minimum lag distance). We normalized the semivariance by simple variance for each of the variograms in order to compare trends in variance across variables (Urban et al. 2000).

We compared the characteristic scaling of measured soil moisture with that of factors highlighted as potentially important to the water regime in the earlier analyses. These included: (1) elevation as an indicator of temperature and precipitation variability; (2) TCI, slope, and Dstrm as topographic measures of drainage and relative slope position; and (3) PRR, HS, and TAspect as measures of radiation (see Table 3.3.2 for definitions of each of the variables). We also examined potentially fine-scale variables that were not included in the regression analysis because they were not available as digital coverages for the entire watershed. Specifically, we investigated the characteristic scaling of: (1) soil depth as a measure of water storage and (2) canopy cover as a modifier of radiation. Thus we analyzed the scaling of both supply terms (precipitation,

drainage and storage) and demand terms (temperature and radiation) of the water balance equation.

Data on these terrain, biotic, and edaphic factors were obtained from the same 60 (20x20 m) plots spread across the HJA landscape. We sampled the terrain-based variables using a 10-m resolution DEM of the HJA. Canopy measurements were taken in the four cardinal directions at each 2x2 m plot. Soil depth was sampled three times and averaged for each 2x2 m plot.

Results

Comparison among permanent TDR sites

Moisture levels were consistently greater for the TDR probes at the high elevation site than the two lower-elevation sites (Table 3.3.3; Figure 3.3.4). The deep soil, in particular, was much wetter at the upper-elevation site.

Precipitation throughfall increased with elevation, reaching its maximum at the high elevation site (Table 3.3.3; Figure 3.3.4). All three of the sites experienced an average of less than 3.5mm of throughfall/day over the three-month period of study, typical for this dry summer system. Figure 3.3.4 illustrates the strong recharge effect of storm events at the low and mid elevation sites. Recharge was not as great at the high elevation site, which had higher pre-storm moisture levels due, at least in part, to greater levels of storage in winter snowpack.

Table 3.3.3. Summary of permanent meteorological station data for the July-September 1999.

	Temperature (°C)		Soil Moisture (volumetric % water)						Throughfall (cm/hr)
	Air	Soil	Upper Slope		Mid Slope		Down Slope		
			0-20cm	80-100cm	0-20cm	80-100 m	0-20cm	80-100cm	
Mean									
MetHigh	15.2	11.0	11.2	26.2	26.7	26.7	19.9	42.2	0.015
MetMid	15.9	12.7	4.0	8.9	9.5	18.8	8.3	21.0	0.012
MetLow	17.6	15.3	12.4	6.4	7.5	9.8	11.0	16.8	0.010
Minimum									
MetHigh	1.3	8.0	7.0	22.3	22.9	25.9	11.7	34.4	0
MetMid	1.2	10.1	2.4	7.7	5.8	14.2	6.2	11.3	0
MetLow	1.2	12.7	10.7	6.1	6.1	8.1	9.2	15.2	0
Maximum									
MetHigh	27.4	14.1	21.2	28.2	33.9	32.0	35.5	49.1	4.1
MetMid	29.9	15.5	6.8	12.3	20.6	22.6	12.8	43.7	2.3
MetLow	32.7	17.9	13.8	7.0	13.6	11.0	22.2	19.5	2.9
Standard Deviation									
MetHigh	5.3	1.3	2.8	1.5	1.9	0.5	4.2	2.1	17.0
MetMid	5.3	1.1	1.0	0.7	2.4	2.3	1.6	6.3	11.8
MetLow	5.9	1.0	0.7	0.2	1.2	0.8	1.8	1.4	10.8

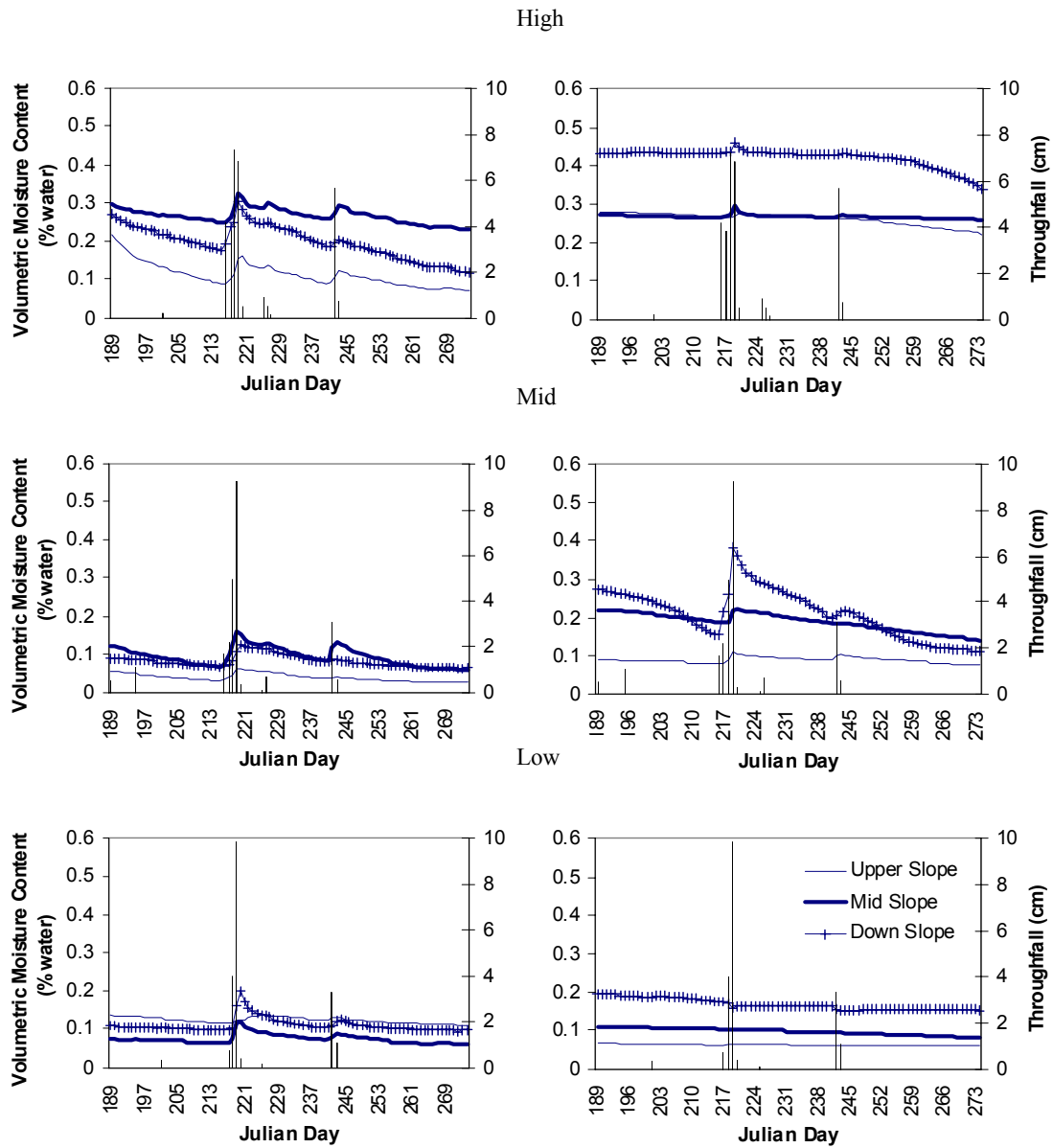


Figure 3.3.4. Soil moisture levels for the permanent TDR sites for the summer 1999. Sensors were placed along a hillslope gradient (upper slope, mid slope and downslope) at each site (high, mid and low elevation). Surface soil measurements are from the top 20 cm of soil; deep soil measurements are from 80-100 cm. Droplines represent throughfall during precipitation events.

Comparison within permanent TDR sites

The average moisture level recorded by the deep soil probes increased from upslope to downslope position within all three sites. The three downslope probes had moisture levels 160 to 260 percent greater than the upslope probes (Table 3.3.3). Differences were less consistent for the surface soil measurements. For eight of the nine locations, the temporal variability at the surface soil sensor was greater than the variability at its corresponding deep soil sensor. Temporal variability also was greater at downslope positions than upslope positions (Table 3.3.3). Because there were a few occasions where the rank order of the wettest to driest probes changed as the soils became desiccated, we decided to conduct future synoptic sampling as early into the summer, dry season as possible (*i.e.*, the beginning of July). Again, we were interested in modeling the spatial distribution of soil moisture primarily for use in vegetation analysis. Early summer represented the period of maximum tree growth. Later in the summer, growth declines, as the system becomes moisture limited. Practical concerns also were considered in choosing the time period for future sampling. Under increasing drought, local controls dominate and terrain influences, which can be easily incorporated in landscape-scale models, are overwhelmed by fine-scale influences (*e.g.*, soil variability), which are less easily incorporated in landscape-scale models.

The permanent TDR data also emphasized the importance of stratifying across elevation and hillslope position. These associations were examined further through the gravimetric sampling.

Gravimetric sampling

A similar increase in moisture with elevation was observed in the gravimetric samples (Figure 3.3.5). Moisture levels were higher in August than July because of the August 5-6 rain event. The importance of elevation as an explanatory variable decreased from July ($r^2 = 0.60$, F-statistic = 30.1, $P < 0.001$) to August ($r^2 = 0.31$, F-statistic = 8.8, $P = 0.008$). After accounting for elevation differences, summer radiation was highlighted as a potential explanatory variable. We, therefore, made certain to stratify across elevation, hillslope position (highlighted in the permanent TDR data analysis), and aspect (highlighted in the gravimetric moisture analysis) in sampling for our empirical model.

Empirical model

According to the regression analyses of the volumetric samples, factors important to deep soil and surface soil moisture patterns are similar but have some important differences (Table 3.3.4). Deep soil moisture was correlated with elevation ($r^2 = 0.19$) and slope ($r^2 = 0.21$). The model for surface soils was slightly more complicated. Local hillslope/drainage factors (distance from stream) and elevation also were important ($r^2 = 0.19$ and 0.21 , respectively), but radiation differences were much more significant than they were for deep soils ($r^2 = 0.08$). Sites with a high solar exposure had significantly drier surface soils than more shaded sites.

The residuals from the surface soil model were normally distributed with a slight skew towards under-predicting values at the wet end of the spectrum (Figure 3.3.6). The

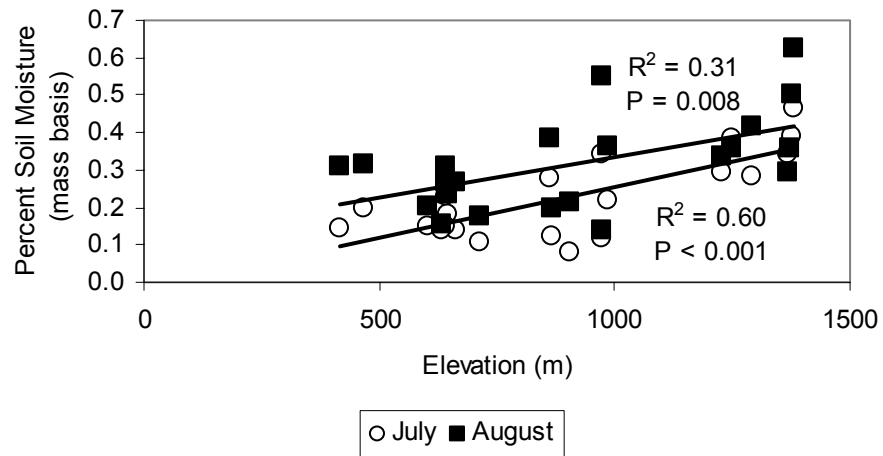


Figure 3.3.5. Gravimetric moisture as a function of elevation for August and July 1999 samples. The August sampling was preceded by a two-day rain event the previous week.

Table 3.3.4. Regression statistics for July 4, 2001 empirical moisture models.

	R^2	F-Statistic	Pr(F)	N
Surface Soil Moisture (0-20cm)				
$\hat{y} = \beta_0 - \beta_1 Dstrm + \beta_2 Elev - \beta_3 PRR$	0.48	25.46	< 0.0001	88
Deep Soil Moisture (80-100cm)				
$\hat{y} = \beta_0 - \beta_1 Slope + \beta_2 Elev$	0.40	4.30	0.04	16

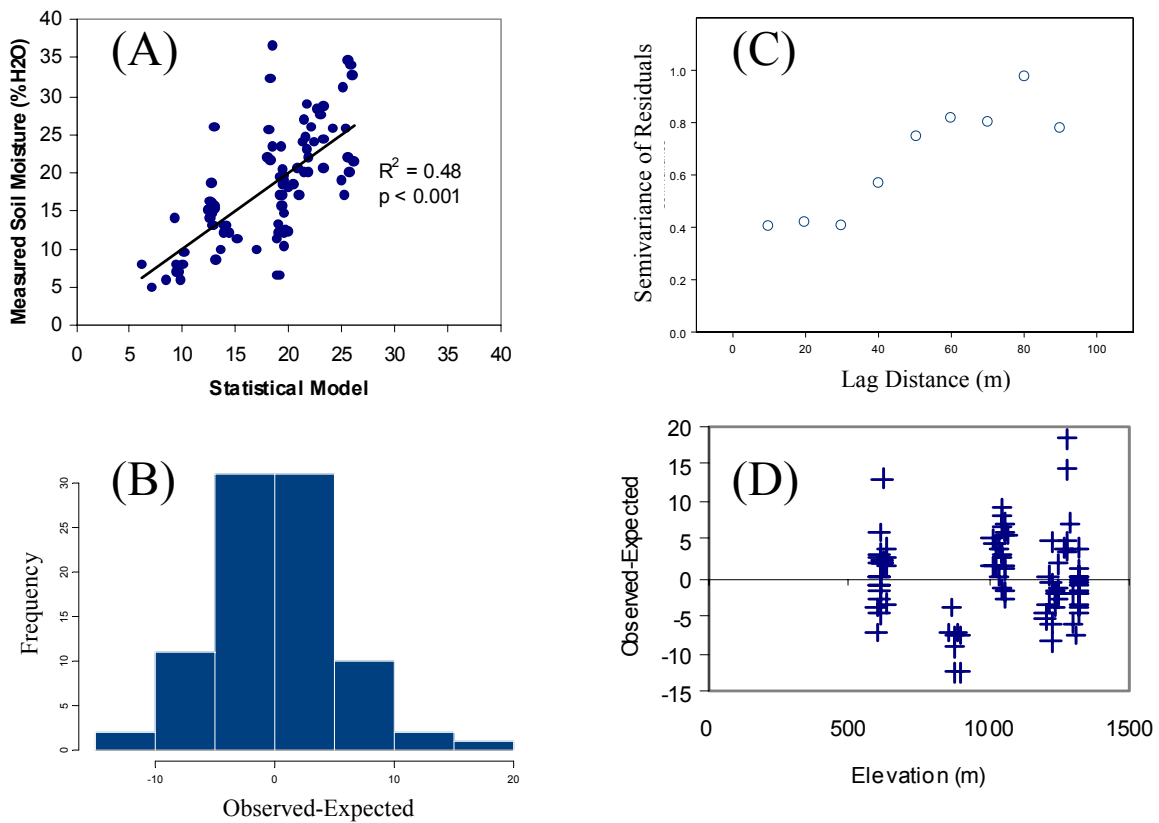


Figure 3.3.6. Comparison of surface soil moisture estimates from the regression model and field data used to construct the model ($N = 88$). (A) The model combines the influences of elevation, distance from stream, and potential relative radiation into a single factor. The residuals are (B) normally distributed, (C) autocorrelated up to 50 m and (D) not significantly related to elevation, although one transect at mid elevation was consistently drier than predicted.

residuals were not significantly correlated with elevation, although there was a cluster of points from one transect between 850 m and 900 m with measured soil moisture values more than one standard deviation below the modeled values (Figure 3.3.6). The residual clustering is likely indicative of the autocorrelation in the data rather than a persistent elevation trend, as model residuals are autocorrelated up to a distance of approximately 50 m (Figure 3.3.6). This distance represents approximately one-half the average transect length. Removing the 850-900 m transect from the analysis improved the regression model fit ($R^2 = 0.58$, F-statistic = 35.4, $P < 0.001$), but the resulting model may be less representative of the diversity of the landscape.

Variograms

The landscape-wide soil moisture samples exhibited variability at multiple scales. Fine-scale variability was indicated by the relatively large nugget variance (Figure 3.3.7). The average variance within the 2x2 m sample quadrats (5.5) and within the 20x20 m sample plots (9.6) also was fairly high relative to the total variance for all 540 samples (16.8). The empirical variogram (points in Figure 3.3.7) did not fit a classic variogram model of increasing variance to an asymptotic sill, and is presented with a lowest-smoothed curve in Figure 3.3.7. The variance did reach a peak at 1500-2000 m, but decreased for separation distances from 2000-4000 m. A second increase in variance was observed at larger distance lags. This complex pattern of variability confirmed that any explanatory model of soil moisture spatial trends would need to account for influences at multiple scales.

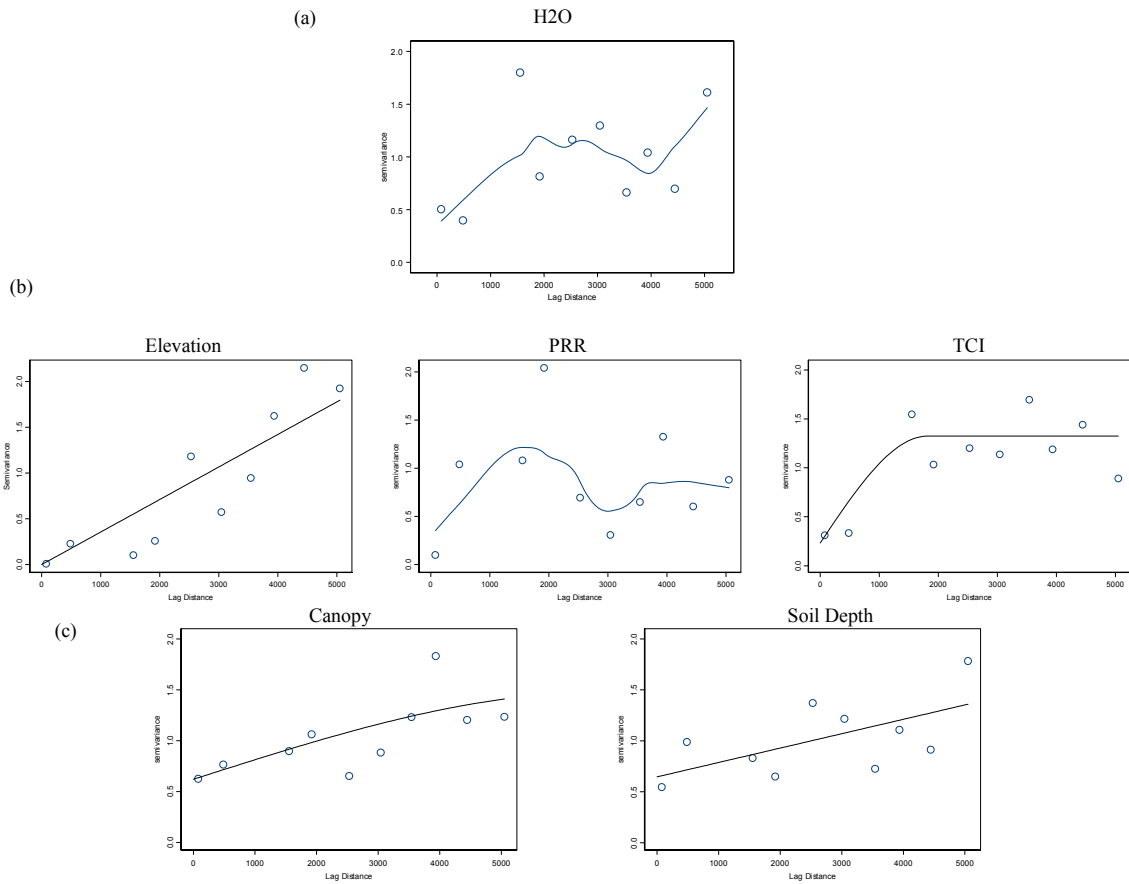


Figure 3.3.7. Spatial scaling of soil moisture and factors important to the water budget as depicted by variograms. Data were obtained from 60 20-m² plots sampled across the HJA landscape (nine measurements taken per plot). All semivariance values have been relativized by total variance for that variable in order to facilitate comparisons across variables. (a) Measured volumetric soil moisture. (b) Terrain-based explanatory variables elevation, summer PRR, and TCI. Values were derived from a DEM. These three variables are representative of the types of curves calculated for terrain variables. (c) Canopy and soil depth. Lag distance was set to 500-m increments and only bins with at least 50 sample pairs were graphed.

The environmental variables that we had determined to be important in our earlier analyses differed considerably in their characteristic ranges. Elevation exhibited a monotonic increase in variance with lag distance, indicative of a simple gradient (Figure 3.3.7). Other DEM-based variables were finer-scaled than elevation. PRR and other measures of radiation reached their maximum values at a range of 1000-2000 m. This distance roughly matches the average hillslope length for the major watersheds contained within the HJA. Like the moisture measurements, these variables did not conform to a classic variogram model, but instead exhibited a decrease in variance at larger lag distances. Though this decrease is undoubtedly a sampling effect (*e.g.*, a complete sampling of the PRR grid for the HJA resulted in no such decrease), it may be important in explaining the similar trend observed for the moisture measurements. TCI and other measures of hillslope position/drainage also were highly related to hillslope length. They reached asymptotic sills at around 1500 m. That this distance corresponds with the peak observed for the soil moisture measurements provides corroborating support that these small-watershed scale topographic variables can be used effectively to describe some of the spatial patterning in soil moisture. The monotonic elevation gradient likely acts as an underlying forcing variable.

The fine-scale variability in soil moisture indicated by the large nugget is probably not a consequence of topography. None of the terrain-based variables had exceptionally large nugget variances.* Canopy cover and soil depth, in comparison, had large nugget variances indicating variation at lag distances finer than were captured in the

* It is important to note that although the smooth curve fit through the PRR data in Figure 3.3.7 does suggest a sizable nugget variance, the variance in the smallest distance class for PRR and the other radiation proxies was very small.

analysis (Figure 3.3.7). These biotic and edaphic factors were highly variable across all spatial scales.

To pursue the large nugget variance in soil moisture, we examined the variation in the soil moisture measurements collected for the empirical modeling, which were gathered at a much finer resolution (Figure 3.3.8). The variation in these measurements increased over the first 100 m in lag distance, indicating some consistency in measurements taken over 10's of m. In other words, measurements taken within 10 m of one another were substantially more similar than measurements taken 100 m apart. We concluded that: (1) variability in soil moisture crosses multiple spatial scales; and (2) the interaction of multiple physical and biological influences (including biotic and edaphic factors on the order of 100 m, slightly larger-scale variability in topography, and an elevation forcing) combine to shape the complex water dynamics of the HJA during this important period of summer drawdown.

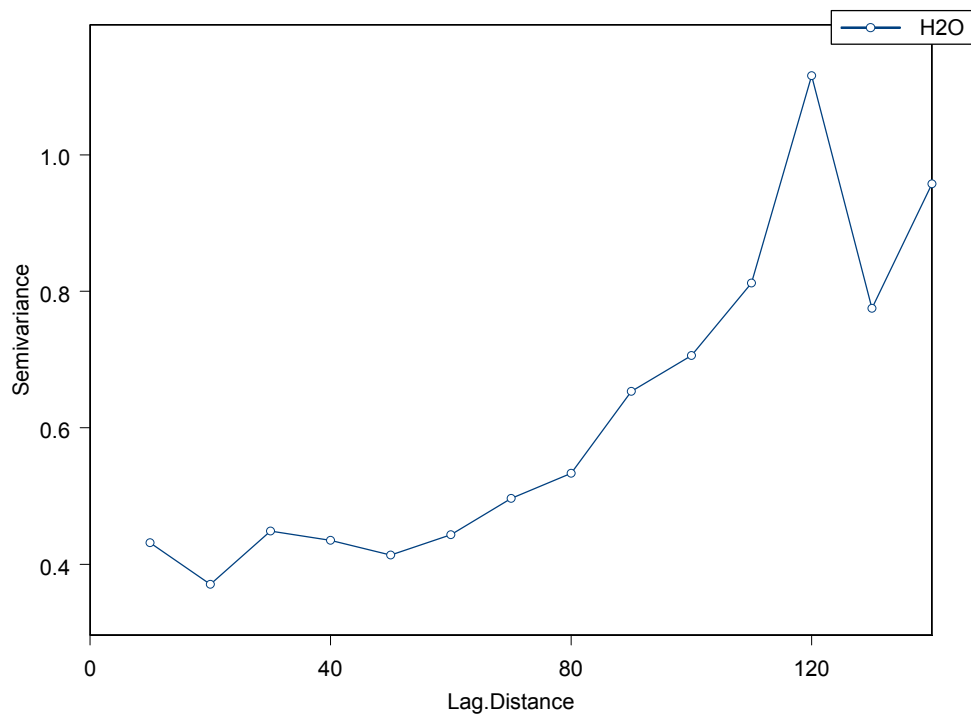


Figure 3.3.8. Variogram of fine-scale trend in moisture content from samples taken in three small watersheds as part of regression analysis ($N = 88$). Samples were taken along short transects (up to 110 m in length) at intervals of 5-10 m. Lag distance was set to 10-m increments.

Discussion

The surface soil regression model was able to combine multiple physical factors with different characteristic spatial scaling into a single coherent equation that explains nearly 50 percent of the variance in the field measurements. A major challenge in describing ecological patterns is that they are sensitive to the scale of observation (Levin 1992). Chen et al. (1999) argue that microclimate has distinct spatial scales corresponding to distinct components of landscape structure. These relationships rarely have been examined across a continuum of spatial scales, because of difficulties in sampling simultaneously across large spatial extents. Technology developments over recent years, however, have greatly increased the feasibility of such studies. For example, we showed in previous research how temperature can vary with proximity to stream on a local scale and elevation on a landscape scale (Lookingbill & Urban 2003). Here, we show how soil moisture varies negatively with elevation on local scales (*i.e.*, water flows downhill) and positively with elevation on landscape scales (*i.e.*, saturated clouds precipitate water when forced to rise over mountains and evapotranspiration decreases with cooler temperatures at higher elevation).

The 1500 m range of soil moisture variability indicated by the variogram analysis may be a reflection of topographically induced patterns in soil moisture associated with shaded north-facing slopes compared to hot, dry south-facing slopes. This distance corresponds with the average hillslope length in the basin. The importance of topographic exposure also is reflected by the radiation term in the regression equation. These findings are consistent with others that have shown that topographic variability is an important

control of spatial differences in July air temperatures for the HJA (Smith 2002, Lookingbill & Urban 2003). Temperature, in turn, can be a significant control on moisture levels.

Although we were able to capture the influences of both macroscale (climate) and mesoscale (topographic drainage and radiation) factors on summer soil moisture in the HJA, we did not have the data to add microscale factors (*e.g.*, soil variability) to the model. The high nugget variance in the landscape-level soil moisture variogram indicates that much of the variability in soil moisture occurred below the sampling grain captured in the 20x20-m plots. Grayson et al. (1997) also found a high-level of local control during the dry season in their seasonal watersheds. In the HJA, Post and Jones (2001) found the greatest exertion of fine-scale influences on the hydrologic regime at the end of the summer drought period.

Quality information on the fine-scale variability of soils is rarely available for even the best-studied systems (Band & Moore 1995). Yet, numerous studies have illustrated that soil properties can be at least as important as terrain-based variables in determining soil moisture content (*e.g.*, Helvey et al. 1972, Boyer et al. 1990, Yeakley et al. 1998). Even if we had the field data to add edaphic variables to the regression model, we would not have the necessary coverages to extrapolate this new model to the entire HJA landscape. Because we posit that much of the fine-grained variability in soil moisture may be due to soil variability, failure to accurately represent variability in soils can compromise substantially the explanatory and predictive capabilities of the model for fine-grained applications.

Our empirical model results corroborate Yeakley et al.'s (1998) conclusion that deep soil water distributions may be very different from surface soil moisture patterns. This finding has important implications for the analysis of ecological processes. For example, the surface soil moisture model that includes radiation as an explanatory factor may be appropriate for predicting seedling establishment. It is probably not the best model for predicting rates of growth for trees whose roots can integrate over a much deeper area than the top 20 cm of soil. A weighted model combining the deep and shallow estimates may be more suitable for this application. Again, we emphasize that any interpretation of the deep soil regression must bear in mind the logistical difficulties of sampling deeper soil layers and the resultant small sample size. We offer these results as a crude comparison with the shallow soil model only.

In the past 20 years, digital terrain based indices have become very popular in describing soil moisture (Beven & Kirkby 1979, Parker 1982, Iverson et al. 1997). This popularity has been driven in part by an increase in computing technology, but also by a lack of field data. Those field measurements that are available are often in locations that are not representative of the landscape as a whole (*e.g.*, watershed base or few prominent peaks; Phillips et al. 1992, Daly et al. 1994). Collecting additional data has been logistically and economically prohibitive. It is important, however, not to forget about field data. Its value is not diminished by the expanse of GIS applications but rather is enhanced. As shown here, field data can be a valuable tool in calibrating relationships for GIS derived variables. Conversely, GIS can be a valuable tool in helping to identify the best sites to locate field samples. For example, the regression model can be used in a

GIS framework to make a predictive map of soil moisture differences for the study area (Figure 3.3.9). This map identifies geographic locations within the HJA that could be targeted in future sampling to test the effectiveness of the model in describing spatial patterns in soil moisture (Chapter 3.4).

It is important to emphasize that the results presented in this analysis are applicable to only a very narrow range of conditions. As with any statistical model, our model should not be extrapolated beyond the range of conditions specified by the input data. These include the topographic and climatic conditions of the study area, the timing of the sampling in mid-summer, and the stand structure of old-growth forest. We were interested in developing a simple moisture model for exactly these conditions as part of an effort to explain landscape-scale patterns in vegetation. We present the approach as an example for others who may be interested in developing models of their own for other specific applications. The empirical approach provides an alternative to more commonly used moisture proxies that rely solely on geographic abstractions of the landscape (*e.g.*, TCI: Beven & Kirkby 1979). If the objective were to develop a more comprehensive spatio-temporal description of the HJA's moisture regime, the data and patterns described in this paper would be of great value as a reality check and calibration tool (Chapter 3.4).

A thorough examination of the major components of the water balance can provide a basis for varied studies of ecological processes in montane systems. We are interested particularly in better understanding the relationship between the distribution of forest vegetation communities and the physical environment. Soil moisture is without question a dominant factor in shaping these distributions. We have shown that factors

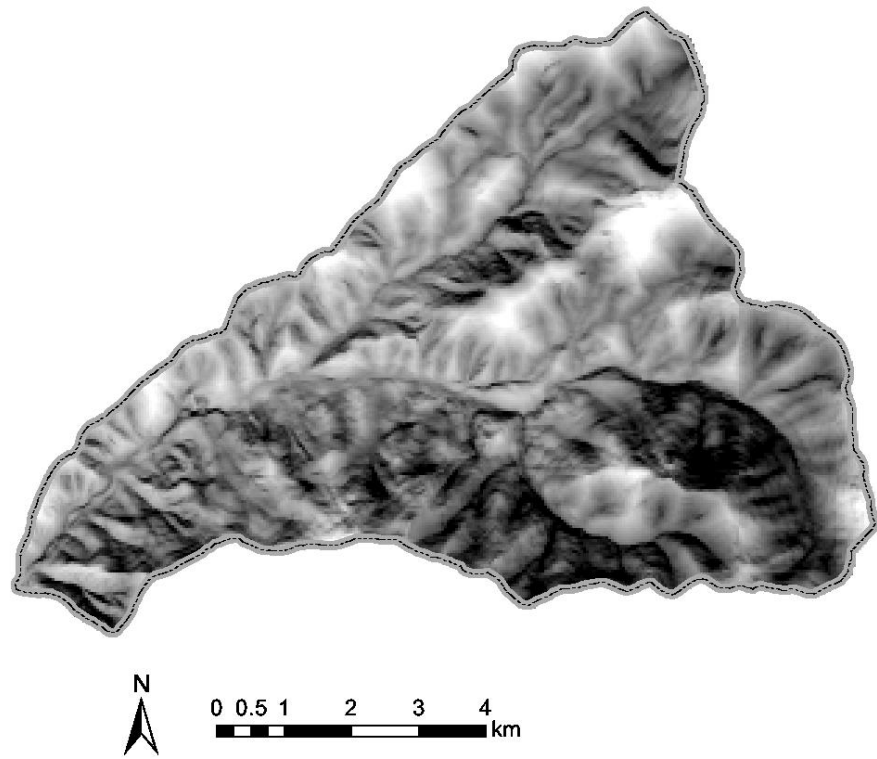


Figure 3.3.9. Statistical model of surface soil moisture mapped back onto the landscape. Darker areas are predicted to be wetter than lighter areas.

important to the summer water balance (as determined by regression analysis) vary at different characteristic spatial scales (as shown through analysis of semivariance); thus, we are able to reproduce the spatial scaling inherent in soil moisture measurements through regression equations of key environmental variables (Figure 3.3.7a and Figure 3.3.10). The regression modeling allows us to extrapolate field measurements of volumetric moisture across similar topographic areas, although we caution that great care should be taken to apply the models only within the restricted domain for which they were built. This type of improved spatial mapping of soil water variability should be beneficial to a wide range of forest community studies and other ecological applications.

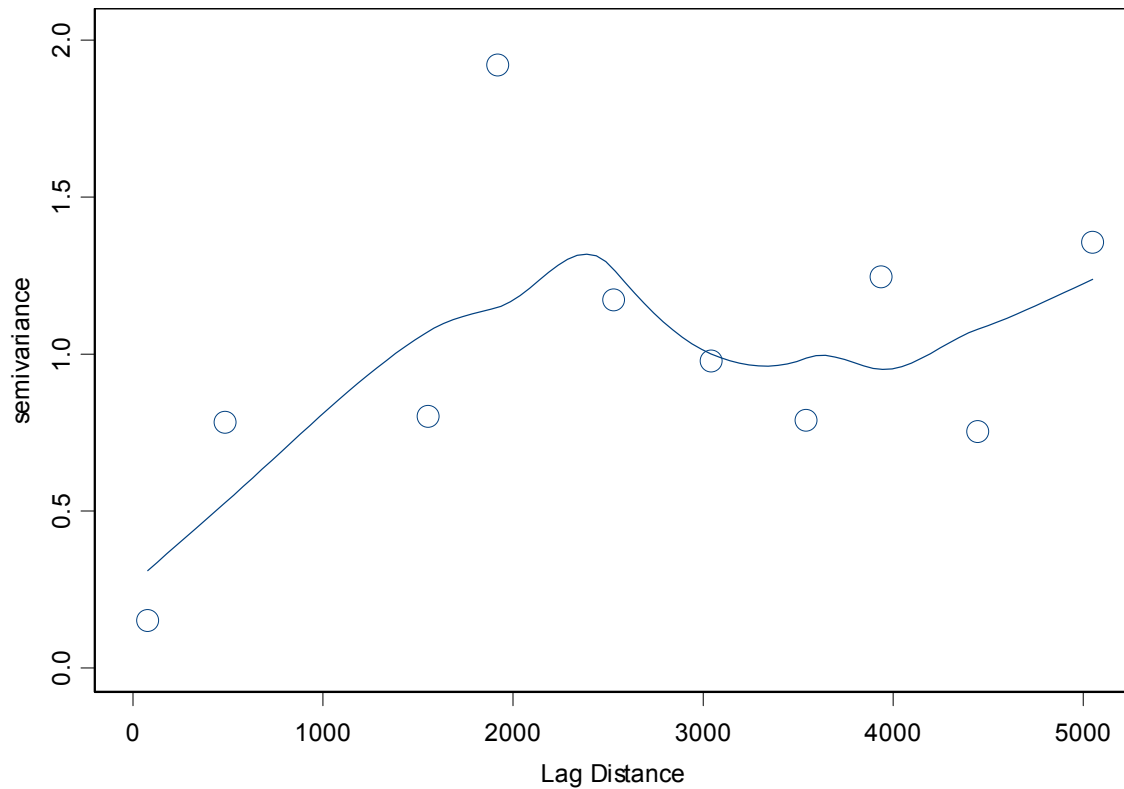


Figure 3.3.10. Variogram of fitted values from regression analysis of surface soil moisture ($N = 60$). The model captures many of the same scaling relationships depicted for field measurements of soil water content (Figure 3.3.7a) by using elevation (increasing trend), radiation (decrease in variance after ~ 2000 m), and distance from stream (sill at ~ 2000 m). Lag distance was set to 500-m increments and only bins with at least 50 sample pairs were graphed.

CHAPTER 3.4 Estimating Spatial Patterns of Summer Soil Moisture: Model Comparison

Abstract

Improved spatial models of primary resource constraints such as soil moisture are needed for landscape-level ecological applications. We have developed five different model descriptions of relative, spatial moisture differences for a well-studied watershed in the Pacific Northwest USA. The models are, in order of increasing complexity: (1) a soil moisture index based solely on local slope angle and upslope contributing area (TCI); (2) a soil moisture index based on both terrain attributes and soil properties (IMI); (3) a statistical model using empirical data to derive the relationship between soil moisture and terrain variables; (4) a steady-state simulation model with spatial evaporation differences (Topog); and (5) a dynamic simulation model that incorporates variable terrain, climate and moisture demand (RHESSys). The use of field studies to test hydrologic models has been under-emphasized. We evaluate the models in terms of their ability to predict two different validation datasets collected through field measurements of soil moisture. Tradeoffs are associated with increasing model complexity, especially when attempting to represent multi-scale spatial processes. Our findings show that spatially implicit statistical models can effectively capture soil moisture variability within specific temporal and spatial domains. For extrapolations beyond these boundaries, more sophisticated models may be warranted. Appropriate model selection ultimately depends on the ecological issue to be addressed and the temporal and spatial domain of application.

Keywords: soil moisture content, spatial variability, landscape-scale, empirical sampling, topographic index, simulation model, H.J. Andrews Experimental Forest

Introduction

Temperature and moisture have long been recognized as primary constraints on forest community composition in montane systems (Dyrness et al. 1976). Unfortunately these factors are difficult to quantify at high resolution for large spatial extents (Chen et al. 1999). Spatial data collection networks for these variables are particularly sparse over mountainous terrain (Phillips et al. 1992, Daly et al. 1994). As a result, elevation is typically used as a proxy variable to describe the relationship between the environmental gradient complex and forest communities (Whittaker 1978). This elevation correlation model greatly oversimplifies the range of variability associated with the physical environment. For example, Stephenson (1990) suggests that both temperature and moisture are influenced by physical factors at multiple spatial scales (*e.g.*, macroscale air currents, mesoscale topography and microscale soil properties). More complex models are required to adequately represent the major components of the physical environment for vegetation analysis and related ecological applications.

Trade-offs exist between model complexity and other desirable attributes of models (Beven 2001, Gardner & Urban *in press*). Increasing the comprehensiveness of a model often requires sacrifices in model simplicity and tractability. The inclusion of additional interactions and feedbacks requires additional parameters and calibration (O'Neill & Gardner 1979). As more information is added, model sins of omission can be replaced by sins of commission (Peters et al. *in review*). Errors are associated with the selection of model formulation, measurement of the input data, and the estimation of parameters (Peters et al. *in review*).

In this study, we compare the ability of models of increasing complexity to describe spatial patterns in soil moisture. Several studies have demonstrated the correlation between soil moisture and plant establishment (Taylor 1995, Woodward 1998, Breshears & Barnes 1999). Spatial patterns of soil moisture help to drive differences in forest productivity (Vertessy et al. 1996), species composition/richness (Hutchinson et al. 1999) and nutrient cycling (Creed & Band 1998). A model of relative moisture, therefore, could be applied to a variety of research and management issues.

Elevation is only one example of a terrain-based index of soil moisture that can be estimated from a Digital Elevation Model (DEM). Other crude moisture indices include measures of slope angle, aspect and slope position. More practical indices can be derived through transformation of these variables (*e.g.*, transformed aspect; Beers et al. 1966). Additional DEM analysis has yielded a number of popular soil moisture indicators. Among the more common of these proxies is a measure of flow accumulation as determined by topographic convergence (Beven & Kirkby 1979). Other DEM-derived measures, such as topographic solar radiation (Dubayah & Rich 1995), provide estimates of spatial patterns in energy for evaporation.

Variability in soil properties also can result in differences in soil moisture content. Several studies have found that soil properties are at least as important as topographic variables in dictating soil water distributions (Helvey et al. 1972, Boyer et al. 1990). In general, soils with high clay content have higher moisture content than sandy soils in similar environments. Similarly, deep soils can hold more water than shallow soils.

Iverson et al. (1997) developed an index that recognizes the importance of both terrain and soil properties on the water balance. Their Integrated Moisture Index (IMI) was used to characterize the soil moisture gradient for oak woodlands in southern Ohio. The IMI combines measures of flow accumulation, slope curvature, radiation shading (all derived from a DEM) and soil water holding capacity (derived from soil depth and texture properties).

Field measurements of moisture can be used to identify significant terrain and soil variables and parameterize their relationships with soil moisture in a statistical model. This approach has been used to evaluate soil moisture predictor variables in small-scale studies of hillslopes (Yeakley et al. 1998), agricultural fields (Hawley et al. 1983), and treefall gaps (Gray and Spies 1995). The development of landscape-scale statistical moisture models has been less practical due to the difficulty in data collection. Advances in technology, including portable sampling devices, have made it more feasible to collect large samples for statistical analysis (Grayson & Western 2001, Noborio 2001). Time Domain Reflectometry (TDR), in particular, is a rapid, nondestructive sampling tool that is growing in popularity for forest research (Gray & Spies 1995). As with any statistical model, issues remain regarding the domain of applicability of these models (Levins 1966).

Mechanistic or process models comprise the most complex model types in this continuum. They base predictions on real cause-effect relationships (Guisan & Zimmerman 2000). As opposed to the indicators previously discussed, hydrologic simulation models explicitly consider the flow of soil water along topographic gradients

(Grayson et al. 1992). Static models assume equilibrium conditions and provide a steady-state description of the system. Dynamic models are not limited by this assumption and can incorporate dynamic weather events and changes in ecophysiology. As a result, they can generate time-series of predictions but require more data to do so.

In this investigation, we compare the spatial representation of relative soil moisture differences in a forested landscape of western Oregon under a series of increasingly complex models. Models are comprised of a DEM-derived proxy, an index combining terrain and soils data, a statistical model derived from empirical soil moisture data, a static process model and a dynamic process model. The models are compared in terms of their ability to predict patterns of relative wetness as captured through field sampling at multiple spatial scales.

Site description

The H.J. Andrews Experimental Forest (HJA) is located on the west slope of the Cascade Mountains. It is comprised of the Lookout Creek watershed, 80 km east of Eugene, Oregon. The Long Term Ecological Research (LTER) site covers 6400 ha and ranges in elevation from 410 m to 1630 m (McKee 1998). At the time of its establishment in 1948, the HJA was an intact forest with about 65 percent of the land in old-growth (*i.e.*, 400-500 years old). Since that time, old-growth forest has been reduced to roughly 40 percent of the total area due to logging activities.

As an LTER site, the HJA maintains an extensive database of meteorological data. Climate is characteristic of the Pacific Northwest, with dry summers and wet winters. Annual precipitation ranges from 2200 mm at the base of the watershed to 3400 mm at upper elevations, with less than 300 mm normally falling during the growing season (Grier & Logan 1977). Soils are mostly deep, well-drained Inceptisols. Rooting occurs almost entirely in the upper 200 cm of soil. Textures range from gravelly, silty clay loam to very gravelly, clay loam (Grier & Logan 1977). Lower-elevation soils are older than upper-elevation soils, dating back to the Oligocene-lower Miocene. Upper-elevation soils are comprised of younger andesite lava flows and High Cascade rocks.

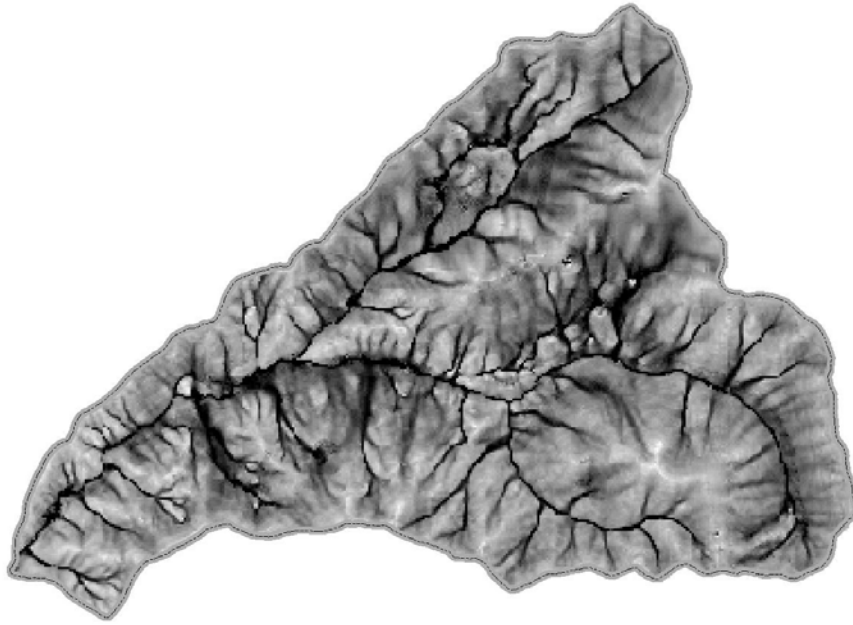
Topographic position is an important control on vegetation in this region (Zobel et al. 1976). *Pseudotsuga menziesii* (Douglas fir), *Tsuga heterophylla* (western hemlock), and *Thuja plicata* (western redcedar) are the dominant species at lower elevations. *Abies amabilis* (Pacific silver fir), *Abies procera* (noble fir), and *Tsuga mertensiana* (mountain hemlock) populate upper elevations (Franklin & Dyrness 1988). Ohmann and Spies (1998) suggest that elevation and associated macroclimate are the major correlates with regional patterns of community composition in Oregon.

Model Descriptions

Soil moisture indices

Two derived moisture indices were considered in this analysis: TCI and IMI (Figure 3.4.1). The first, a simple topographic convergence index (Beven & Kirkby 1979), was calculated using a 10-m resolution DEM according to the formula:

A)



B)

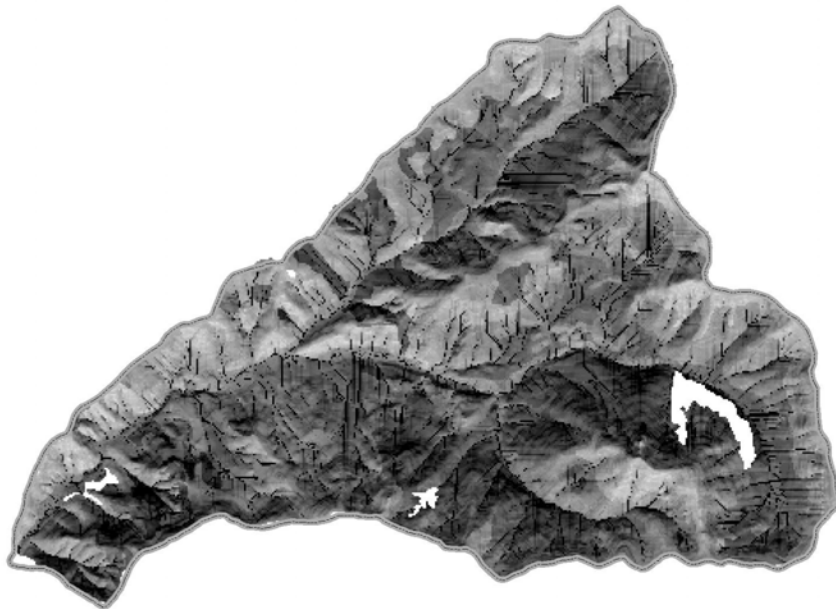


Figure 3.4.1. Soil moisture indices. A) Topographic Convergence Index after Beven and Kirkby (1979). B) Integrated Moisture Index after Iverson et al. (1997). Dark areas are estimated to be locations of high moisture.

$$TCI = \ln(a/\tan\beta) \quad (\text{eqn. 3.4.1})$$

where a is the upslope contributing area, and β is the local slope angle. Sites of high convergence should accumulate water and be wetter than sites of low convergence. This index represented an effort to describe spatial patterns in soil moisture based solely on placement within the topographic complex.

The integrated moisture index (Iverson et al. 1997) combined important terrain attributes with information on soil properties to estimate moisture patterns. The index combined four environmental factors that influence soil moisture levels: flow accumulation, slope curvature, radiation and soil water holding capacity.

The first three factors were derived from a 10-m DEM of the HJA. We developed a flow accumulation coverage from the DEM following the principles of topographic convergence used in the TCI calculation. Slope curvature was characterized as concave or convex based on the height of the cell and surrounding cells in the DEM. High values represented convex landforms, associated with drier soils; low values represented concave landforms, associated with wetter soils. Solar exposure levels were estimated by placing the HJA into the larger context of its surrounding landscape and calculating the incident solar exposure after accounting for topographic shading. We applied a southern exposure (180°) at mid-day (45° solar angle) for this calculation. Low values represented exposed, south-facing slopes and high values represented lower radiation slopes.

Soil water holding capacity was estimated from soil texture and soil depth coverages of the HJA (<http://www.fsl.orst.edu/lter>). Soil depth was classified into three

depth classes: 1 = 1 – <3 ft, 2 = 3 – 10 ft, and 3 = >10 ft. Soil texture was classified into 10 classes that represented increasing water-holding capacity with increasing pixel value:

- 1 = quarries
- 2 = cobbly sandy loam
- 3 = gravely loam
- 4 = dark poorly drained
- 5 = gravely sandy loam
- 6 = bedrock talus
- 7 = cobbly heavy loam
- 8 = gravely clay loam
- 9 = light clay loam.

Texture and depth values were multiplied together to provide an estimate of water holding capacity that increased with improving soil type and increasing depth.

All four coverages were scaled from 1-100 with higher values representing potentially wetter conditions. They were then combined into a single index (IMI) based on weights recommended by Iverson et al. (1997) for predicting hillside moisture availability (flow accumulation - 30%, curvature - 10%, hillshaded radiation - 40%, and water holding capacity - 20%).

Statistical model

We developed a statistical model of relative soil moisture based on synoptic time domain reflectometry (TDR) sampling within three small watersheds of the HJA

(Chapter 3.3). We used handheld probes (Hydrosense, Campbell Scientific Incorporated) in order to collect measurements rapidly over a large area. The three sampling areas were located at low (mean elevation of samples = 613 m), mid (989 m) and high (1285 m) elevation sites within the HJA. Two sampling stations were located in the *T. heterophylla* vegetation zone; the third was located in the *A. amabilis* zone.

A total of 79 moisture samples were taken on July 4, 2001. Each sample represented the average of three measurements taken within 1 m². Measurements were taken along short transects representing different hillslope aspects and positions within each of the sampling areas. Samples were separated by a minimum of 5 m and integrated over the top 0-20 cm of soil. The beginning and endpoint of each transect were recorded using a PRO/XRS 12 channel Trimble GPS, which reported 95 percent confidence intervals of 1-2 m. An additional nine measurements were added to the analysis from water content reflectometer probes (Campbell Scientific Incorporated) hooked to permanent meteorological stations at the center of each of the three sampling areas, bringing the total number of measurements to 88: 22 at low elevation, 34 at mid elevation and 32 at high elevation. From these data, we developed a regression equation to describe surface soil moisture trends.

Forward stepwise regression analysis (Sokal & Rohlf 1995) was used to select the most important variables to explain the observed trends in moisture. Each of the variables chosen as a candidate for the models was selected because of its potential influence on soil moisture. Additionally, all of the variables could be derived easily from commonly available geographic information systems data. We overlaid the sample locations on a

10-m resolution DEM to estimate those variables derived from terrain data. We considered elevation, slope, distance from stream, relative slope position (0 = valleys; 100 = ridges), TCI, and a wide variety of radiation proxies ranging from simple transformed aspect (Beers et al. 1966) to a potential relative radiation (PRR) measure developed from DEM data. Chapter 3.1 describes the radiation proxies in detail. The PRR index, developed specifically for use in community level vegetation analysis, is a measure of how topography translates to spatial differences in relative radiation. It both accounts for hillshading effects and integrates over time to account for the fact that solar position changes over the course of the day and year.

The following variables were flagged as the strongest explanatory variables and combined additively in the regression model:

$$\hat{y} = \beta_0 - \beta_1 Dstrm + \beta_2 Elev - \beta_3 PRR \quad (\text{eqn. 3.4.2})$$

where *Dstrm* is distance from stream, *Elev* is elevation, and *PRR* is cumulative radiation over the entire summer. Relative soil moisture values were mapped back across the entire HJA using this statistical model (Figure 3.3.9). Chapter 3.3 describes the model development in greater detail.

Process models

We examined two different mechanistic process models: TOPOG in its steady-state formulation and RHESSys as a dynamic simulator (Chapter 3.4.2). Both explicitly consider the flux of soil water along topographic flowpaths, though the flowpaths are derived slightly differently.

A)



B)

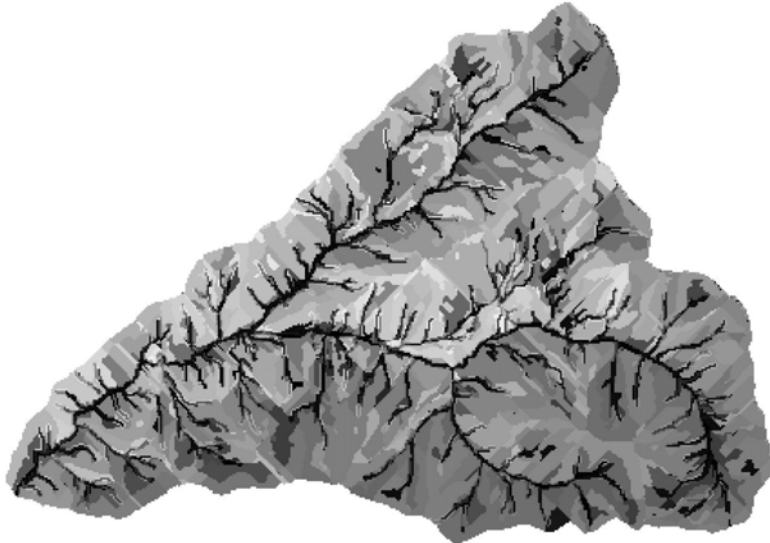


Figure 3.4.2. Process Models. A) Topog with evaporation weighted as a function of radiation. B) RHESSys run for July 17, 2002. Dark areas are estimated to be locations of high moisture.

TOPOG

TOPOG is a terrain analysis-based hydrologic modelling package developed by CSIRO Land and Water and the Cooperative Research Centre for Catchment Hydrology, Australia (O'Loughlin 1986). We used TOPOG version 9.21 (May 2000) for our analysis. It is a deterministic hydrologic modelling package comprised of over 30 FORTRAN and C programs. Common applications include its use to describe the topographic attributes of complex three-dimensional terrain, to simulate the transient hydrologic behaviour of catchments and how this is affected by changing catchment vegetation, and to model the growth of vegetation and how this impacts the water balance (Vertessy et. al 1993, Dawes et. al 1994, Wu et. al 1994).

One of the primary strengths of TOPOG is that it makes use of a sophisticated digital terrain analysis model, which accurately describes the topography of complex landscapes. Water is distributed among catchment elements, which can be irregularly shaped and therefore are free to more closely match the structure of the terrain than a rigidly defined grid. TOPOG is intended for application to small catchments (up to a maximum 10 km² and generally smaller than 1 km²). The application of the model to the HJA watershed (64 km²), therefore, is stretching the normal bounds of operation. Due to this limitation, we restricted the application of TOPOG to its steady-state mode in this analysis and did not use it to model dynamic responses to weather and plant processes.

The foundation for the TOPOG simulation is the three-dimensional representation of the landscape. Since elements are defined by the intersection of elevation contours

and perpendicular flow trajectories, the number of elements in a watershed is dependent on both of these factors. We used a combination of 30-m elevation contours and a trajectory spacing of 120 m along the contours to define 6700 relatively square elements. Elements varied in size depending on their placement in the landscape, but the median element size was 84x84 m. Even this relatively coarse network contained too many elements to conduct dynamic simulations for this version of TOPOG.

Steady-state simulations were run in two modes. The first computed a drainage index following O'Loughlin's (1986) initial formulation of the model. The normal drainage index (W) was calculated for each element in accordance with the local slope, contributing area, evaporation rate, and soil transmissivity.

$$W(x, y) = \frac{1}{mbT} \int qdA \quad (\text{eqn. 3.4.3})$$

where:

m = slope (m/m),

b = length of contour at base of element (m),

T = local soil transmissivity (m^2/d),

A = element area (m^2), and

q = net subsurface drainage flux; precipitation-evaporation-vertical drainage (mm/d).

Both the net subsurface drainage flux and the transmissivity were assumed to be spatially uniform for these simulations. The subsurface drainage flux was set to 1.0 mm/d , which resulted in an output baseflow value similar to that given in the radiation

weighted simulations described below. Soil transmissivity was varied along a reasonable range of values (1 m²/d to 15 m²/d) to explore the influence of this parameter on model output. Increasing the soil transmissivity resulted in drier soils, more stream and baseflow, and less exfiltration. A transmissivity value at the upper end of the range (10 m²/d) was viewed as providing a compromise between having too large a proportion of the landscape saturated (33 percent for the T = 1 m²/d simulation), but maintaining saturated riparian areas and terrain depressions.

In the second TOPOG formulation, the net subsurface drainage flux was not assumed to be spatially uniform. In particular, the evaporation rate was varied as a function of the potential radiation of each element and the cube-root of soil moisture:

$$E(x, y) = \frac{\alpha r_s(x, y) + \beta r_h * W^{1/3}}{2.2248} \quad (\text{eqn. 3.4.4})$$

where:

α = efficiency of transpiration; fraction of solar energy converted to net radiant energy; factor that scales down radiation due to attenuation by clouds and atmospheric dust (set to 0.50 for clear sky summer conditions),

$r_s(x, y)$ = total solar radiation for each element; function of slope and aspect,

β = fraction of solar energy converted to radiant energy for a shaded horizontal surface (set to 0.02),

r_h = total solar radiation for a horizontal surface,

W = drainage index; used as a proxy for soil moisture, and

2.2248 = conversion factor used to convert radiation units to equivalent transpiration units [(MJ/m/d)/(mm/d)].

Since q uses W and is used to calculate W , the radiation-weighted drainage index (W_r) must be solved by iteration until stable values are obtained (Vertessy et al. 1990). Simulations were run for the summer (solar declination of +23.5). Precipitation input was set to 7.7 mm/d (annual average of 2800 mm divided by 365 days) and soil transmissivity was set to 10 m²/d as in the steady-state runs. Although nearly 8 mm of rain per day may seem like an unrealistically high estimate for the summer season, recall that the simulations portray steady state conditions. The precipitation input is a description of not only summer rainfall but also antecedent precipitation present in the system in the form of snowmelt or stored soil water. Simulations that were run with typical summer precipitation rates of 3 mm/d (~300 mm for the summer period) had so little water in the system that the entire landscape was uniformly dry.

RHESSys

RHESSys (Regional HydroEcological Simulation System) is a hydroecological modeling package implemented in C (Band et al. 1991, 1993; Tague 1999). The object-oriented approach facilitates the substitution of different process algorithms at different scales. For example, climate and canopy processes can be modeled at completely different levels within the hierarchical representation of the landscape from patch to zone to hillslope to basin. As a consequence of this scale-dependent stratification of process

algorithms, RHESSys can be run for much larger areas than TOPOG (*e.g.*, areas in the 10-1000s km²).

An additional strength of RHESSys is that terrain partitioning can occur on ecologically meaningful units rather than strictly defined grid cells. Patches, the smallest level of aggregation in the model, are defined as areas of similar soil moisture characteristics. Partitioning is free to take advantage of patterns of relevant variability within the landscape. For our model, hillslopes were defined using standard watershed delineation techniques to produce sub-basins corresponding to an accumulated drainage area threshold of 300 (30 m) grid cells. Each sub-basin contained two hillslopes, one on either side of the stream. Each hillslope was partitioned further into patches based on elevation and distance to the stream. Patches were defined such that finer resolution was maintained in areas near to the stream in order to capture finer scale variable source areas during wetting and drying periods in these areas. Mean patch size was 9 grid cells or 90x90 m, approximately the same size as for the TOPOG simulations.

RHESSys is comprised of three primary submodels: (1) a climate submodel (MTN-CLIM; Running et al. 1987); (2) an ecophysiological submodel (BIOME-BGC; Running & Coughlan 1988); and (3) a distributed hydrology submodel using either implicit (TOPMODEL; Beven & Kirkby 1979) or explicit (a distributed hydrological soil and vegetation model - DHSVM; Wigmosta et al. 1994) flow routing. Each of these submodels requires extensive input data including distributed forest, terrain, and soil data and nondistributed climate data and forest physiological parameters. In this case, vegetation and soil parameters were based on standard values for *P. menziesii* forest

cover and gravelly clay loam soils as described in Tague and Band (2001). Climate data input included daily minimum and maximum temperature taken from the Upper Lookout meteorologic station, which is located at an elevation of 1294 m in the southeast region of the basin. To spatially interpolate these inputs, a temperature lapse rate of 5.8 °C/km elevation was used. Spatial interpolation of rainfall was based on annual rainfall isohyets estimated by PRISM (Daly et al. 1994), which incorporates rainfall data from several stations within the Lookout Creek basin. Radiation and other meteorologic variables were computed internally in the model, based on MTN-CLIM routines.

Saturated hydraulic conductivity at the surface (K_{sat0}) and the decay of that conductivity with depth are the two calibrated parameters in RHESSys. The initial spatial patterns of these parameters were based on maps of soil texture and soil depth, assuming an exponential decay of hydraulic conductivity with depth. Note that this assumption implicitly defines a hydrologic soil depth that may include some flow within fractured bedrock layers. Because calibrated hydraulic conductivity values are typically higher than those based on soil texture and reflect preferential flow paths, basin-wide scaling of these two parameters was done to optimize correspondence between observed and modeled daily streamflow. Calibration used a Monte-Carlo based approach to optimize the Nash-Sutcliffe efficiency metric. Calibration resulted in a mean basin K_{sat0} of 750 m/d and an effective hydrologic soil depth (*i.e.*, depth at which hydraulic conductivity was reduced to 90 percent of its surface value) of 10 m.

Prior to simulation of soil moisture values for comparison, the model was run for 250 years to spinup soil and vegetation carbon and nitrogen pools (*i.e.*, model run to

reach a steady-state, old-growth forest condition). For the simulation period, the model was run on a daily timestep from January 1, 2001 through July 31, 2002 to produce spatial patterns of soil moisture over the entire Lookout Creek watershed. Comparison with observed sites, however, was done only for a small fraction of the total area of the HJA where there were undisturbed stands without harvest units present in their upslope contributing area. We were careful in selecting such stands in conducting our validation sampling.

Validation Data

We collected two different test sets with which to compare the different models. The first was within the original domain of sampling used in constructing the statistical model. This approximated the maximum amount of area that could be covered on a single day of sampling. The second extended more broadly across the entire HJA landscape. This effort stretched over two weeks of sampling.

On July 4, 2002 we returned to the three hillslopes we had sampled exactly one-year previously. We again laid out short transects representing different hillslope aspects and positions, similar in location and methods but not overlapping with the previous year's effort. A total of 136 new samples were collected: 47 from the high elevation site, 44 from the mid elevation site and 45 from the low elevation site. Individual field measurements from the sampling varied from four percent to 45 percent volumetric water content with an average of 18 percent.

From July 10 to July 24, 2002 we collected georeferenced data on soil moisture at 60 (20x20 m) plots spread throughout the HJA (Figure 3.4.3). To elucidate similarities and differences between the models, separate maps were made for each model identifying areas that were greater than 1.5 standard deviation (+ or -), between 1.5 and 0.5 standard deviation (+ or -), and within 0.5 standard deviation from the mean estimate of that model. These five categories divided the maps into five discrete areas over which samples could be stratified. Figure 3.4.3 presents the output from the statistical regression model as an example. Similar maps were generated for all the models. The relativized maps were then compared to identify geographic areas for sampling within the HJA that covered a range of predicted soil moisture values. Exact locations were selected from among 175 (20x20 m) sample plots for which we had extensive data on the biotic and physical environment (Chapter 2). All of the plots were located in old-growth forest in order to control for the effects of vegetation age as a factor. Three 2x2 m quadrats were located randomly within each plot. Three volumetric soil moisture readings were taken in each quadrat. The three quadrats then were averaged to arrive at a plot level moisture value (average of nine measurements). Average plot moisture values varied from seven percent to 26 percent with a mean of 13 percent across the plots and an average standard deviation of 2.8 percent within each of the 60 plots.

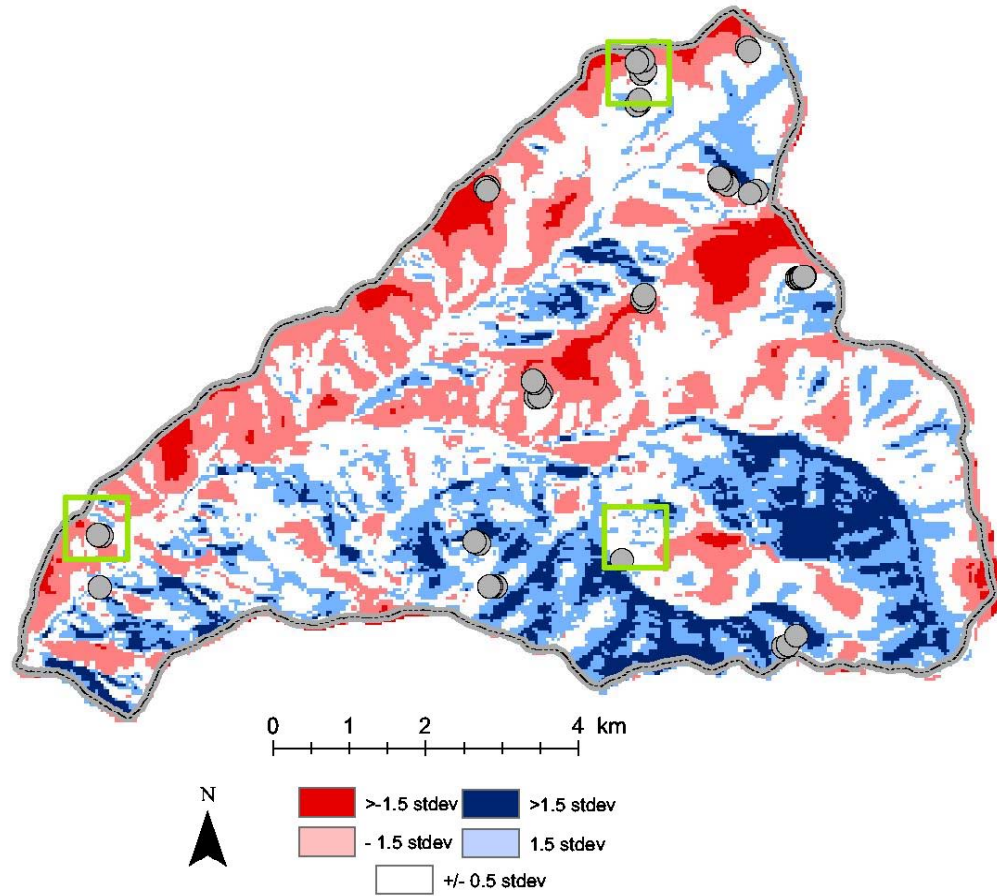


Figure 3.4.3. Locations of samples collected from July 10-24, 2002. Watersheds from which July 4 samples were collected are boxed. Sample locations are overlaid on predicted deviations from the mean wetness value as determined from the statistical model (see text).

Model Comparisons

Three watersheds, single day

All models agreed in having wet drainage areas and relatively dry upslope conditions. The models had varying effectiveness in predicting the July 4, 2002 field measurements, however, as measured by the error residuals in a regression framework (Table 3.4.1). The average squared prediction error (ASPE) is a statistic representing the expected total error of the different models in predicting the validation data (Reynolds & Chun 1986). It is calculated as

$$\text{ASPE} = \frac{1}{n} \sum_{i=1}^n D_i^2 \quad (\text{eqn. 3.4.5})$$

where D = observed – predicted values and n = sample size. TCI was the poorest estimator of differences in moisture among these samples. IMI was better. The statistical model provided the best estimates of relative differences in the samples. The process models had mixed results in predicting these data. They performed better than TCI but worse than IMI.

A closer examination of the prediction errors for all the models found significant spatial trends in the residuals. Nine of the 13 most under-predicted values came from a single transect, which paralleled and once crossed a small hillslope seep. In addition, eight of the top 13 most over-predicted values came from an extremely rocky, midslope transect with shallow soil. Removing these two transects from the analysis improved

Table 3.4.1. Regression tests of model predictions for samples collected from three small watersheds ($N = 136$). ASPE = average squared prediction error.

Model	r^2	F Value	Pr(F)	ASPE
TCI	0.08	12.2	0.001	56.4
IMI	0.16	25.5	<0.001	50.8
Statistical Model	0.36	75.4	<0.001	38.9
Topog (steady-state)	0.09	13.2	<0.001	55.1
Topog (radiation)	0.10	13.6	<0.001	55.0
RHESSys (7/4)	0.14	21.9	<0.001	53.4

Table 3.4.2. Regression tests of model predictions for samples collected from three small watersheds after removing two transects with large prediction error ($N = 114$). ASPE = average squared prediction error.

Model	r^2	F Value	Pr(F)	ASPE
TCI	0.16	21.3	<0.001	35.1
IMI	0.12	15.1	<0.001	35.9
Statistical Model	0.33	56.4	<0.001	28.0
Topog (steady-state)	0.14	17.7	<0.001	35.8
Topog (radiation)	0.16	19.9	<0.001	35.1
RHESSys (7/4)	0.23	34.0	<0.001	33.0

Table 3.4.3. Regression tests of model predictions for samples collected from entire landscape ($N = 60$). ASPE = average squared prediction error.

Model	r^2	F Value	Pr(F)	ASPE [†]
TCI	0.032	1.95	0.17	7.8
IMI	0.001	0.01	0.91	8.0
Statistical Model	0.001	0.06	0.81	8.0
Topog (steady-state)	0.003	0.17	0.68	8.0
Topog (radiation)	0.010	1.10	0.29	7.9
RHESSys (7/17)	0.007	0.41	0.52	8.0
RHESSys (7/10-7/24)	0.023	1.38	0.25	7.8

[†] ASPE values are lower than in Tables 1 and 2 because the landscape-wide samples used in this validation test had considerably lower variability than the validation data used in the previous analyses.

the explanatory power of those models (TCI and process models) that relied heavily on topographic drainage in generating their predictions (Table 3.4.2). IMI, which incorporated differences in soil properties, actually performed worse after removing these transects.

Landscape, multiple days

None of the models accurately predicted differences among the landscape-wide samples (Table 3.4.3). The simple TCI proxy performed as well as any of the more sophisticated models. The statistical model, which described moisture patterns well within the geographic area for which it was originally calibrated, performed poorly when attempting to predict moisture from different regions within the study area. Although adding radiation-weighted differences in evapotranspiration did improve the predictive ability of the Topog model, neither formulation described the observed measurements very well ($P = 0.68$ and 0.29 respectively). By using the dynamic simulator RHESSys, we were able to improve our predictive capability, slightly, chiefly by matching the model output with the specific day of sampling ($P = 0.25$). Permanent soil moisture probes within the HJA did exhibit minor temporal trends within the sample period (Figure 3.4.4). This average decrease of 2.3 percent during the sample period is relatively small, however, in comparison to the observed spatial range from seven percent to 26 percent.

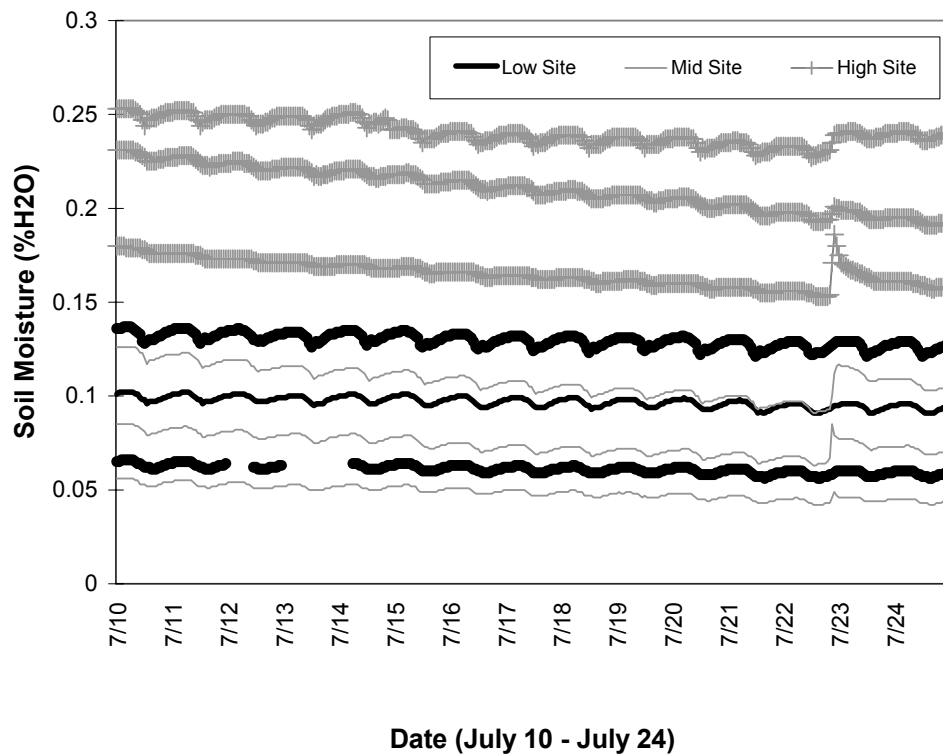


Figure 3.4.4. Hourly soil moisture measurements from permanent sampling stations located in three small sample watersheds of the HJA from July 10-24, 2002. The gray, hatched lines are from three locations within the high-elevation watershed; the dotted lines are from the mid-elevation site; and the thick, black lines are from low elevation. One small rain event occurred on the evening of July 22 (from 9pm-midnight with a total throughfall of less than 1.5 cm at all sites). Diel patterns driven by hydraulic redistribution of soil water (Bond et al. 2001, Brooks et al. 2002) result in volumetric changes of less than 1 percent.

Discussion

In total, we developed five different model descriptions of the relative, spatial moisture differences of the HJA in mid-summer: (1) a soil moisture index based solely on local slope angle and upslope contributing area (TCI); (2) a soil moisture index based on both terrain attributes and soil properties (IMI); (3) a statistical model using empirical data to derive the relationship between soil moisture and terrain variables; (4) a steady-state simulation model with spatial evaporation differences (Topog); and (5) a dynamic simulation model that incorporates variable terrain, climate and moisture demand (RHESys). These models have been described generally in order of increasing complexity.

In comparing the models using two different validation datasets we conclude the following:

- 1) Both IMI and TCI capture a substantial amount of the variability in soil moisture at fine scales. In particular, IMI is able to capture fine-scale differences in soil properties that may be important when evaluating areas of high local variability in soil texture or depth. Although TCI is able to explain more of the variance in the landscape-scale data than any of the other models considered, none of the models capture these patterns effectively.
- 2) The statistical model provides better predictions than the other models for the samples collected within the small watersheds, but performs poorly at the landscape scale. The spatial domain of applicability of this model is limited to specific areas for which the model was built, a general rule that is too often ignored in ecological studies.

3) For samples collected beyond the spatial domain of the statistical model: TCI, Topog with radiation weighting, and the dynamic RHESSys simulation perform better than the statistical model but still show significant error. The advantage of including temporal dynamics in RHESSys is limited to the small temporal variation in soil moisture during the July sampling period.

Moving between models requires trade-offs between precision, generality, realism and simplicity (Gardner & Urban *in press*, Peters et al. *in review*). In particular, there is a cost to including additional processes, which may increase the physical realism, but require additional calibration. Though not mechanistic, statistical models can perform quite well within their appropriate ranges of applicability. Unfortunately, even with improved sampling technology, it may be logistically prohibitive to acquire sufficient field samples to construct landscape-scale statistical models of soil moisture for many areas. In which case, process models like RHESSys provide an opportunity to extrapolate across large spatial scales, but require site-specific calibrations of individual driving processes (*e.g.*, spatial distributions of rainfall and snowmelt). Simple terrain-based proxies provide the best tools for estimating moisture when such resources are not available or such an intensive representation is not justified.

Moisture proxies are tractable and relatively simple to develop, but do not include some of the major components of the water balance. For example, averaging away temporal variability in moisture conditions is not appropriate for many applications in the Pacific Northwest or other ecological systems of highly variable annual precipitation. The dynamic capabilities of RHESSys would be absolutely essential were we interested

in simulating highly dynamic states such as during the fall wet-up or a more prolonged period of summer draw-down. Only with the most complicated model in which we were able to match the specific date of sampling with model output for that day would we be able to describe these patterns. In addition, topographic differences may be understated by not including plant growth and transpiration in the simpler models. All things being equal, it could be argued that simple models should be preferred to complex models (O'Neill 1979, Hillel 1986, Reynolds & Acock 1985). Because all model outputs are not typically equal, model selection is a more subtle art.

In addition to their varying degrees of complexity, the different models also can be contrasted in terms of how they treat spatial relationships within the landscape. Peters et al. (*in review*) describe three classes of models that differ in their treatment of spatial processes: nonspatial, spatially implicit and spatially explicit. Nonspatial models provide predictions using independent variables measured without regard to spatial location. Spatially implicit models rely upon correlated and spatially structured explanatory variables; therefore, spatially structured output are created even if no explicit location is referenced in the model. Spatially explicit models incorporate neighborhood effects and/or explicitly simulate the fluxes of materials, organisms, energy, etc.

Our model selection process can be viewed in terms of these three classes of models and the importance of spatial processes to the phenomenon of study. The lateral flux of soil water through a landscape is an inherently spatial process (White and Running 1994, Band & Moore 1995), so a nonspatial model would not be appropriate. This process may not be captured adequately through spatially implicit statistical

relationships for highly variable terrain, in which case a spatially explicit model such as RHESSys may be required. Alternatively, spatially implicit models may be sufficient for specific areas given adequate empirical data with which to parameterize the statistical relationships. For example, our statistical model works well within the watersheds for which it was derived and for the anniversary date from the date in which the calibration data were collected. The implicit relationships break down when attempting to extrapolate the statistical model beyond these bounds.

An analysis of the landscape-level error residuals highlighted elevation as a potential forcing variable not captured by the process models. The moisture levels at high elevation were generally under-predicted by the models, while sites at low elevation were predicted to be wetter than they actually were. For the Topog model, these findings are not surprising. Elevation trends in soils and precipitation were not included in the calibration. Topog was developed primarily as a small watershed model rather than a landscape model. As such, it focuses on small-scale processes such as drainage flux along hillslope gradients, rather than landscape-level patterns.

The relatively poor performance of RHESSys at the landscape scale may also be partially explained by problems with model calibration. On the hillslope scale, water flows downhill and RHESSys captures this dynamic fairly well (*e.g.*, the model predicted the small-watershed data well and the landscape-scale residuals were not correlated with TCI). On the landscape scale, however, locations further down the mountain generally were observed to be drier than higher elevation sites, because at the time of sampling snowmelt was still a contributing factor to soil recharge at high elevations but not low

elevations. Our current formulation of RHESSys does not effectively replicate this elevation gradient in soil moisture at the time of year when we did our sampling.

Snowfall and melt are highly variable processes that might require better calibration, both spatially and temporally, to describe accurately the hydrologic patterns of this catchment.

As a separate analysis, we can construct a new linear regression model to fit rather than predict the landscape samples. In this model, elevation and TCI are the most important explanatory variables and a significant amount of the variation is explained by the equation ($P = 0.003$). This model should not be compared to the others because it is a simple data fit, rather than a test with independent samples. The fact that different explanatory variables are identified by this analysis than by the statistical model built from the small-watershed data is informative, however. It suggests that the watersheds sampled for the initial model might not capture the larger-scale trends in moisture sufficiently. A larger, more diverse sampling of the entire HJA would be required to build a landscape-scale statistical model. The data and analyses provided in this study could be used to help identify locations that should be sampled to construct this landscape model in an iterative approach to model development (Urban et al. 2002).

Four caveats are worth mentioning regarding how our method of sampling may have influenced model performance. First, the scale of field samples was, in many instances, finer than the scale of the models. This mismatch of scale was most severe for the process models. A common trade-off occurs in model development between increasing sophistication of the model and decreasing resolution. The gap between the coarse-scale resolution required to run landscape-scale simulations and the fine-scale

resolution desired of the output has been shrinking with increases in computing technology and resolution of remotely sensed input data, but it has not yet been eliminated. For example, the interval spacing (and resulting element size) in Topog was constrained by computational difficulties associated with generating a high-resolution, large-extent flow network. As a result, the grain of both the small-watershed sample quadrats (1x1 m) and the landscape sample quadrats (20x20 m) was much finer than that of the Topog element network (median element size of 84x84 m). Because more than one field measurement were contained within a single element, the model could not represent the fine-scale variability of the field data.

A similar argument could be made for RHESys, which also had a mean patch size much larger than the size of the sampling quadrats (90x90 m). As perhaps a more realistic test of the ability of the RHESys patches to predict field moisture values, we aggregated the landscape scale moisture samples to the RHESys patch level. The correlation between these patch-level measurements and the RHESys output was no better ($r^2 = 0.02$, $P = 0.5$, $N = 27$ for the sample date-corrected comparison), however, suggesting that scale differences were not the primary explanation for the observed inability of the model to explain a high proportion of the variability in field moisture.

A second sampling issue that may have influenced model performance was the timing of data collection. Grayson et al. (1997) suggest the existence of two distinct states in spatial soil moisture patterns: a dry state, in which the landscape can be disconnected and local controls dominate; and a wet state, which is more strongly controlled by horizontal fluxes (*i.e.*, topographic drainage). We only examined a short

period of time, mostly for logistical reasons. We chose the beginning of the summer because we are interested in soil moisture patterns at the peak of the growing season and how these patterns may be correlated with spatial patterns of plant dynamics. The relative performance of these models may have been very different if we had tested them during a different time of year. In fact, it is possible that the short delay between the July 4, small-watershed sampling and the July 10-24, landscape-level sampling may have been long enough for a switch in states to occur. The statistical model built to describe the wet state would have very little predictive power for samples collected during the dry state. More broadly, none of the models, which are all heavily terrain-based, would be expected to accurately predict moisture patterns under a dry, disconnected state in which local controls dominate.

The switching between these two states can be sudden, and is described by Grayson et al. (1997) as a threshold phenomenon. Soil moisture draw down can be extremely fast over the summer months in this forest and is highly spatially variable. The range in moisture values decreased from 9-45 percent for the July 4 samples to 7-26 percent for the July 10-24 samples, though the difference in sample locations should not be ignored in drawing comparisons between these two datasets. We did not observe large changes in moisture levels at the permanent sampling locations during the July 10-24 period (Figure 3.4.4). In a separate analysis, however, we found substantial decreases in moisture from repeated measures of locations on June 20, 2002 and again on July 20, 2002 (Chapter 4). All of these samples ($N = 277$) were from an elevation band (1225 – 1350 m) that maintained patches of snow into the summer months. Values decreased by

an average of 7.5 percent between the two sample dates. Seventeen points decreased by over 20 percent, while other locations changed by only one or two percent. Without a perfectly calibrated spatio-temporal model, errors can be quite large during this highly dynamic period.

A third issue to consider is related to the depth of sampling. Our field samples were all from the top 20 cm of soil, while many of the models integrate moisture over the entire soil profile (*e.g.*, Topog and RHESSys provide lumped estimates for the entire unsaturated zone). We limited our field effort to the upper profile mainly for logistical reasons related to the increased time required to sample deeper soil layers. The problem is that estimates of soil moisture integrated to the water table do not decrease as quickly as the top 20 cm of soil as the system dries out. It is even theoretically possible for lumped unsaturated zone estimates to increase as formerly saturated portions of the soil profile are converted to wet areas within the unsaturated zone. As a consequence, the elevation trend that was observed in the field samples but not the process models may be due to differences in their representation of the soil profile. While lower elevations may have lower upper soil moisture levels in the field, this might not be reflected well by estimates of total unsaturated zone moisture content.

These differences raise an important concern about model selection. Ultimately, the appropriateness of a model can be evaluated only relative to the specifics of the intended application (Rykiel 1996, Guisan & Zimmermann 2000, Gardner & Urban *in press*). It is possible that a model may be well-suited to describe certain ecological processes but poorly-suited to describe others. The model evaluation we have presented

here is relevant only to the ability of the models to predict relative surface soil moisture. These differences may explain patterns of seedling establishment but may be inappropriate to describe patterns of growth or mortality where adult trees can access much deeper reserves. For the latter applications, model evaluation would require field samples that integrated across a larger portion of the soil profile. Overall model performance may increase for these types of samples, which would more closely match many of the model formulations. Crave and Gascuel-Oudou (1997) provide a more detailed discussion of why surface measurements of soil moisture may not always match distributions predicted by topographic-based indices.

A fourth and final sampling issue was that although we tried to maximize the variance in the landscape-scale validation dataset by using the models to guide our sampling, we were hampered in this effort by difficulties in translating GIS predictions into the field and constraints imposed by limiting our choices of locations to the 175 vegetation plots for which we already had considerable ancillary data. For the validation data gathered from the three small sample areas, we were freer to locate samples at a wider range of topographic locations. As a result, the variance in the landscape-wide samples ($s^2 = 8.1$) was much smaller than the variance in the small-watershed samples ($s^2 = 57.2$). The ASPE statistic is not sensitive enough to differentiate between models given the compression of moisture variability in the landscape samples (Table 3.4.3). The models also may have performed differently had we collected a more variable test data set for the landscape-wide analysis.

Improved estimates of basic environmental resources such as soil moisture are needed to try to explain and predict ecological processes (Parker 1982). Grayson et al. (1992) and more recently Beven (2000) argue that hydrologic model development is too often carried out in the absence of field programs designed to test the models. Too little discussion has been centered on model shortcomings, giving the impression that model complexity is positively correlated with confidence in results. It is insufficient to offer theoretical model validations. Field tests are needed to establish links between the models and reality. We have developed and compared five models for estimating spatial soil moisture differences for a well-studied LTER site in the Pacific Northwest. The models vary in their representation of soil water fluxes from spatially implicit to spatially explicit with an associated increase in model complexity. Appropriate model selection in our case study, as in most situations, depends on the ecological issue to be addressed and the temporal and spatial domain of application.

SECTION 4: A FOCUSED INVESTIGATION

CHAPTER 4 Factors Controlling Community Transition at the *Tsuga heterophylla*/*Abies amabilis* Ecotone

Abstract

Major vegetation zones typically are described along elevation gradients. Trees are not affected by elevation, however, but rather by variables such as temperature and precipitation that covary with elevation. Because these variables are difficult to measure at large spatial scales, I propose a method of tactically sampling the landscape at locations that are most meaningful for learning about forest community dynamics. Ecotones are landscape linkages between adjacent communities. As such, they provide logical targets for focused study of forest community pattern. I used landscape-scale correlations between forest composition and environmental factors to locate five high-resolution study plots within the dominant forest ecotone in the Western Cascades of central Oregon. Within these relatively small sample units, I examined explicitly the relationship between ecologically important environmental variables (temperature, radiation, soil moisture, and snow) and tree demography (establishment, growth and mortality). The effect of temperature on growth rates might be important in limiting the downslope migration of *Abies amabilis*, but the upper elevation boundary of *Tsuga heterophylla* was associated with a more complex interaction of temperature and soil moisture on patterns of regeneration. The potential of ecotone studies for the monitoring of ecological response to environmental change such as that predicted under climate change scenarios is discussed.

Keywords: community ecotone, environmental proxies, old-growth forest, spatial analysis

Introduction

Ecologists historically have focused on homogeneous environments in their attempts to understand ecological processes (*e.g.*, Whittaker 1956, Peet 1981). Fonda and Bliss (1969) summarize this perspective in their study of the vegetation of the Olympic Mountains in Washington state:

“Rather than impose a random net of stands for sampling on the mountains, stands were selected based upon the recognition of relatively homogenous populations of the tentative community types. Transition areas between the tentative community types were too narrow to include in the sampling.”

In the 1980s, Weins et al. (1985) called for more studies of ecological dynamics at areas of transition (*i.e.*, ecotones). Risser (1995) echoed this appeal ten years later. Only recently, however, are these calls beginning to be answered with ecotone studies at the landscape level (*e.g.*, Stohlgren et al. 2000, Camarero et al. 2000). The utility of studying community transitions is manifold: (1) These are areas of maximum habitat variability and often maximum diversity (Neilson 1991). As such, these biologic hotspots have much to offer investigations of biodiversity. (2) Many current models of ecosystem dynamics are at too large a spatial scale to provide insights into the complex interactions of ecological systems (Camill & Clark 2000). Ecotone studies provide the opportunity to examine these interactions at a fine spatial grain. (3) Because many species are at the competitive limits of their ecological tolerances at ecotones, these regions may be especially sensitive to environmental change (Milne et al. 1996, Fortin et al. 2000). For example, the analysis and continued monitoring of community ecotones may be the most

effective means of detecting and predicting ecological response to greenhouse warming (di Castri et al. 1988).

During periods of natural climatic transition, the average rate of climate change has been approximately one degree centigrade per 1000 years (Hidinger & Glick 2000). The projected rate of climate change in the short-term future is 1.4 to 5.8 degrees centigrade over the next 100 years (IPCC 2001). From these projections have come general predictions of a poleward and upslope shift of many species and communities (Peters & Darling 1985, Fujiwara & Box 1999). High mountain landscapes are viewed as particularly vulnerable (Taylor 1995, Fujiwara & Box 1999). Several recent reviews have shown that species range shifts are beginning to be observed (Parmesan & Yohe 2003, Walther 2002). In general, however, this evidence is for mobile animals and short-lived species. There has been limited field evidence to support theoretical predictions of rapid migrations for long-lived plant species, though the paleoecology literature is rich in accounts of tree migrations in response to changes in climate (Flenley 1979, Davis 1981).

Ecotone studies provide the opportunity not only to monitor shifts in plant communities, but also to improve predictions of forest response to future environmental conditions by providing more knowledge about the mechanisms of transition. Attempts to predict ecological response to global climate change must start with an understanding of the local factors influencing current vegetation patterns (Halpin 1997, Woodward 1998). Noble (1993) noted that the potential value of an ecotone as a monitoring tool is dependent upon the mechanisms of transition at that ecotone. In many of our best-studied systems these mechanisms are still poorly understood. Previous studies have examined

the potential response to changes in climate at the boundaries between continental climatic regimes (Crumley 1993), grassland-woodland transitions (Clark et al. 2001), woodland-forest boundaries (Grimm 1983), and treeline ecotones (Noble 1993). Loehle (2000) suggested that ecotones between different forest communities are more likely to exhibit measurable and interpretable changes.

In this study, I attempt to better understand the mechanisms behind the transition from the *Tsuga heterophylla* vegetation zone to the *Abies amabilis* vegetation zone in the Western Cascades. This ecotone is a compelling case study because it is the dominant community transition in these old-growth ecosystems. Lessons drawn from a detailed examination of the biotic processes and physical constraints dictating this transition can be applied to more general models of landscape pattern.

Ecotone hypotheses

The transition from the *T. heterophylla* vegetation zone to the *A. amabilis* vegetation zone has been described in great detail (Fonda & Bliss 1969, Zobel et al. 1976, Franklin & Dyrness 1988), but efforts to identify the causes of this transition have been minimal and often contradictory. In this study, I look for evidence to support or refute competing hypotheses regarding the mechanisms of transition. I focus on the relative importance of temperature, moisture, radiation, and snowpack on community patterns. The argument has been made that while the upper-elevation (or northern) limits of species' ranges are bound by physiological constraints (*e.g.*, frost), lower-elevation (or southern) limits are determined by competition and the trade-offs between physiological tolerances and maximum growth (Smith & Huston 1989; Loehle 2000). In studying a

forest-forest ecotone, I must consider both the upper limit of one species (*T. heterophylla*) and the lower limit of another (*A. amabilis*). I will address each in turn. I summarize below the hypotheses that will be explored and the data that will be used to test each hypothesis.

T. heterophylla upper limit:

Snow – In perhaps the most detailed investigation of this ecotone to date, Thornburgh (1969) suggested that mechanical pressures associated with snowpack may be critical to the transition. According to his argument, *T. heterophylla* seedlings do not germinate until up to a month after the first snowmelt, while *A. amabilis* can germinate almost immediately. The *T. heterophylla* seedlings, therefore, have limited growth over their first growing season. This low growth combined with their general drooping nature make *T. heterophylla* seedlings highly susceptible to damage by snowpack and associated debris over their first winter. Although the logic of this theory is compelling, empirical support is limited. I generate spatial estimates of snow depth and timing of spring melt, and test whether these factors are correlated with *T. heterophylla* regeneration at the edge of its range.

Frost tolerance - A long history of gradient analysis provides a second potential explanation. Implicit in these studies is the assumption that community transitions are governed by trade-offs in tolerances and growth rates. Following this general model as described by Smith and Huston (1989), *T. heterophylla* may not be competitive at higher elevations because of their limited cold tolerance.

Considerable frost damage has been observed in *T. heterophylla* stands at high elevation in the Rockies (Packee 1990). Further, the germination rate has been shown to be extremely sensitive to temperature (Edwards 1976). I test this hypothesis by comparing patterns in January mean and minimum temperatures with the distribution of *T. heterophylla* regeneration at the edge of its range.

A. amabilis lower limit:

Growth rates – At its lower-elevation limit, *A. amabilis* may be bound by slower growth rates than *T. heterophylla*. According to the Smith and Huston (1989) community model, species that develop high tolerances do so at the cost of reduced growth rates. I measure growth rates throughout the HJA watershed to determine if such a trade-off is evident for *A. amabilis*.

Drought tolerance – Kotar (1972) suggested that *A. amabilis* seedlings were less drought tolerant than *T. heterophylla* seedlings, which prevented them from successfully competing in drier climates. Krajina (1969) described a moisture gradient from *P. menziesii* to *T. heterophylla* to *A. amabilis*. Thornburgh (1969) did not believe that the distributions of these species were governed by soil moisture. This hypothesis is complicated by the confounding effects of temperature and radiation on moisture. I test the hypothesis by sampling soil moisture directly and by developing spatial estimates of moisture differences at seedling locations.

Heat/evapotranspiration stress – Others have countered that temperature is more important than moisture (Fonda & Bliss 1969, Packee 1990). They argue that

higher temperatures produce a number of physiological effects that *A. amabilis* cannot tolerate. This hypothesis is more in line with conventional community ecology ordinations that separate major vegetation zones along a temperature axis and use moisture to divide community associations within those zones (*e.g.*, Whittaker 1967, Dyrness et al. 1976). I measure summer temperature levels to evaluate this hypothesis.

Dispersal limitation – Poor dispersal capabilities also may affect the range of *A. amabilis* (Schmidt 1957). Its seeds are fire sensitive and very heavy, which results in the late invasion of the species into disturbed stands even at high elevations. Additionally, seeds are produced only every other year and a low percentage of the seeds are viable due to a variety of factors described by Owens and Molder (1977), including long periods of pollen dormancy and a low number of archegonia that abort quickly if not fertilized. I draw inferences about the dispersal characteristics of these species through point pattern analysis of trees and seedlings.

A. procera lower limit and competition with *A. amabilis*:

Growth rates – As with *A. amabilis*, *A. procera* may be limited by low growth rates relative to downslope species. I compare growth across its range relative to *T. heterophylla*. I also compare average growth rates of *A. procera* relative to *A. amabilis* and *T. heterophylla* within the transition zone.

Radiation constraints – *A. procera* is a shade-intolerant co-dominant in the *A. amabilis* vegetation zone. I test the importance of radiation to regeneration

patterns by examining seedling distributions relative to fine-scale canopy and hillslope radiation influences.

Dispersal limitation – *A. procera* is another heavy-seeded disperser with a high percentage of unviable seeds. I use point pattern analysis at the lower boundary of its distribution to evaluate dispersal processes as a potential constraint.

The competing hypotheses have different implications under greenhouse warming scenarios. Nobody has attempted to reconcile these competing hypotheses with a focused study of areas of transition, and with the possible exception of Thornburgh (1969), nobody has attempted to test the hypotheses with explicit measurements of plant-relevant environmental variables such as temperature, soil moisture, and snowpack and melt. In this paper, I provide a detailed examination of the patterns of transition from *T. heterophylla* to *A. amabilis* and *A. procera* dominated forest. I begin with a brief description of the biology of these species. I describe the collection of field data at ecotone focus plots and the processing of these data to estimate spatial patterns in demography (regeneration, growth, and mortality) and the environment (radiation, soil moisture, snow, and temperature). I present an overview of the biotic and environmental conditions observed on the plots. I then compare trends in demography with trends in environmental condition. First, I take a more traditional gradient analysis approach and examine changes in mortality and growth with elevation. To address these trends, I use data collected from a sampling of forest stands broadly distributed across the landscape. I also examine the relationships between the landscape data and the estimates of temperature, radiation, and soil moisture described in Chapter 3. I then focus on the area

of transition between these two community types, and test whether demographic patterns are correlated with environmental microcondition. Finally, I test the dispersal limitation hypothesis through point pattern analysis of plot stem maps.

Study area

The H.J. Andrews Experimental Forest (HJA) is located on the west slope of the Cascade Mountains. It is comprised of the Lookout Creek watershed, 80 km east of Eugene, Oregon. The Long Term Ecological Research (LTER) site covers 6400 ha and ranges in elevation from 410 m to 1630 m (McKee 1998). The watershed lies within the Blue River Adaptive Management Area, one of 10 such areas devoted to the development and evaluation of progressive management strategies for northwestern forests (Cissel et al. 1999). At the time of its establishment in 1948, the HJA was an intact forest with about 65 percent of the land in old-growth (*i.e.*, 400-500 years old). Since that time, old-growth forest has been reduced to 40 percent of the total area due to logging activities.

Climate is characteristic of the Pacific Northwest, with dry summers and wet winters. Annual precipitation ranges from 2200 mm at the base of the watershed to 3400 mm at upper elevations, with less than 300 mm normally falling during the summer growing season (Grier & Logan 1977). Soils are mostly deep, well-drained Inceptisols with most roots concentrated in the upper 200 cm of soil. Zobel et al. (1976) argued that topography is more important than soil differences in controlling vegetation in this region. *Pseudotsuga menziesii* (Douglas-fir), *Tsuga heterophylla* (western hemlock), and *Thuja plicata* (western red cedar) are the dominant species at lower elevations, while *Abies amabilis* (Pacific silver fir), *Abies procera* (noble fir), and *Tsuga mertensiana*

(mountain hemlock) dominate upper elevations (Franklin & Dyrness 1988). On a regional basis, Ohmann and Spies (1998) suggested that elevation and associated macroclimate are the major correlates with community composition throughout Oregon.

***Tsuga heterophylla* [Raf.] Sarg. (western hemlock)**

T. heterophylla comprises the most common potential climax species in the most extensive vegetation zone in western Oregon and Washington. The *T. heterophylla* zone extends broadly throughout both states, from the Klamath Mountains in southern Oregon to British Columbia. The vegetation zone's elevation range in the Cascade Mountains extends from near sea level to upwards of 1,000 m (Franklin & Dyrness 1988). In a separate analysis (Chapter 2), I showed that the zone extends above 1,200 m within the HJA. *T. heterophylla* itself has been observed at elevations as high as 2,130 m and is often found in mixed stands within the *A. amabilis* vegetation zone (Packee 1990). Within the *T. heterophylla* vegetation zone, *T. heterophylla* is successional from *P. menziesii* except on the driest stands. Despite its shade tolerance, however, *T. heterophylla* decreases in importance at higher elevations and more northerly latitudes. Relatively little research has been conducted regarding the mechanisms of this decrease, though some evidence suggests the important influences of winter snow (Thornburgh 1969) and/or cold temperatures (Edwards 1976, Packee 1990).

***Abies amabilis* [Dougl.] Forbes (Pacific silver fir)**

Abies amabilis is the major climax species in the *A. amabilis* vegetation zone. This zone is typically found upslope from the *T. heterophylla* zone at elevations ranging

from 1,000 to 1,500 m in the Oregon Cascades (Franklin & Dyrness 1988). Franklin (1979) distinguished the zones climatically by the 1-3 m snowpacks common to the *A. amabilis* zone, but absent from the *T. heterophylla* zone. Late-successional forest composition in the *A. amabilis* zone is characterized by mixed stands of *A. amabilis*, *T. heterophylla*, *P. menziesii*, and *A. procera*, with poles and regeneration dominated by *A. amabilis*. Although *A. amabilis* is capable of growing at lower elevations, it does not compete well there with *T. heterophylla* (Franklin & Dyrness 1988). Factors that may contribute to its competitive inferiority include slower growth rates, lower drought tolerance (Kotar 1972) and susceptibility to heat stress (Fonda & Bliss 1969). *A. amabilis* also are notoriously poor dispersers (Schmidt 1957).

***Abies procera* Rehd. (noble fir)**

Abies procera is a common codominant in the *A. amabilis* vegetation zone. Relative to *A. amabilis*, it is early successional, as evidenced by a comparison of the size class distribution of the two species on mixed stands on the study plots (Figure 4.1). It is one of the most important timber species in the Pacific Northwest. It has the strongest wood of any of the true fir species and is a productive subalpine species, whose long-term productivity exceeds even that of *P. menziesii* (Franklin 1964). *A. procera* also is the western true fir with the most limited distribution. Rarely does it occur in pure stands, but instead is found most commonly mixed with *A. amabilis*. Geographically, my study area in the McKenzie River Basin represents the southernmost extent of the range of genetically pure trees. *A. procera* is most common between 1,070 m and 1,500 m in the central Oregon Cascades, and has been observed with most frequency on warmer, south-

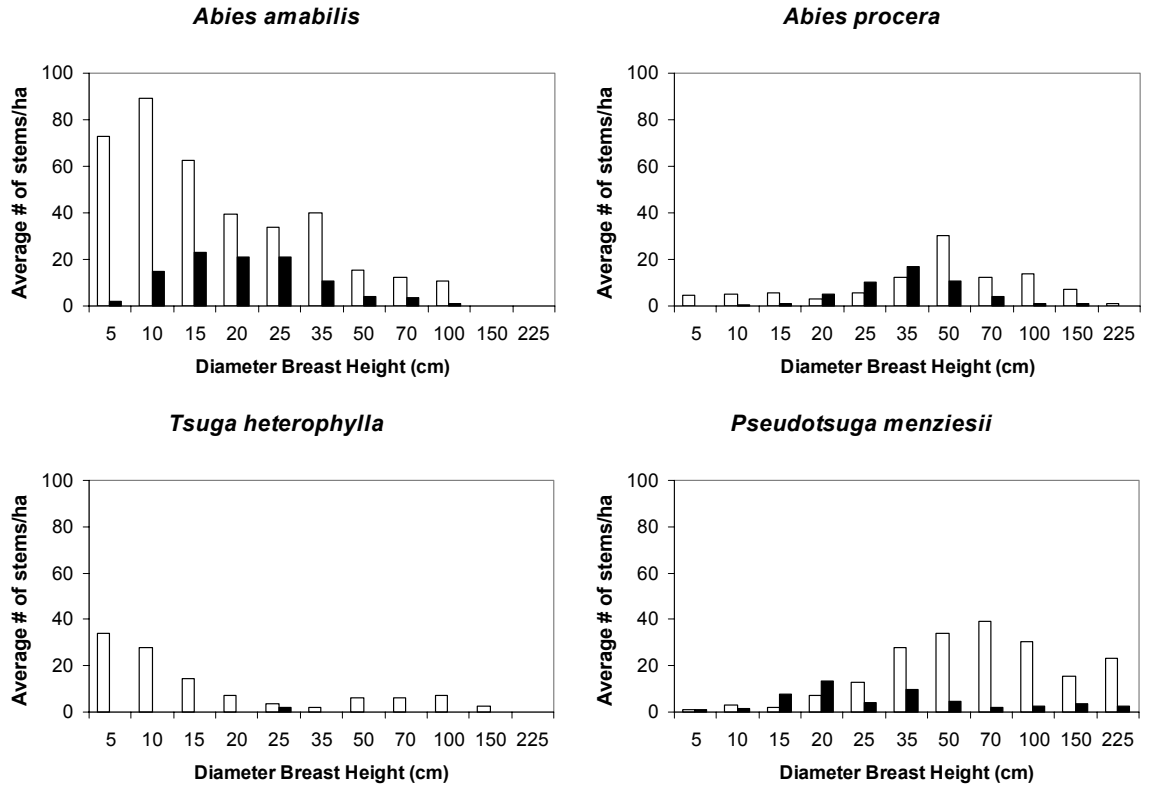


Figure 4.1. Histograms of average size distributions for four major species across five ecotone study plots. Open bars are live trees; closed bars are dead. *A. procera* and *P. menziesii* are early successional, shade-intolerants. *A. amabilis* and *T. heterophylla* are later successional, shade-tolerants.

facing aspects (Thornburgh 1969, Dyrness et al. 1974). Because it can be very productive at lower elevations, it is thought to be restricted to higher elevations because of competitive disadvantages rather than any physiological tolerances (Packee 1990). Like *A. amabilis*, it has a low percentage of viable seed, and seeds are not widely dispersed (Thornburgh 1969). There is some evidence that it prefers soils with high nutrient levels, high moisture levels, and good drainage capabilities (Franklin 1964, Franklin & Dyrness 1988). *A. procera* is considered shade intolerant. Though slightly more tolerant than *P. menziesii*, it typically requires disturbance such as fire to establish successfully.

I include *A. procera* in this analysis because it is a major component of the *A. amabilis* zone. Unlike *P. menziesii*, the primary shade-intolerant species of the *T. heterophylla* zone, *A. procera* seedlings were commonly observed in my study plots. When referring to *A. amabilis* and *A. procera* collectively, I will use the terminology *A. spp.* Otherwise, conventional genus-species nomenclature is followed.

Methods

Ecotones were sampled explicitly through a set of microsite focus plots. The focus plots were aimed at capturing fine-scale demographic and environmental constraints along active community transitions. This approach differs from traditional intensive sampling (*e.g.*, reference stands), which typically is done on homogeneous sites representative of single vegetation zones (*e.g.*, Acker et al. 1998 in the HJA).

Plot selection

I relied upon earlier analyses of forest community pattern across the HJA (Chapter 2) to guide this sampling. The results of a statistical model of 164 (20x20 m) vegetation samples stratified across the landscape were used in a geographic information systems (GIS) framework to highlight specific geographic locations on which to sample. These earlier analyses suggested terrain “proxy” variables most important in discriminating among community types (*e.g.*, elevation). The ecotone plots were designed to refine my description of this transition by explicitly considering more plant-relevant explanatory variables at sites where their variation would have noticeable effects on vegetation. The guiding principle was to hold elevation relatively constant and focus on the effects of variability in moisture, radiation, temperature, and snow. The approach is analogous to a regression analysis that focuses on the variance in the residuals. To maximize this variance, the plots covered a range of slope/aspect/watershed positions.

Specifically, I chose sites to meet the following criteria through a process of successive filtering:

- (1) sites within the area identified as “transition zone” in the landscape-level community analysis (Figure 4.4);
- (2) locations that fit criterion 1 and covered all major geomorphic features of the HJA:
 - a. Carpenter Mountain
 - b. Frissell Ridge
 - c. Lookout Mountain;

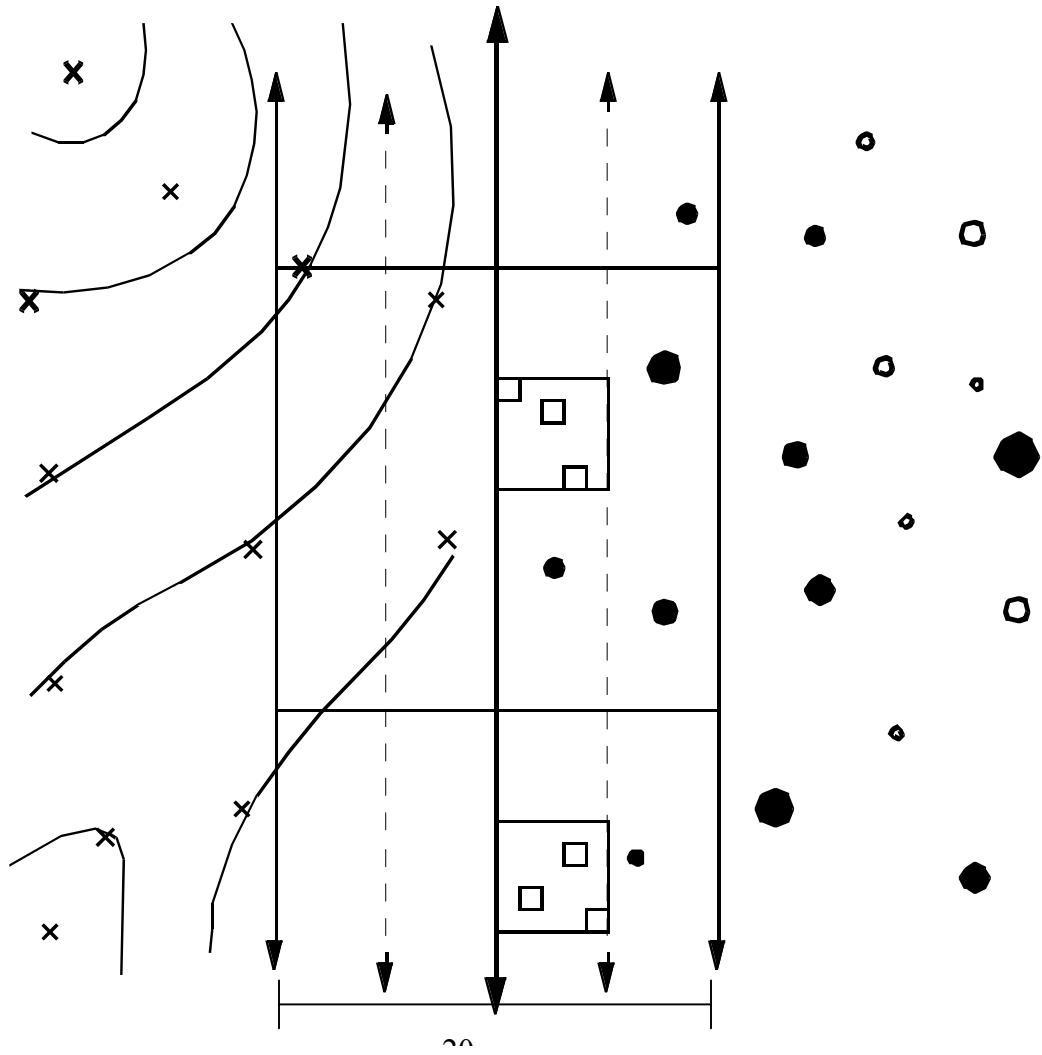
- (3) areas that fit criteria 1 and 2 that could include within a 100-200 m transect two 20x20 m plots that differed in community composition (*i.e.*, one dominated by *T. heterophylla* and one dominated by *A. spp*); and
- (4) orientations that fit criteria 1-3 and created a portfolio of case studies that incorporated a range of topographic contrasts (*i.e.*, changes in elevation, slope and aspect).

Field methods

Ecotone transects were 20 m in width and 100-180 m in length. Within each of the ecotone transects, all dead and live trees were measured at breast height, cored for age and growth rate, and mapped using a laser surveying system (Impulse Laser, Laser Technologies Incorporated; Figure 4.2). In addition, potential seed trees outside the transect were identified according to a plotless sampling design. Using a 2.5-factor basal area prism, any tree sighted as a potential seed source for seedlings along the centerline was measured and cored. For example, this would include a 1-m diameter tree at a distance of 40 m from the centerline. Nested within each transect were 3 (1x1 m) quadrats per 20 m in which all seedlings were tallied by size class (young of the year, 0-10 cm in height, 10-50 cm in height, 50-137 cm in height). The large number of empty quadrats and the resulting small seedling sample sizes made the analysis of these data problematic. As a result, I also mapped all seedlings within 1 m and all saplings (greater than 137 cm in height, but less than 2.5 cm in diameter at breast height) within 5 m of the transect centerline. These individually mapped seedlings were the focus of the analysis. A

topographic position:

tree sampling and stem mapping:



subset of saplings and seedlings were harvested for growth rate analysis. From these data, rates of critical demographic processes (*e.g.*, growth, seedling establishment, mortality) were derived in a spatial context.

The physical template also was sampled intensively within these transects. Critical topographic points (VIPs) were mapped using the laser surveying system. Sufficient VIPs were recorded to interpolate a high-resolution digital elevation model (DEM) of the site. An average of nearly forty measurements were taken for every 20 m of transect. Surface soil moisture (0-20 cm in depth) was recorded synoptically at a subset of the VIP locations and all seedling quadrats using a handheld volumetric moisture sampling device (Hydrosense, Campbell Scientific, Incorporated). Measurements were taken twice in the summer of 2002 (June 20 and July 20). Three soil depth measurements also were taken at each of the moisture locations using a 1-m tile probe. Canopy closure was estimated at the seedling quadrats using a concave spherical densiometer. Temperature sensors (HOBOS, Onset Corporation) were located at several key locations along each transect. These sensors recorded temperature at breast height (1.37 m) at half-hourly increments. Several complementary approaches were used to quantify snow levels and melt on the plots. On May 10-12, 2002, I measured snow depth (up to a maximum depth of 100 cm) at 1-m intervals along the centerline of three of the transects. Average height at which lichens began growing on tree boles was recorded for each 20-m segment. According to Winkler and Schultz (2000), lichen height acts as a reasonable proxy for the average maximum snow depth. Finally, I distributed temperature sensors (additional HOBOS; hereafter referred to as SNOBOs) at ground

level across the plots. These sampling devices allowed me to monitor remotely the beginning and end of winter snowcover for specific locations on the plots. When covered with snow, these sensors would consistently record a temperature of 0 °C. When snowfree, the half-hourly measurements were much more variable.

GIS methods - development of spatial data layers

For each ecotone plot, I developed multiple geospatial estimates of the biotic characteristics, light/radiation, soil moisture, snow coverage, and temperature (Table 4.1).

Biotic – Biotic layers consisted of point coverages of all live and dead trees, all seedlings within 1 m of the centerline, and all saplings within 5 m of the centerline. All of these data were gathered directly in the field and did not require subsequent post-processing. Tree cores were analyzed to evaluate spatial patterns in growth rates. For each live tree, I recorded the mean annual growth increment from 1990-1995 using a VELMEX data encoder (Velmex Incorporated) and MEASUREJ2X software (VoorTech Consulting). Cores were read using a microscope to a precision of 0.001 mm.

Light – Potential radiation was modeled on several different spatial scales. These estimates considered differences in canopy cover and hillslope radiation.

- (1) Corresponding to those seedlings that I did find in the initial sampling of 90 (1x1 m) seedling quadrats, I recorded densiometer measurements in each of the four cardinal directions. These measurements were averaged to give an average percent canopy cover for the 1x1 m quadrat. Because canopy cover is such a fine-scaled, highly variable attribute and I had

only three measurements per 20 m, I did not attempt to interpolate these data to estimate canopy in areas where I did not take measurements. The original seedling quadrat data, therefore, were the only information available to evaluate the importance of canopy cover. The importance of canopy cover was the only environmental relationship for which I used the 90 seedling quadrats rather than the more intensively sampled seedling transects along the plot centerlines.

- (2) On a larger spatial scale, radiation is influenced by hillslope orientation. I used the elevation values from the VIPs to create a surface from which hillslope orientation could be estimated for specific points in the plots. Several techniques are available for interpolating point measurements to a continuous surface. I explored inverse-distance weighting (IDW) and kriging. IDW is one of the simplest interpolation techniques, as it relies solely on the linear distance to known measurements to estimate values for new locations. Kriging modifies the weighting of measurements through semi-variogram analysis of spatial autocorrelation. In this analysis, kriging performed better than inverse distance weighting in both a cross-validation check of the data used to construct the DEM and a true validation test with independent elevation data (Figure 4.3). The kriged 1-m resolution DEMs were used to derive fine-scale estimates of aspect. These estimates were transformed along a northeast-southwest axis using the following transformation: $-\cos(45-\text{aspect})$ (after Beers et al. 1966).

4.1. Summary of geospatial data layers built for analysis.

	<u>Variable</u>	<u>Comment</u>
Biotic	Trees	Location, dbh, species, growth rate of all trees
	Mortality	Location, dbh, and species of all identifiable snags
	Seedling/sapling transect	Location, size class, species of all seedling and saplings along centerline
	Seedling quadrats	Location and tally of all seedlings by size class in 1x1m plots
Light	Canopy cover	Densimeter readings in four cardinal directions at each seedling quadrat
	Transformed Aspect	Aspect derived from 1-m and 10-m DEMs and transformed to a NE-SW axis
Soil Moisture	Focal concavity grid	Focal mean elevation for 3 cell radius - local elevation using 1-m DEM
	TCI	$\ln(a/\tan\beta)$ where upslope area (a) is based on the surrounding watershed
	Surface soil moisture	Surfaces built from regression and kriging of June moisture measurements
Snow	Snow depth transect	Spline of 1m measurements along centerline
	Lichen height	Average value for each 20m segment
	SNOBOs	Kriged surface using SNOBO point values
Temperature	HOBOS	Kriged surface for June and January mean, minimums and maximums

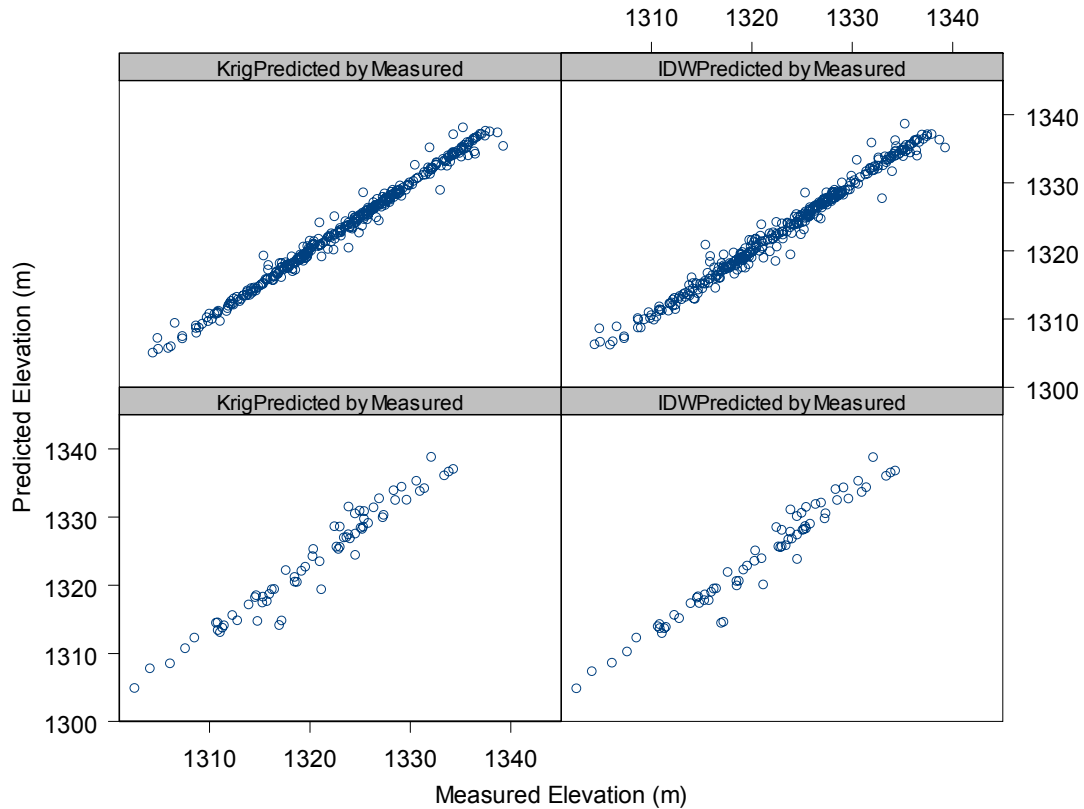


Figure 4.3. Comparison of kriging vs. IDW as interpolation techniques to create a high-resolution DEM from VIP points. Top panels present a cross-validation analysis of 340 points used to construct DEM for Plot 2. Kriging root mean square error (RMSE) = 0.83 m. IDW RMSE = 1.06 m. Bottom panels present a validation analysis with 70 independent measurements of elevation. Kriging RMSE = 3.60 m. IDW RMSE = 3.71 m.

- (3) Coarser estimates of radiation also were derived by calculating transformed aspect from a 10-m USGS DEM of the HJA.

Moisture – Because radiation influences evaporative demand it is highly related to moisture. Soil moisture variability was estimated directly using a number of different methods. I developed two DEM-based indices of soil moisture: a focal concavity index (FCI) and a topographic convergence index (TCI). I also interpolated field measurements of June surface soil moisture.

- (1) FCI accounted for topographic context as:

$$\text{FCI} = \text{Focal Mean Elevation (3 cell radius)} - \text{Local Elevation} \quad (\text{eqn. 4.1})$$

where focal mean elevation is the average elevation value for a circle centered on the cell of interest with a radius of three neighboring cells.

Local elevation is the elevation value at the cell of interest. The index was calculated using the 1-m DEM. Following the example of McNab's (1989) terrain shape index, positive FCI values are returned for sites that are low relative to their neighbors and, therefore, collect water. Convex sites have negative values and more quickly disperse water.

- (2) TCI was calculated as in Beven and Kirkby (1979):

$$\text{TCI} = \ln(a/\tan\beta) \quad (\text{eqn. 4.2})$$

where a is the upslope contributing area and β is the local slope angle.

Because the focus plots were not physically separated from their surroundings, estimates of topographic drainage must consider the larger

spatial context. I used the 1-m focus plot DEMs to estimate the local slope angle (β), but used a 30-m DEM of the entire HJA to calculate the upslope contributing area (a) beyond the extent of the focus plots.

- (3) The soil moisture measurements were interpolated across the plots using two approaches. The June 2002 data were used for these analyses because they captured the largest variability in wetness. Soil depth was estimated by kriging soil probe measurements across the plots. These estimates along with plot-level terrain data (elevation, slope, aspect, tci) were used in regression equations for all plots combined and for each plot individually. As a complementary approach, surfaces were constructed by kriging the moisture measurements.

Snow – Snow cover was included in the analysis as a potential influence on seedling establishment; therefore, I needed to develop estimates for this variable along the seedling transect down the plot centerlines. I tried three approaches to capture the large spatial and temporal variability in snow. Each had its limitations.

- (1) Measurements of snow depth at 1-m intervals along the centerlines were splined to create a continuous estimate. These measurements represent conditions for a single day and were taken at only three of the five plots.
- (2) The average lichen height on six to eight trees in each 20-m segment was assigned to each seedling within that 20-m segment. Relative differences in lichen height should correspond to relative differences in winter snow depth for this coarse resolution estimator.

(3) The dates at which each SNOBO became snow free were kriged to create a continuous surface. I did not have enough of these loggers to get a systematic coverage (also ~1 every 20 m) and I mainly was experimenting with them as a proof of concept.

Temperature - Coverages were created for June and January averages, minimums and maximums by kriging the HOBO point data. Loggers were installed at each 20-m marker along the transect centerlines.

Statistical methods

I compared patterns in radiation, temperature, soil moisture and snow cover to the demographic patterns for the different species using a combination of t-tests, logistic regression, and classification tree analysis. To examine potential dispersal limitations, I considered spatial patterns of trees and seedlings within the plots using bivariate Ripley's K analysis.

Logistic regression is a regression technique used for characterizing binary responses such as presence-absence (Jongman et al. 1995). It uses maximum likelihood to fit a model to describe the log transformation of the probability (p) of some condition being met. Maximum likelihood is used rather than least-squares regression because the regression errors are not normally distributed, a necessary condition of least-squares regression. Instead, errors are binomially distributed based on whether or not presence/absence observations are correctly predicted. The logit transformation is used to

stretch the p -interval of 0 to 1 to $-\infty$ to $+\infty$, which allows for linear regression (Yee & Mitchell 1991, Jongman et al. 1995):

$$p() = \frac{e^{\mu}}{1 + e^{\mu}} \quad (\text{eqn. 4.3})$$

where μ is the linear predictor equation. In this analysis, I used logistic regression to model the presence or absence of (1) a seedling of any type, (2) *T. heterophylla*, (3) *A. amabilis*, or (4) *A. procera* seedlings in the 1x1-m seedling sample quadrats based on canopy measurements from the quadrats. I also used it to examine the importance of the different predictor variables in explaining the distribution of *T. heterophylla* seedlings relative to the distribution of the *A. spp* seedlings.

Classification and regression tree (CART) analysis is a divisive analysis that attempts to partition a data set by recursively dividing it into subsets based on the strongest predictor variable (Breimann et al. 1984). The technique offers several advantages over the regression approach. It allows the distribution of multiple categories of data to be considered simultaneously. The interpretation of the tree is rather intuitive and can be easily converted to a geographic information system for visualization of results (Moore et al. 1991). The data structure allows for the incorporation of substitution and compensatory relationships. The hierarchical structure of the model allows the data to be partitioned at multiple levels of complexity. Finally, because each branch of the tree is defined independently of other branches and the decision rules rely on no assumptions regarding the underlying model structure, CART allows a data set to be classified with great accuracy. Unfortunately the high degree of accuracy may result in

an over-fitting of many ecological data sets. To account for this tendency to over-fit, I used cross-validations of one-tenth of the entire data set to prune less important branches from the trees. Classification accuracy was determined from an average of these 10 cross-validated trees. The effect of this cross-validation was to penalize trees that over-fit the data. The final trees were trimmed to eliminate branches that caused an increase in the misclassification rate of the entire data set. In this analysis, I used CART to complement the logistic regression analysis in identifying important variables for differentiating between species type for seedlings observed in the seedling transects along the plot centerlines.

Point pattern analysis can be a valuable tool for interpreting the spatial functioning of ecosystems (Moeur 1993). Ripley's K analysis (Ripley 1976) is a point-pattern analysis that considers the cumulative distribution of observed points relative to the distribution of points generated by a random process. The Ripley's K function differs from conventional nearest neighbor analyses in that it considers distances between all observed points and not just the first or second nearest neighbor. An advantage of preserving all spatial relationships in the data is that Ripley's K tests can assess pattern at multiple scales, and thus it can be used to evaluate spatial scales of clustering, in a univariate sense, or attraction/repulsion, in a bivariate sense. To test the dispersal limitation hypotheses, I conducted a bivariate label permutation test of seedlings and trees in each of the plots. All trees and seedling locations were held constant, while I randomly reassigned the species labels of the seedlings. The distances from seedlings to conspecific adults for 99 of these randomized trials were then compared to the distances

for the actual data to assess significance ($P < 0.01$). Observations higher than the randomized data were considered to be positively associated. Observations lower than the randomized data were considered to be negatively associated. The scale of any positive association should be reflective of that species' dispersal distance.

Results

Plot descriptions

In total, four plots were installed in 2001 and a fifth was installed in 2002 (Table 4.2; Figure 4.4). Plots varied in length from 100 to 180 m and in elevation from 1225 to 1397 m. Two of the plots were aligned along the dominant elevation gradient (Plots 5 and 6). A third hillslope gradient plot crossed a small shoulder at the upper end (Plot 3). One of the plots captured contrasting aspects separated by a discrete ridgeline (Plot 4). Finally, Plot 2 was oriented to capture multiple hillslope aspects in undulating terrain.

Biotic patterns

A. amabilis was slightly more abundant than *T. heterophylla*, though both species were well-represented on the plots (Figure 4.1). *A. procera* and *P. menziesii* also were present, with size-class distributions typical of early successional species. Mortality of *A. spp* was considerably greater than for the two other species. Only one dead *T. heterophylla* was found on all of the plots. Percent mortality for *A. spp* ranged from highs of 25 percent (Plot 4) and 46 percent (Plot 2) to lows of 11 percent (Plot 6), 13

Table 4.2. Summary of five ecotone plots.

Plot	Location	UTME	UTMN	Elevation	Aspect	Slope	Transect Length	Orientation	Notes
2	Carpenter Mtn	567042-150	4902642-800	1304-1340	SE-SW	0-20	180	Across undulating ridges	Area of high fir mortality
3	Frissell Ridge	568129-240	4901209-254	1278-1312	NW-W	15-24	110	Over a small shoulder	Clearing near top with few live trees
4	Lookout Mtn	570142-234	4894840-928	1377-1397	SW-N	0-32	100	Opposite sides of ridgetop	Abrupt transition at ridgetop
5	Lookout Mtn	565107-208	4895900-930	1225-1256	NW	5-22	100	Hillslope gradient; flattens upslope	Very gradual transition
6	Frissell Ridge	569160-279	4899935-990	1274-1352	W	34	120	Hillslope gradient	Gradual transition

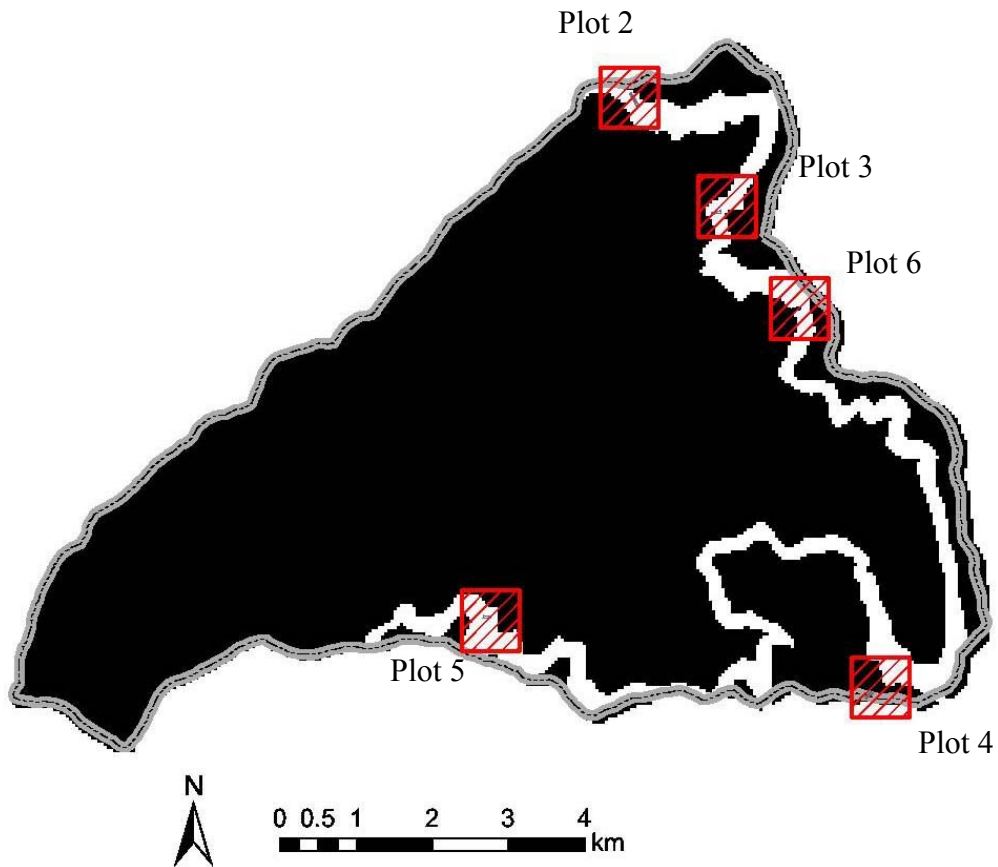
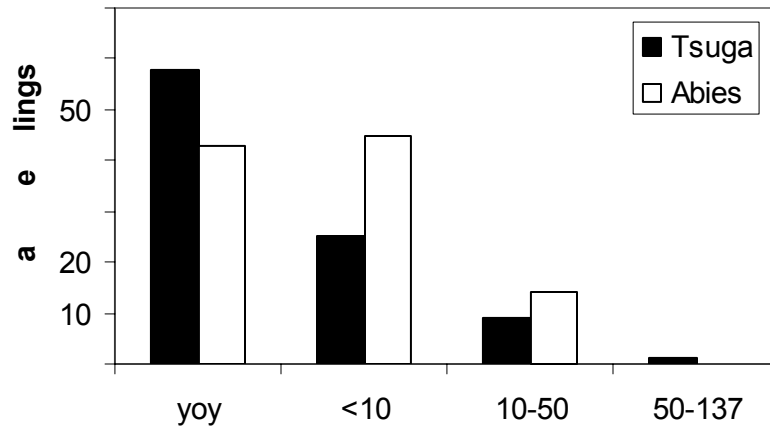


Figure 4.4. Ecotone plot locations. White area represents transition zone as identified by the community model in Chapter 2.

percent (Plot 3) and 14 percent (Plot 5). *P. menziesii* mortality was more evenly distributed: Plot 4 had 27 percent mortality and all other plots had between 15 percent and 20 percent. Total basal area was approximately three times greater on Plot 6 (260 m²/ha) and Plot 5 (305 m²/ha) than on Plot 4 (92 m²/ha). The basal area of *A. spp* was evenly distributed among the plots (25 m²/ha to 50 m²/ha) except for on Plot 5 (122 m²/ha).

A. spp seedlings were slightly more abundant than *T. heterophylla* seedlings (Figure 4.5). Thirty-seven out of the 90 seedling quadrats had seedlings in them. Of the 198 seedlings observed in these quadrats, 93 were *T. heterophylla*. Nearly all the remaining seedlings were *A. spp*, with only three *P. menziesii* seedlings found in the quadrats. Of the 1488 seedlings recorded along the line transects, 835 were *A. spp* and 653 were *T. heterophylla*. The size class distribution of *T. heterophylla* was skewed much more heavily towards young-of-the-year than the *A. spp* for both the quadrat and transect samples. More than 50 percent of seedlings in their first growing season were *T. heterophylla*. In the next smallest size class recorded (second growing season through 10 cm in height), that percentage had dropped to 27 percent. Plot 6 had the fewest total number of seedlings (75 along the transect and only one quadrat with any seedlings). Plots 5 and 6 had approximately four times as many *T. heterophylla* seedlings as *A. spp* seedlings. Plot 2 had just over twice as many *A. spp* seedlings as *T. heterophylla* seedlings, and Plot 4 had 353 *A. spp* seedlings but only 1 *T. heterophylla* seedlings. Plot 3 had nearly equal amounts of the two seedling types.

(A)



(B)

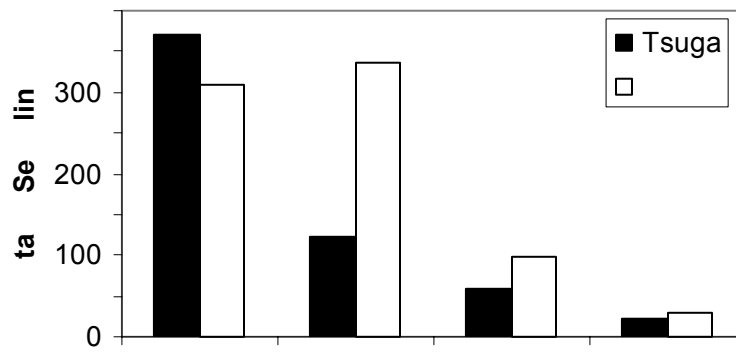


Figure 4.5. Seedling histograms. (A) Seedlings from three (1x1 m) seedling quadrats placed randomly every 20 m. (B) Seedlings measured along continuous 2-m wide transect down the middle of the plot. Young of year (yoy) are first year germinants.

Environmental patterns

Light/radiation – Canopy cover was generally high throughout, ranging from plot means of 90-95 percent, but differences between plots were significant (Table 4.3, ANOVA: $F = 8.6$, $P = 0.004$). In addition to having the highest average canopy opening, Plot 6 also had one of the most southwesterly hillslope orientations. Plot 2 was southwest facing, while Plot 3 and 5 received less direct radiation (Table 4.3). Plot 4 crossed a distinct ridgeline and encompassed two extremely contrasting aspects. At 1-m resolution, terrain was highly variable and mean aspect differences among plots were not significant (ANOVA: $F = 1.0$, $P = 0.31$). When aspect was derived from the 10-m resolution USGS DEM data, within-plot variability was reduced and among-plot differences were significant (ANOVA: $F = 10.9$, $P = 0.001$).

Soil moisture – Plots were sampled twice in 2002: once in June at the beginning of the summer dry down, and a second time approximately a month later when soils had dried out substantially. Soil moisture ranged from 10-48 percent in June and from 6-25 percent in July. Values decreased an average of 7.5 percent per sample location between the two sample dates ($\sigma = 5.9$). The plots in the southern part of the watershed lost much more moisture than those in the northern part. Seventeen points decreased by over 20 percent. Of these, 12 were on Plot 5 and the remaining five were on Plot 4. These two plots were significantly wetter at the beginning of the sample period (Table 4.4). By the July sampling, all the plots had dried down to a similar level.

Differences in soil moisture were significantly associated with radiation differences. For the 283 June samples collected at all plots combined, geographic location

Table 4.3. Percent canopy opening and Transformed Aspect (NE = -1; SW =1) for 90 seedling quadrats. Average plot values are shown along with standard deviations. Transformed aspect values are provided from both the 1-m and 10-m DEMs.

Plot	Canopy Opening (%)	TAspect 1-m	TAspect 10-m
2	4.8 (2.6)	0.75 (0.23)	0.96 (0.05)
3	5.2 (4.5)	0.14 (0.42)	0.38 (0.16)
4	4.9 (5.7)	0.03 (0.82)	0.42 (0.74)
5	6.9 (5.0)	-0.21 (0.54)	-0.6 (0.03)
6	9.3 (6.3)	0.84 (0.09)	0.83 (0.04)

Table 4.4. Summary of soil moisture measurements. Moisture was sampled in the top 0-20 cm of soil.

Plot	June 2002				July 2002			
	Mean	Range	St.Dev.	N	Mean	Range	St.Dev.	N
2	19.0	(12-26)	2.8	92	12.7	(7-18)	2.2	95
3	16.4	(11-24)	2.8	54	12.4	(7-18)	2.1	57
4	27.7	(21-41)	5.0	18	9.1	(6-14)	2.1	17
5	30.2	(13-48)	7.7	43	14.0	(6-25)	4.8	50
6	17.4	(10-34)	3.6	76	12.6	(6-23)	2.9	77

was the strongest explanatory factor in a regression model of surface soil moisture ($r^2 = 0.35$ and 0.15 , respectively for Northing and Easting UTM coordinates). When the UTM coordinates were not included in the analysis, transformed aspect was the strongest explanatory variable of moisture ($r^2 = 0.12$, $P < 0.001$). Aspect was particularly important in explaining soil moisture differences on the two plots that crossed ridges (Plot 3 and Plot 4). Elevation also was an important explanatory variable for the moisture regression models built for several of the individual plots. No terrain variables significantly described observed differences in moisture on Plot 6. The average root mean square error (RMSE) of the residuals from the regression model fits was 3.3 percent. I also used the spatial autocorrelation in the moisture measurements to interpolate continuous surfaces across the plots using kriging (Figure 4.6). This approach had similar success in fitting the data (average RSME = 4.1 percent), and it generated estimates for Plot 6 for which no regression equation could be developed. The kriged and regression-based estimates were highly correlated ($r = 0.92$, $P < 0.001$).

Snow – The snow depth measurements corresponded well with both the average lichen height on trees in the plots ($r = 0.70$, $P < 0.001$) and with the snowmelt data from the SNOBOs ($r = 0.44$, $P < 0.001$). The snow depth transects provided the finest resolution measure (Figure 4.7). I was able to reach three very different plots for this sampling: (1) Plot 2, which stretched across an undulating ridge; (2) Plot 3, which was a more classic hillslope gradient; and (3) Plot 4, which included opposing sides of a ridgeline. Snow depths at the time of sampling ranged from 0 cm to much greater than 100 cm. None of the plots were completely snow free and none of the plots were

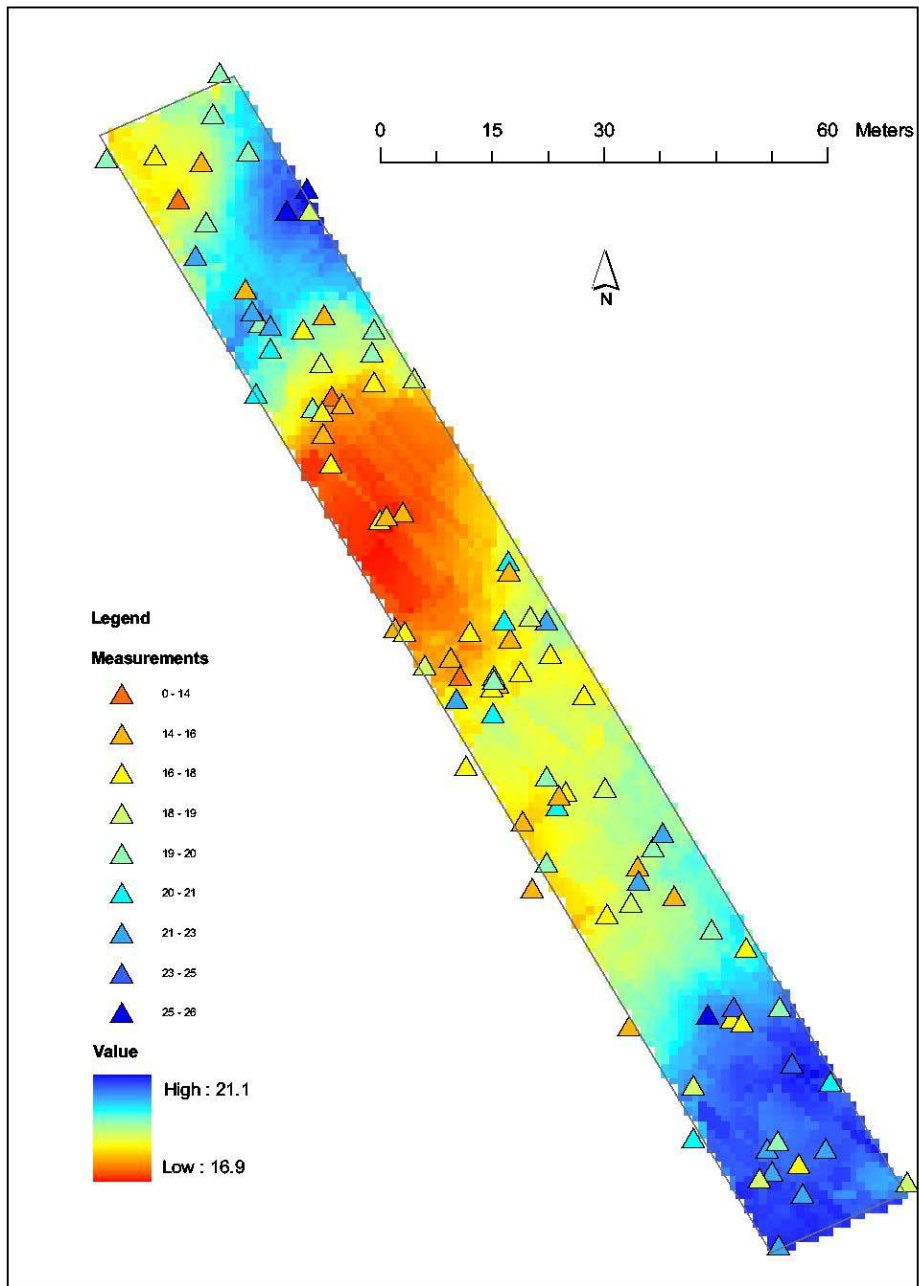


Figure 4.6. Example kriged soil moisture coverage with sample points overlaid (Plot 2).

Focus Plot 2 (Snow Depth)

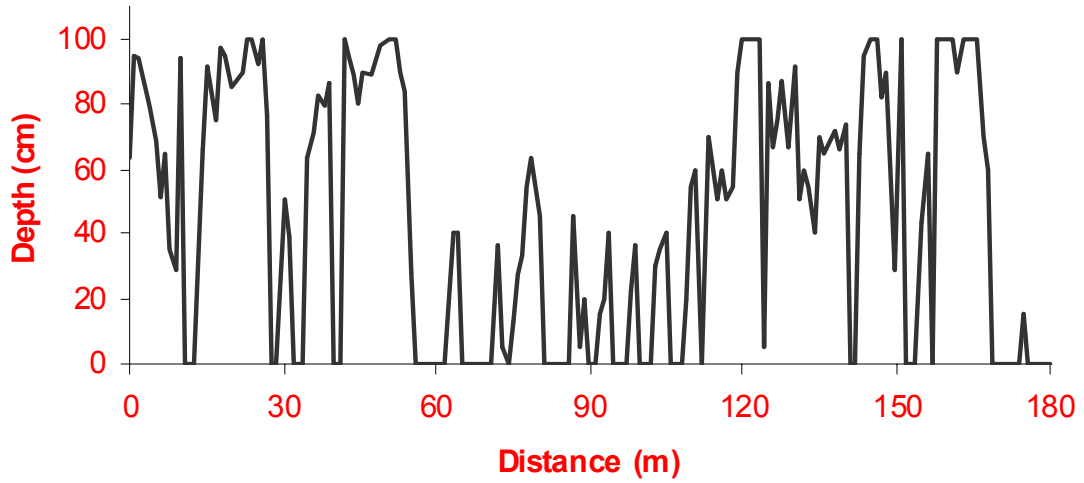


Figure 4.7. Example snowdepth transect. Depth measurements were taken each 1 m along the centerline and splined to create a continuous surface (Plot 2).

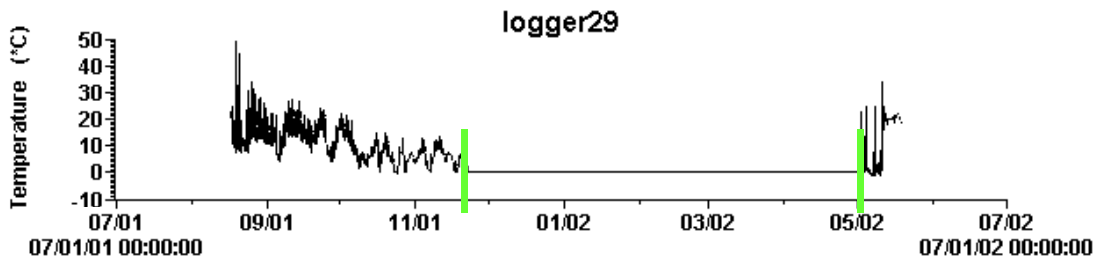


Figure 4.8. SNOBO melt data for a location on Plot 2. Snow cover is indicated by the straight line at 0 °C from 11/22/01 to 5/03/02.

completely covered in snow. The pattern of snowmelt, however, differed considerably among the three plots. Snow depth on Plot 2 was highly variable at fine spatial scales with a noticeable trend of lower depth at the ridge located in the middle of the plot. Depth on the classic gradient plot (Plot 3) generally increased with increasing elevation. Snow on Plot 4 was absent from the south-facing aspect and deeper than the 100 cm tile probe on the entire north-facing aspect. The finding of the deepest snow of any of the sample sites on this north-facing aspect on Lookout Mountain is consistent with other studies that suggest this area is the coldest and wettest region of the HJA (Smith 2002). This plot also had the highest elevations included in the study.

The SNOBO sensors were effective in capturing snow dynamics over the winter 2001-2002. A few isolated snow events were recorded in the early fall, but temperature was still highly variable at all sites until November 22. After this major snowstorm, temperatures recorded by the SNOBOs remained within 1° of 0 °C until spring snowmelt (Figure 4.8). Very few snowfree days were observed before the final spring melt. Snowoff, measured as the date at which temperature rose above 1°C and variation increased, was obvious for all the sensors. The average snowoff date was May 17. Although the network of sensors was sparse (~1 sensor every 20 m), both within and among site trends were observed in the SNOBO data. The average standard deviation within a plot was 8 days, with the undulating terrain plot (Plot 2) having the largest range in snowoff for its sensors (35 days). Plot 2 also was the last to have all of its sensors become snowfree, which did not occur until June 4. For comparison, 6 SNOBOs were distributed in the *T. heterophylla* zone from 1140 m to 1180 m in elevation, directly

downslope from Plot 2. Snowoff occurred from April 20 to 28 at these sensors, up to a full month earlier than in the transition zone 160 m upslope in elevation.

Temperature – By controlling for elevation, I also severely limited the range of temperature values observed on the plots (Table 4.5). Weather related damage and vandalism resulted in the recovery of only three to six portable temperature sensors per plot. The within-plot ranges of the mean June values for the different sensors were less than 0.5 °C, and the within-plot variations in January means were even smaller. Among-plot variation also was small and less in January than June. The more southern plots (Plots 4 and 5) were slightly cooler than the plots in the northern portion of the watershed. Plot 5, which was located on a northwest-facing local slope along the generally north-facing Lookout Ridge, was consistently coolest despite the fact that it was at the lowest elevation of any of the plots.

The temperature data were associated with the small differences in elevation within the plots, though the associations were not consistent across the plots. Examining the relationship across the entire dataset, January temperatures were significantly negatively correlated with elevation, but June maximum temperatures were not. On a plot-by-plot basis, however, June maximums were consistently negatively correlated with elevation (r -coefficients from -0.43 to -0.89). The different measures of temperature (June mean, June maximum, January mean, and January minimum) were significantly positively correlated with each other except for January means with June maximums.

Table 4.5. Summary of temperature data gathered from portable microloggers. N is the number of sensors per plot. Mean is the overall mean temperature recorded from all sensors combined. St.Dev. is the standard deviation of the individual mean sensor values for the plot. Abs. Range is the absolute lowest and absolute highest values recorded on the plot.

Plot	N	June			January		
		Mean	St.Dev.	Abs. Range	Mean	St.Dev.	Abs. Range
2	6	11.6	0.17	-0.19 - 30.33	1.2	0.12	-7.56 - 10.38
3	4	11.9	0.14	-0.47 - 29.95	1.2	0.18	-7.99 - 11.02
4	3	11.0	0.11	-1.14 - 25.73	1.1	0.06	-8.35 - 9.67
5	4	11.5	0.21	0.23 - 27.27	1.2	0.11	-6.53 - 9.94

Environmental controls on demography

I discuss below how demographics relate to environmental patterns in temperature, radiation, snow and moisture. First, I briefly describe the associations for the entire watershed. Then, I address the associations at the ecotone level.

Landscape-level associations

Abundance data from an earlier analysis of forest community pattern across the HJA (Chapter 2) indicated a relatively sharp transition in species type at approximately 1300 m in elevation (Figure 4.9). While *A. amabilis* seedling density was still relatively high below this threshold, *T. heterophylla* seedling density began to decline well before reaching this threshold. *T. heterophylla* mortality was low throughout its range, while *A. amabilis* and *A. procera* mortality rates were high at or below their lower-elevation threshold. These trends suggest that the regeneration phase may be limiting the upslope migration of *T. heterophylla*, whereas the range of the *A. spp* may be limited by high mortality at low elevations. I examined the growth rates of these species in more detail to determine if changes in relative competitive advantage coincided with the high *A. spp* mortality.

Environmental correlations with growth rates may be sufficient to explain the inability of *A. spp* to compete successfully at lower elevations, but *T. heterophylla* growth was not strongly associated with environmental factors. I examined the mean annual increment (rw) from 1990-1995 of 1723 trees cored throughout the entire HJA watershed from 1997-1999 (943 *T. heterophylla*, 547 *A. amabilis*, and 234 *A. procera*). Trees

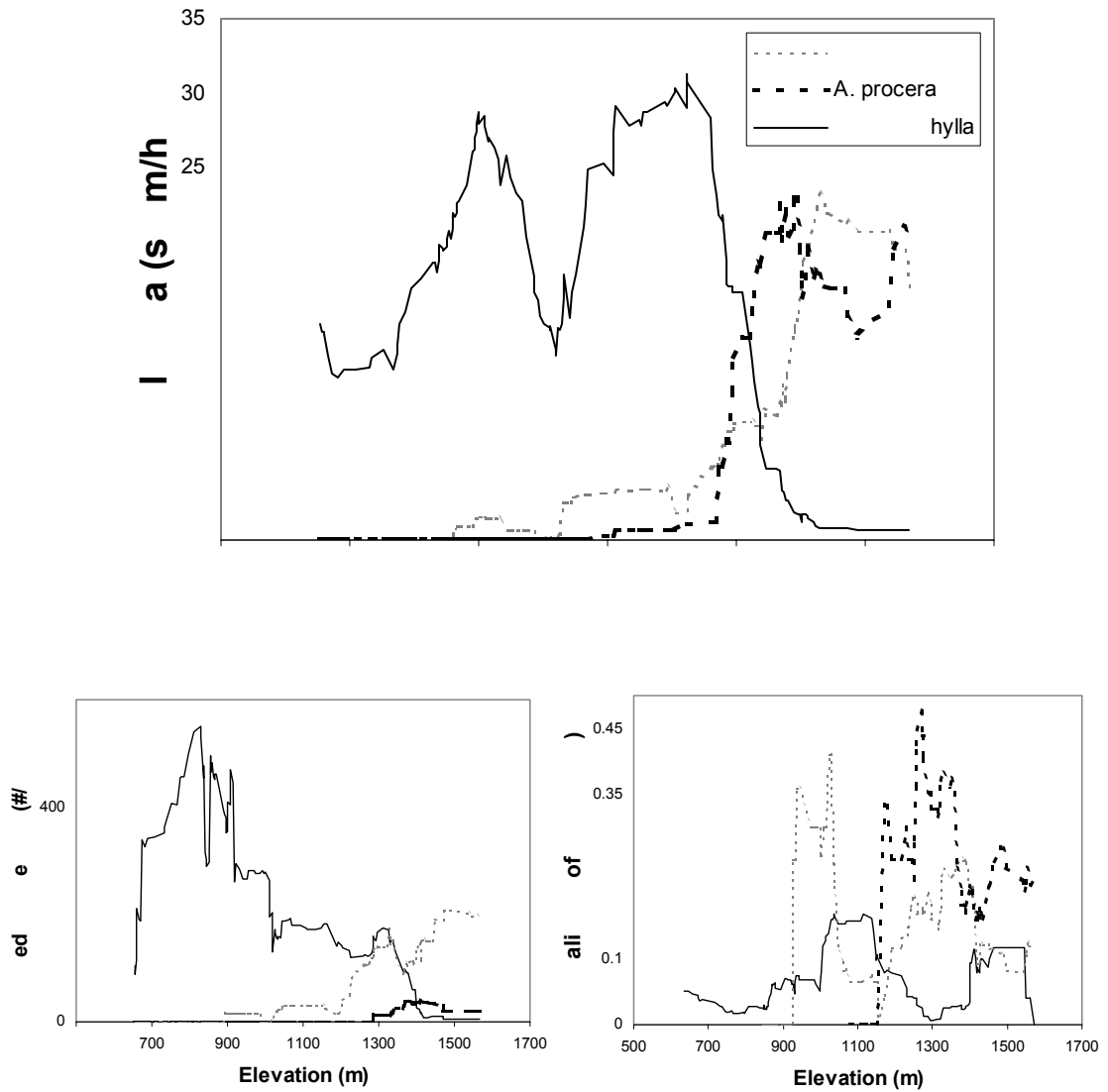


Figure 4.9. Elevation trends observed from 175 (20x20 m) sample plots spread across the entire HJA watershed. The top panel present the average basal area of each species on the plots. The bottom panels present the seedling density and mortality for the different species. Lines are 20-point running averages.

ranging in size from 5-190 cm diameter at breast height (DBH) were included in the analysis, resulting in a space-filling graph of the mean growth increment plotted against elevation (Figure 4.10A). The first step in the analysis of tree growth rates was to develop equations for the diameter-corrected mean annual increment for each of the species. A series of increasingly more complicated models considering elevation, basal area (BA), and the environmental factors modeled in Chapter 3 (summer radiation, temperature and soil moisture) were compared to these simple equations. The models were nested so the significance of new terms could be evaluated by likelihood ratio tests (Sokal & Rohlf 1995). The following, most parsimonious models resulted:

$$T. heterophylla: \ln(rw) = -1.0 + 0.5\ln(DBH) - 0.001BA \quad (\text{eqn. 4.4})$$

$$A. amabilis: \ln(rw) = 0.3 + 2.0\ln(DBH) - 0.3(\ln(DBH))^2 - 0.18TEMP - 0.008BA \quad (\text{eqn. 4.5})$$

$$A. procera: \ln(rw) = -2.8 + 2.4\ln(DBH) - 0.3(\ln(DBH))^2 - 0.12TEMP \quad (\text{eqn. 4.6})$$

I log transformed the growth rate and diameter data to: (1) improve the normality of these datasets and (2) improve the linearity of the relationships with these variables. The negative quadratic terms in the *A. spp* equations indicate that growth rates in these species began to decline after a certain size. After accounting for diameter effects, the growth rates of both the *A. spp* were negatively associated with temperature. Growth rates for *T. heterophylla* were fairly consistent across temperatures. Growth declined with increasing basal area for the two shade-tolerants. *A. procera* growth rates were not significantly associated with basal area, most likely because trees of this shade-intolerant species would not even be present in the understory of heavily stocked stands. A plot of the predicted growth rates of average sized trees (27.5 cm dbh) in a stand of average basal area (83 m²/ha) suggests that *T. heterophylla* should be competitively

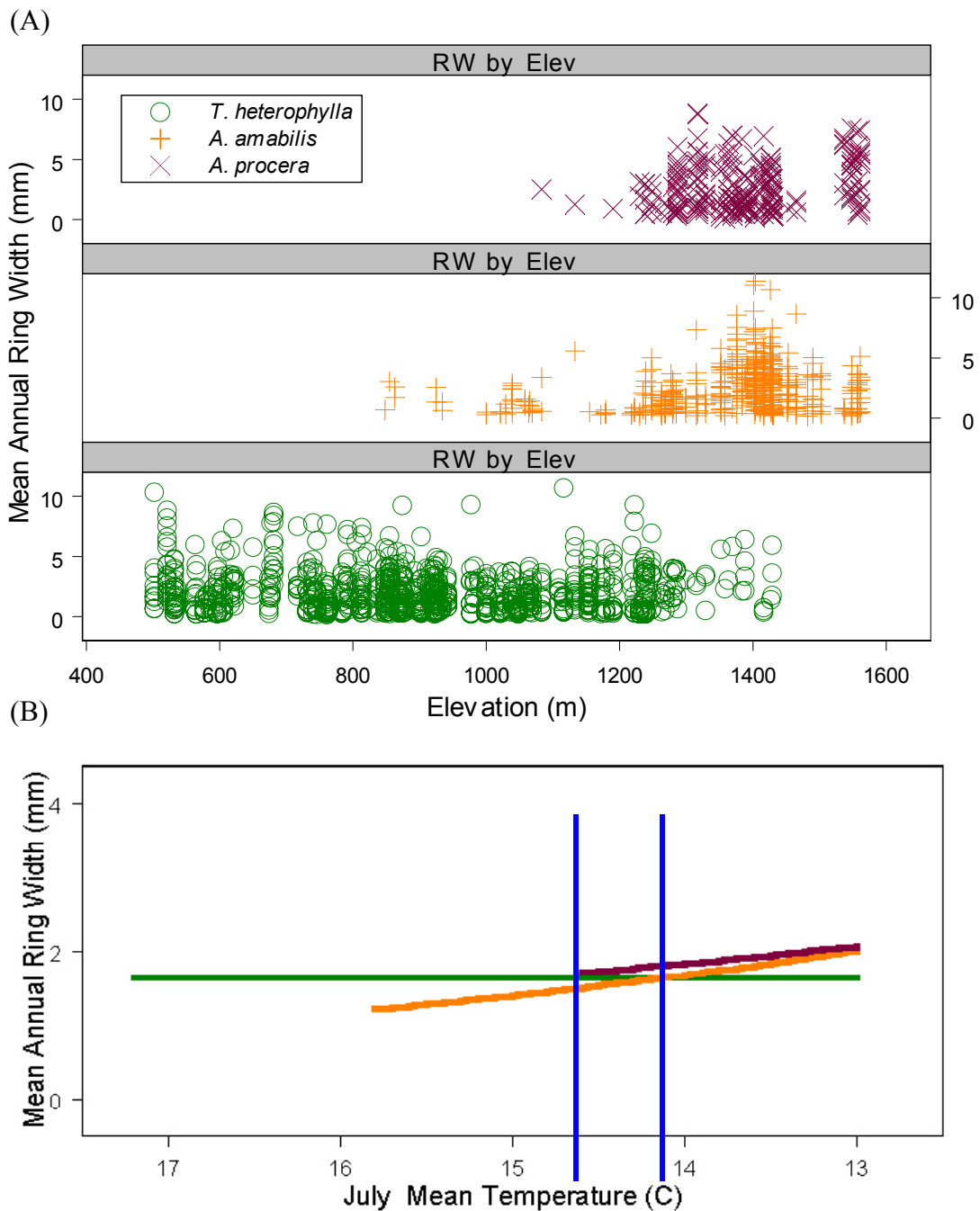


Figure 4.10. Landscape trends in relative growth rates. (A) Five-year mean annual ring width against elevation for trees found on the 175 landscape-wide plots. (B) Fitted mean annual ring width against temperature, the strongest environmental correlate with growth for the *A. spp.* Regression equations account for any significant relationships with tree size and stand basal area. Competition favors *T. heterophylla* at temperatures greater than the blue lines.

superior to *A. spp* above the temperature at which the lines cross (Figure 4.10B). The absolute values in temperature in Figure 4.10B should not be interpreted strictly, as the temperature model predicts relative temperatures only (see Chapter 3.2). The crossing of the growth curves does correspond with the elevation of the ecotone (~1200 m).

I also compared the ability of temperature, soil moisture and radiation to explain patterns in regeneration at the landscape level. In particular, since the direct ordination of *T. heterophylla* seedling density against elevation suggested that regeneration of this species may be influenced by environmental gradients, I conducted a regression tree analysis on these seedlings with the more plant-relevant variables. Temperature was the first splitting variable in the tree. Soil moisture was important in limiting the fine-scale distribution of seedlings within the upper temperature zone (Figure 4.11). The highest density of seedlings were found at sites of high temperature and high moisture.

Ecotone level associations

Growth and mortality trends were not significant for any of the species on the ecotone plots. I found only one dead *T. heterophylla* tree on the ecotone plots. Mortality of *A. spp* in the ecotone plots was highly variable, but consistently greater than *T. heterophylla* mortality. Growth rates were not significantly associated with elevation, temperature or any of the other environmental variables (Figure 4.12). The remainder of this section focuses on significant influences on regeneration

Only thirty-seven of the 90 (1x1 m) seedling quadrats had seedlings present. *A. spp* seedlings were present in 26, *T. heterophylla* were present in 13, and *P. menziesii*

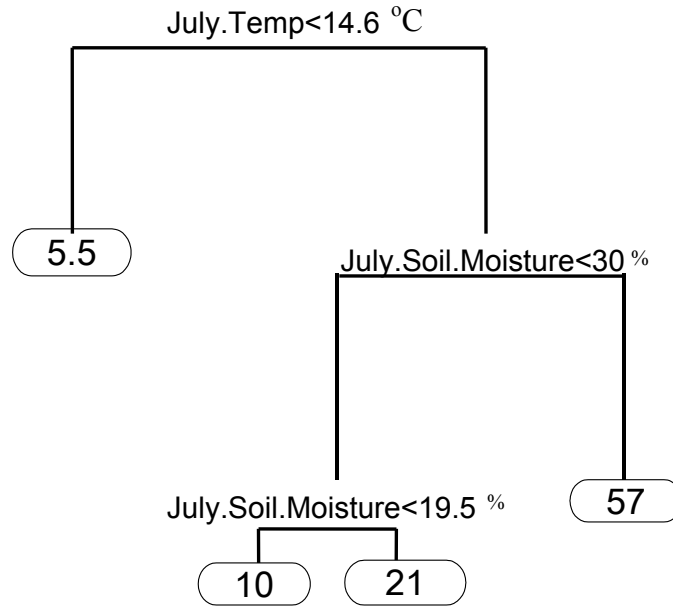


Figure 4.11. Regression tree model of *T. heterophylla* seedling density on 175 landscape-wide plots. Circles provide mean number of seedlings for the plots described by that end-node. Length of branch corresponds to the amount of variance explained by that variable.

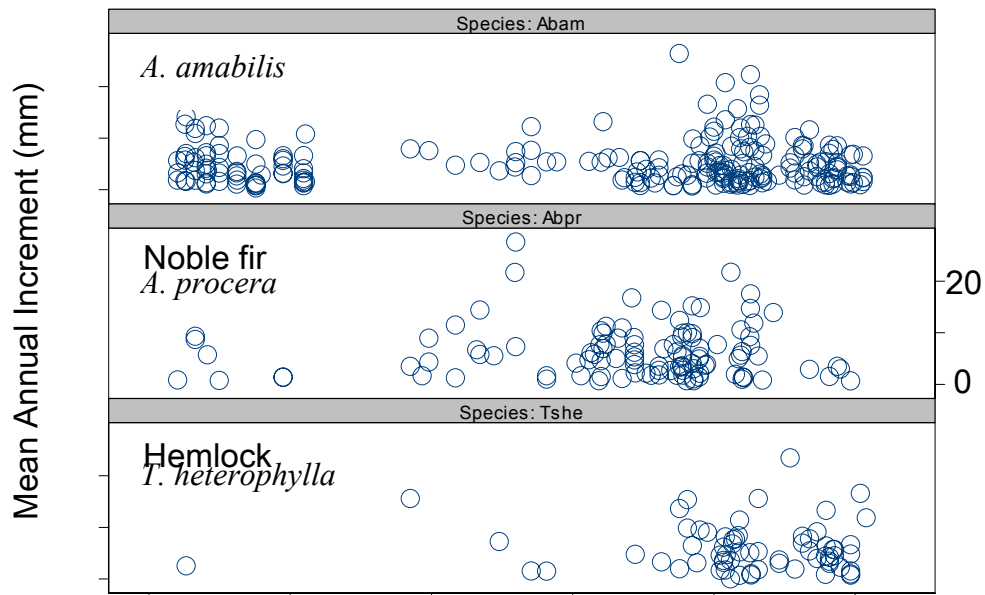


Figure 4.12. Ecotone trends in relative growth rates. Growth was not significantly associated with any of the environmental variables considered.

were present in 3. Only 3 plots had both *A. spp* and *T. heterophylla* seedlings. Logistic regression equations using canopy measurements taken at these quadrats significantly predicted *T. heterophylla* presence/absence (positive association with canopy cover, $r^2 = 0.06$, $P = 0.007$), but were not significant in describing the distribution of either of the *A. spp*.

By examining the individual seedlings along the centerline transects, I was able to increase the sample sizes considerably (N = 653 *T. heterophylla* seedlings, 603 *A. amabilis* seedlings, and 232 *A. procera* seedlings). I used the derived environmental coverages of light, snow, temperature and moisture to group seedling observations by species in classification tree and logistic regression analyses. Because I did not have information on each of the variables for all of the plots (Table 4.2 provides a description of each of the variables), I examined each plot separately in addition to aggregating across all plots.

The distributions of seedlings on plots dominated by *T. heterophylla* seedlings were less easily explained by the classification tree analyses than were the distributions of seedlings on plots that contained a more even mix of seedling types (Table 4.6). Plot 4 was dominated by *A. spp* seedlings to the point that *T. heterophylla* seedlings were not even present. Plots 2 and 3 provide the best opportunities to examine the limitations on *T. heterophylla* regeneration. The combination of moisture and temperature was best able to explain the seedling distributions on these plots. The difference in explanatory variables between the plots suggests that multiple mechanisms may be important. On Plot 2, *T. heterophylla* were observed on drier sites. On Plot 3, *T. heterophylla* were found on

Table 4.6. Summary of most important plant-relevant variables identified by classification tree. Variables are provided in the order in which they were added to the classification tree. Significance was tested by two sample t-tests. The number of seedlings of each species is provided at the bottom of the table. Average snowdepth measurement was deeper for *A. spp* seedlings than *T. heterophylla* seedlings on Plot 3, though the difference was not statistically significant ($P = 0.08$). Too few *T. heterophylla* seedlings were available for tests on Plot 4. Snowdepth measurements were not available for Plot 5, and snowdepth, SNOBO, and temperature was not available for Plot 6.

	Plot 2	Plot 3	Plot 4	Plot 5	Plot 6
	Summer Temperature	Moisture	---	Moisture	None
	Moisture	Radiation		Radiation	
	Winter Temperature	Winter Temperature			
		Snow (n.s.)			
<i>T. heterophylla</i>	124	70	1	397	61
<i>A. amabilis</i>	119	53	334	84	13
<i>A. procera</i>	176	27	17	11	1

wetter sites as the shade-intolerant *A. procera* dominated drier, southwest-facing aspects. Snowdepths were not significantly different for the different species on either plot. Depths were slightly deeper for *A. spp* seedlings on Plot 3, but were less deep on Plot 2.

Results of the logistic regression analyses corroborated the importance of temperature and moisture as explanatory variables, but reemphasized the high plot-to-plot variability. For this group of analyses, the total amount of variance explained by each variable independently as examined rather than the combined influence of multiple factors as in the classification trees. Temperature differences were highlighted as the strongest predictor of *T. heterophylla* seedling presence/absence across all plots (Figure 4.13). Relationships were not consistent, however. Summer temperature differences were important in classifying *T. heterophylla* seedlings on Plot 2 only. January temperatures but not June temperatures were significantly different on Plot 3. Soil moisture was again the strongest predictor variable for Plot 3.

One difference between the logistic regression and classification tree results was in the relative importance of radiation. When considered independently in the logistic regression analysis, radiation was consistently the least important of the potential explanatory variables. When considered after accounting for moisture effects in the classification tree analyses for Plots 3 and 5, radiation was the second most important explanatory variable.

The point pattern analysis confirmed that the heavier seeded *A. spp* may be more prone to dispersal limitations than *T. heterophylla*, but none of the species were constrained by dispersal within the extents of the ecotone plots.

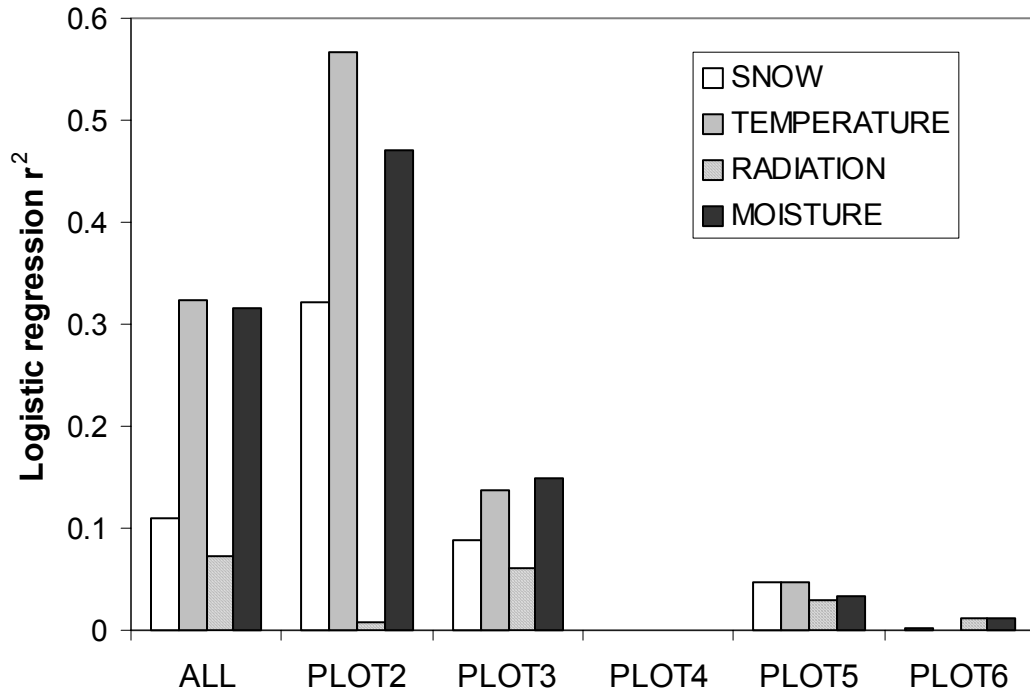


Figure 4.13. Summary of amount of variation in *T. heterophylla* distribution explained by logistic regression equations with each of the four environmental variables. Too few *T. heterophylla* seedlings were available for tests on Plot 4. Snowdepth measurements were not available for Plot 5, and snowdepth, SNOBO, and temperature was not available for Plot 6.

Discussion

In this study, I explored potential mechanisms of transition in a Pacific Northwest old-growth ecotone. I was interested specifically in comparing the relative importance of temperature, soil moisture, light, and snow to differences in growth and establishment. The results support a combination of factors that influence species sorting at the *T. heterophylla*/*A. amabilis* ecotone. On landscape scales, temperature associations with growth appear to be limiting the downward expansion of *A. spp.* Higher growth rates of *A. spp.* at cooler temperatures could be limiting the upslope migration of *T. heterophylla*. Temperature and moisture associations with regeneration also are highly associated with the distribution of *T. heterophylla* seedlings.

These same factors are most associated with the distribution of *T. heterophylla* seedlings in the fine-scale ecotone plots, though effects are variable from plot to plot. Radiation effects are highlighted at the ecotone level. Growth rates are not significantly related to changes in the environmental setting at this fine scale.

T. heterophylla

I found no relationship between *T. heterophylla* growth rates with any of the environmental variables, and, therefore, concluded that growth was probably not controlling the upper-elevation boundary of this species. It is possible that higher growth rates of *A. spp.* at high elevation give these species a competitive advantage over *T. heterophylla*, but no strong elevation trend was observed in *T. heterophylla* mortality and extremely low mortality was observed in the ecotone plots. These findings are consistent

with those of Acker et al. (1996) who found low *T. heterophylla* mortality relative to *A. spp* mortality in a 27-year study of a forest stand at 1290 m in the HJA. If differences in growth rates were leading to *A. spp* excluding *T. heterophylla* at high elevations, higher mortality of *T. heterophylla* trees should have been observed at upper elevations.

The results suggest that regeneration is likely to be limiting the range of *T. heterophylla* either through snow, temperature, or moisture limitation. Support for Thornburgh's (1969) snow hypothesis was equivocal. I did not find a consistent relationship between *T. heterophylla* regeneration and any of the estimates of snow depth and melt. The snow theory does have an intuitive appeal, as snow is an integrator of precipitation, temperature and radiation. It is possible that my measures of snow were not adequate to identify associations. Though the three approaches to recording snow were highly correlated with each other, at least two of the metrics (SNOBOs and lichen height) may have been at too coarse a grain to capture the fine-scale snowmelt dynamics that may be critical to regeneration. I had 1-m resolution measurements of snow depth for only two of the plots that had *T. heterophylla* seedlings. On one of the plots (Plot 3), *T. heterophylla* seedlings were found in areas of only slightly lower snow depth than were the *A. spp* seedlings. On the other plot (Plot 2), *A. spp* seedlings were found in areas of lower snow depth. This result contradicts Thornburgh's (1969) snow hypothesis, but supports Brooke (1964), who suggested that *A. amabilis* seedlings rather than *T. heterophylla* seedlings should be found in areas of early snow melt at higher elevations. He proposed that because of their early germination, *A. amabilis* seedlings have few available safe sites for establishment in areas that maintain snowcover into the summer

months. Those seedlings that try to establish on snow dry out and die, and only those seeds that find free locations are successful.

I also did not find *T. heterophylla* seedlings preferentially on south-facing slopes or canopy openings. The finding that *T. heterophylla* seedlings were more common under dense canopies than canopy gaps is contrary to one of Thornburgh's (1969) direct predictions, but it may indirectly support his overall snow accumulation theory. *T. heterophylla* seedlings may be found around large trees because of the influence of these trees on patterns of snow accumulation and melt. Snowfall interception by branches and needles can substantially decrease the amount of accumulation under tree crowns. The rate of snowmelt also is modified considerably in the vicinity of large stems that can re-radiate longwave radiation. The combination of these two influences results in the commonly observed melt cone around tree trunks (Anderson 1963). It is possible that *T. heterophylla* establishment in the transition zone, and by extension *T. heterophylla* migration upslope, is aided by these melt cones.

Given the weak support for the snow hypothesis, I cannot discount other potential mechanisms. Temperature differences were highlighted as the strongest predictor of *T. heterophylla* seedling presence/absence across the aggregated ecotone plot data. The mechanism by which temperature would limit the upward expansion of *T. heterophylla* in this system is not clear. Temperatures do not get below the USDA prescribed *T. heterophylla* frost tolerance of -23.2°C in these forests (Table 4.5). Seedlings also would be buffered by winter snowpack. One possible mechanism is that cool temperatures delay the start of germination. The germination rate of *T. heterophylla* is

more sensitive than that of *A. spp*, as the number of days required for germination is nearly doubled for every 5 °C below the optimum temperature of 20 °C (Packee 1990).

One potential mechanism not examined is the importance of nurse logs to *T. heterophylla* regeneration. *T. heterophylla* are unusual in their regeneration pattern in that nearly 100 percent of seedlings are found on decaying logs (Christy & Mack 1984). It is possible that successful establishment requires a certain type of rotting log. Harmon et al. (1986) reported a decay half-life of 166 years for *P. menziesii*, which also has a rough-textured bark. This extremely slow decay rate and bark consistency are two attributes that may make *P. menziesii* a more suitable substrate for regeneration than *A. spp* (Thornburgh 1969). Recently fallen logs can be low in available nutrients and too high off the ground for successful establishment and growth (Harmon & Franklin 1989). Because there are fewer old, decaying *P. menziesii* logs at high elevation, *T. heterophylla* regeneration may be substrate limited in the *A. amabilis* zone.

A. amabilis

Thornburgh (1969) found this species everywhere at high elevations, even south-facing slopes. He describes a threshold elevation, below which it was not observed and did not even speculate an explanation for this threshold. I also found *A. amabilis* widely distributed across all aspects at high elevation. I conclude that competition most likely controls the lower-elevation boundary of *A. amabilis*'s range. Lower growth rates at lower elevations (associated with higher temperatures) result in increased mortality and competitive exclusion by *T. heterophylla*. Teskey et al. (1984) reported a decreased net photosynthesis of *A. amabilis* at temperatures above 15 °C. Without providing additional

detail, Fonda and Bliss (1969) also suggested that *A. amabilis* were less competitive at higher temperatures due to their sensitivity to heat stress.

It is important to emphasize that the projected shift in competitive advantage associated with the landscape-level tree cores is not driven by an increase in *T. heterophylla* growth rate, but rather by a decrease in *A. amabilis* growth rate with increasing temperature. This finding supports a functional response curve where species exhibit reduced growth at the lower-elevation boundary of their range. It contradicts Loehle's (1998) asymptotic response function, which hypothesizes that trees growing above their elevation range limit (or northern limit) should show decreased growth, but below their elevation range limit (or southern range limit) should not show a decline in growth.

From this study it is not possible to separate cleanly a pure temperature effect from a temperature-associated drought effect at low elevation driven by increased potential evapotranspiration. There is some evidence of drought intolerance for *A. amabilis*. Soil moisture was nearly as strong a factor in explaining *A. amabilis* growth rate trends at the landscape scale as was temperature. With a better model of soil moisture, this factor might have been more significant. At the ecotone level, mean soil moisture values were significantly higher at *A. amabilis* seedling locations (27.1 percent) than *T. heterophylla* locations (24.4 percent; $t = 7.6$, $P < 0.001$). The gradient from wet *A. amabilis* sites to drier *T. heterophylla* sites is consistent with the moisture gradient described by Krajina (1969). It is likely that drought intolerance of *A. amabilis* is

dictating this difference in seedling distributions, because it is unclear how wetter soils could limit the establishment of *T. heterophylla*.

A. procera

This species is frequently associated with south-facing aspects at high elevations (Franklin & Dyrness 1988) but an explanation for either the elevation or the aspect preference is lacking (Thornburgh 1969). Growth of *A. procera* in my study was negatively associated with temperature. The rate of decline with increasing temperature was slightly lower than for *A. amabilis*, resulting in a lower-elevation threshold to its distribution. As to the issue of *A. procera*'s preference for south-facing slopes, I found that this pattern could not be explained simply by growth differences. I did not find any significant differences in growth for either *A. procera* or *A. amabilis* on different aspects. Across much of its range, the growth rate of *A. procera* is considerably greater than that of *A. amabilis* (Figure 4.10B). For 350 *A. spp* trees cored in the ecotone plots, the diameter corrected mean growth increment of *A. procera* was nearly 25 percent greater than that of *A. amabilis*. Once established, therefore, *A. procera* is not limited by growth at upper limitations, which suggests an establishment constraint.

Establishment is constrained to areas of very high light for this shade intolerant. The seedling distribution was significantly associated with southwest-facing aspects (Figure 4.14). Because potential dispersers were present on northeast-facing slopes, light rather than dispersal is more likely to be limiting their range.

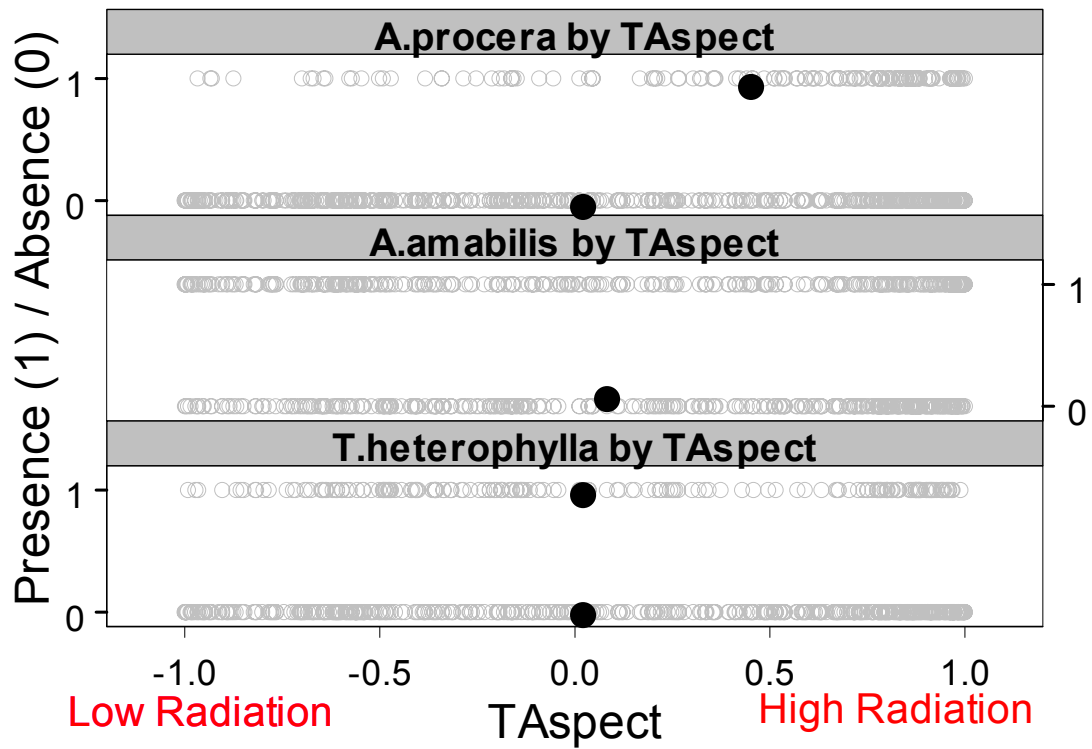


Figure 4.14. Distribution of different species with respect to aspect. Dark circles represent mean values.

Conclusions

These plots have already provided valuable information in the effort to understand the mechanisms of change at one of the major forest ecotones in the Pacific Northwest. Gradient analyses in the past have focused on patterns of abundance only and have not addressed adequately the demographic mechanisms behind community transitions. Here, I examined directly regeneration, growth and mortality as potential mechanism of community patterns. I also addressed species responses with respect to more plant-relevant environmental variables than are typically considered in a gradient analysis. These analyses benefited greatly from focused sampling in areas of highest competition.

The plots have further potential as monitoring tools for future environmental change. The study provides a baseline analysis of an ecotone that can be revisited to monitor possible effects of climate change. Though ecotones have been advocated as valuable sites for the detection of climate change (di Castri et al. 1988, Hansen & di Castri 1992), some have argued that they are not suitable for this purpose. Most notably, Noble (1993) argued that the slow response and highly variable ecotone front make these areas problematic for monitoring of climate change. Demographic processes such as growth and regeneration are less susceptible to the time lags that are expected to complicate monitoring of forest response to changes in climate. The large amount of variation between the different ecotone plots, however, suggests that replicated studies are critical to any potential monitoring program

CHAPTER 5 Summary and Conclusions

In this chapter, I present a summary of the overall findings and approach, I present an example of how the study could be relevant to management under potential climate change scenarios, and I discuss how the methods can be transferred to other montane systems. In short, I address how demographic processes and physiologically important physical variables provide more valuable descriptions of forest community transitions than simple trends in tree composition and elevation.

Summary

I have described an approach to identify ecologically important environment-tree associations that can be applied widely to montane watersheds. I have presented a study in old-growth forest of the Pacific Northwest as an example application. A summary of the major findings of the study is presented below.

- (1) The initial landscape-level analysis (Chapter 2) found that elevation was highly correlated with the transition in basal area from *T. heterophylla* to *A. amabilis*. In many studies this result may be viewed as the end-product of the investigation. Here, I used it as a point of departure (working model) to try to identify more physiologically meaningful variables and demographic mechanisms underlying the elevation gradient.
- (2) Using the tools of landscape ecology (including geographic information systems data and portable electronic monitoring equipment), landscape-scale models were constructed to estimate spatial patterns in radiation, temperature, and soil

moisture. The following observations were made for the H.J. Andrews watershed in the Oregon Cascades, but are probably more universally applicable.

- a. Radiation: hillshading by adjacent topography and temporal variability in sun angle had significant effects on radiation estimates (Chapter 3.1).
- b. Temperature: the representativeness of simple lapse rate models were improved by incorporating radiation (for temperature maximums and means) and distance from stream (for temperature minimums and means) into the models (Chapter 3.2).
- c. Soil moisture: surface soil moisture was modeled statistically using elevation, radiation, and relative slope position. Deeper soil moisture was less affected by radiation differences (Chapter 3.3). Statistical models can perform as well or better as more sophisticated process models under conditions similar to those from which the models were built, but they might not be effective at extrapolating to new environmental settings (Chapter 3.4).
- d. For all three of these factors, variability was a function of the scale of observation. For example, temperature varied with proximity to stream on a local scale and elevation on a landscape scale. Soil moisture varied negatively with elevation on local scales (*i.e.*, water flows downslope) and positively with elevation on landscape scales (*i.e.*, precipitation increases upslope). It is important to account for these multiple influences in

constructing broadly applicable models of environmental variability
(Chapter 3).

(3) When confronting the landscape-scale working model with these new data, temperature and soil moisture were better explanatory variables for patterns of tree composition than elevation (Chapter 4).

(4) The effect of temperature on growth rates might be important in limiting the downslope migration of *A. amabilis*, but the upper elevation boundary of *T. heterophylla* was associated with a more complex interaction of temperature and soil moisture on patterns of regeneration (Chapter 4).

(5) Focus plots can be useful tools for continued monitoring of biotic and abiotic change that may accompany global climate change or other shifts in environmental condition (Chapter 4).

Beyond Elevation

The long and distinguished history of gradient analysis (Merriam 1899, Whittaker 1956, Kessell 1979) leaves the impression that species sort along elevation gradients. My initial investigation of the dynamics of this system support the observations of Zobel et al. (1976), Franklin and Dyrness (1988), Ohmann and Spies (1998), and others, that dominant forest communities are highly associated with specific elevation bands (Chapter 2). Yet, as discussed in Chapter 1, elevation is not directly relevant to plants. The ubiquitous elevation gradient is comprised of a complex combination of environmental variables. I developed a series of simple models to provide improved spatial estimates of

relative differences in radiation, temperature, and soil moisture over landscape extents (Chapter 3). Acquiring a better understanding of these physiologically more important environmental variables will yield better predictive power and management information for responding to shifts in environmental condition such as those expected under global climate change scenarios.

Demographics are Important, too

Few studies of landscape pattern have focused on demographic states other than mature trees (see Clark et al. 1999, Diaz-Delgado et al. 2002 for exceptions), but to understand the mechanisms behind community pattern requires an investigation of the growth, mortality and reproduction patterns that underlie trends in forest composition. I investigated the relationship between the physical template and alternative demographic states at both the landscape and ecotone level.

Because many species are at the competitive limits of their ecological tolerances at ecotones, these regions are well-suited to a detailed study of the response of forest demographics to environmental variability (Fortin et al. 2000). By focusing on these relatively small geographic regions, I was able to gather data to test specific hypotheses regarding the importance of temperature, moisture, radiation and snowpack on establishment, growth and mortality (Chapter 4). From these data, I concluded that the effect of temperature on growth rates may be important in limiting the downslope migration of the *Abies* species. Additional evidence supported drought limitations for *A. amabilis* regeneration and light limitations for *A. procera* regeneration. The upslope migration of *T. heterophylla* appears to be limited by a complex interaction of

temperature and soil moisture on regeneration, with the importance of snow and nurse logs yet unresolved.

It is important to emphasize that the projected shift in competitive advantage associated with the growth data is not driven by an increase in the growth rate of *T. heterophylla* (the lower-elevation dominant species), but rather by a decrease in the growth rate of *A. amabilis* (the upper-elevation dominant species) with increasing temperature. This result is consistent with the argument that vegetation sorting along environmental gradients results from trade-offs between resource tolerances and growth rates (Smith & Huston 1989). The details, however, are not consistent with the typical application of this theory, in which species are believed to be limited by low levels of a resource at the upper-elevation limit of their range and by competition at the lower end. Instead, *A. amabilis* growth appears to be negatively influenced by high-temperature levels at its lower-elevation limit.

From this study it is not possible to separate cleanly a pure temperature effect from a temperature-related drought effect at low elevations due to increased potential evapotranspiration. It is possible that with better spatial representations of soil moisture and/or snow variability, one of these factors could prove to be a better correlate with community pattern (*e.g.*, the landscape-scale growth rates were nearly as highly correlated with the statistical model of soil moisture as they were with the temperature model). Nonetheless, the current model, which emphasizes temperature-growth rate associations, has important implications for how these forests may respond to any future changes in climate.

Implications for Global Climate Change

In response to rising atmospheric CO₂ levels, temperature is projected to increase by 1.4-5.8 °C over the next 100 years (IPCC 2001). Previous studies have focused on the buffering abilities of primary forests to this environmental change because of the long life spans of trees (Sprugel 1991, Noss 2001). Because trees can survive for decades to centuries and take years to establish, they may not immediately show obvious impacts of climate change. For example, Pacific Northwest forests take over 200 years to show the old-growth characteristics associated with the plots sampled in this study (Christensen et al. 2000). Even so, slow shifts in composition are expected along environmental gradients in these forests (Franklin et al. 1991). Given the associations between *A. amabilis* growth rates and temperature, I can predict regions of the HJA where the *A. amabilis* should have a competitive growth advantage and areas where *T. heterophylla* should have a competitive advantage (Figure 5.1). These predictions map on the current distribution of forest types fairly well (e.g., see Figure 4.4).

I also can make predictions as to how competitive advantages may shift with an increase in temperature (Figure 5.1). Though compositional shifts may be lagged due to the longevity of trees (Urban et al. 1993), disturbance can interact with climate change to affect more immediate responses (Dale et al. 2001). Management actions in these potentially sensitive areas should consider how these interactions might complicate forest recovery to activities such as logging or fire.

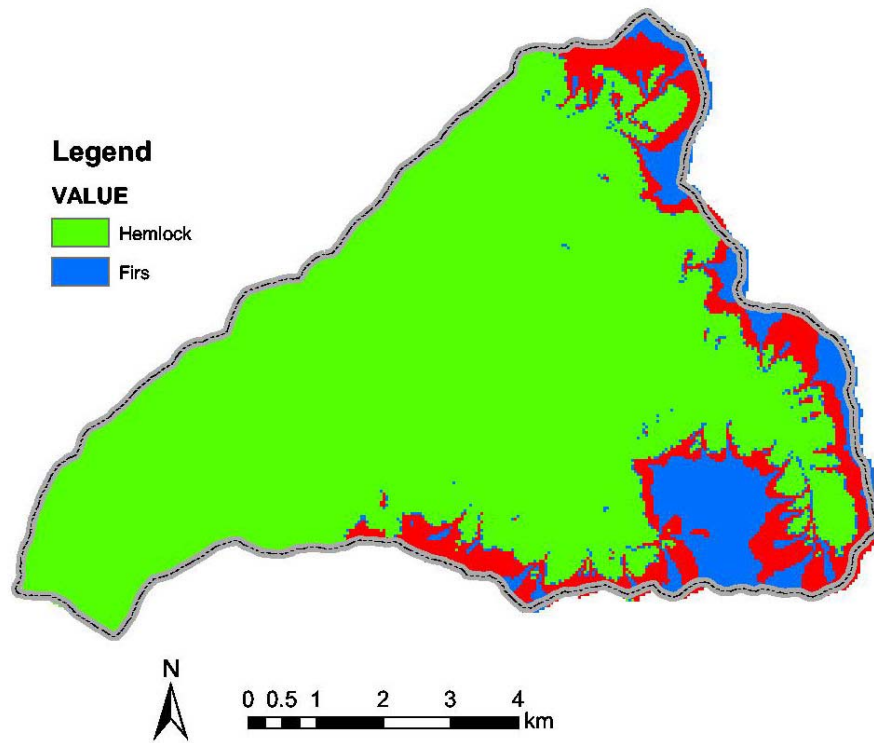


Figure 5.1. Areas sensitive to change given a 1°C change in climate. The major vegetation zones are mapped in green and blue based on growth differences of *T. heterophylla* (western hemlock) and *A. amabilis* (silver fir) at different summer temperatures. Areas in red are locations where firs should have a competitive advantage under current climate, but hemlocks would have a competitive advantage given an increase in temperature of 1°C.

Applicability of Approach to Other Montane Systems

Finally, though specific findings may not be applicable beyond the Pacific Northwest old-growth forest system in which this study was conducted, the general approach is applicable to many montane systems as an extension to traditional gradient analysis. For example, as part of a cross-site comparative study, we (Lookingbill et al. 2001) are interested in comparing landscape-level vegetation-environment relationships at four forested, montane sites with contrasting climates, terrain and geologic history: H.J. Andrews Experimental Forest (Cascades, Oregon), Sequoia National Park (Sierra Nevada, California), Hubbard Brook Experimental Forest (White Mountains, New Hampshire), and Coweeta Hydrologic Laboratory (Southern Appalachians, North Carolina). We are just beginning to apply the sampling and statistical methods described in this dissertation to these sites. In the western systems, environmental gradients are steep and the approach outlined here has been successful in replacing proxy factors such as elevation with more biologically meaningful explanatory variables. In the eastern systems, where elevation gradients are less steep and fine-scale factors are more important, the methods are the same, but the focus must shift to developing better representations of soil variability.

The general approach, therefore, is more generic than this specific case study. It provides a framework for an iterative ecology; field studies are used to build models, which guide future sampling to answer new hypotheses and build better models. The importance of field data is not diminished by the increasing use of models, nor can complex ecological phenomenon be described at large spatial extents without some form

of simplifying model. One supports the other in a synthetic approach to conducting community ecology at the landscape scale.

REFERENCES

- Acker, S.A., M.E. Harmon, T.A. Spies and W.A. McKee. 1996. Spatial patterns of tree mortality in an old-growth *Abies-Pseudotsuga* stand. *Northwest Science* 70:132-138.
- Acker, S.A., W.A. McKee, M.E. Harmon and J.F. Franklin. 1998. Long-term research on forest dynamics in the Pacific Northwest: a network of permanent plots. Pages 93-106 in F. Dallmeier & J.A. Comiskey (eds.), *Forest Biodiversity in North, Central and South America, and the Caribbean: Research and Monitoring*. Parthenon Press: New York.
- Ambrose, B. 1995. Topography and the water cycle in a temperate middle mountain environment: the need for interdisciplinary experiments. *Agricultural and Forest Meteorology* 73:217-235.
- Anderson, H.W. 1963. *Managing California's snow zone lands for water*. Sacramento, CA. U.S. Department of Agriculture, Forest Service, Pacific Southwest Research Station. 26 p.
- Austin, M.P. 1987. Models for the analysis of species' response to environmental gradients. *Vegetatio* 69:35-45.
- Bailey, J.D., C. Mayrsohn, P.S. Doescher, E. St.Pierre, and J.C. Tappeiner. 1998. Understory vegetation in old and young Douglas-fir forests of Western Oregon. *Forest Ecology and Management* 112:289-302.
- Band, L.E. and I.D. Moore. 1995. Scale: landscape attributes and geographical information systems. *Hydrological Processes* 9:401-422.
- Band, L.E., D.L. Peterson, S.W. Running, J. Coughlan, R. Lammers, J. Dungan and R. Nemani. 1991. Forest ecosystem process at the watershed scale: basis for distributed simulation. *Ecological Modelling* 56:171-196.
- Band, L.E., P. Patterson, R. Nemani and S.W. Running. 1993. Forest ecosystem processes at the watershed scale: incorporating hillslope hydrology. *Agricultural and Forest Meteorology* 63:93-126.
- Barry, R.G. 1992. *Mountain Weather and Climate*. Routledge, London.
- Beers, T.W., P.E. Dress and L.C. Wensel. 1966. Aspect transformation in site productivity research. *Journal of Forestry* 64:691-692.
- Beven, K. 2000. Uniqueness of place and process representations in hydrological modelling. *Hydrology and Earth System Sciences*. 4:203-213.

- Beven, K. 2001. How far can we go in distributed hydrological modelling? *Hydrology and Earth System Sciences*. 5:1-12.
- Beven, K J and M J. Kirkby 1979. A physically based variable contributing area model of basin hydrology. *Hydrologic Science Bulletin* 24:43-69.
- Beven, K. and M.J. Kirkby. (eds.) 1993. *Channel Network Hydrology*. Wiley, Chichester.
- Bierlmaier, F.A and A. McKee. 1989. Climatic summaries and documentation for the primary meteorological station, H.J. Andrews Experimental Forest, 1972-1984. Gen. Tech. Rep. PNW-GTR-223. Portland, OR: U.S. Department of Agriculture, Forest Service, Pacific Northwest Research Station. 26 p.
- Bolstad, P.V., L. Swift, F. Collins and J. Regniere. 1998. Measured and predicted air temperatures at basin to regional scales in the southern Appalachian mountains. *Agricultural and Forest Meteorology* 91:161-176.
- Bolstad, P.V., W. Swank and J. Vose. 1998. Predicting southern Appalachian overstory vegetation with digital terrain data. *Landscape Ecology* 13:695-707.
- Bonan, G.B. 1988. Environmental processes and vegetation patterns in boreal forests. Ph.D. Thesis, University of Virginia: Charlottesville.
- Bonan, G.B. 2002. *Ecological Climatology*. Cambridge University Press, Cambridge.
- Bond, B.J., J.A. Jones, G. Moore, N. Phillips, D.A. Post and J.J. McDonnell 2002. The zone of vegetation influence on baseflow revealed by diel patterns of streamflow and vegetation water use in a headwater basin. *Hydrological Processes*. 16:1671-1677.
- Boyer, D.G, R.J. Wright, W.M. Winant and H.D. Perry. 1990. Soil water relations on a hilltop cornfield in central Appalachia. *Soil Science* 149:383-392.
- Brady, N.C. and R.R. Weil. 1999. *The Nature and Properties of Soils*. Upper Saddle River, NJ, Prentice Hall.
- Bray, R.J. and J.T. Curtis. 1957. An ordination of the upland forest communities of southern Wisconsin. *Ecological Monographs* 27: 325-349.
- Breiman, L., J.H. Friedman, R.A. Olshen and C.J. Stone. 1984. *Classification and Regression Trees*. Wadsworth and Brooks/Cole, Monterey, CA.
- Breshears, D.D. and F.J. Barnes. 1999. Interrelationships between plant functional types and soil moisture heterogeneity for semiarid landscapes within the grassland/ forest continuum: a unified conceptual model. *Landscape Ecology* 14:465-478.

- Brockway, D.G. 1998. Forest plant diversity at local and landscape scales in the Cascade Mountains of southwestern Washington. *Forest Ecology and Management* 190:323-341.
- Brooks, J.R., F.C. Meinzer, R. Coulombe and J. Gregg 2002. Hydraulic redistribution of soil water during summer drought in two contrasting Pacific Northwest coniferous forests. *Tree Physiology*. 22:1107-1117.
- Brown, D.G. 1994. Predicting vegetation types at treeline using topography and biophysical disturbance variables. *Journal of Vegetation Science* 5: 641-656.
- Buffo, J. Fritschen, L.J. and Murphy, J.L. 1972. Direct solar radiation on various slopes from 0 to 60 degrees north latitude. USDA Forest Service Research Paper PNW-142. Portland, OR.
- Callaway, R.M., Clebsch, E.E.C. and White, P.S. 1998. A Multivariate analysis of forest communities in the western Great Smoky Mountains national park. *American Midland Naturalist* 118(1): 107-118.
- Camarero, J.J., E. Gutierrez and M.-J. Fortin. 2000. Spatial pattern of subalpine forest-alpine grassland ecotone in the Spanish Central Pyrenees. *Forest Ecology and Management* 134:1-16.
- Camill, P. and J.S. Clark. 2000. Long-term perspectives on lagged ecosystem responses to climate change: permafrost in boreal peatlands and the grassland/woodland boundary. *Ecosystems* 3:534-544.
- Campbell, G.S. and Norman, J.M. 1998. *An Introduction to Environmental Biophysics*. Springer: New Jersey
- Chen, J., S.C. Saunders, T.R. Crow, R.J. Naiman, K.D. Brosofske, G.D. Mroz, B.L. Brookshire and J.F. Franklin. 1999. Microclimate in forest ecosystem and landscape ecology. *BioScience* 49:288-297.
- Christensen, N.L., A.M. Bartuska, J.H. Brown, S. Carpenter, C. D'Antonio, R. Francis, J.F. Franklin, J.A. MacMahon, R.N. Noss, D.J. Parsons, C.H. Peterson, M.G. Turner and R.G. Woodmansee. 1996. The report of the Ecological Society of America committee on the scientific basis for ecosystem management. *Ecological Applications* 6:665-691.
- Christensen, N.L., S.V. Gregory, P.R. Hagenstein, T.A. Heberlein, J.C. Hendee, J.T. Olson, J.M. Peek, D.A. Perry, T.D. Schowalter, K. Sullivan, G.D. Tilman and K.A. Vogt. 2000. *Environmental Issues in Pacific Northwest Forest Management*. Washington, D.C., National Academy Press.

- Christy, J.E. and R.N. Mack. 1984. Variation in demography of juvenile *Tsuga heterophylla* across the substratum mosaic. *Journal of Ecology* 72:75-91.
- Cissel, J.H., F.J. Swanson and P.J. Weisburg. 1999. Landscape management using historical fire regimes: Blue River, Oregon. *Ecological Applications* 9:1217-1231.
- Clark, J.S. 1990. Landscape interactions among nitrogen mineralization, species composition, and long-term fire frequency. *Biogeochemistry* 11:1-22.
- Clark, J.S., E.C. Grimm, J. Lynch and P.G. Mueller. 2001. Effects of Holocene climate change on the C₄ grassland/woodland boundary in the northern plains, USA. *Ecology* 82:620-636.
- Clark, J.S., M. Silman, R. Kern, E. Macklin, and J. HilleRisLambers. 1999. Seed dispersal near and far: patterns across temperate and tropical forests. *Ecology* 80:1475-1494.
- Clements, F.E. 1933. Competition in plant societies. *News Service Bulletin*, Carnegie Institution of Washington.
- Clinton, B.D., Boring, L.R., and Swank, W.T. 1994. Regeneration patterns in canopy gaps of mixed-oak forests of the Southern Appalachians: Influences of topographic position and evergreen understory. *American Midland Naturalist* 132: 308-319.
- Cole, K. 1990. Geologic controls of vegetation in the Purisima Hills, California. *Madrono* 27:79-89.
- Cramer, W., R. Leemans, E.-D. Schulze, A. Bondeau and S. R.J. 1999. Data needs and limitations for broad-scale ecosystem modelling. pages 88-105 in B. Walker, W. Steffen, J. Canadell and J. Ingram (eds.), *The Terrestrial Biosphere and Global Change: Implications for Natural and Managed Ecosystems*. University Press, Cambridge.
- Crave, A. and C. Gascuel-Oudou. 1997. The influence of topography on time and space distribution of soil surface water content. *Hydrological Processes* 11:203-210.
- Creed, I.F. and L.E. Band. 1998. Exploring functional similarity in the export of nitrate-N from forested catchments: A mechanistic modeling approach. *Water Resources Research* 34:3079-3093.
- Crumley, C.L. 1993. Analyzing historic ecotonal shifts. *Ecological Applications* 3:377-384.
- Daly, C., R.P. Neilson and D.L. Phillips. 1994. A statistical-topographic model for mapping climatological precipitation over mountainous terrain. *Journal of Applied Meteorology* 33:140-158.

- Davis, F. W. and S. Goetz. 1990. Modeling Vegetation Pattern Using Digital Terrain Data. *Landscape Ecology* 4: 69-80.
- Davis, M.B. 1981. Quaternary history and the stability of forest communities. Pages 132-153 in D.C. West, H.H. Shugart and D.B. Botkin (eds.), *Forest Succession: Concepts and Application*. Springer-Verlag: New York.
- Dawes, W.R. and D.L. Short 1994. The significance of topology for modelling the surface hydrology of fluvial landscapes. *Water Resources Research* 30:1045-1055.
- Day, F.P. and Monk, C.D. 1974. Vegetation patterns on a southern Appalachian watershed. *Ecology* 55: 1064-1074.
- di Castri, F., A.J. Hansen and M.M. Holland (eds.) 1988. A New Look at Ecotones. *Biology International*, Special Issue 17.
- Díaz-Delgado, R., F. Lloret, X. Pons, and J. Terradas. 2002. Satellite evidence of decreasing resilience in Mediterranean plant communities after recurrent wildfires. *Ecology* 83: 2293–2303.
- D'Odorico, P., L. Ridolfi, A. Porporato and I. Rodriguez-Iturbe. 2000. Preferential states of seasonal soil moisture: The impact of climate fluctuations. *Water Resources Research* 36:2209-2219.
- Donnegan., J. A. and Rebertus, A.J. 1999. Rates and mechanisms of subalpine forest succession along an environmental gradient. *Ecology* 80(4): 1370-1384.
- Dozier, J. and Frew, J. 1990. Rapid calculation of terrain parameters for radiation modeling from digital elevation data. *IEEE Transaction on Geoscience and Remote Sensing* 28(5): 963-969.
- Dubayah, R.C. 1994. Modeling a solar radiation topoclimatology for the Rio Grande River Basin. *Journal of Vegetation Science* 5: 627-640.
- Dubayah, R.C. and P.M. Rich. 1995. Topographic solar radiation models for GIS. *International Journal of Geographical Information Systems* 9: 405-419.
- Dufrene and Legendre. 1997. Species assemblages and indicator species: the need for a flexible asymmetrical approach. *Ecological Monographs* 67:345-366.
- Dyrness, C.T., Franklin, J.F., and Moir, W.H. 1974. A preliminary classification of forest communities in the central portion of the Western Cascades in Oregon. *Forestry Sciences Laboratory, USDA Forest Service, Corvallis, OR*.
- Edwards, D.G.W. 1976. Seed physiology and germination in western hemlock. In *Proceedings, Western Hemlock Management Conference*. pp. 126-127. W.A. Atkinson and R.J. Zasoski (eds.) University of Washington: Seattle, WA.

- ESRI. ARC/Info 7. 1994. Environmental Systems Research Institute. Inc. Redlands. CA.
- Fasham, M. J. R. 1977. A comparison of nonmetric multidimensional scaling, principal components and reciprocal averaging for the ordination of simulated coenoclines, and coenoplanes. *Ecology* 58: 551-561.
- Flenley, J.R. 1979. The Late Quaternary vegetational history of the equatorial mountains. *Progress in Physical Geography* 3: 488-509.
- Fonda, R. W., and L. C. Bliss. 1969. Forest vegetation of the montane and subalpine zones, Olympic Mountains, Washington. *Ecological Monographs* 39:271-301.
- Fortin, M. J., and J. Gurevitch. 1993. Mantel tests: spatial structure in field experiments. Pages 342-359 in S. M. Scheiner and J. Gurevitch (eds.), *Design and Analysis of Ecological Experiments*. Chapman and Hall, New York.
- Fortin, M.J. and G.M. Jacquez. 2000. Randomization tests and spatially autocorrelated data. *Bulletin of the Ecological Society of America* July: 201-205.
- Frank, E.C. and Lee, R. 1966. Potential solar beam irradiation on slopes: tables for 30 to 50 latitude. Rocky Mountain For. Range Exp. Stn. Gen. Tech. Rep. U.S.D.A Forest Service.
- Franklin, J.F. 1964. Some notes on the distribution ecology of noble fir. *Northwest Science* 38:1-13.
- Franklin, J.F. 1965. Tentative ecological provinces within the true fir-hemlock forest area of the Pacific Northwest. U.S. Forest Service Research Paper PNW-22. Pacific Northwest Forest and Range Experiment Station: Portland, OR.
- Franklin, J.F. 1979. Vegetation of the Douglas-fir region. Pages 93-112 in P.E. Heilman, H. W. Anderson and D.M. Baumgartner (eds.), *Forest Soils of the Douglas-Fir Region*. Washington State Cooperative Extension: Pullman, WA.
- Franklin, J.F. 1998. Predicting the distribution of shrub species in southern California from climate and terrain-derived variables. *Journal of Vegetation Science* 9: 733-748.
- Franklin, J.F. and C.T. Dyrness. 1988. *Natural Vegetation of Oregon and Washington*. Corvallis, Oregon State University Press.
- Franklin, J.F. and C.B. Halpern. 2000. Pacific Northwest Forests. Pages 121-159 in M.G. Barbour and W. D. Billings (eds.), *North American Vegetation*, Cambridge University Press, New York.
- Franklin, J.F., P. McCullough and C. Gray. 2000. Terrain variables used for predictive mapping of vegetation communities in Southern California. Pages 331-354 in J.P.

- Wilson and J.C. Gallant (eds.), *Terrain Analysis: Principle and Applications*. John Wiley and Sons: New York.
- Franklin, J.F., W.H. Moir, G.W. Douglas and C. Wiberg. 1971. Invasion of subalpine meadows by trees in the Cascade Range, Washington and Oregon. *Arctic and Alpine research* 3:215-224.
- Franklin, J.F., F.J. Swanson, M.E. Harmon, D.A. Perry, T.A. Spies, V.H. Dale, A. McKee, W.K. Ferrell, J.E. Means, S.V. Gregory, J.D. Lattin, T.D. Schowalter and D. Larsen. 1992. Effects of global climatic change on forests in northwestern North America. Pages 244-257 in R.L. Peters & T.E. Lovejoy (eds.), *Global Warming and Biological Diversity*. New Haven, CT, Yale University Press.
- Frew, J.E. 1990. *The Image Processing Workbench*. Ph.D, University of California, Santa Barbara. Santa Barbara.
- Fujiware, K. and E.O. Box. 1999. Climate change and vegetation shift. Pages 121-126 in A. Farina (ed.), *Perspectives in Ecology*. Backhuys Publishers, Leiden.
- Gardner, R.H. and D.L. Urban. *in press*. Model validation: Past lessons, present concerns, future prospects. in C. D. Canham, J. C. Cole and W. K. Lauenroth (eds.), *Understanding Ecosystems: The Role of Quantitative Models in Observation, Synthesis, and Prediction*. Princeton, NJ, Princeton University Press.
- Gauch, H.G. Jr. and R.H. Whittaker. 1981. Hierarchical classification of community data. *Journal of Ecology* 69:537-557.
- Gauch, H.G. Jr., R.H. Whittaker and S.B. Singer. 1981. A comparative study of nonmetric ordinations. *Journal of Ecology*. 69: 135-152.
- Geiger, R.J. 1965. *The Climate Near the Ground*. Harvard University Press: Cambridge. MA.
- Goodall, D. W. 1954. Objective methods for the classification of vegetation. III. An essay in the use of factor analysis. *Australian Journal of Botany* 2:304-324.
- Gray, A.N. and T.A. Spies 1995. Water content measurement in forest soils and decayed wood using time domain reflectometry. *Canadian Journal of Forest Research*. 25:376-385.
- Grayson, R.B and A.W. Western. 2001. Terrain and the distribution of soil moisture. *Hydrological Processes* 15:2689-2690.
- Grayson, R.B., A.W. Western, F.H.S. Chiew and G. Bloschl. 1997. Preferred states in spatial soil moisture patterns: Local and nonlocal controls. *Water Resources Research* 33:2897-2908.

- Grayson, R.B., I.D. Moore and T.A. McMahon. 1992. Physically based hydrologic modeling: 2. Is the concept realistic? *Water Resources Research* 26:2659-2666.
- Greene, S.E. and M. Klopsch. 1985. Soil and air temperatures for different habitats in Mount Rainier National Park. Res. Pap. PNW-342. Portland, OR: USDA, Forest Service, Pacific Northwest Forest and Range Experiment Station.
- Greenland, D. 1994. The Pacific Northwest regional context of the climate of the H.J. Andrews Experimental Forest. *Northwest Science* 69:81-96.
- Greenland, D. 1996. Potential solar radiation at the H. J. Andrews experimental forest. Pacific Northwest Research Station. U.S.D.A. Forest Service.
- Grier, C.C. and R.S. Logan. 1977. Old-growth *Pseudotsuga menziesii* communities of a western Oregon watershed: biomass distribution and production budgets. *Ecological Monographs* 47:373-400.
- Griffith, D. A. 1992. What is spatial autocorrelation? Reflections on the past 25 years of spatial statistics. *L'Espace géographique* 3:265-280.
- Grimm, E.C. 1983. Chronology and dynamics of vegetation change in the prairie woodland region of southern Minnesota, USA. *New Phytol* 93:311-350.
- Guisan, A. and N.E. Zimmerman. 2000. Predictive habitat distribution models in ecology. *Ecological Modeling* 135:147-186.
- Guisan, A., Theurillat, J., and Kienast, F. 1998. Predicting the potential distribution of plant species in an alpine environment. *Journal of Vegetation Science* 9: 65-74.
- Halpin, P. 1997. Global climate change and natural-area protection: management responses and research directions. *Ecological Applications* 7:828-843.
- Halverson, N., R.D. Leshner and R.H. McClure. 1986. Major Indicator Shrubs and Herbs on National Forests of Western Oregon and Southwestern Washington. USDA Forest Service PNW: Region R6-TM-229-1986.
- Hansen, A.J. and F. di Castri (eds.) 1992. *Landscape Boundaries: Consequences for Biotic Diversity and Landscape Flows*. Ecological Studies 92. Springer-Verlag, New York.
- Harmon, M., J. Franklin, F. Swanson, P. Sollins, S. Gregory, S. Lattin, J. Latin, N. Anderson, S. Cline, N. Augmen, J. Sedell, G. Lienkaemper, J. K. Cromack and K. Cummins. 1986. Ecology of coarse woody debris in temperate ecosystems. *Advances in Ecological Research* 15:133-302.
- Harmon, M.E. and J.F. Franklin, J.F. 1989. Tree seedlings on logs in *Picea – Tsuga* forests of Oregon and Washington. *Ecology* 70:48-59.

- Hawley, M.E., T.J. Jackson and R.H. McCuen. 1983. Surface soil moisture variation on small agricultural watersheds. *Journal of Hydrology* 62:179-200.
- Helvey, J.D., J.D. Hewlett and J.E. Douglass. 1972. Predicting soil moisture in the southern Appalachians. *Soil Science Society of America Proceeding* 36:954-959.
- Henderson-Sellers, A. and K. McGuffie. 1987. *A Climate Modelling Primer*. Wiley, New York.
- Herkelrath, W.N., S.P. Hamburg and F. Murphy. 1991. Automatic, real-time monitoring of soil moisture in a remote field area with time domain reflectometry. *Water Resources Research* 27:857-864.
- Hidinger, L. and R. Glick. 2000. A change in the weather: how will plants and animals respond to climate change? *Bulletin of the Ecological Society of America* 81:216-218.
- Hillel, D. 1986. Modeling in soil physics: A critical review. Pages 35-42 in *Future Developments in Soil Science Research*. Soil Science Society of America, Madison, Wisconsin.
- Hitchcock, C.L. and A. Cronquist. 1973. *Flora of the Pacific Northwest*. University of Washington Press, Seattle.
- Hobbs, R. 1997. Future landscapes and the future of landscape ecology. *Landscape and Urban Planning* 37:1-9
- Hutchinson, T.F., R.E.J. Boerner, L.R. Iverson, S. Sutherland and E.K. Sutherland. 1999. Landscape patterns of understory composition and richness across a moisture and nitrogen mineralization gradient in Ohio (U.S.A.) *Quercus* forests. *Plant Ecology* 144:177-189.
- Intergovernmental Panel on Climate Change. 2001. *Climate Change 2000. The Science of Climate Change. Contribution of working group I to the third assessment report of the Intergovernmental Panel on Climate Change.*, Cambridge University Press, Cambridge.
- Iverson, L.R., M.E. Dale, C.T. Scott and A. Prasad. 1997. A GIS-derived integrated moisture index to predict forest composition and productivity of Ohio forests (U.S.A). *Landscape Ecology* 12:331-348.
- Jenny, H. 1980. *The Soil Resource*. Springer-Verlag, New York.
- Jongman, R.H.G., C.J.F. ter Braak, and O.F.R. van Tongeren. 1995. *Landscape Analysis in Community and Landscape Ecology*. Cambridge University Press: New York.

- Kessell, S.R. 1979. Gradient Modeling: Resource and Fire Management. Springer-Verlag: New York.
- Klein, S. A. 1977. Calculation of monthly average insolation on tilted surfaces. Solar Energy 19: 325-329.
- Kotar, J. 1972. Ecology of *Abies amabilis* in relation to its altitudinal distribution and in contrast to its common associate *Tsuga heterophylla*. Ph.D. dissertation. University of Washington, Seattle.
- Kozlowski, T.T., Kramer, P.J., and Pallardy, S.G. 1991. The Physiological Ecology of Woody Plants. Academic Press: New York.
- Krajina, V.J. 1969. Ecology of forest trees in British Columbia. Ecology of Western North America 2:1-146.
- Kruskal, J.B. 1964. Multidimensional scaling by optimizing goodness of fit to a nonmetric hypothesis. Psychometrika 29:1-27.
- Leduc, A., P. Drapeau, Y. Bergeron, and P. Legendre. 1992. Study of spatial components of forest cover using partial Mantel's tests and path analysis. Journal of Vegetation Science 3:69-78.
- Legendre, P. and L. Legendre. 1998. Numerical Ecology. Elsevier, New York.
- Legendre, P. and M.J. Fortin. 1989. Spatial pattern and ecological analysis. Vegetatio 80:107-138.
- Legendre, P., and M. Troussellier. 1988. Aquatic heterotrophic bacteria: modeling in the presence of spatial autocorrelation. Limnol. Oceanogr. 33:1055-1067.
- Levin, S.A. 1992. The problem of pattern and scale in ecology. Ecology 73:1943-1967.
- Levins, R., 1966. The strategy of model building in population ecology. American Scientist 54:421-431.
- Loehle, C. 1998. Height growth rate tradeoffs determine northern and southern range limits for trees. Journal of Biogeography 94:13-15.
- Loehle, C. 2000. Forest ecotone response to climate change: sensitivity to temperature response functional forms. Canadian Journal of Forest Research 30:1632-1645.
- Lookingbill, T. and D. Urban. 2003. Spatial estimation of air temperature differences for landscape-scale studies in montane environments. Agricultural and Forest Meteorology 114:141-151.

- Lookingbill, T., K. Pierce, and D. Urban. 2001. A cross-site comparative study of physical correlates with community transition. 86th Annual Ecological Society of America Proceedings 2001:311.
- Mackay, D.S. and L.E. Band. 1997. Forest ecosystem processes at the watershed scale: dynamic coupling of distributed hydrology and canopy growth. *Hydrological Processes* 11:1197-1217.
- Mackey, B.G., Mullen, I.C., Baldwin, K.A., Gallant, J.C., Sims, R.A., and McKenney, D.W. 2000. Towards a spatial model of boreal forest ecosystems: The role of digital terrain analysis. Pages 391-427 in J. P. Wilson and J. C. Gallant (eds.), *Terrain Analysis: Principle and Applications*. John Wiley and Sons: New York.
- Mantel, N. 1967. The detection of disease clustering and a generalized regression approach. *Cancer Research* 27:209-220.
- McCay, D.H., Abrams, M.D. and DeMeo, T.E. 1997. Gradient analysis of secondary forests of eastern West Virginia. *Journal of the Torrey Botanical Society* 124: 160-173.
- McCune, B. and Dylan, K. 2002. Equations for potential annual direct incident radiation and heat load. *Journal of Vegetation Science* 13: 603-606.
- McCune, B. and J.B. Grace. 2002. *Analysis of Ecological Communities*. MjM Software Design, Gleneden Beach, OR.
- McCune, B. and M.J. Mefford. 1999. *PC-ORD: Multivariate Analysis of Ecological Data*. Version 4.09. MjM Software, Gleneden Beach, OR.
- McCutchan, M.H. and D.G. Fox. 1986. Effect of elevation and aspect on wind, temperature and humidity. *Journal of Clim. Appl. Met.* 25:1996-2013.
- McKee, A. 1998. Focus on field stations: H.J. Andrews Experimental Forest. *Bulletin of the Ecological Society of America* 79:241-246.
- McNab, W.H. 1989. Terrain shape index: quantifying effect of minor landforms on tree height. *Forest Science* 35:91-104.
- Merriam, C.H. 1899. Results of a biological survey of Mount Shasta, California. *North American Fauna* 16:1-179.
- Mielke, P.W. 1984. Meteorological applications of permutation techniques based on distance functions. Pages 813-830 in P.R. Krishnaiah and P.K. Sen (eds.), *Handbook of statistics*, vol 4. Elsevier, Amsterdam, The Netherlands.
- Miller, C. and D.L. Urban. 1999. Fire, climate and forest pattern in the Sierra Nevada, California. *Ecological Modeling* 114:113-135.

- Miller, C. and D.L. Urban. 1999. Forest pattern, fire, and climatic change in the Sierra Nevada. *Ecosystems* 2:76-87.
- Milne, B.T. A.R. Johnson, T.H. Keitt, J. David, C.A. Hatfield and R. Hraber. 1996. Detection of critical densities associated with pinon-juniper woodland ecotones. *Ecology* 77:805-821.
- Moer, M. 1993. Characterizing spatial patterns of trees using stem-mapped data. *Forest Science* 39:756-775.
- Moore, D. M., B. G. Lees, and S. M. Davey. 1991. A new method for predicting vegetation distributions using decision tree analysis and geographic information system. *Environmental Management* 15:59-71.
- Moore, I.D., G.J. Burch and D.H. Mackenzie. 1988. Topographic effects on the distribution of surface water and the location of ephemeral gullies. *Transactions of the American Society of Agricultural Engineering*. 31:1098-1107.
- Moore, I.D., R.B. Grayson and A.R. Ladson. 1991. Digital terrain modelling: a review of hydrological, geomorphological, and biological applications. *Hydrological Processes* 5:3-30.
- Naden, P.S., E.M. Blyth, P. Broadhurst, C.D. Watts, and I.R. Wright. 2000. *Hydrological Processes* 14:785-809.
- Neilson, R.P. 1991. Climatic constraints and issues of scale controlling regional biomes. *Ecotones: The Role of Landscape Boundaries in the Management and Restoration of Changing Environments*. Pages 31-51 in M. M. Holland, P. G. Risser and R. J. Naiman (eds.). Chapman and Hall, New York
- Nikolov, N.T. and Zeller, K.F. 1992. A solar radiation algorithm for ecosystem dynamic models. *Ecological Modelling* 61: 149-168.
- Noble, I.R. 1993. A model of responses of ecotones to climate change. *Ecological Applications* 3:396-403.
- Noborio, K. 2001. Measurement of soil water content and electrical conductivity by time domain reflectometry: a review. *Computers and Electronics in Agriculture* 31:213-237.
- Norman, G.R. and D.L. Streiner. 2000. *Biostatistics*. Decker, Lewiston, NY.
- Noss, R.F. 2001. Beyond Kyoto: Forest management in a time of rapid climate change. *Conservation Biology* 15:578-590.
- Nusser, S.M., F.J. Breidt and W.A. Fuller. 1998. Design and estimation of investigating the dynamics of natural resources. *Ecological Applications* 8:234-245.

- O'Neill R.V. and R.H. Gardner. 1979. Sources of uncertainty in ecological models. Pages 447-463 in B.P. Zeigler, M.S. Elzas, G.J. Kliv and T.I. Oren, editors. Methodology in Systems Modelling and Simlulation. North-Holland Publishing Co.
- O'Neill, R.V. 1979. Natural variability as a source of error in model predictions. Pages 23-32 in G.S. Innis and R.V. O'Neill, editors. Systems analysis of ecosystems. International Co-operative, Fairland, Maryland, USA.
- Ohmann, J.L. and T.A. Spies. 1998. Regional gradient analysis and spatial pattern of woody plant communities of Oregon forests. Ecological Monographs 68:151-182.
- O'Loughlin, E.M. 1986. Prediction of surface saturation zones in natural catchments by topographic analysis. Water Resources Research 22:794-804.
- Owens, J. H. and M. Molder. 1977. Sexual reproduction of *Abies amabilis*. Canadian Journal of Botany 55:2253-2667.
- Packee, E. C. 1990. *Tsuga heterophylla* (Raf.) Sarg. western hemlock. In: Burns, Russell M.; Honkala, Barbara H., technical coordinators. Silvics of North America. Volume 1. Conifers. Agricultural Handbook 654. Washington, DC: U.S. Department of Agriculture, Forest Service.
- Palmer, M.W. 1993. Putting things in even better order: the advantages of canonical correspondence analysis. Ecology 74:2215-2230.
- Park, A.D. 2001. Environmental influences on post-harvest natural regeneration in mexican pine-oak forests. Forest Ecology and Management 144:213-228.
- Parker, A.J. 1982. The topographic relative moisture index: an approach to soil-moisture assessment in mountain terrain. Physical Geography 3:160-168.
- Parker, A.J. 1995. Comparative gradient structure and forest cover types in Lassen Volcanic and Yosemite National Parks, California. Bulletin of the Torrey Botanical Society 122:58-68.
- Parmesan, C. and G. Yohe. 2003. A globally coherent fingerprint of climate change impacts across natural systems. Nature 421:37-42.
- Pastor, J. and W.M. Post. 1988. Response of northern forests to CO₂-induced climate change. Nature 334:55-58.
- Peet, R.K. 1981. Forest vegetation of the Colorado Front Range. Vegetatio 43:3-75.
- Peters, D.P.C, D.L. Urban, R.H. Gardner, D.D. Breshears and J.E. Herrick. *in review*. Strategies for ecological extrapolation.

- Peters, R.L. and J.D. Darling. 1985. The greenhouse effect and nature reserve design. *BioScience* 35:707-717.
- Phillips, D.L., J. Dolph and D. Marks. 1992. A comparison of geostatistical procedures for spatial analysis of precipitation in mountainous terrain. *Agricultural and Forest Meteorology* 58:119-141.
- Platt, J.R. 1964. Strong inference. *Science* 146:347-353.
- Pojar, J and A. MacKinnon. 1994. *Plants of the Pacific Northwest Coast*. Lone Pine, Redmond, WA.
- Post, D.A. and J.A. Jones. 2001. Hydrologic regimes of forested, mountainous, headwater basins in New Hampshire, North Carolina, Oregon, and Puerto Rico. *Advances in Water Resources* 24:1195-1210.
- Raven, P.H., Evert, R.F. and Eichhorn, S.E. 1992. *Biology of Plants*. Worth Publishers: New York.
- Reynolds, J.F. and B. Acock. 1985. Predicting the response of plants to increasing carbon dioxide: a critique of plant growth models. *Ecological Modelling* 29:107-129.
- Reynolds, J.M.R. and J. Chung. 1986. Regression methodology of estimating prediction error. *Canadian Journal of Forest Research* 16:931-938.
- Richardson, C.W. 1981. Stochastic simulation of daily precipitation, temperature and solar radiation. *Water Resources Research*. 17:182-190.
- Ripley, B.D. 1976. The second-order analysis of stationary point processes. *Journal of Applied Probability* 13:255-266.
- Risser, P.G. 1995. The status of the science of examining ecotones. *BioScience* 45: 318-325.
- Rosentrater, L.D. 1997. *The Thermal Climate of the H.J. Andrews Experimental Forest, Oregon*. Masters Thesis. Department of Geography. Eugene, OR: University of Oregon.
- Rowe, J.S. 1956. Uses of undergrowth plant species in forestry. *Ecology* 37:461-473.
- Running, S.W. and J. Coughlan. 1988. A general model of forest ecosystem processes for regional applications: Hydrologic balance, canopy gas exchange and primary production processes. *Ecological Modeling* 42:125-154.
- Running, S.W., R.R. Nemani and R.D. Hungerford. 1987. Extrapolation of synoptic meteorological data in mountainous terrain and its use for simulating forest

- evapotranspiration and photosynthesis. *Canadian Journal of Forest Research* 17:472-483.
- Rykiel, E.J. 1996. Testing ecological models: the meaning of validation. *Ecological Modeling* 90:229-244.
- Salmela, S., R. Sutinen, and P. Sepponen. 2001. Understorey vegetation as an indicator of water content in Finnish Lapland. *Scandinavian Journal of Forest Research* 16:331-341.
- Schmidt, R.G. 1957. The silvics and plant geography of the genus *Abies* in the coastal forests of British Columbia. Tech. Publ. T.46. Victoria, BC: British Columbia Department of Lands and Forests, British Columbia Forest Service. 31 p.
- Sea, D.S. and C. Whitlock. 1995. Postglacial vegetation and climate in the Cascade Range, Central Oregon. *Quaternary Research* 43:370-381.
- Shreve, F. 1922. Conditions indirectly affecting vertical distribution on desert mountains. *Ecology* 3:269-274.
- Smith, J. 2002. Mapping the Thermal Climate of the H.J. Andrews Experimental Forest, Oregon. Oregon State University, Corvallis, OR.
- Smith, T.S. and M. Huston. 1989. A theory of the spatial and temporal dynamics of plant communities. *Vegetatio* 83:49-69.
- Smouse, P. E., J. C. Long, and R. R. Sokal. 1986. Multiple regression and correlation extensions of the Mantel test of matrix correspondence. *Systematic Zoology* 35:627-632.
- Sneath, P.H.A. and R.R. Sokal. 1973. *Numerical Taxonomy*. W.H. Freeman, San Francisco.
- Society of American Foresters. 1984. Scheduling the harvest of old growth. Society of American Foresters, Bethesda, MD.
- Sokal, R.R. and R.J. Rohlf. 1995. *Biometry*. Third edition. Freeman, San Francisco, California.
- SPLUS 2000. 1999. Mathsoft Inc. Data Analysis Products Division. Seattle, WA.
- Sprugel, D.G. 1991. Disturbance, equilibrium, and environmental variability: what is 'natural' vegetation in a changing environment? *Biological Conservation* 58:1-18.
- Stephenson, N.L. 1990. Climatic controls on vegetation distribution: the role of the water balance. *American Naturalist* 135:649-670.

- Stephenson, N.L. 1998. Actual evapotranspiration and deficit: biologically meaningful correlates of vegetation distribution across spatial scales. *Journal of Biogeography* 25:855-870.
- Stohlgren, T.J., A.J. Owen and M. Lee. 2000. Monitoring shifts in plant diversity in response to climate change: a method for landscapes. *Biodiversity and Conservation* 9:65-86.
- Swanson, F.J., Kratz, T.K., Caine, N., and Woodmansee, R.G. 1988. Landform effects on ecosystem patterns and processes. *Bioscience* 38: 92-98.
- Tague, C. 1999. Modeling seasonal hydrologic response to forest harvesting and road construction: The role of drainage organization. PhD dissertation. Department of Geography. University of Toronto, Toronto.
- Taylor, A.H. 1995. Forest Expansion and Climate Change in the Mountain Hemlock (*Tsuga mertensiana*) Zone, Lassen Volcanic National Park, California, U.S.A. *Arctic and Alpine Research* 27:207-216.
- ter Braak, C.J.F. 1985. Correspondence analysis of incidence and abundance data: properties in terms of unimodal response model. *Biometrics* 41:859-873.
- Therneau, T.M. and E.J. Atkinson. 1997. An introduction to recursive partitioning using RPART routines. Mayo Foundation. (distributed in postscript format with RPART package).
- Thornburgh, D.A. 1969. Dynamics of the true fir-hemlock forests of the west slope of the Washington Cascade Range. Ph.D. dissertation. University of Washington, Seattle.
- Thornton, P.E., S.W. Running and M.A. White. 1997. Generating surfaces of daily meteorological variables over large regions of complex terrain. *Journal of Hydrology* 190:214-251.
- Urban, D., S. Goslee, K. Pierce and T. Lookingbill. 2002. Extending community ecological analyses to landscape scales: a multi-phased approach based on distance measures. *Ecoscience* 9:200-212.
- Urban, D.L. 2002. Tactical monitoring of landscapes. *in* S. Liu and W. Taylor (eds.), *Integrating Landscape Ecology into Natural Resources Management*. Cambridge University Press.
- Urban, D.L. M.E. Harmon and C.B. Halpern. 1993. Potential response of Pacific Northwestern forests to climatic change, effects of stand age and initial composition. *Climatic Change* 23:247-266.

- Urban, D.L., C. Miller, P.N. Halpin, and N.L. Stephenson. 2000. Forest gradient response in Sierran landscapes: the physical template. *Landscape Ecology* 15:603-620.
- Urban, D.L., R.V. O'Neill and H.H. Shugart, Jr. 1987. Landscape ecology. *Bioscience* 37:119-127.
- USDA. 1990. *Silvics of North America*. U.S. Forest Service Agricultural Handbook 654. December 1990. Washington, D.C.
- Vankat, J.L and J. Major. 1978. Vegetation changes in Sequoia National Park, California. *Journal of Biogeography* 5:377-402.
- VEMAP participants (J.M. Melillo and 26 others). 1995. Vegetation/ecosystem modeling and analysis project (VEMAP): comparing biogeography and biogeochemistry models in a continental-scale study of terrestrial ecosystem responses to climate change and CO₂ doubling. *Global Biogeochemical Cycles* 9:407-437.
- Vertessy, R.A., C.J. Wilson, D.M. Silburn, R.D. Connolly and C.A. Ciesiolka. 1990. Predicting erosion hazard areas using digital terrain analysis. Pages 298-308 in *Proceedings of IAHS International Symposium on Research Needs and Applications to Reduce Erosion and Sedimentation in Tropical Steeplands*. Suva, Fiji.
- Vertessy, R.A., T.J. Hatton, P.J. O'Shaughnessy and M.D.A. Jayasuriya 1993. Predicting water yield from a mountain ash forest catchment using a terrain analysis based catchment model. *Journal of Hydrology* 150:665-700.
- Vertessy, R.A., T.J. Hatton, R.G. Benyon and W.R. Dawes. 1996. Long-term growth and water balance predictions for a mountain ash (*Eucalyptus regnans*) forest catchment subject to clear-felling and regeneration. *Tree Physiology* 16:221-232.
- Walker, P.A. 1990. Modelling wildlife distributions using a geographic information system: kangaroos in relation to climate. *Journal of Biogeography* 17:279-289.
- Walther, G.-R., E. Post, P. Convey, A. Menzel, C. Parmesani, T.J.C. Beebee, J.-M. Fromentin, O. Hough-Guldberg and F. Bairlein. 2002. Ecological responses to recent climate change. *Nature* 416:389-395.
- Wang, G.G. 2000. Use of understory vegetation in classifying soil moisture and nutrient regimes. *Forest Ecology and Management* 129:93-100.
- Ward, J.H. 1963. Hierarchical grouping to optimize an objective function. *Journal of American Statistics Association*. 58:236-244.

- Western, A.W., G. Bloschl and R.B. Grayson. 1998. How well do indicator variograms capture the spatial connectivity of soil moisture? *Hydrological Processes* 12:1851-1868.
- White, J.D. and S.W. Running. 1994. Testing scale dependent assumptions in regional ecosystem simulations. *Journal of Vegetation Science* 5:687-702.
- Whittaker, R.H. 1956. Vegetation of the Great Smoky Mountains. *Ecological Monographs* 26:1-80.
- Whittaker, R.H. 1960. Vegetation of the Siskiyou Mountains, Oregon and California. *Ecological Monographs* 30: 279-338.
- Whittaker, R.H. 1967. Gradient analysis of vegetation. *Biological Reviews* 42:207-264.
- Whittaker, R.H. 1978. Ordination of Plant Communities. *Handbook of Vegetation Science* 5. 2nd ed. Junk, The Hague.
- Wiens, J.A., C.S. Crawford and J.R. Gosz. 1985. Boundary dynamics: a conceptual framework for studying landscape ecosystems. *Oikos* 45:421-427.
- Wiens, J.A., N.C. Stenseth, B. Van Horne and R.A. Ims. 1993. Ecological mechanisms and landscape ecology. *Oikos* 66:369-380.
- Wigmosta, M.S. and S.J. Burges. 1997. An adaptive modeling and monitoring approach to describe the hydrologic behavior of small catchments. *Journal of Hydrology* 202:48-77.
- Wilson, J.P. and Gallant, J.C. 2000. Secondary topographic attributes. Pages 97- 132 *in* J.P. Wilson and J.C. Gallant (eds.), *Terrain Analysis: Principle and Applications*. John Wiley and Sons, New York.
- Winkler, J.B. and F. Schultz. 2000. Seasonal variation of snowcover: inexpensive method for automatically measuring snow depth. Pages 381-338 *in* B. Schroeter, M. Schlenso, and T.G.A. Green (eds.), *New Aspects in Cryptogamic Research: Contributions in Honour of Ludger Kappen*. *Bibliotheca Lichenologica* 75. Cramer, Berlin, Stuttgart.
- Woodward, A. 1998. Relationships among environmental variables and distribution of tree species at high elevation in the Olympic Mountains. *Northwest Science* 72:10-22.
- Wu, H., E.J Rykiel Jr., T. Hatton and J. Walker 1994. An integrated rate methodology (IRM) for multi-factor growth rate modelling. *Ecological Modelling* 73: 97-116.
- Wu, J. and O.L. Loucks. 1995. From balance of nature to hierarchical patch dynamics: a paradigm shift in ecology. *The Quarterly Review of Biology* 70:439-466.

- Yeakley, J.A., W.T. Swank, L.W. Swift, G.M. Hornberger and H.H. Shugart. 1998. Soil moisture gradients and controls on a southern Appalachian hillslope from drought through recharge. *Hydrology and Earth System Sciences* 2:41-49.
- Yee, T.W. and N.S. Mitchell. 1991. Generalized additive models in plant ecology. *Journal of Vegetation Science* 2:587-602.
- Zobel, D.B., A. McKee, G.M. Hawk and C.T. Dyrness. 1976. Relationships of environment to composition, structure, and diversity of forest communities of the central western Cascades of Oregon. *Ecological Monographs* 46:135-156.